The Sizewell C Project

PDB-1 Modelling of the Temporary and Permanent Beach Landing Facilities at Sizewell C

SizewellC
Doing the power of *good* for Britain

eDF *CGN*

NOT PROTECTIVELY MARKED

Modelling of the Temporary and Permanent Beach Landing Facilities at Sizewell C

Table of contents

List of Tables and Figures

Tables

Figures

TR543 MODELLING OF THE TEMPORARY AND PERMANENT BLF AT SZC

NOT PROTECTIVELY MARKED

TR543 MODELLING OF THE TEMPORARY AND PERMANENT BLF AT SZC

NOT PROTECTIVELY MARKED

NOT PROTECTIVELY MARKED

Executive Summary

The Sizewell C Development Consent Order (DCO) Application was submitted in May 2020 (the Application). An Environmental Statement (ES) was submitted as part of the Application. Since the submission of the Application, SZC Co. has continued to engage with the local authorities, environmental organisations, local stakeholder groups and the public with regard to the Application. This process has identified potential opportunities for changing the Application to further minimise impacts on the local area and environment in many cases, whilst reflecting the further design detail that has come forward in preparation for implementation of the Sizewell C Project. In January 2021, SZC Co. submitted information on a number of proposed changes to the Sizewell C Project which were described in detail in an ES Addendum. One of those changes is the subject of this report:

> *Change 2: An enhancement of the permanent beach landing facility and construction of a new, temporary beach landing facility (described in detail in Chapter 2 of the ES Addendum)*

The Application included a permanent beach landing facility (BLF), for use in both the construction and operational phases of the Sizewell C. It would be located on the coast directly in front of the Northern Mound at the northern end of the sea defences, with an associated private access road connecting it to the main platform. The primary purpose of the BLF was to import large deliveries, known as Abnormal Indivisible Loads (AILs), to Sizewell C by sea on barges. Since submission of the Application, further design work has been carried out which has identified that there is potential for more material to be brought to the site by sea than is currently provided for in the Application. This would be achieved by:

- enhancing the design of the permanent BLF; and

- providing a new temporary BLF.

The Sizewell C Environmental Statement Addendum (ESA) (SZC Co) provided details of these changes and presented the results of Environmental Impact Assessments (EIA) for the BLFs, which were performed using Expect Judgement based on previous modelling of jetty and BLF design iterations. Due to uncertainty, some effects were assessed on a precautionary basis. The ESA concluded that the revised BLF and new BLF, and their associated activities, would have no significant effect on any coastal geomorphology receptors, which was the same conclusion that was reached in Application ES.

Since the submission of the ESA, a large number of detailed modelling studies has been undertaken with an aim to determine whether the Expert Judgement-based assessment was appropriate and that no potentially significant effects were overlooked.

Outline description of the BLFs

The two BLFs proposed for SZC are required for transporting Abnormal Indivisible Loads (AILs – large station components), rock armour and bulk construction material that cannot be delivered by the road and rail network. The enhanced permanent BLF[1] will be present for both the construction and operational phases of the station, whilst the temporary BLF will only be present during the construction phase.

---

[1] The enhanced BLF is a revision of the originally proposed permanent BLF. It is positioned at the same Northing and is approximately 16 m longer than the original BLF.

The enhanced permanent BLF would consist of a 101 m long structure built across the beach and out into the sea, consisting of 28 permanent piles in total. It would receive AIL deliveries via barges that ground on a 100 m x 30 m grounding structure on the seabed (the grillage) during the construction phase. During the operational phase, barges would ground in a dredged grounding pocket. The required bed reprofiling for the grounding pocket and access would affect both the inner and outer longshore bars for up to 149 m in the cross shore and 83 m in the longshore.

The temporary BLF consists of a 506 m long structure built across the beach and out into the sea, consisting of 114 piles in total. The temporary BLF would receive aggregates and other freight via ships docked at the BLF head, which is in sufficient water depth that no navigational dredging is required.

Modelling studies undertaken

This report investigates the impacts (including the combined impacts where there is temporal overlap) of the temporary and permanent BLFs and their associated activities (grillage, dredging, moored vessels). Nine different combinations of the structures and vessels were investigated representing the possible combinations during the SZC construction and operational phases. The magnitude of change in the absolute bed shear stress was calculated for each case and compared with the critical bed shear stress (the threshold at which sediment is mobilised). To assess the potential for effects on coastal geomorphological receptors, the bed shear stress at different locations "with BLFs" was compared with the predicted values for the baseline conditions ("without BLFs") to judge whether there were any changes that were sufficient to cause changes in sediment mobilisation.

A total of 58 model scenarios were investigated which included combinations of: the temporary BLF, permanent enhanced BLF, grillage and dredging, vessels – barge and ship, 1 in 20-year wave – NE and SE, peak ebb and peak flood tidal currents, 1.5 m wave (ship working limit) – NE and SE and 0.5 m wave (barge working limit) – NE and SE. Each scenario represents a static moment in time. Therefore, the scenarios can be considered as representative of the instantaneous worst cases at key points in the tidal cycle.

Numerical simulations were carried out using high-resolution ARTEMIS and TELEMAC2D models to provide information regarding the impacts of the BLFs and vessels on the wave and current fields, respectively. For each of the nine combinations of structures and vessels, four scenarios were considered in ARTEMIS with different combinations of wave heights, wave directions and water levels (coincident with peak flood and ebb tidal conditions, extracted from TELEMAC2D results). Three wave heights were considered: a 1 in 20-year return interval wave height (no vessels), critical wave height (H_s)=1.5 m (working limit for ships at the temporary BLF) and H_s= 0.5 m (working limit for barges at the enhanced permanent BLF).

In all the model meshes, except for the baseline mesh, the presence of the nearshore outfalls (the Combined Drainage Outfall (CDO) and the two Fish Recovery and Return outfalls (FRR)) has been included. Whilst the CDO and FRRs may not temporally overlap with the temporary BLF, these structures have been included as a worst case.

The bed shear stress changes were modelled for all scenarios and a detailed analysis was presented for the scenario corresponding to the greatest magnitude change, which was from south-easterly waves with peak ebb tidal currents. The absolute change in bed shear stress was calculated considering the maximum bed shear stress in excess of the critical threshold value, using the condition with no BLF structures or vessels as a baseline to investigate the effect of their introduction.

Modelling Results

The results are presented as changes in absolute bed shear stress. An increase in bed shear stress does not necessarily mean an increase in erosion, nor does a decrease lead to an increase in deposition of sediment.

NOT PROTECTIVELY MARKED

The critical threshold of motion reference point, calculated from the Sizewell subtidal sand samples, is 0.216 N/m^2 – i.e. bed shear stress above 0.216 N/m^2 implies sandy sediment is in motion. Results show that the baseline bed shear stresses (when no BLFs are present) over the entire model domain are above the critical threshold of motion. There are no areas of change, as a result of the BLF structures or vessels, where a reduction in bed stress reduces below the critical threshold or increases above the threshold where it was not previously already above that threshold.

For all the scenarios presented there is an area of increased bed shear stress ranging between 2-6 N/m^2 extending north up to 460 m into the Minsmere SPA/SAC during the construction phase and 230 m in the operational phase. This increase in bed shear stress is small compared to the modelled baseline conditions (40-60 N/m^2), is well within natural variation along the Minsmere SPA/SAC frontage and unlikely to result in a detectable topographic change.

SZC construction phase

For the scenario considering only the temporary and enhanced permanent BLF piles (1 in 20-year wave height), the enhanced permanent BLF leads to an alternating increase/decrease pattern in bed shear stress along the shore, as the waves and flow interact with the BLF. However, as the BLF piles are transmissive, they would not block sediment transport. The temporary BLF causes a small reduction in the leeward side of the structure with an equally small increase in bed shear stress on the windward side. However, these changes are very small compared to the baseline. Alternating patterns of bed shear stress would not persist in the same locations, due temporal changes in the currents and the waves. Patches of altered bed shear stress are sufficiently small in magnitude and scale that they are not expected to cause detectable change to the shoreline.

The presence of the CDO and FRR structures show no detectable change in bed shear stress beyond their immediate scour pits and show no interaction with the temporary or permanent BLF.

The grillage would be used at the permanent BLF for approximately four years during the SZC construction period and would increase the area of changed bed shear stress compared to the BLF piles alone. In the lee of the grillage, a reduction of 15-22 N/m^2 extends approximately 45 m over the inner longshore bar, compared to a baseline of 40-50 N/m^2. The shoreward end of the grillage would sit above the bed, deflecting currents shoreward and increasing the bed shear stress at the seaward deck piles of the permanent BLF. However, the grillage does not act as a blockage as currents still pass over the top. Much like the BLF structures alone, the grillage and deck piles create a localised patchwork of increased and decreased bed shear stress, which reflect the non-persistent and variable state of the tide and direction of waves. They are not expected to cause detectable change to the shoreline.

The introduction of a ship at the temporary BLF combined with the permanent BLF (without grillage or dredging) results in reduction in bed shear stress in the lee of the prevailing wave direction. The ship is treated as a barrier to wave energy in the model, however, in reality the ship does not occupy the full water column and would heave with the passage of waves, meaning that the model results show greater increases and decreases in bed shear stress than would be expected in reality. The reduction is between 15-20 N/m^2 along both the inner and outer longshore bar, compared to a baseline of 20-30 N/m^2 and 40-50 N/m^2, for the respective longshore bars. The wave shadow caused by a ship in dock during large SE waves leads to a reduction in bed shear stress which mean less sediment in suspension. However, the differences in bed shear stress along the shoreline are small compared to baseline, meaning that deposition and salient formation is very unlikely, as a long period of persistent wave conditions (non-varying, directionally) would be required. The differences associated with the maximum wave height considered lessen with a reduction in wave height. Ships would not be present all of the time and would be least present in winter when natural bed shear stress differences would be greatest. When ships are absent the reduction in stress would disappear. Treating the

NOT PROTECTIVELY MARKED

ship as a breakwater (but noting the earlier comment that it would not fully block wave energy), the ship's length and its distance from shore is sufficient that no deposition (i.e., a salient) is expected to occur. In summary, therefore, salient formation is very unlikely and, were it to occur, would amount to a very small transient feature. As the differences in bed shear stress near the shore are very subtle and shown to be incapable of salient formation for several reasons, they would also not affect longshore transport in a detectable way.

As a salient formation is very unlikely, and longshore transport will not be affected, the BLFs and associated structures and vessels are not considered to act as a potential barrier to the restorative processes of the beach following natural erosion over the winter. The recovery phases of the beach and the landward movement of sand occur mainly during summer months when the waves are lower, meaning the reduction due to the presence of the ship is very small.

When the grillage is present at the permanent BLF in conjunction with a ship docked at the temporary BLF, the combined impacts of the grillage and ship are no greater than the ship in isolation, seaward of the grillage. In the lee of the grillage, the magnitude of reduction along the inner longshore bar is similar (15-20 N/m^2), however, although this extends over a wider area compared to the ship only case it is still within the footprint of the wave shadow of the ship only case.

Unlike the grillage, which sits slightly proud of the seabed for part of its length, the grounded barge acts a barrier to the shore parallel tidal flows, as it occupies the entire water column once grounded. This barrier causes the flow to divert around the shoreward and seaward ends of the barge, although it is important to note that barges would only be present for up to 22% of the April – October period (and would be infrequent during winter) so the impacts described below are very transient. The flow accelerates between the shore and the end of the barge, with a peak increase in tidal currents of 0.34 m/s between the last two pairs of piles of the permanent BLF. This increase in velocity returns to within 0.1 m/s within 140 m. The reduced flow to the north of the barge on the ebb tide returns to within 0.1 m/s within 835 m.

Despite the resulting increase in the current induced bed shear stress shoreward of the barge, results show that the blockage effect to the waves leads to an overall reduction in bed shear stress between the shoreline and the barge. This is because the wave induced bed shear stress is significantly larger in the shallow waters than the current induced bed shear stress, even with a 0.5 m wave. The reduction in bed shear stress along the inner longshore bar between the barge and the shore is between 15-20 N/m^2, compared to a baseline of 20-25 N/m^2. There is no area where a reduction in bed shear stress reduces below the critical threshold. These conditions are variable with the state of tide and waves, meaning the peak impact shown in the model results is not persistent over a tidal cycle and are not expected to cause detectable change to the shoreline.

The bed shear stress in the ship lee decreases substantially, as shown in the significant wave height of 0.5 m barge model case. The decreased bed shear stress is most noticeable in the shallow waters associated over the outer longshore bar. As a result, the change in bed shear stress due to the presence of both the ship and the barge is similar to the barge only.

SZC Operational phase

During the operational phase, when only the permanent BLF is present, the spatial pattern of the magnitude of change is almost the same as for the construction phase (permanent and temporary BLFs). The patchwork of increased and decreased bed shear stress due to the piles is dependent on the state of the tide and direction of waves. These conditions would vary with the changing state of tide and waves, meaning the peak impact modelled would not persist over a whole tidal cycle. Patches of altered bed shear stress are sufficiently small in magnitude and scale that they are not expected to cause detectable change to the shoreline.

The dredging of a grounding pocket during the operational phase leads to an alternating pattern of increase/decrease in bed shear stress. The deepest parts of the grounding pocket lead to a reduction of 10-15 N/m^2, with areas of a 8-10 N/m^2 increase in the shallow regions of the pocket. The baseline within the grounding pocket is 25-30 N/m^2. The patchwork of increased and decreased bed shear stress due to the grounding pocket would vary with the changing state of tide and waves, meaning the peak impact modelled would not persistent over a whole tidal cycle. Furthermore, reprofiling the grounding pocket would only occur once every 5-10 years. Therefore, it would have no effect on the shoreline.

Conclusions

For all of the scenarios considered in this report, the BLF structures and their associated activities are not considered to result in any detectable change to bed levels along the shoreline. Therefore, there would be no change beyond those caused by natural processes to the supratidal beach. As a result, there will be no additional change to the 'annual vegetation of drift lines' habitat (Minsmere to Walberswick Heaths and Marshes SAC) or the potential nesting sites for little tern (*Sterna albifrons*) (Minsmere to Walberswick SPA). The assessment of the impact on the annual vegetation drift lines or potential nesting sites is not conducted in this report but is conducted in the shadow Habitats Regulation Assessment (HRA).

All the modelled predictions are consistent with the overall conclusions presented in the SZC Environmental Statement Addendum and original Environmental Statement namely that there is no significant effect on coastal geomorphology receptors due to the presence of the BLFs and/or associated operations.

1   Introduction

As detailed in the Sizewell C Environmental Statement Addendum (ESA), the design of the Beach Landing Facilities (BLF) at Sizewell C (SZC) have changed. The Environmental Impact Assessments (EIA) of the BLFs in the ESA were conducted using Expect Judgement based on previous modelling of jetty and BLF design iterations. It concluded that the amended and new designs would have no significant effect on coastal geomorphological receptors, which was the same conclusion reached in the original Environmental Statement (ES). The purpose of this report is to present the results of a detailed modelling assessment of the changes to the BLF designs described in the ESA and to determine whether the Expert Judgement based assessment was appropriate and that no potentially significant effects had been overlooked.

Marine freight (including Abnormal Indivisible Loads (AIL), rock armour and bulk construction material) will be delivered to SZC on large barges and ships docking at two BLFs. The enhanced permanent BLF (hereafter the permanent BLF) will be present for both the construction and operational phase of the station. The temporary BLF will only be present during the construction phase.

During the SZC construction phase, the permanent BLF would be in place early in the construction phase to support construction of the power station by enabling delivery of some AILs by sea. Up to 100 beach landings per annual campaign (approximately 1 April to 31 October) are anticipated over a four-year period during the construction phase.

To reduce the amount of construction material that would otherwise need to be delivered by land, a temporary BLF would be used during the construction phase only, to receive bulk construction materials, such as aggregate and potentially other materials (e.g., marine tunnel segments for marine works). Up to 400 deliveries between April and October (inclusive) are expected from self-propelled ships, with up to 200 additional deliveries for the remainder of the year, for each of the eight years of operation. The temporary BLF would be located approximately 165m to the south of the permanent BLF. The temporary BLF would be removed at the end of its use during the construction phase.

During the operational phase of the station, the permanent BLF would only be used once every 5-10 years for maintenance activities. Notwithstanding unexpected poor weather, it would be in operation for less than four weeks during each maintenance phase. The most likely operational window would be April to October, when wave heights are typically low, however, this does not rule out potential use during calm winter conditions.

Deliveries to the permanent BLF would access the SZC site using a haul route, whilst a conveyor would be used along the length of the temporary BLF.

The BLF characteristics and a general overview of the modelling tools used in this report are described in the following sections.

1.1   Temporary and permanent BLFs

The permanent BLF would be built across the beach and out into the sea and consist of 28 permanent piles in total – 24 (12 seaward of Mean High Water Springs, MHWS) 1 m diameter piles would support the BLF deck and four mooring dolphins/fender piles (approximately 2.5 m diameter) would be seaward of the deck. The BLF would be 101 m in total length, with a cross shore pile spacing of 9.2 m and an alongshore pile spacing of 12 m. The permanent BLF would be located at approximately 264446 m Northing (British National Grid (BNG)).

TR543 MODELLING OF THE TEMPORARY AND PERMANENT BLF AT SZC

NOT PROTECTIVELY MARKED

The temporary BLF would be built across the beach and consist of 114 piles (of which approximately 12 would be located above MHWS). It would be 506 m long and up to approximately 12 m wide. A jetty head, comprising 24 piles, at the seaward end would be up to approximately 62 m wide. The temporary BLF would extend seaward of the outer longshore sand bar and would not require dredging as vessels could berth alongside with sufficient under keel clearance. The length of the vessel could be up to approximately 120 m (this length has been used for the inclusion of the ship in the modelling). The piles would be 1.2 m in diameter, except for two berthing dolphins and two mooring dolphins (each 2.5 m in diameter). Raking piles and cross braces may be required at the seaward end of the unloading platform for stability. However, these have not been included in the model as the 2D models cannot represent a diagonal structure. The omission of these small structures will not materially affect the results of the modelling. The temporary BLF would be located at approximately 264281 m Northing (BNG).

Figure 1 shows location map of the enhanced permanent BLF and barge/grillage (to the north), the temporary BLF and ship, and the nearshore outfalls (CDO and FRRs).
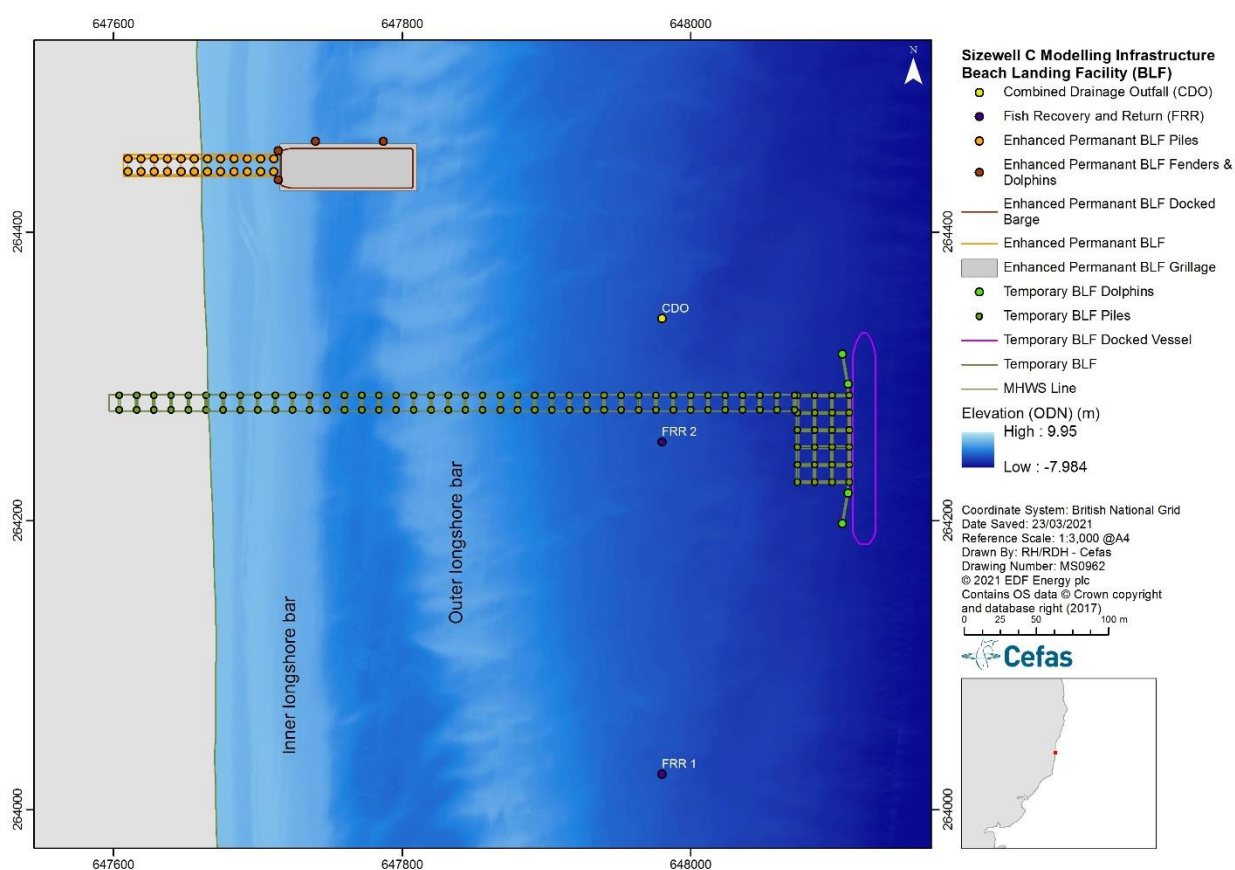
Figure 1: Location map showing the enhanced permanent BLF and barge/grillage (to the north), the temporary BLF and ship, and the nearshore outfalls (CDO and the two FRR outfalls).

1.2   Permanent BLF docking during the construction phase – grillage

For deliveries at the permanent BLF, a barge would approach the BLF approximately one hour before high tide, with the assistance of two tugboats. Once the barge has docked against the end of the BLF, it would alter

its ballast to sink with the falling tide, such that it will rest fully on a non-erodible grounding platform (herein referred to as the grillage). The grillage would be 100m in length and 30m wide. The shoreward tip of the grillage is expected to protrude above the seabed by approximately 1m with a 1:28 slope along the 100m length. The grillage would be removed at the end of its use period within the construction phase.

1.3   Permanent BLF docking during the operational phase – grounding pocket

During the operational phase, every 5-10 years, dredging of a 1:28 planar surface (a grounding pocket) would be required for barges to ground upon. Once the barge has docked against the end of the BLF, it would alter its ballast to sink with the falling tide, such that it will rest fully on the seabed at low tide.

For this study, a North Sea barge was assumed and has been used to assess the dredging needed for the grounding pocket. North Sea barges are 94 m long and 27.4 m wide. The dredged profile is similar to the natural profile (i.e., minimal depth change) except on the landward flank of the outer bar (Figure 2), which needs a deeper cut in order to accommodate the grounded barge. A 28° angle of repose was used for the slopes of the dredged area (as recommended by Soulsby, 1997) to reduce infilling. The outer bar was clipped to a height of -3.5 m ODN to allow clearance of the tugs over the outer bar (see Section 1.4).

In addition to the desired dredge profile, Figure 3 shows the area over which the dredging would be required. The total area includes the width of the barge to rest centred in front of the BLF plus the length of the tugboat to work tangentially to the barge to provide clearance for safe working. The edges of the dredge areas use a 28° angle of repose to return from the dredge depth to the surrounding bathymetry.

To investigate the influence of bed lowering arising from dredging, the bathymetry of the model's domain was lowered accordingly (as indicated in cross-section in Figure 2 over the area shown in Figure 3). The total dredged area is 1.22 ha.
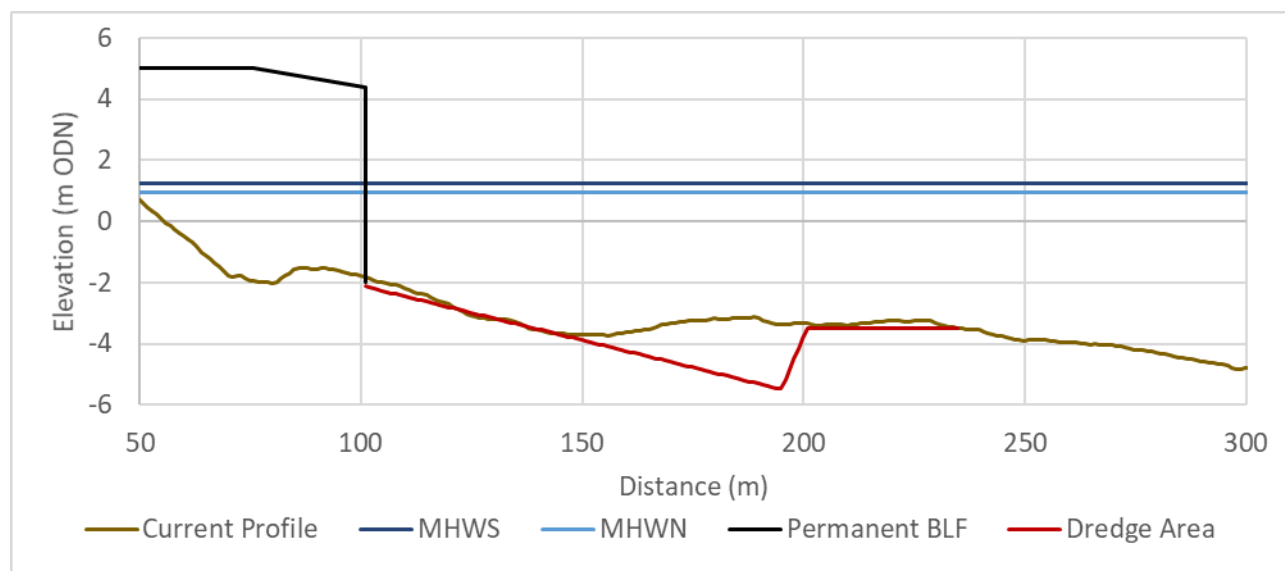
Figure 2: Desired dredge profile (red) required for a North Sea barge to dock at the BLF (black), compared to the 2017 bathymetry (brown).
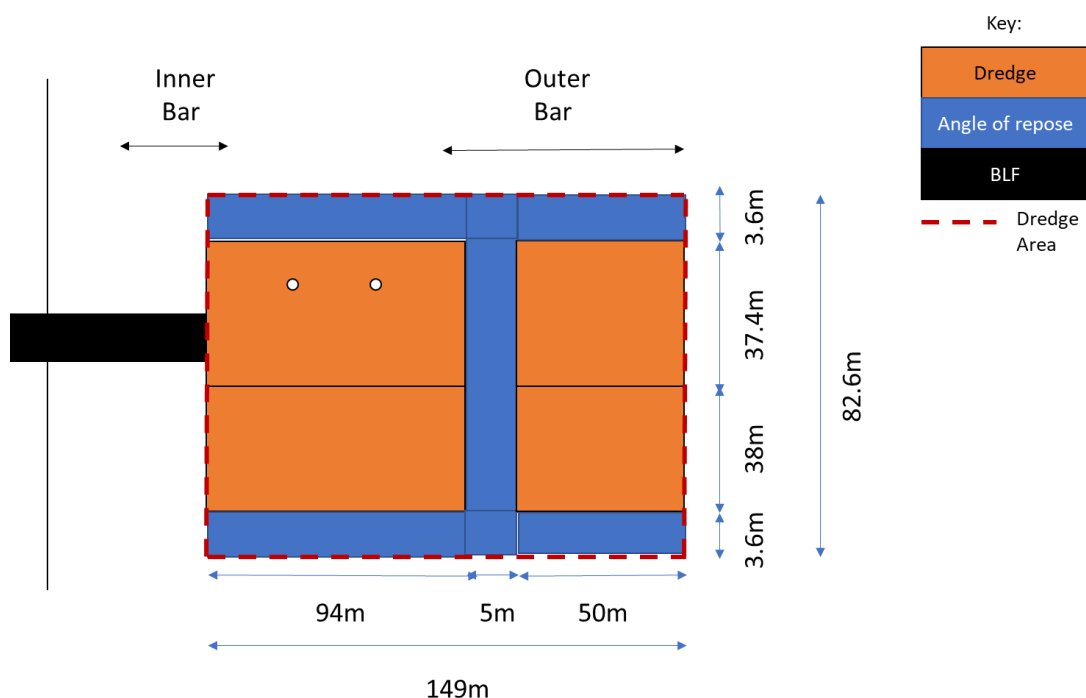
Figure 3: Dredge area required for the BLF navigational approach. Dredge area includes barge grounding and clearance for tugboat safe working.

1.4 Permanent BLF access dredging

In order for the barge to dock at the end of the permanent BLF during both construction and operational phases, the barge and the tugboats would need to transit over the outer longshore bars. One tugboat would push from the aft of the barge and the other will guide from the port side, due to flood currents still flowing southwards just before high tide. For safe navigation, the outer longshore bar will require dredging to a height of -3.5 m ODN for sufficient clearance. The dredging required is minimal as the bar crest is typically around -3.5 m ODN.

1.5 The ARTEMIS and TELEMAC models

TELEMAC-MASCARET is an integrated suite of numerical modelling packages that allows the computation of free surface flows, wave propagation and sediment dynamics. The two modules used here are TELEMAC2D and ARTEMIS. An overview of the Sizewell TELEMAC models is described in BEEMS Technical Report TR224. TELEMAC models have previously been used to simulate tides and waves at Sizewell. The Sizewell regional model provided the boundary forcing conditions for this study. The setup and validation of the model used to simulate the tidal currents and waves is described in BEEMS Technical Reports TR233 Edition 2 and TR232 Edition 2, respectively.

ARTEMIS is one of two modules for simulating wave action in the TELEMAC-MASCARET suite. It is used in a stand-alone mode, independently of other parts of a hydrodynamic system, and computes the wave field only. ARTEMIS is a phase-resolving wave model, meaning it simulates the free water surface and therefore can compute the interaction between surface waves and hard structures such as walls, breakwaters and coastal defence infrastructure. It includes all the sources and sinks of wave energy included in the TOMAWAC

NOT PROTECTIVELY MARKED

wave model[2] as well as two additional and important parameters that allow wave reflection by an obstacle and wave diffraction in the lee of an obstacle to be considered. These effects are crucial, particularly when coupled with refractive effects of bottom variation. ARTEMIS may be used to simulate either regular waves or mono-directional and/or multidirectional random waves. It includes the effects of bathymetry and energy dissipation both due to bottom friction and wave breaking (EDF, 2012).

ARTEMIS does not include the effect of wave refraction by a steady current (hence there is no requirement to create an internal coupling between tides and waves) and is not able to handle drying areas inside the domain (as TOMAWAC and TELEMAC2D are able to). The intertidal area at Sizewell is very small and this limitation of the model is not considered significant. For the simulations carried out on the temporary and permanent BLFs, a constant tidal level is used corresponding with either the peak flood or ebb tide, in order that no drying areas are created. The ARTEMIS wave model is a steady state simulation and results represent a snapshot in time and space of the computed wave field over the whole domain. This is based upon constant wave inputs at the boundaries as initial conditions.

Wave incidence in ARTEMIS is given in mathematical notation (0 radians on the x-axis) rather than geographic notation (0° from North). This conversion is programmed to allow the results to be consistent with all other TELEMAC output. However, all wave angles mentioned in this report are made with reference to geographic notation.

Although an internal coupling was not made between ARTEMIS and TELEMAC2D for this study, an external coupling was made. This allows forcing from steady linear tidal currents and orbital wave currents to be considered separately, simulated by their respective models, and then combined as a post-processing operation. The methodology for calculating the combined bed shear stress from waves and tides is discussed in detail in Appendix A, with the results presented in Section 4.

---

[2] TOMAWAC is the spectral wave model used to propagate waves from deep-water to the nearshore ARTEMIS domain; see BEEMS Technical Report TR232 Edition 2 for model details.

2 Determining Bed Shear Stress

2.1 Relationship between bed shear stress and sediment transport

Sediment erosion of the seabed takes place when shear stress generated by the frictional force of the water over the sediment overcomes the force of gravity acting on the sediment grains, as well as frictional or cohesive forces which adhere particles to the underlying bed. For currents, the shear stress is proportional to the square of the mean current speed; for waves it is the square of near bed orbital velocity amplitude. A complex boundary condition exists between the bed and the flow above (Leeder, 1999). Movement of sediment grains begins when shear stress at the bed overcomes a critical threshold level. This critical bed shear stress is usually expressed in a dimensionless form known as the threshold Shields parameter (Soulsby, 1997).

The two main modes of granular sediment transport are bedload and suspended load transport. Bedload transport consists of particles sliding, rolling and saltating near the bed. It takes place when the fluid forces are sufficient to move sediment but not raise it substantially into the water column (i.e., there is permanent or intermittent contact with the bed and flow induced drag and gravity forces dominate). When bed shear stress increases significantly, for stronger flows, sediment is entrained into the water column by turbulence, and is transported as suspended load (Van Rijn, 1993). This is particularly relevant for finer sediment particles that will move into suspension more readily, remaining there as long as their settling velocity is exceeded by the vertical velocity components of turbulent eddies.

A characteristic of steady tidal flows, such as the rectilinear tidal currents at Sizewell, are that bedforms are generated on the seabed. Bedforms are produced by both waves and currents and their precise form, shape and size depends upon current speed, sediment grain size and water depth. Bedforms have a strong influence on boundary layer frictional characteristics and turbulence formation in flows, affecting bed shear stress and hence sediment transport (Soulsby, 1997; Van Rijn, 1993; Nielsen, 1992). With varying current speed, bed features change their nature and dimensions such that friction at the bed is continually developing during the period of a tide's phase.

2.1.1 Friction

Bed friction is a crucial factor in determining sediment transport rates in the nearshore zone. The frictional property of the bed is the dominant component that affects the critical threshold value for bed shear stress. The overall bed friction is reliant upon several components, which collectively are described as the roughness length. The sediment itself displays a skin friction factor z_{0s} (dependent upon sediment size) that determines the capacity for grains to start to move. Once bedload transport has been initiated and grains are in motion along the bed, bedforms may be generated, which adds a second component of friction known as the form friction factor z_{0f}. A third component is the sediment transport factor z_{0t}, generated by particle interaction and momentum transfer occurring as particles collide.

The overall friction factor is the sum of these components such that the roughness length z_0:

$$z_0 = z_{0s} + z_{0f} + z_{0t} \qquad (1)$$

In this study, a roughness length associated with a rippled bed has been used. Soulsby (1997) estimates this to be 6 mm for a rippled sandy bed, across both tidal and wave models universally.

2.2   Combined wave and current bed shear stress

Determination of the frictional force exerted on the bed by waves propagating inshore has been made using methods described fully by Soulsby (1997). The methodology is fully detailed in Appendix A and describes a clear and straightforward process using a series of sequential steps to evaluate each part of the computation. Where any deviation in the procedure from this source is made, full reference is given.

The bed shear stresses due to currents only, τ_c, and waves only, τ_w, can be combined to give an enhanced total bed shear stress. The notion of an enhancement to the bed shear stress, according to Soulsby (1993), is illustrated in Figure 4 and features the maximum combined bed shear stress (τ_{max}), the mean combined bed shear stress (τ_m) and the enhancement due to the combination of both. Many variations of this idea have been developed over time by different research groups, and Soulsby (1997) describes these fully. The method of Grant and Madsen (1979) gives a good all-round performance and is used in this study.
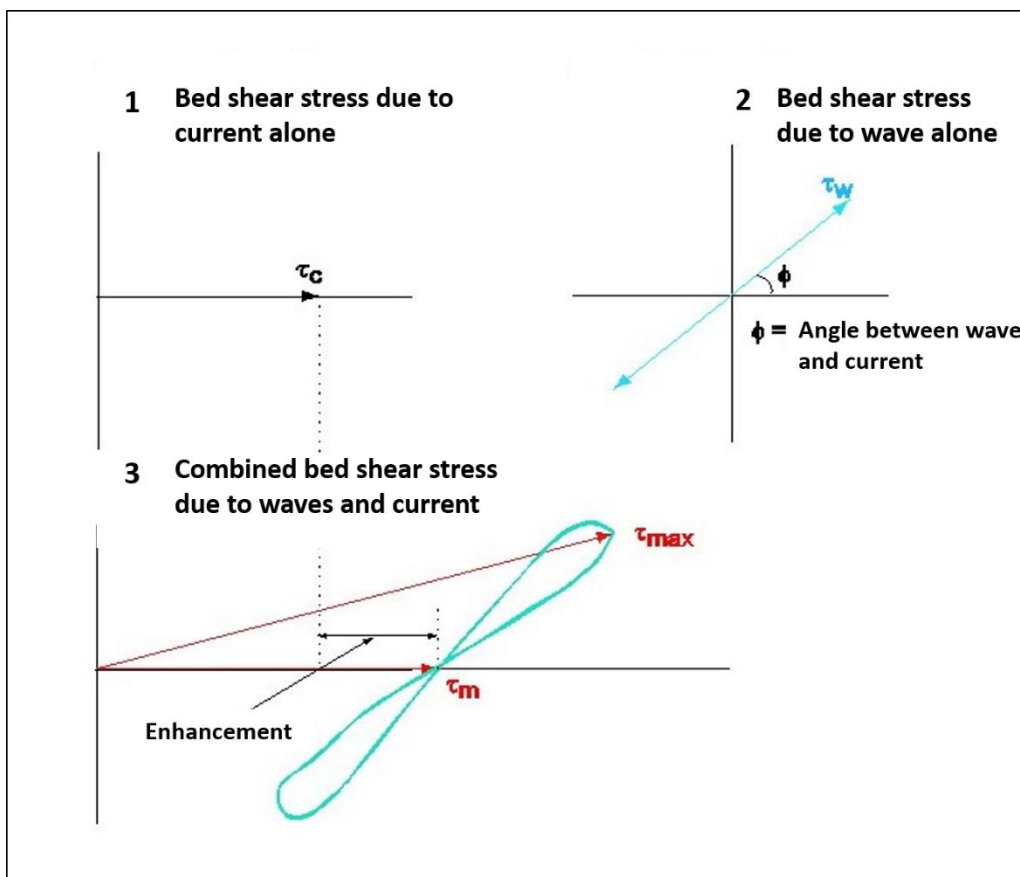
Figure 4: Enhancement of bed shear stress due to combined waves and currents (in Soulsby (1997), adapted from Soulsby (1993)).

3 Modelling the Temporary and Permanent BLFs

3.1 Introduction

This study uses numerical models to simulate the wave climate and tidal velocities as a result of transformed waves arriving at the BLF piles, having propagated over the Sizewell - Dunwich Banks. The results are then combined to calculate the bed shear stress exerted on the seabed near the BLFs. The computation of bed shear stress is considered in two modes:

1. Frictional stresses generated by currents only and waves only (i.e. wave orbital current stress at the bed), which are dominant during storms.

2. Bed shear stress generated by waves and currents combined – quasi-steady tidal currents combined with orbital wave currents produce a non-linear enhancement to bed shear stress.

The two models used in this study are TELEMAC2D, for the hydrodynamics, and ARTEMIS, for the wave climate. This chapter outlines the development and set up of the two models, as well as the model scenarios investigated.

3.2 Mesh design

Construction of a mesh for modelling tides and waves around the BLF structures, to provide a basis for assessment of morphological change, is a complex process due to conflicting numerical demands of the separate parts of the modelled hydrodynamic processes. The TELEMAC models generally used for tides, waves and sediment transport over the sandbanks and other aspects of the model application at Sizewell each use a coincident mesh, as their numerical and operational parameters remain within orders of magnitude (numerical stability criteria, advection schemes). However, to simulate hydrodynamics around the BLF piles, the model requires a resolution finer that the pile dimensions.

For both TELEMAC2D and ARTEMIS model domains, the mesh was built in a parametric way, where the triangular element sizes and location can be specified using a script. The mesh constructed for this study was built with the following criteria:

1. Simulate the rectilinear tidal currents between the shoreline and the end of the BLFs.

2. Replicate the structure of the BLF piles (diameter and spacing between piles) to a very fine resolution (20 cm).

3. Provide a resolution suitable to allow the model to be numerically stable and for waves to be resolved in length.

Further details on the mesh design can be found in Appendix B. Figure 5 shows the ARTEMIS and TELEMAC2D mesh structure which is identical around the temporary and permanent BLFs. In addition to the temporary and permanent BLF, the Combined Drainage Outfall (CDO) and the two Fish Recovery and Return outfalls (FRR) have also been included. Whilst the construction of the CDO and FRRs may not temporally overlap the use of the temporary BLF, the structures have been included as a worst case.

As the hydrodynamic model is two dimensional, the model treats the inclusion of the ship as a full water column feature. This effectively models the ship as a breakwater; where in reality there is water under the keel and

the vessel will heave with waves. Therefore, any effect of a reduction in wave height in the lee of the ship as shown in the results section (Section 4) is conservative.
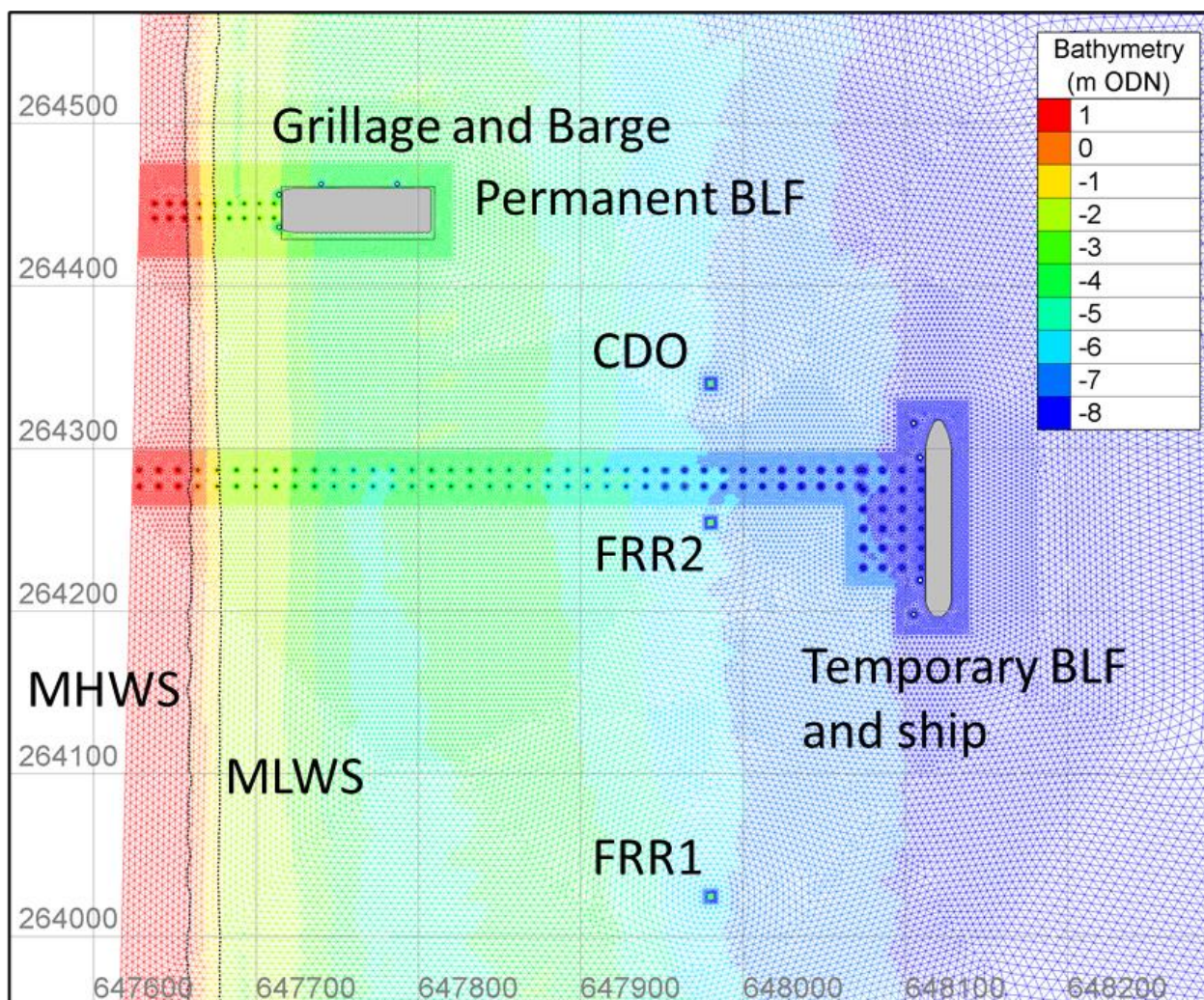
Figure 5: ARTEMIS and TELEMAC2D mesh structure, including the ship at the temporary BLF, the grillage and barge at the permanent BLF, and the CDO and FRR outfalls. The MHWS and MLWS contours are also represented by black dashed lines.

3.3   Grillage

To include the influence of the grillage at the permanent BLF (in place for the construction phase only), the bathymetry was modified with the shoreward tip of the grillage starting a -1.4 m ODN, and a 1:28 slope over the 100 m length. The resulting bathymetry and local scour lowering used in the ARTEMIS and TELEMAC2D mesh around the permanent BLF and grillage is shown in Figure 6. Scour is included as the grillage will only be present after the permanent BLF piles have been installed. Note there is a vertical exaggeration in the plot to aid the view of the grillage.
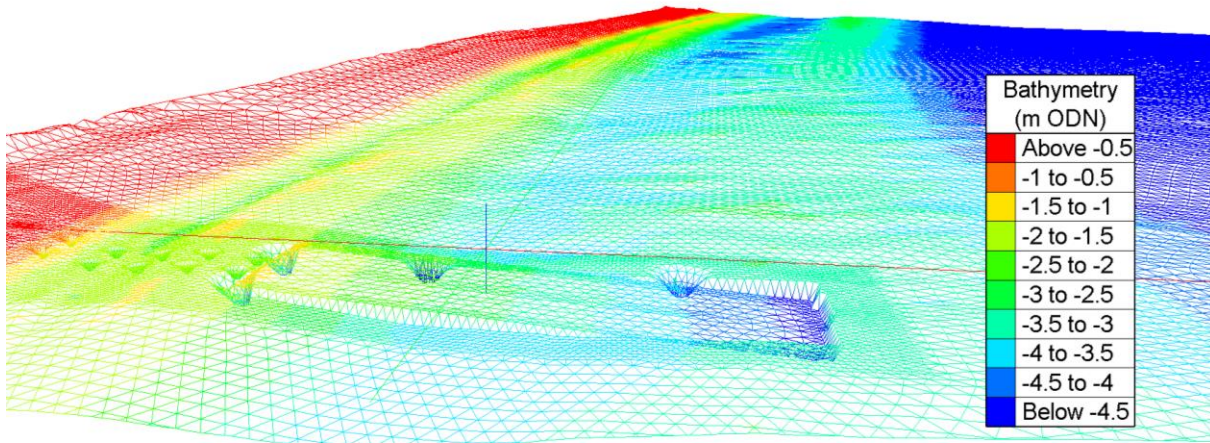
Figure 6: Bathymetry around the permanent BLF including the grillage and scour around the jetty piles.

3.4   Reprofiled bathymetry for the access dredging and barge grounding area

To include the influence of the reprofiled bathymetry required for the access dredging (clipping the outer longshore bar to -3.5 m ODN) during construction and operation, along with the grounding pocket for docked barges during the operational phase, the bathymetry was lowered according to the profile shown in Figure 2. The resulting bathymetry is shown in Figure 7 and Figure 8 shows the bathymetric difference between the baseline and reprofiled beds. The greatest bathymetric change would be on the inner flank of the outer longshore bar (at the most seaward dolphin) where the bathymetry would be lowered by a maximum of 2.1 m. The area of the reprofiled bathymetry has an extent of approximately 149 m cross shore and 83 m longshore.
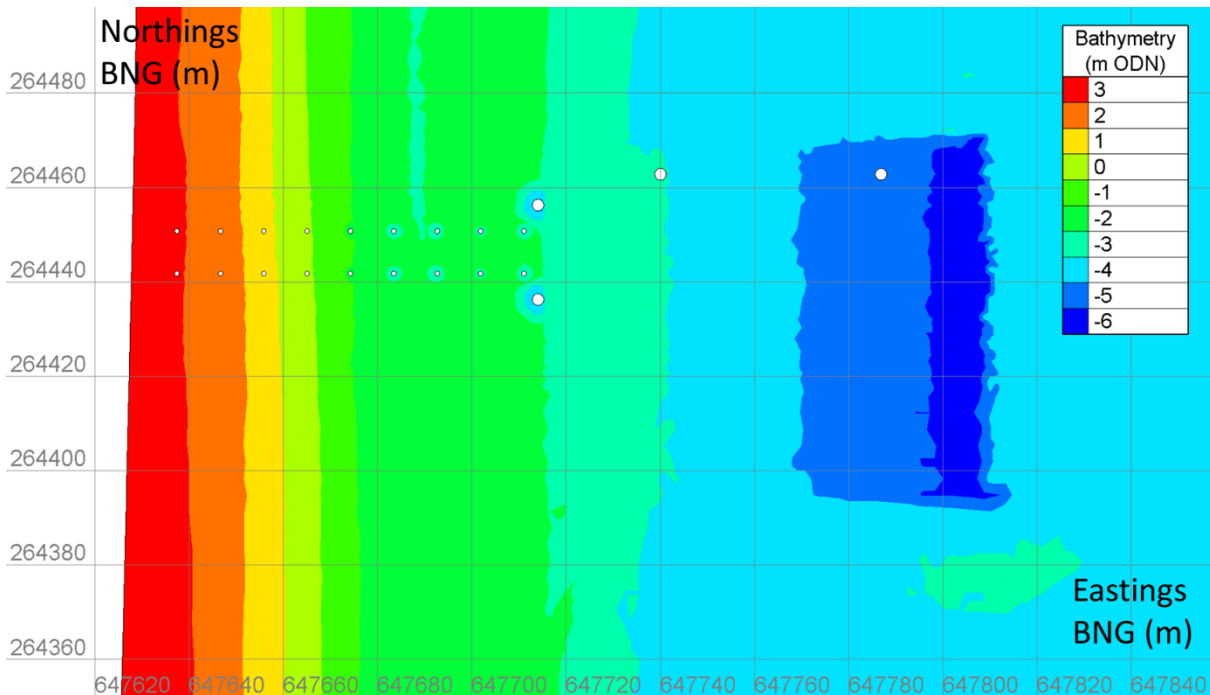
Figure 7: ARTEMIS BLF in use mesh showing the bathymetry and associated dredge reprofiling.
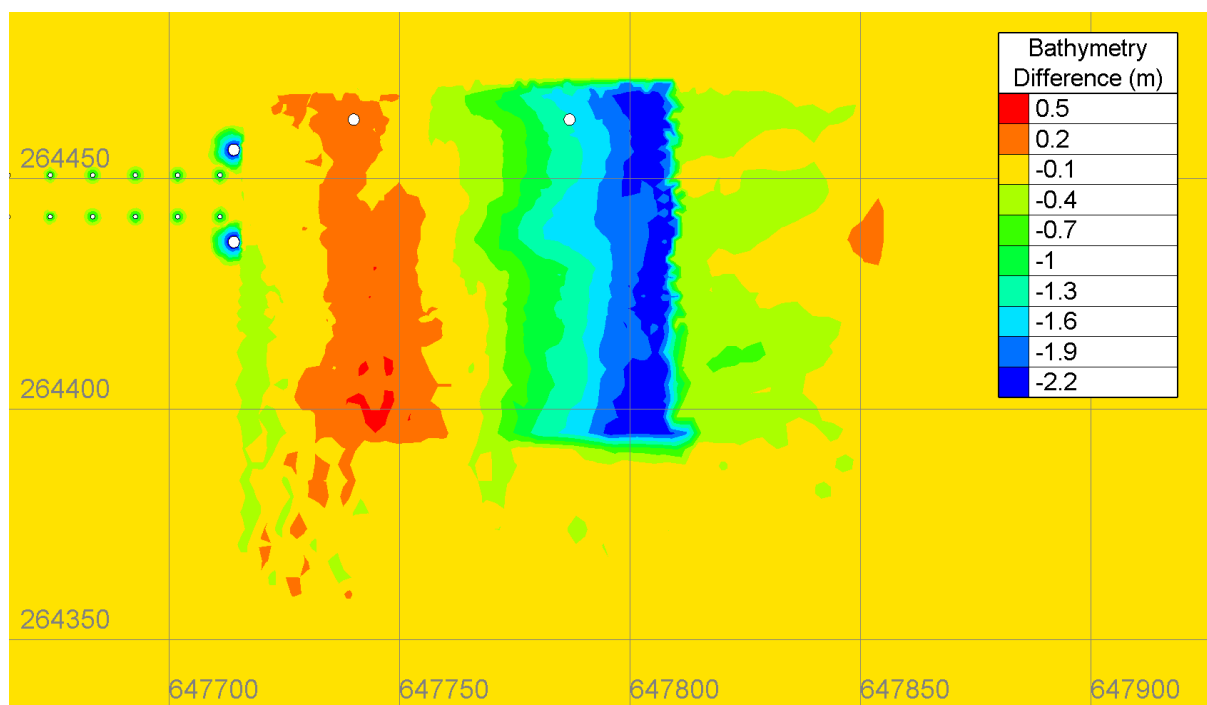
Figure 8: ARTEMIS mesh: bathymetric differences due to the reprofiled bathymetry.

3.5 Model scenarios

3.5.1   Tidal currents

To calculate the contribution of tidal currents to the combined bed shear stress, two tidal flow conditions were considered: peak flood and peak ebb. These correspond to the maximum flows during a flood and ebb tide. Tidal flows in the Sizewell region are rectilinear and flow north-south. The relationship between the wave inputs, tidal currents, and the respective domains over which these separate parts of the model are run, are shown in Figure 9.
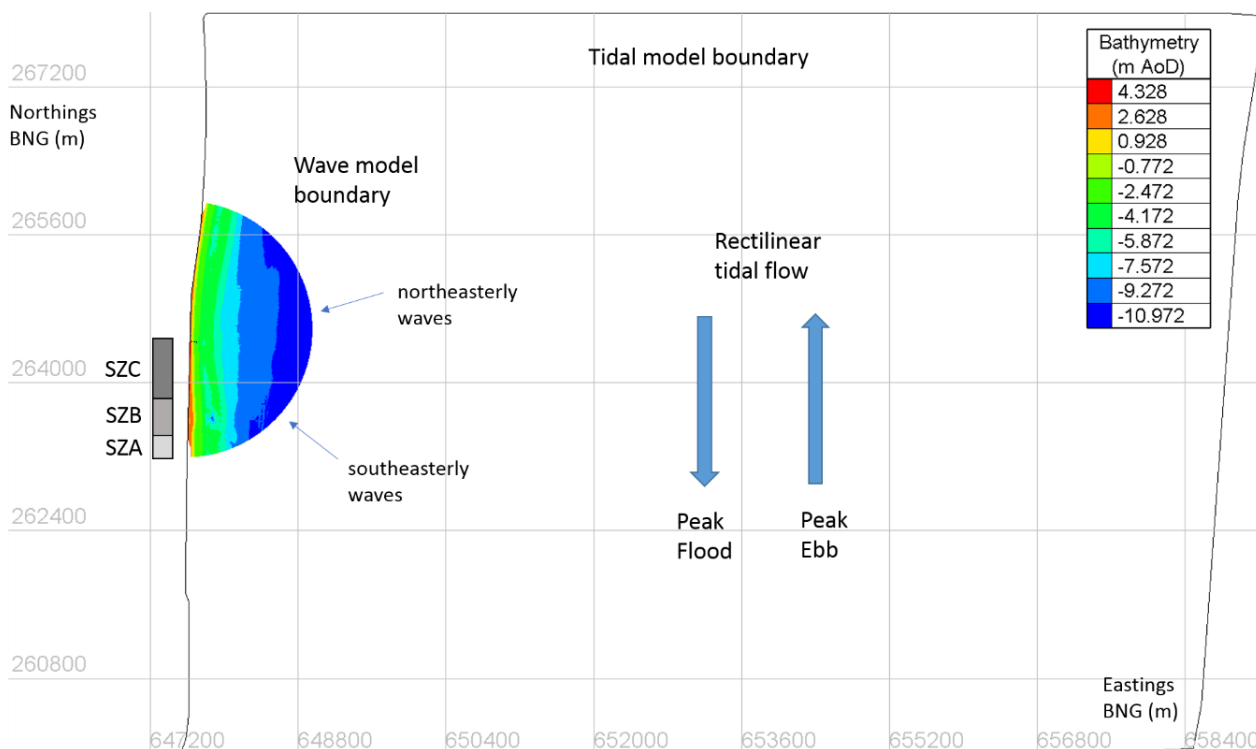
Figure 9: The open boundaries of the ARTEMIS and fine TELEMAC2D domains, with the main wave and current directions also represented.

To calculate the peak flood and ebb conditions, velocities and elevations were extracted from the full regional tidal model at the open boundaries of nested model, and the nested model was run for a 48-hour period that corresponds to the peak spring period. The fine density of the nodes around the piles (0.2 m) demands a very short internal time-step (0.1 s) leading to long run-times for the model. Figure 10 shows a time series of the current speed and free surface elevation, extracted at approximately 6km offshore, over the peak spring conditions.

The results show that the peak flood magnitude is 1.139 m/s and the peak ebb magnitude is 1.080 m/s. As the ARTEMIS model is a steady state simulation, a constant initial water level is fixed for each run. For this study, the two water levels that correspond to the time of peak flood and ebb have been used to provide the constant initial water level considered in ARTEMIS. The results show that the elevation corresponding to peak flood was 0.71 m ODN and -0.57 m ODN for the peak ebb tide.
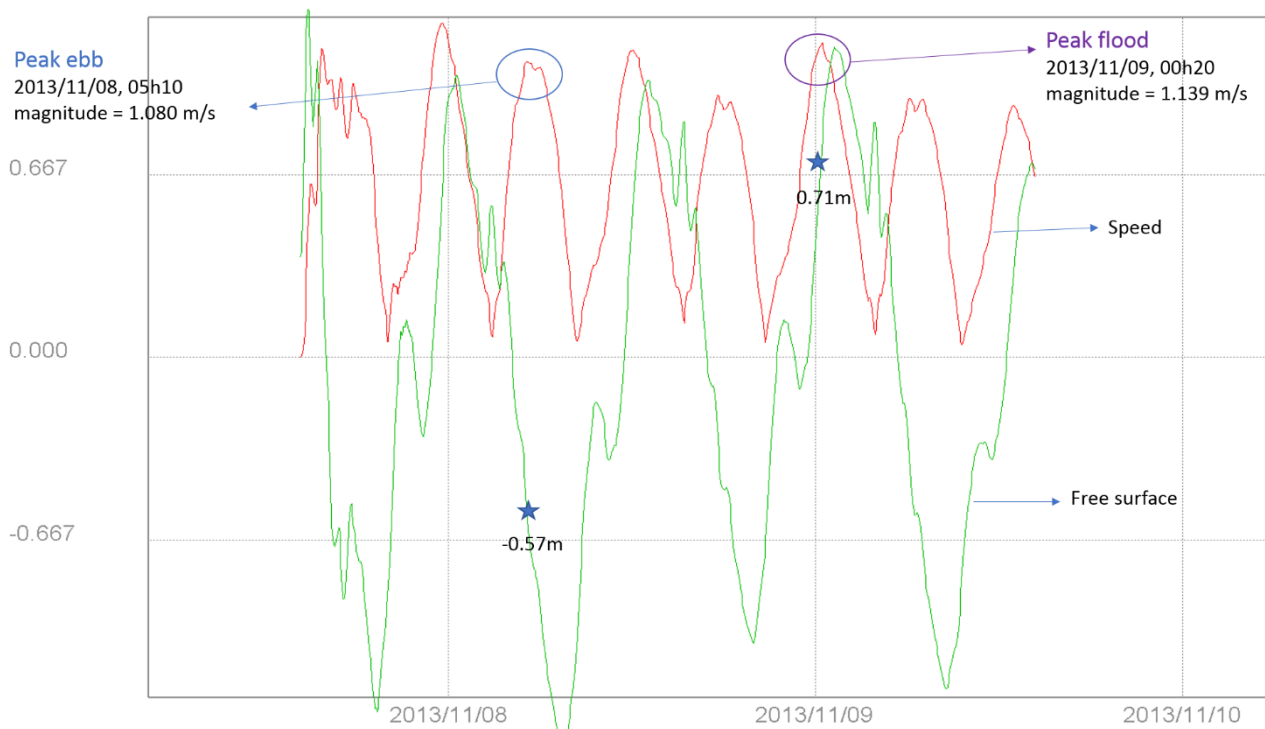
Figure 10: Peak ebb and peak flood conditions identified for the speed (green) and the free surface (red), extracted from the nested tidal model run.

3.5.2 Waves

The wave characteristics used in ARTEMIS were derived from TOMAWAC simulations, with the significant wave height, wave direction and peak period extracted at the most offshore point of the ARTEMIS domain boundary. The TOMAWAC model is a high-resolution coastal wave model that can replicate the behaviour of wave propagation over the complex bathymetry from the offshore to the nearshore. Therefore, it can provide accurate boundary conditions for the ARTEMIS domain based on extreme conditions observed further offshore.

For the present report, wave conditions from the UK Meteorological Office (Met Office) 'ReMap' European wave hindcast model[3] prediction point 950 was used, considering 22 years (1991 to 2012) of the time series, to generate offshore extreme wave return intervals (BEEMS Technical Report TR319). As point 950 is approximately on the offshore boundary of the TOMAWAC domain, this was considered as suitable boundary conditions to drive the simulations. At this location, the predominant wave directions are from 55° and 172° and were used at TOMAWAC offshore boundary. The wave rose of this location is shown in Figure 11, and represents the model derived offshore wave conditions with a significant wave height greater to 3 m. Wave heights below this have been disregarded as only the highest waves are of interest. The offshore waves were transformed into inshore to the ARTEMIS boundary using the TOMAWAC model.

---

[3] Met Office 'ReMap' European wave model, http://wavenet.cefas.co.uk/hindcast
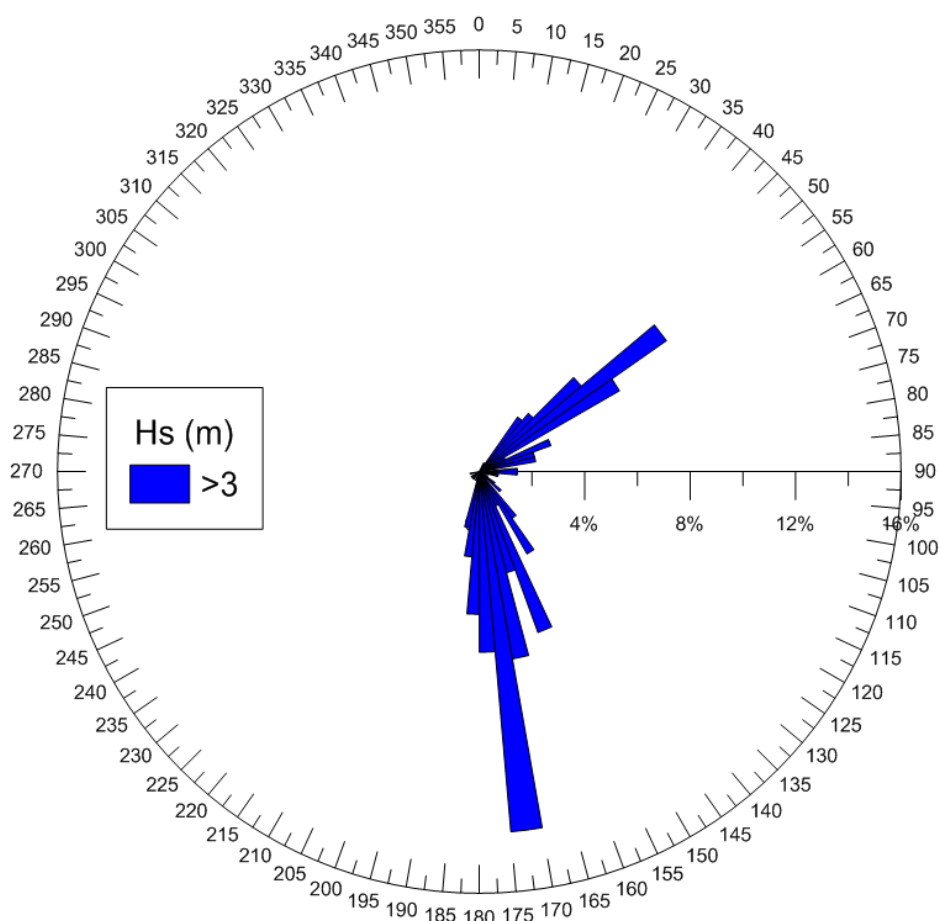
Figure 11: Model derived offshore waves with a significant wave height greater than 3 m, at TOMAWAC offshore boundary (Wave Model prediction point 950 for the period 1991-2012).

A multidirectional random wave was used as the input condition on the seaward boundary of ARTEMIS domain. The model simulates the directional spreading of the wave energy, according to a pre-defined number of directions/periods and minimum and maximum angles of propagation/spectral period, where the angles are discretised into equal energy bands across of the directional spread (tests showed minimal influence of the selected number of directions on the output results). For each of the ARTEMIS runs, the number of directions and periods were split by 8 and 6, respectively. The overall computation time can be gauged by taking the runtime for a regular wave computation and multiplying by the product of other parameterisations.

Three wave heights have been considered as boundary conditions for the ARTEMIS model. The first is a 1 in 20 year return interval wave height, based upon the return intervals derived in BEEMS Technical Report TR319. This offshore wave condition was run on the TOMAWAC model to transform to the ARTEMIS boundary. The wave transformation was required as the significant wave height at TOMAWAC offshore boundary was quite different from the wave height at inshore ARTEMIS boundary (5.39 m vs 3.18 m). The differences between the inshore and offshore wave heights are due to waves breaking on the offshore Sizewell-Dunwich bank. In this way, 5 m offshore waves are only slightly larger inside the banks when compared to 3 m waves. Therefore, running larger waves, such as a 1:100 years wave events will be similar too. A 1 in 100 year return interval wave from the NE is 6.11 m at the boundary of the TOMAWAC model, but is only 3.02 m at the ARTEMIS boundary (BEEMS Technical Report TR319). A 1:20 year wave event is the

largest inshore wave that would represent a realistic scenario. Additionally, the scour depths at the location of the BLF are tidally driven and the methodology for scour prediction shows waves (such as a 1 in 100 year event) would infill the scour holes (BEEMS Technical Report TR310 Edition 2). Therefore, considering larger waves would reduce the scour depths considered in Table 2.

In addition to the 1 in 20 year return interval, two further wave conditions are considered in relation to the working limits of the ship at the temporary BLF (1.5 m) and the barge at the permanent BLF (0.5 m). The docked limit of each vessel is not the same as the transit limit, which is higher. As the 1 in 20 year return interval wave height is much larger than the working limits of the vessels, that condition is only applied to the scenarios where both vessels are not present.

For each of the three wave heights considered, a total of four model scenarios have been devised. These four scenarios represent the wave heights from a north-easterly and south-easterly wave direction with water levels corresponding to the peak flood and peak ebb tidal conditions. All the boundary parameters for the four scenarios are summarised in Table 1. The spectral period range was obtained by extracting the TOMAWAC wave spectra at the most offshore point of the ARTEMIS domain boundary.

Table 1: Wave and physical parameters used in ARTEMIS wave simulations.

Run	Wave direction	Significant wave height	Peak period	Water level	Spectral period range	T_z
	(°)	(m)	(s)	(m)	(s)	(s)
1	77	3.18	10.71	0.71	2 – 19	5.19
2	129	2.90	7.52	0.71	2 – 12	4.61
3	77	2.72	10.69	-0.57	2 – 19	4.71
4	126	2.50	7.08	-0.57	2 – 12	4.23
5	77	1.50	6.52	0.71	2 – 19	3.78
6	129	1.50	5.37	0.71	2 – 12	3.11
7	77	1.50	6.52	-0.57	2 – 19	3.78
8	126	1.50	5.37	-0.57	2 – 12	3.11
9	77	0.50	3.89	0.71	2 – 19	2.26
10	129	0.50	3.5	0.71	2 – 12	2.03
11	77	0.50	3.89	-0.57	2 – 19	2.26
12	126	0.50	3.5	-0.57	2 – 12	2.03

TR543 MODELLING OF THE TEMPORARY AND PERMANENT BLF AT SZC

NOT PROTECTIVELY MARKED

4   Results

Results are presented for all the possible combinations of the temporary BLF, the permanent BLF, the grillage, the presence of the barge at the permanent BLF and the ship at the temporary BLF. The differences in bed shear stress caused by the presence of structures and vessels are all compared against baseline conditions with no structures. These were all run under present day sea levels. The effect of sea level rise has not been considered in this report as previous evidence provided in the Application E S showed that sea level rise reduced the effects of the BLF presence This is caused by the increase in water depth which reduces the wave orbital velocities along the seabed.

For each combination of structures and vessels, four scenarios were modelled to investigate the potential effect of the BLFs on the wave conditions, for both north-easterly and south-easterly waves with two water levels associated with peak flood and ebb tidal currents (Table 1). A total of fifty-eight wave and tidal scenarios were modelled on the ARTEMIS and TELEMAC2D meshes. As such, detailed results are presented for the run (scenario) corresponding to the worst-case impact only (south easterly wave at peak ebb), as defined by the greatest change in bed shear stress, with the remaining simulation results shown in Appendix D.

Although the tidal currents from the TELEMAC2D results were obtained for all tidal levels, the ARTEMIS results were run for the constant water levels associated with peak flood currents (0.71 m ODN) and peak ebb currents (-0.57 m ODN), which would generate the maximum combined wave-current bed shear stresses.

For the calculation of bed shear stress, the methodology outlined in Appendix A was followed. It should be noted that in Eq. 13, Eq. 14 and Eq. 15, the value of the critical Shields parameter and critical bed shear stress is dependent upon the physical properties of sediment and water only (parameterised sediment size, viscosity, density, etc). In the ARTEMIS and TELEMAC2D models used for this study, these properties (sediment, water density, etc.) are fixed as constant in time and space for the model's duration. The most dominant parameter is sediment diameter (d_{50}). For this study, some 300 sediment samples were analysed to determine the characteristic d_{50} value and in the critical bed shear stress calculation it was assigned a uniform value of d_{50}= 350 μm for sediment grain size. Using Eq. 13, Eq. 14 and Eq. 15, a threshold bed shear stress of 0.216 N/m^2 was obtained.

The model results are expressed in terms of absolute bed shear stress. As a result, any value above the critical threshold represents a bed shear stress available to mobilise sediment at the bed and into the water column for transport by tidal currents and waves.

A direct comparison between the baseline conditions model scenarios requires that the results are both on the same ARTEMIS mesh structures. As the TELEMAC2D mesh structure is slightly different to the ARTEMIS domain, the hydrodynamic results were mapped on to the ARTEMIS mesh.

4.1   Baseline conditions

For visual reference and comparison to the changes in bed shear stress resulting from the combinations of the temporary and permanent BLF structures and vessels, Figure 12 to Figure 15 present the baseline current only bed shear stress during peak ebb and the baseline wave only bed shear stress associated with a 1 in 20 year return interval wave height, 1.5 m wave and 0.5 m wave, respectively.

TR543 MODELLING OF THE TEMPORARY AND PERMANENT BLF AT SZC

NOT PROTECTIVELY MARKED
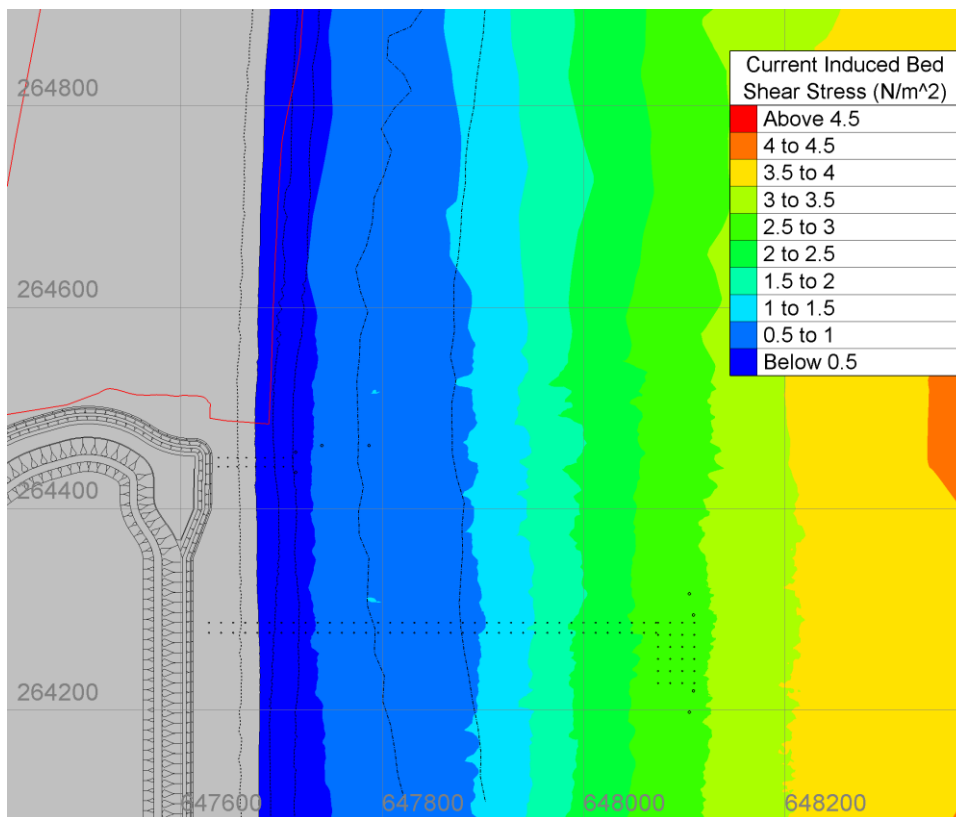
Figure 12: Baseline current induced bed shear stress (τ_c) during peak ebb.
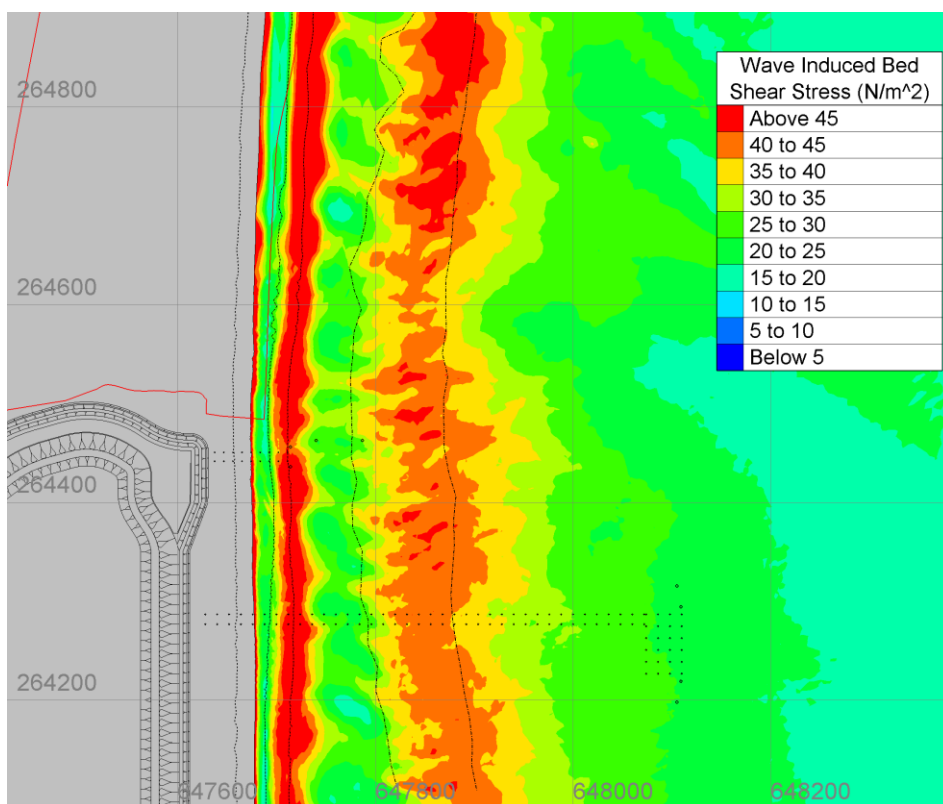
Figure 13: Baseline wave induced bed shear stress (τ_w) for 1in 20yr SE wave during peak ebb.
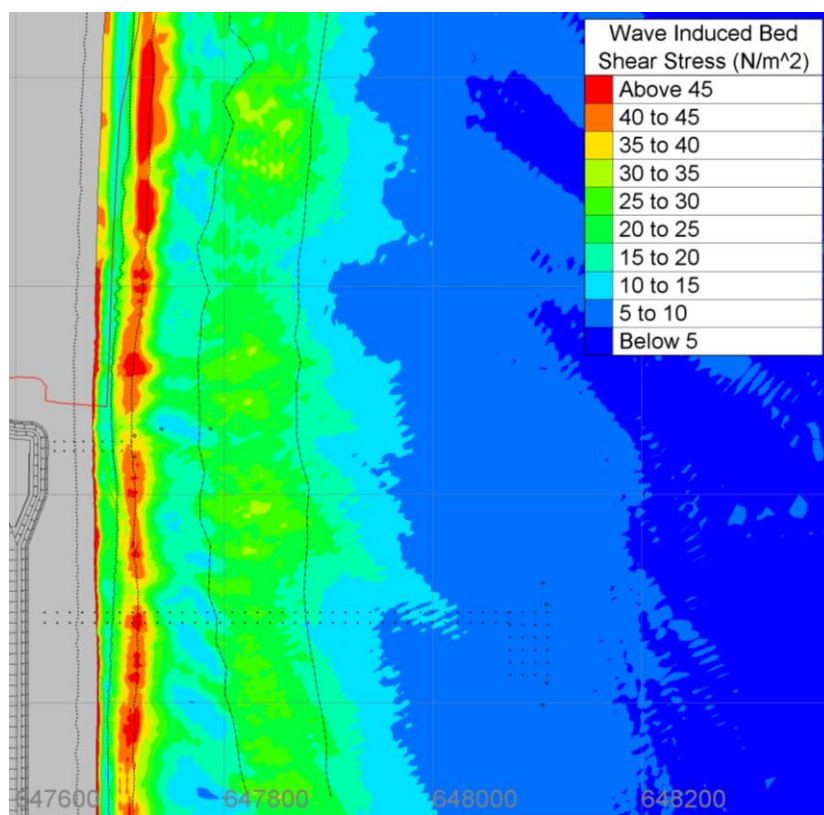
Figure 14: Baseline wave induced bed shear stress (τ_w) for 1.5 m SE wave during peak ebb.
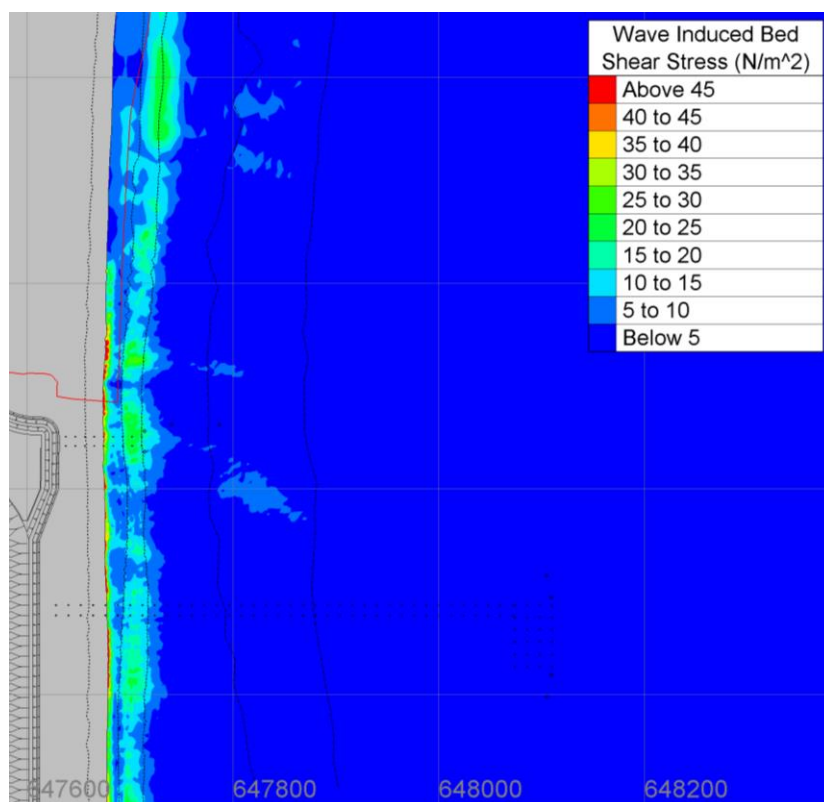
Figure 15: Baseline wave induced bed shear stress (τ_w) for 0.5 m SE wave during peak ebb.

4.2   Temporary and Permanent BLF structures only

To investigate the effect of introducing the two BLFs into the domain, the peak ebb velocities, wave energy and bed shear stress results were compared to the baseline conditions with a 1 in 20 year return interval wave. This scenario would occur when both BLFs are not in use and the requirement for the permanent BLF during construction has finished.

4.2.1   Tidal current induced bed shear stress

Baseline flow velocities across the domain were extracted at peak spring ebb and are shown in Figure 16. To highlight the influence of the BLF piles, Figure 17 shows the flow velocities around the temporary and permanent BLF with Figure 18 showing the difference in velocities compared to the baseline.

Figure 17 and Figure 18 show that the BLF structures slightly interrupt the shore parallel flow. For the permanent BLF there is a small decrease in the tidal currents in the lee of the piles, with flows returning to within 0.1 m/s within 5 m. There is also a minor increase in flows created shoreward of the mooring fenders. The reduction in tidal flows along the temporary BLF is small. The largest change occurs at the head of the temporary BLF where there is the greatest combination of piles and mooring fenders in parallel with the main tidal flow. Tidal currents return to within 0.1 m/s within 330 m of the temporary BLF head.

TR543 MODELLING OF THE TEMPORARY AND PERMANENT BLF AT SZC

NOT PROTECTIVELY MARKED
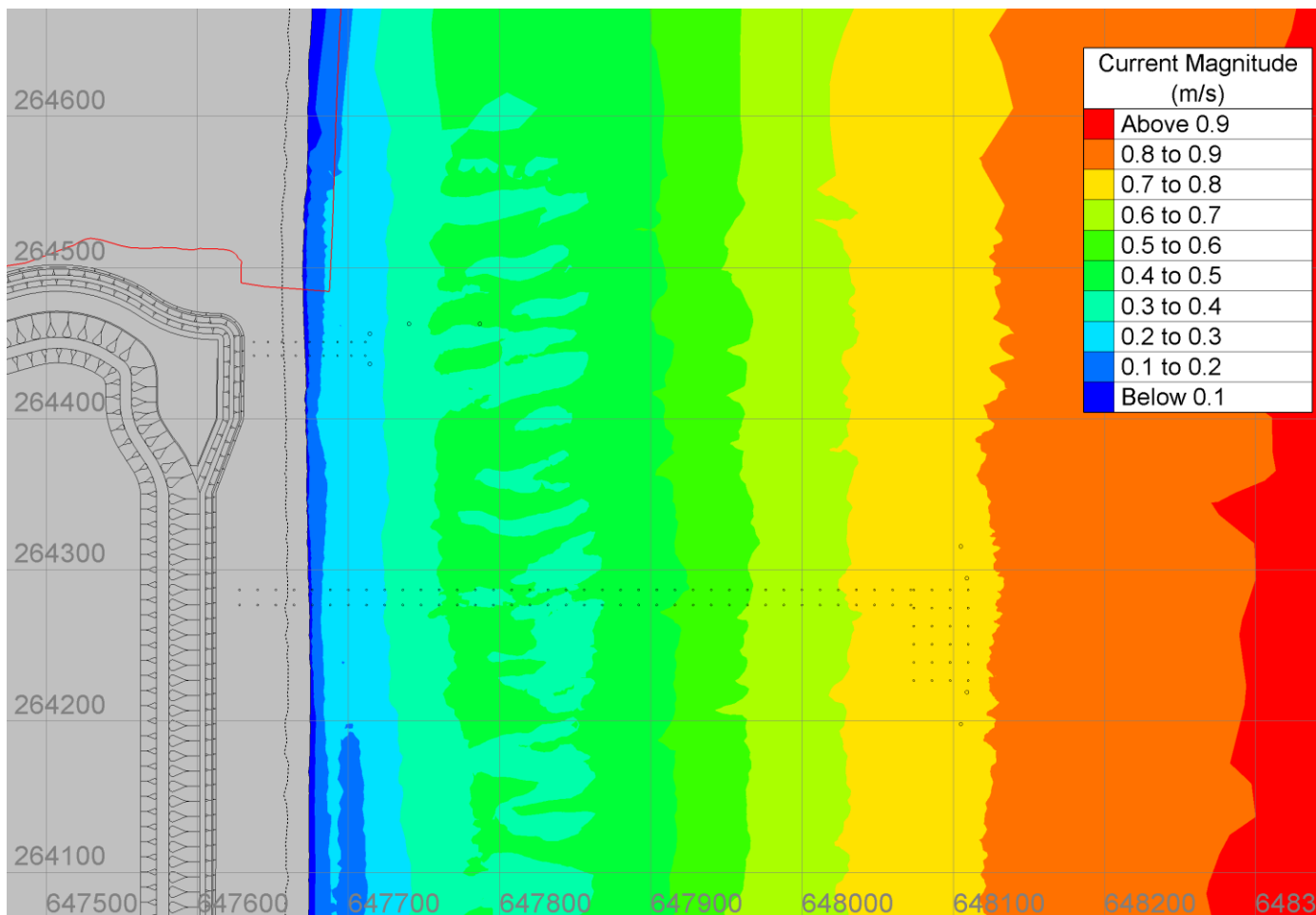
Figure 16: Baseline peak spring ebb velocities. Jetty piles included for visual reference (not in model mesh).

TR543 MODELLING OF THE TEMPORARY AND PERMANENT BLF AT SZC

NOT PROTECTIVELY MARKED
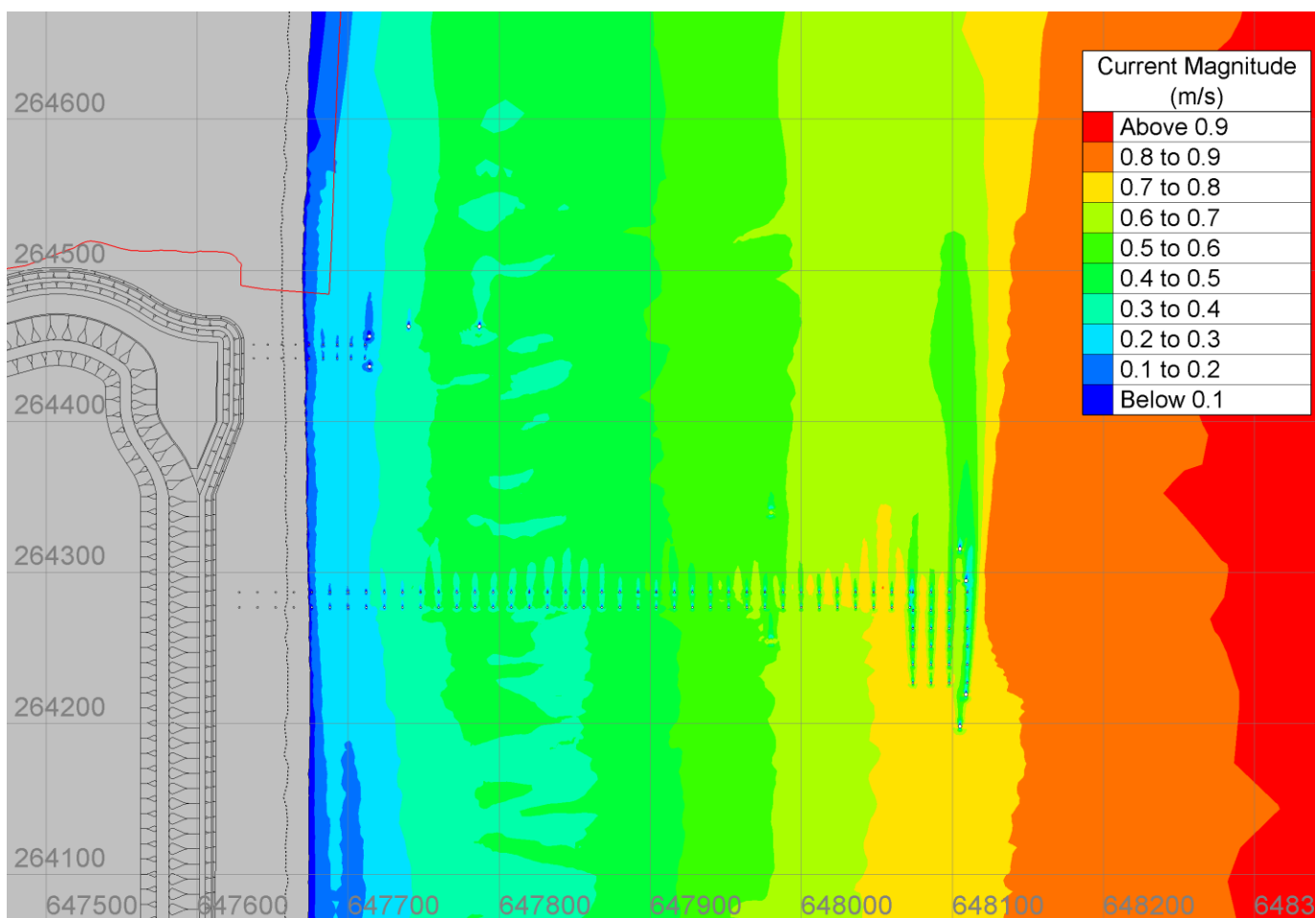
Figure 17: Peak ebb velocities around temporary and permanent BLF.

TR543 MODELLING OF THE TEMPORARY AND PERMANENT BLF AT SZC

NOT PROTECTIVELY MARKED
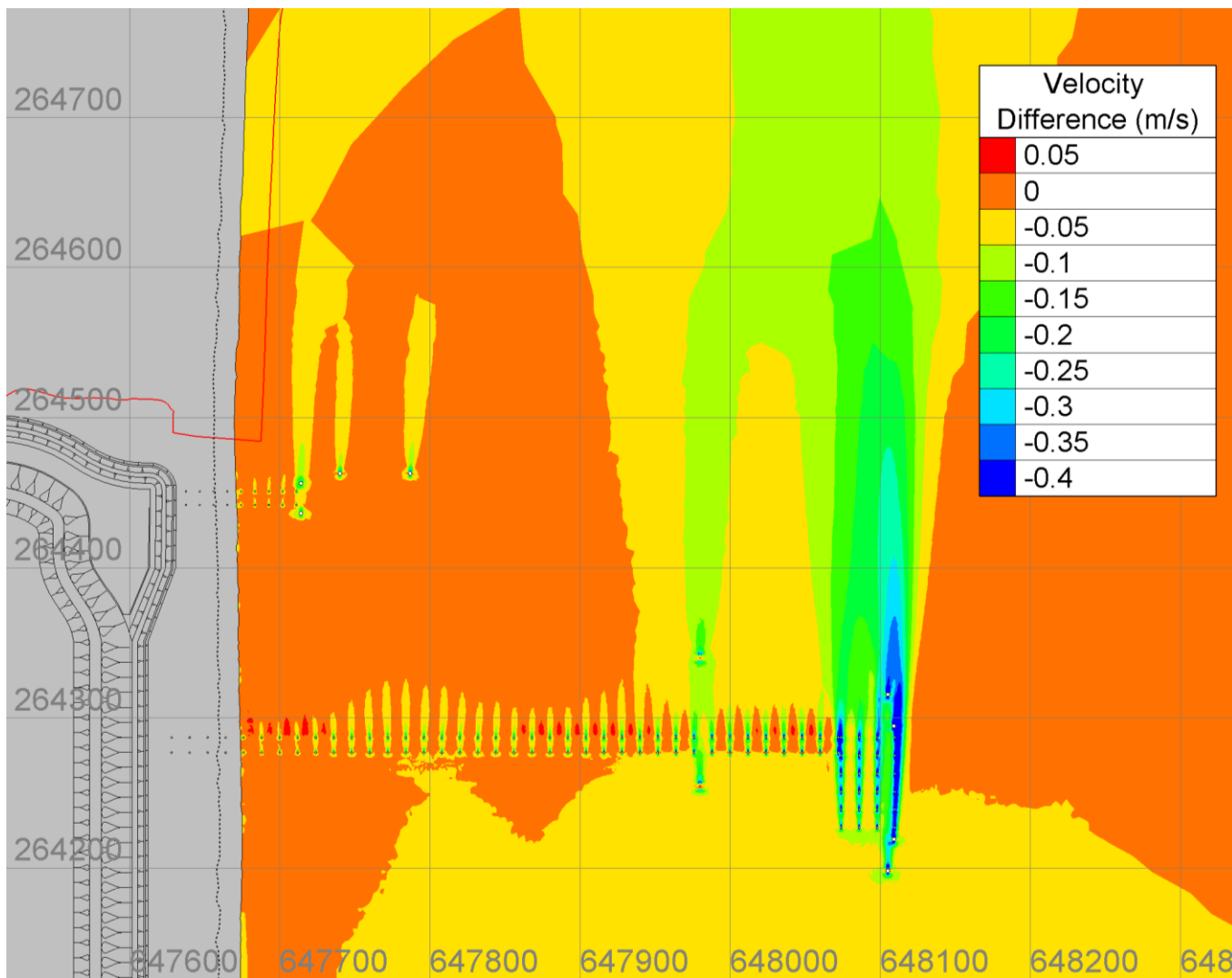
Figure 18: Difference in peak ebb velocity between the structures only and baseline case.

Figure 19 shows the current-only (τ_c) bed shear stress for the temporary and permanent BLF structures only during peak ebb. The effect of the jetty piles on the bed shear stress can be seen to be very localised around the jetty piles, due to the reduction caused by the scour pits around each pile. The larger extension for the reduction in τ_c is related to the decrease in the velocity along the last row of piles at the head of the temporary BLF.
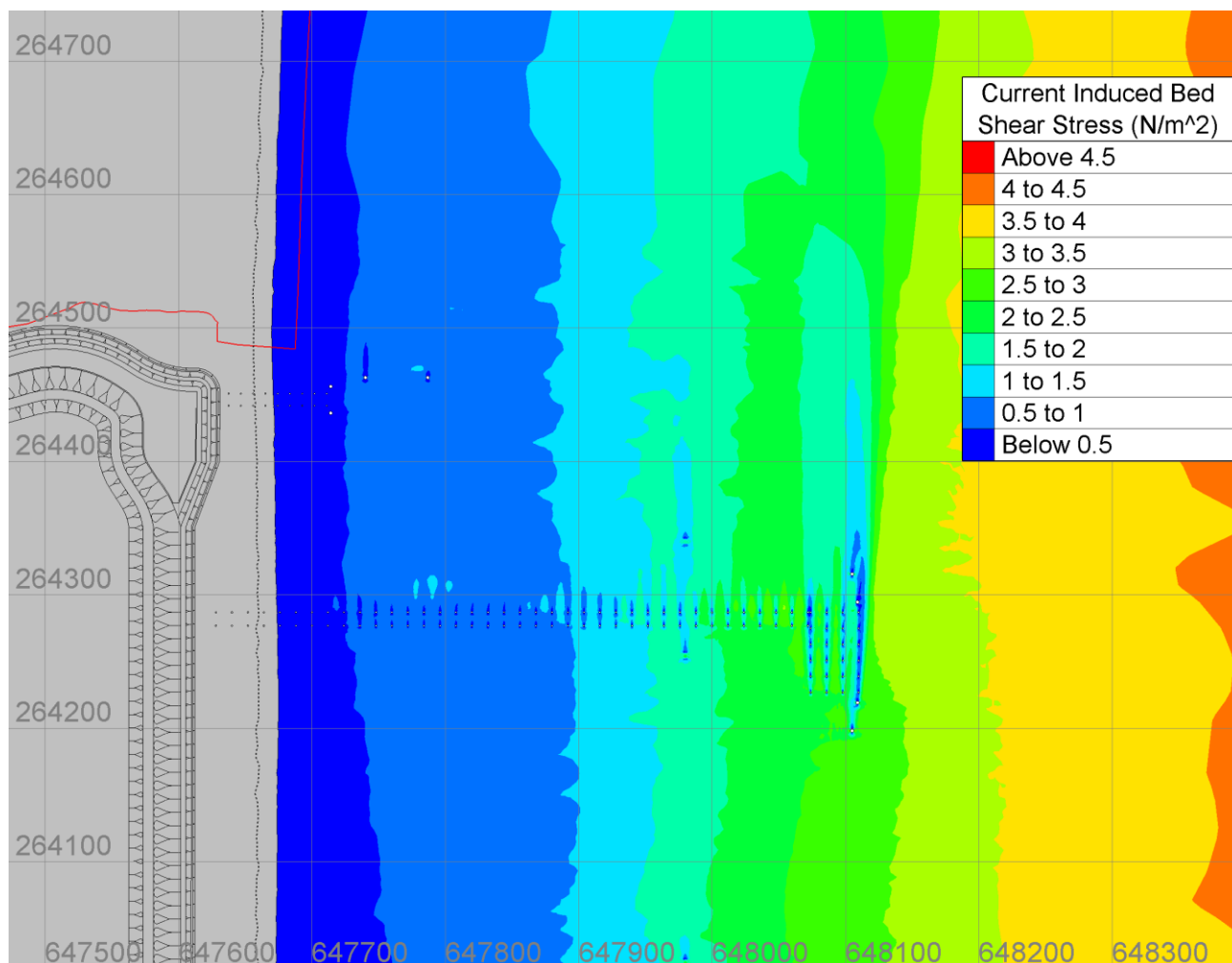
Figure 19: Current-only (τ_c) bed shear stress for the temporary and permanent BLF structures only (peak ebb).

4.2.2 Wave induced bed shear stress

Figure 20 shows wave-only (τ_w) bed shear stress for the temporary and permanent BLF structures only for a 1 in 20 year SE wave during peak ebb.

The respective magnitudes for τ_c and τ_w clearly show that the area is wave dominated with the wave-only bed shear stresses being approximately 30 times larger than the currents-only bed shear stresses. The effect of the jetty piles on the wave induced bed shear stress is very localised around the piles, with reductions in τ_w for approximately 3-5 m from the centre of the piles and fenders, respectively. The effect of the temporary jetty head is much less pronounced for the wave induced bed shear stress (Figure 20) compared to the tidal currents (Figure 19).
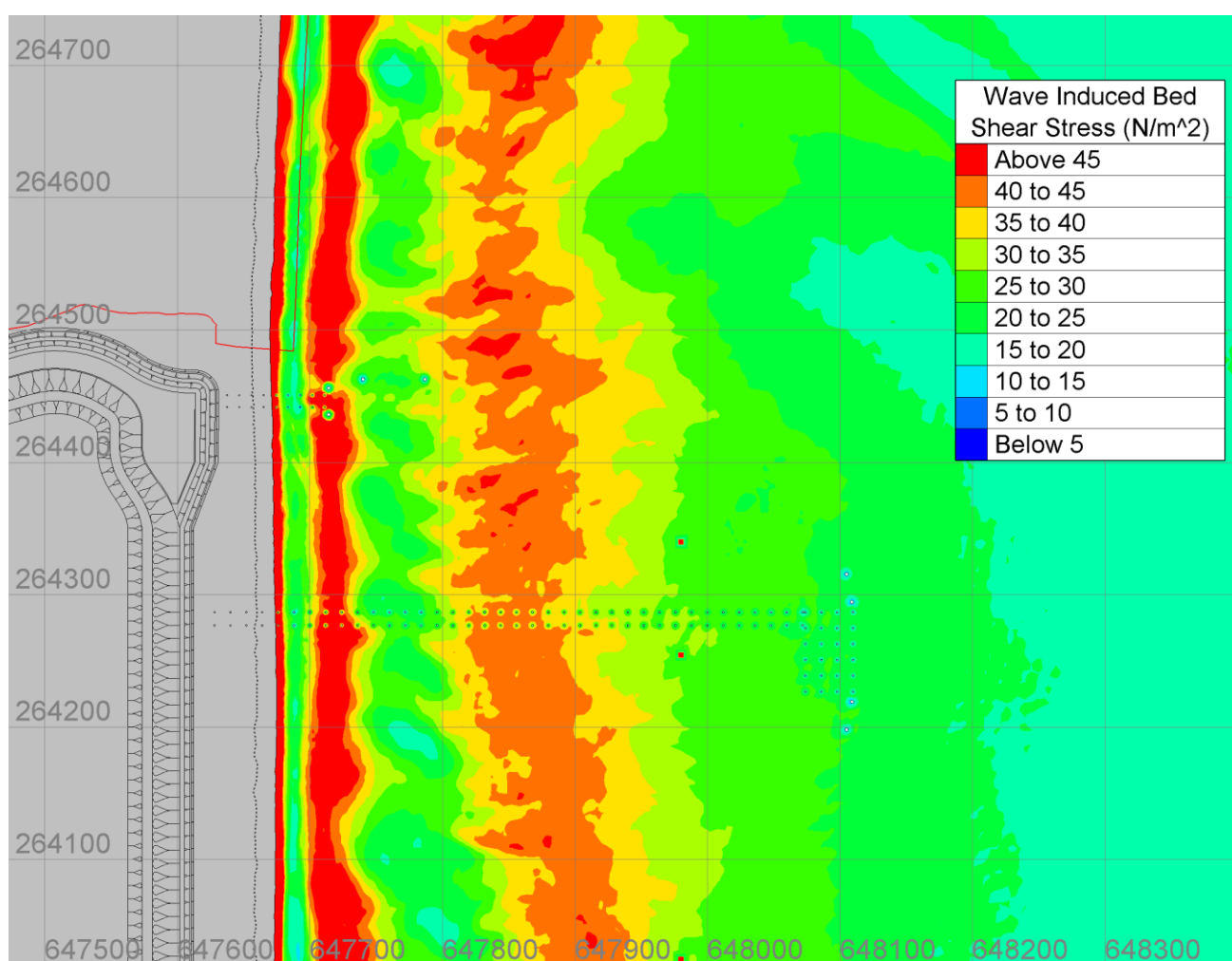
Figure 20: Wave-only (τ_w) bed shear stress for the temporary and permanent BLF structures only (1 in 20 year SE wave, peak ebb).

4.2.3 Combined wave and current bed shear stress

Figure 21 and Figure 22 show the mean (τ_m), and maximum (τ_{max}) combined bed shear stresses, respectively, for the temporary and permanent BLF structures only run. The mean combined bed shear stress depends mostly on the current-only bed shear stress (see Eq. 11), explaining the similar patterns in Figure 19 and

Figure 21. As such, the decrease in the velocities in the lee of the piles (Figure 18) in those locations can also be seen as a reduction in τ_c and τ_m. The maximum combined bed shear stress depends mostly on the waves-only bed shear stress (see Eq. 12), meaning the patterns in Figure 20 and Figure 22 are very similar. The effect of the inner and outer longshore bars is evident, leading to an increase in the wave-only and maximum bed shear stress along the bars.
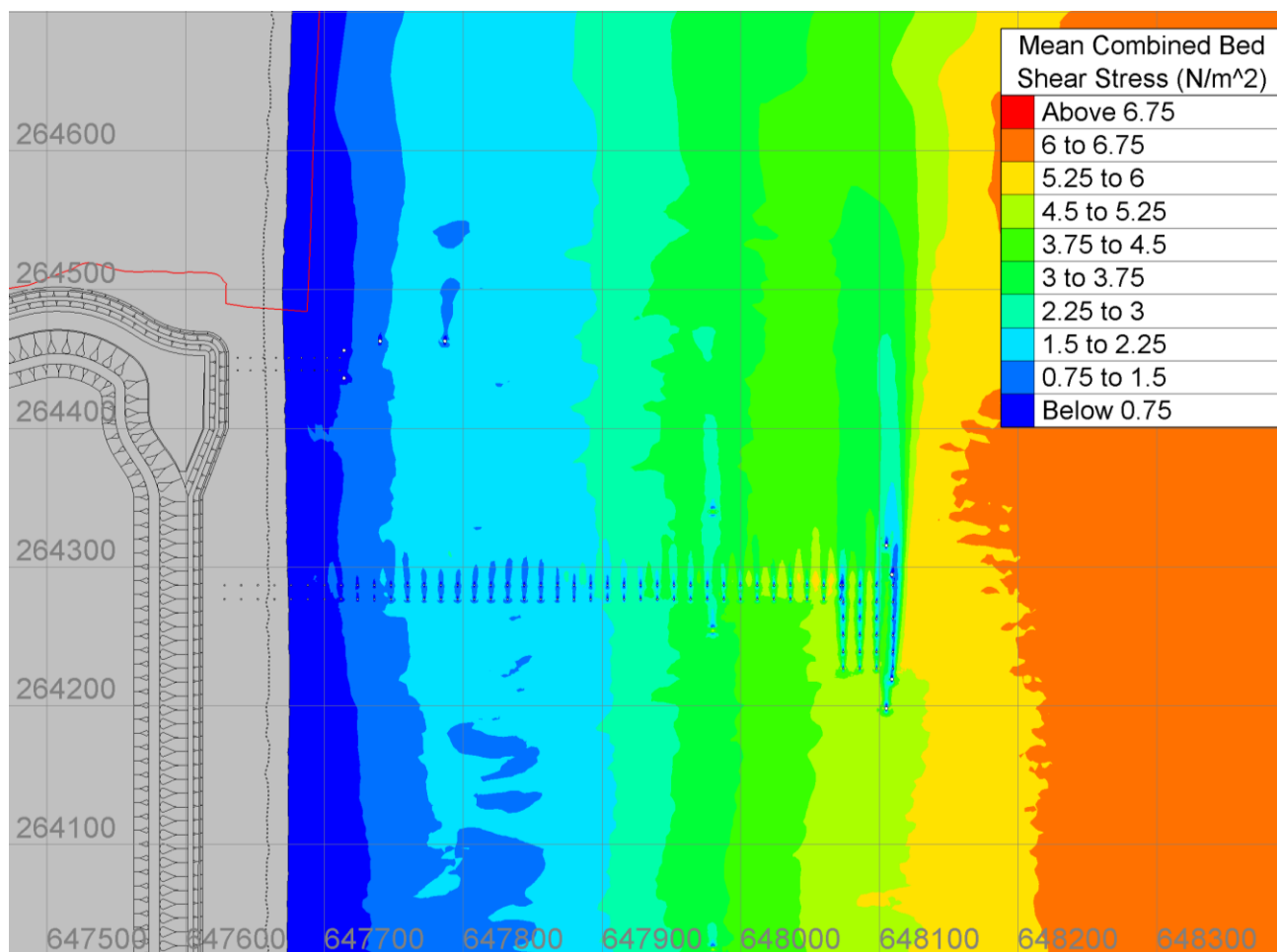
Figure 21: Mean combined bed shear stress (τ_m) for the temporary and permanent BLF structures only (1 in 20 year SE wave, peak ebb).
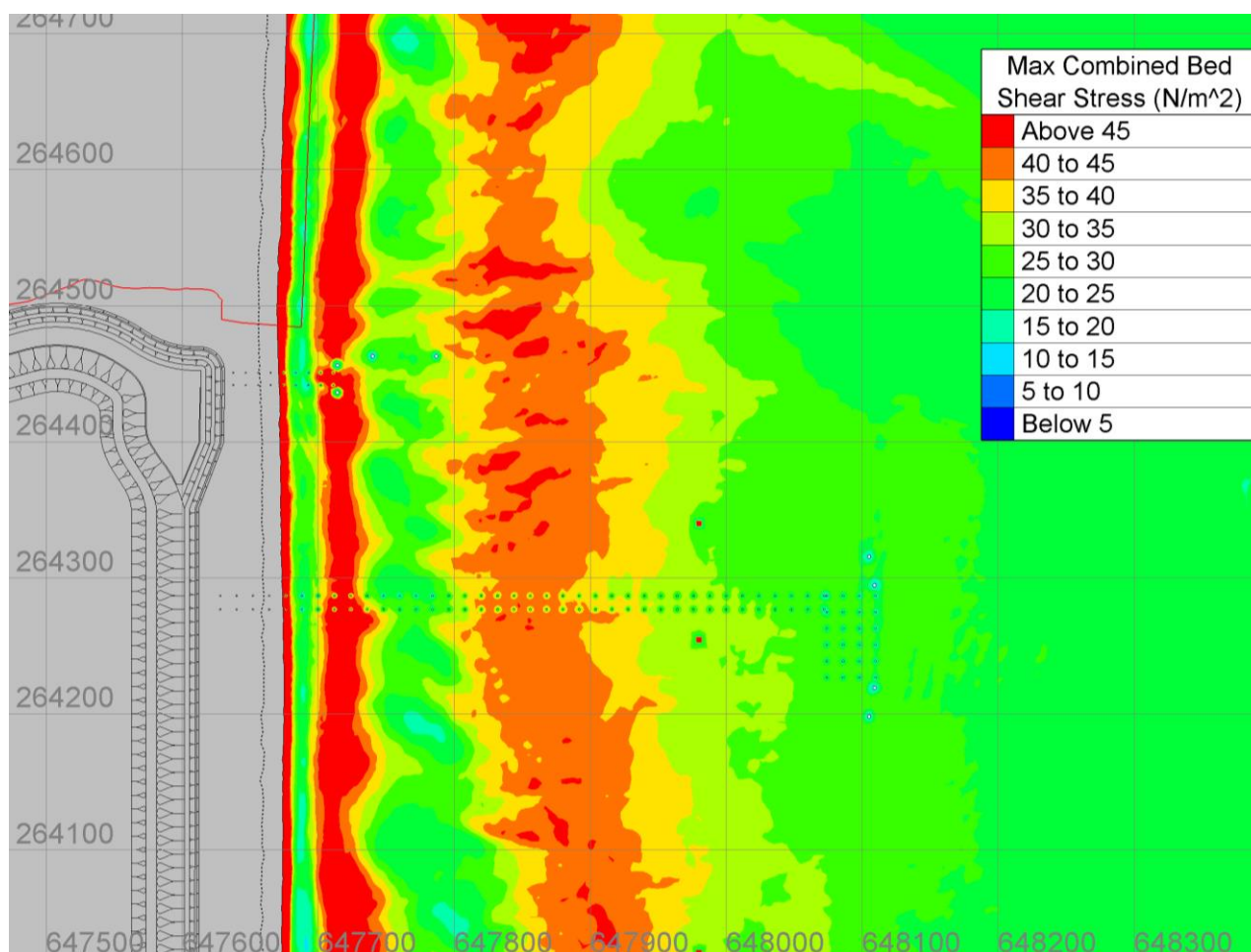
Figure 22: Maximum combined bed shear stress (τ_{max}) for the temporary and permanent BLF structures only (1 in 20 year SE wave, peak ebb).

The effect of the BLF structures on the combined bed shear stress as represented by a percentage change is shown in Figure 23. The BLFs effect on bed shear stress is very small in almost all locations, with the highest changes occurring where the permanent jetty piles/fenders are closer to each other (maximum increase +20%, maximum decrease -10%). However, immediately around the piles/fenders/dolphins a larger reduction in the bed shear stress (up to 60% over a 3 m distance) was observed which arises because of the implementation of scour pits in the modelled bathymetry. The area of bed shear stress change that is greater than five percent (± 5%) extends approximately 565 m along the Sizewell frontage, including a small increase in bed shear stress above 5% extending 20 m into the Minsmere SPA/SAC.

In the following plots, an increase or reduction in bed shear stress does not equal erosion or deposition. Whilst the 5% change metric is a commonly used convention and can be useful as an indicative measure, percentage change on its own can be misleading. What is more relevant from a coastal geomorphology perspective are the absolute bed shear stresses, the absolute differences and their relation to the critical bed shear stress. Figure 24 is a more meaningful plot and shows the effect of the BLF structures on the combined bed shear stress as represented by a difference in magnitude.

TR543 MODELLING OF THE TEMPORARY AND PERMANENT BLF AT SZC

NOT PROTECTIVELY MARKED
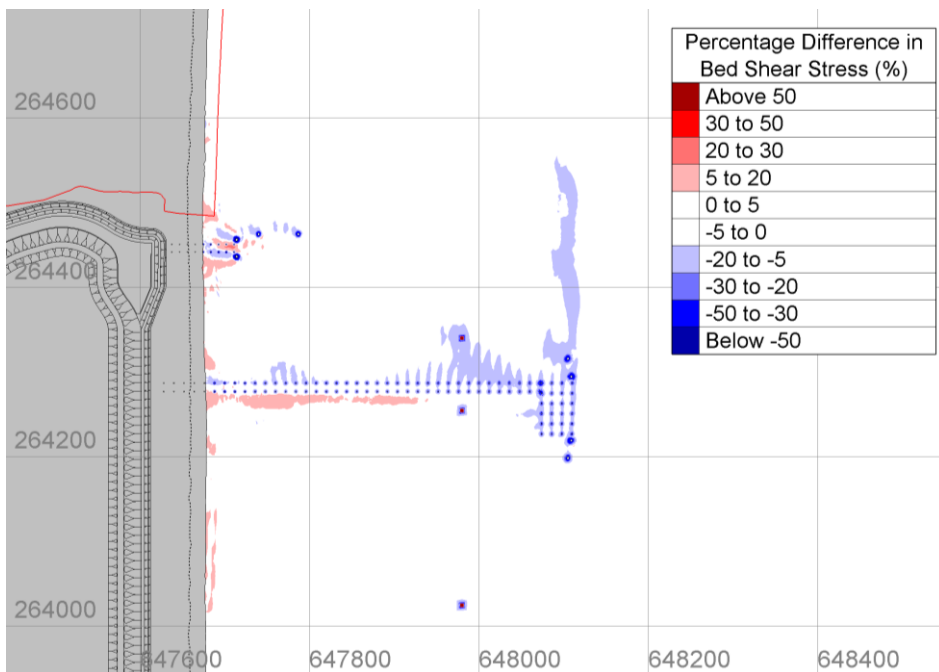
Figure 23: Percentage change in maximum bed shear stress for the temporary and permanent BLF structures only (1 in 20 year SE wave, peak ebb).
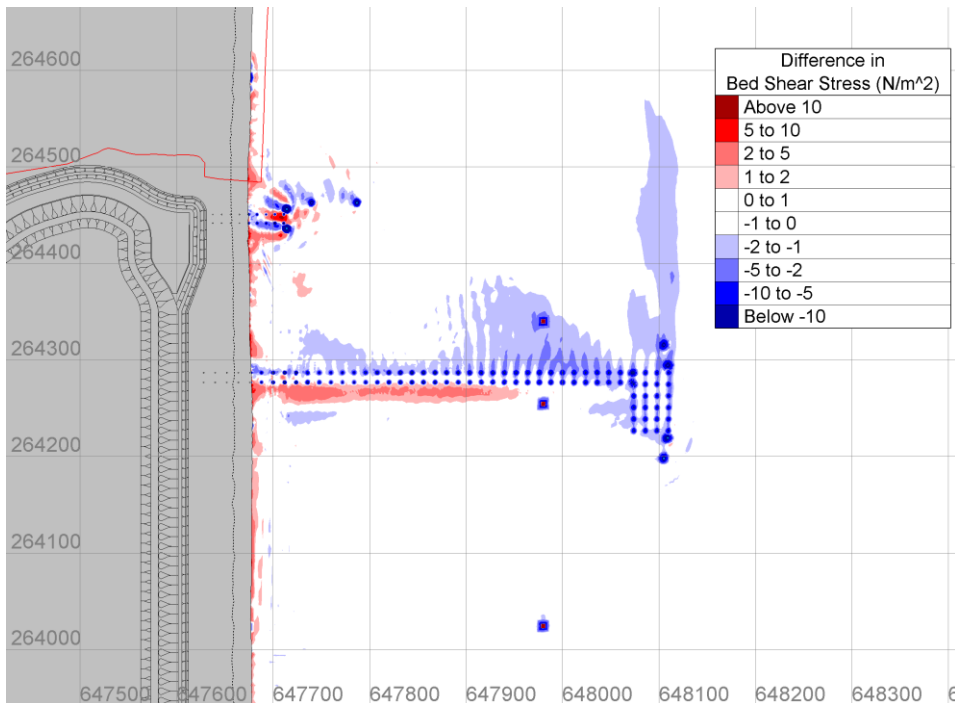
Figure 24: Magnitude of change in maximum bed shear stress for the temporary and permanent BLF structures only (1 in 20 year SE wave, peak ebb).

It is important to note (when examining any of the figures in this report) that an increase in bed shear stress does not mean an increase in erosion, nor does a decrease lead to an increase in deposition of sediment. The critical threshold of motion reference point, calculated from the Sizewell subtidal sand samples, is 0.216 N/m^2 – bed shear stress above 0.216 N/m^2 implies sandy sediment is in motion. Results show that the baseline bed shear stresses over the entire model domain are above the critical threshold of motion.

The change bed shear stress across the designated frontage is very small (2-5 N/m^2) and unlikely to result in a detectable topographic change. This is because the background stress on which the 2-5 N/m^2 is superimposed is 40-60 N/m^2, some 185 to 277 times larger than the critical threshold. As the sediment is already substantially in motion, such small changes will not register detectable change at the bed.

An interesting feature observed in the model is the alternate increase/decrease in bed shear stress along the shore, as the waves and flow interact with the permanent BLF structure. The BLF piles are transmissive and would not block sediment transport. The peak increase in bed shear stress within the permanent BLF is 11 N/m^2 compared to a baseline of 50 N/m^2 in that location. However, that very localised increase is still within the wider baseline variation along the Sizewell C frontage of 30-65 N/m^2 (for a 1 in 20 yr wave height). The patchwork of alternating bed shear stress due to the piles would change continuously with the state of the tide and direction of waves. These conditions are variable with the state of tide and waves, meaning the peak impact is not persistent over a tidal cycle. There are no areas of change within the model where a reduction in bed stress reduces below the critical threshold or an increase above the threshold where it was not previously. Patches of altered bed shear stress are sufficiently small in magnitude and scale, and would migrate continuously, so that they are not expected to cause detectable change to the shoreline.

The presence of the CDO and FRR structures also show no detectable change beyond their immediate scour pits and show no interaction with the temporary or permanent BLF (FRR2 is sufficiently far from the temporary BLF piles that group scour is not considered). The temporary BLF causes a 2-3 N/m^2 reduction in the leeward side of the structure from the prevailing wave direction with an 2-3 N/m^2 increase in bed shear stress on the windward side of the structure. The baseline bed shear stress in this area is 30-40 N/m^2. These conditions are variable with the state of tide and waves, meaning the peak impact is not persistent over a tidal cycle and is not expected to cause detectable change to the shoreline.

4.3   Temporary and Permanent BLFs plus grillage

To investigate the effect of the grillage (only in pace for the construction phase and removed thereafter) in combination with the permanent and temporary BLFs into the domain, the peak ebb velocities, wave energy and bed shear stress results were compared to the baseline conditions with a 1 in 20 year return interval wave. This scenario will occur when only the temporary BLF is in use during the winter, but the permanent BLF is still required. As the grillage will only be installed once the permanent BLF has been installed, there is no scenario where the grillage will be present in isolation so that scenario has not been modelled.

4.3.1   Tidal current induced bed shear stress

To highlight the influence of the jetty piles, Figure 25 shows the flow velocities around the temporary and permanent BLF with Figure 26 showing the difference in velocities compared to the baseline.

Figure 25 and Figure 26 show that the last pair of jetty piles, fenders and the shoreward tip of the grillage slightly disturbs the shore-parallel flow. This is where the shoreward tip of the grillage sits slightly above the bathymetry. The grillage does not act as a blockage as currents still pass over the top. This small decrease in the tidal currents in the lee of the piles and grillage returns to within 0.1 m/s within 45 m. There is also a minor increase of 0.1 m/s in flows created shoreward of the mooring fenders. Over the grillage there is a small

increase of 0.075 m/s, although the grillage itself is a non-erodible structure so a small increase has no effect on the grillage itself.

Figure 27 shows the current-only (τ_c) bed shear stress for the temporary and permanent BLF structures plus grillage during peak ebb. The effect of the grillage on the bed shear stress can be seen to be very localised to the grillage, with a small reduction leeward of the shoreward tip of the grillage.
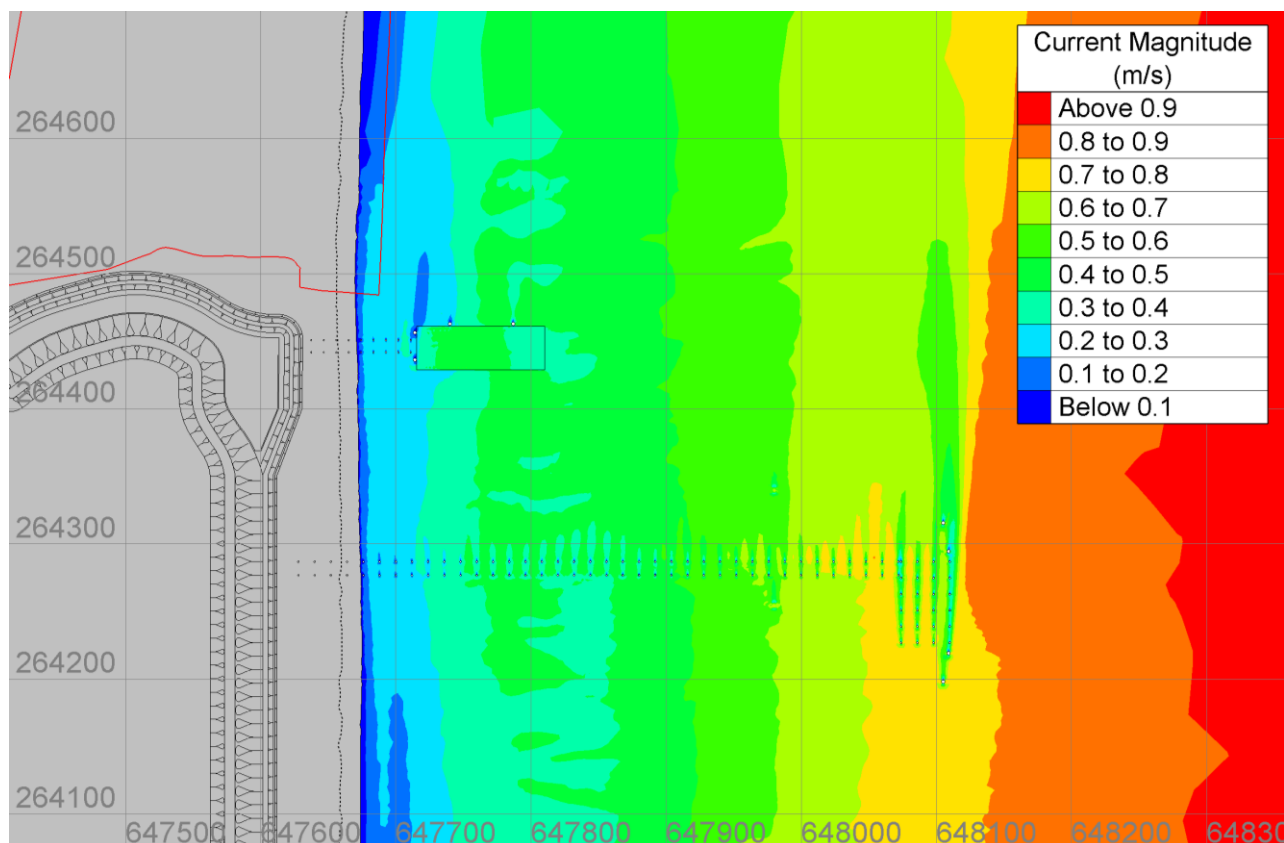
Figure 25: Peak ebb velocities around temporary and permanent BLF plus grillage.

TR543 MODELLING OF THE TEMPORARY AND PERMANENT BLF AT SZC

NOT PROTECTIVELY MARKED
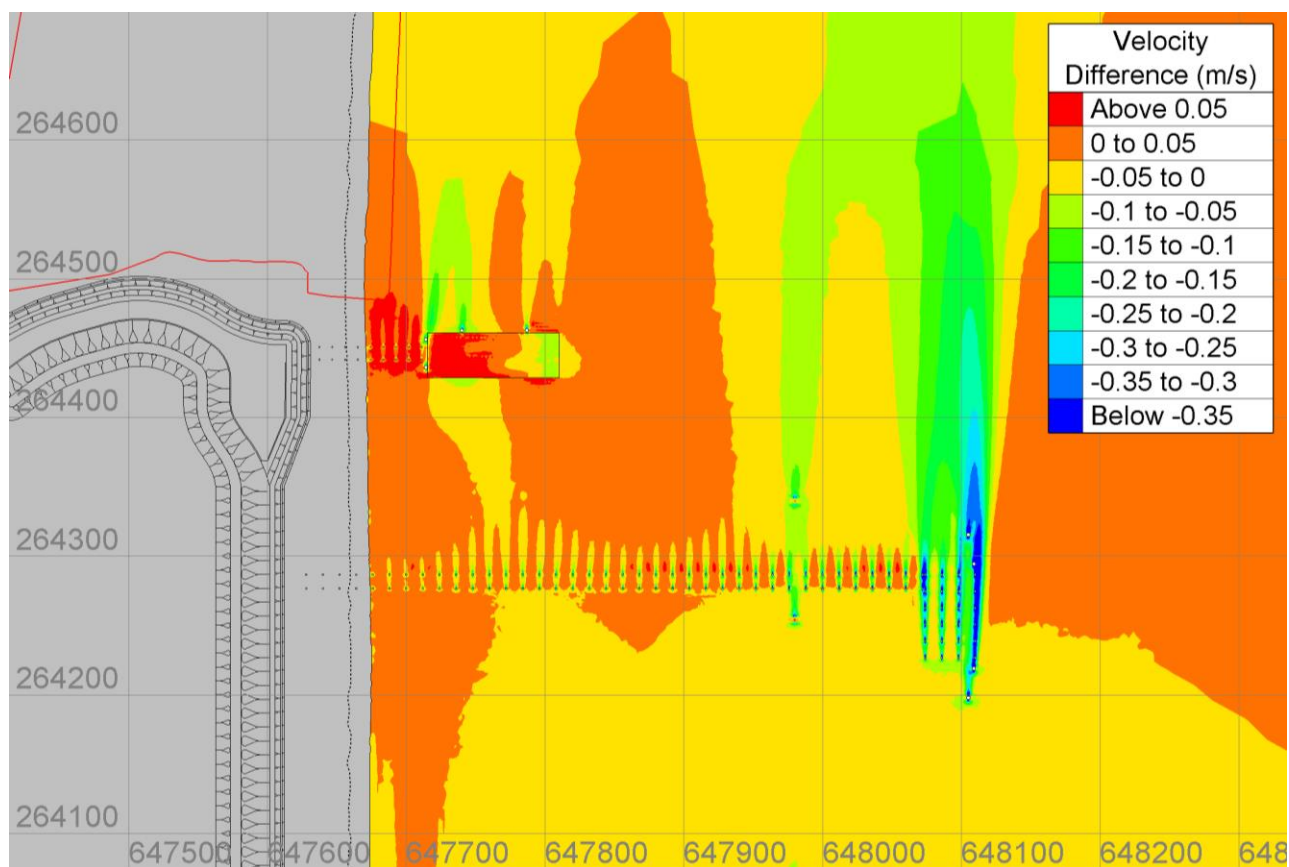
Figure 26: Difference in peak ebb velocity between the structures plus grillage and baseline case.
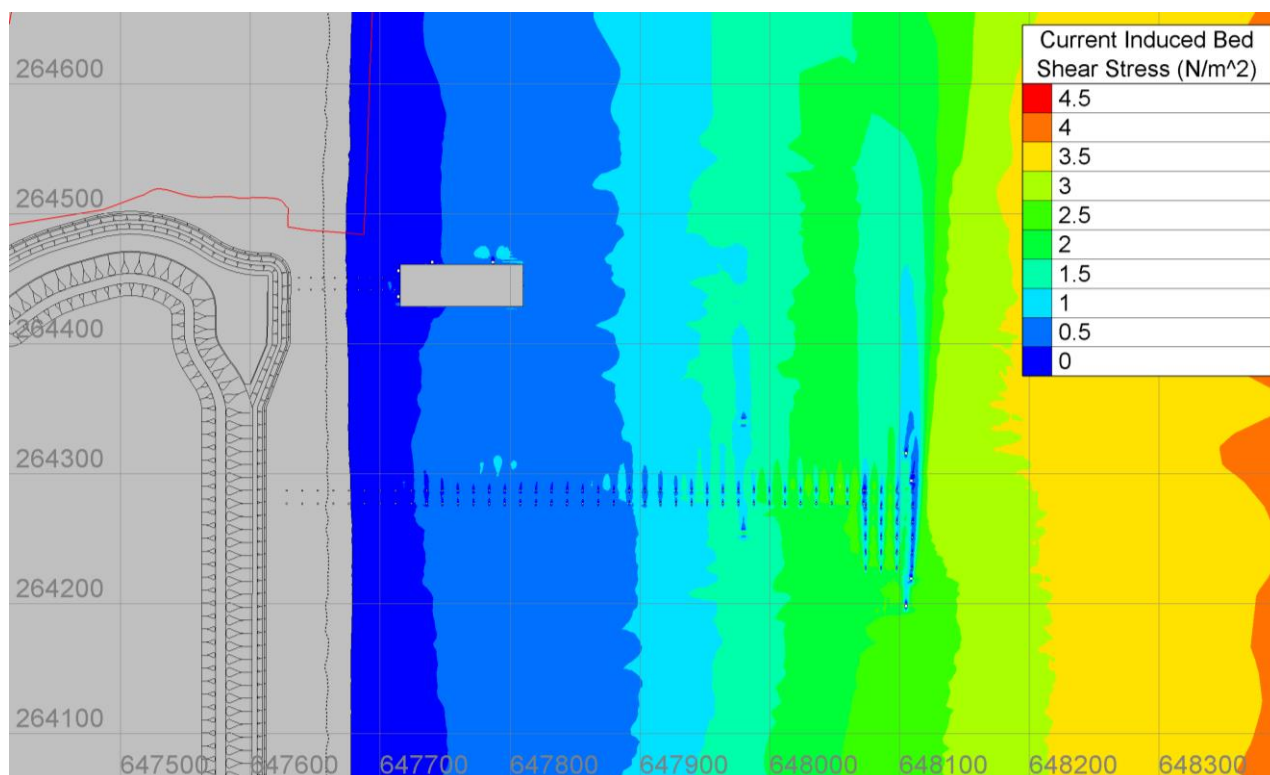
Figure 27: Current-only (τ_c) bed shear stress for the temporary and permanent BLF structures plus grillage (peak ebb).

4.3.2 Wave induced bed shear stress

Figure 28 shows wave-only (τ_w) bed shear stress for the temporary and permanent BLF structures plus grillage for a 1 in 20 year SE wave during peak ebb.

The effect of the grillage on the wave induced bed shear stress is localised to the shoreward edge of the grillage, with reductions in τ_w for approximately 40 m along the inner longshore bar. However, results show that the wave induced bed shear stress is still in excess of 100 times larger than the critical threshold, meaning sediment is still in motion along the bar.
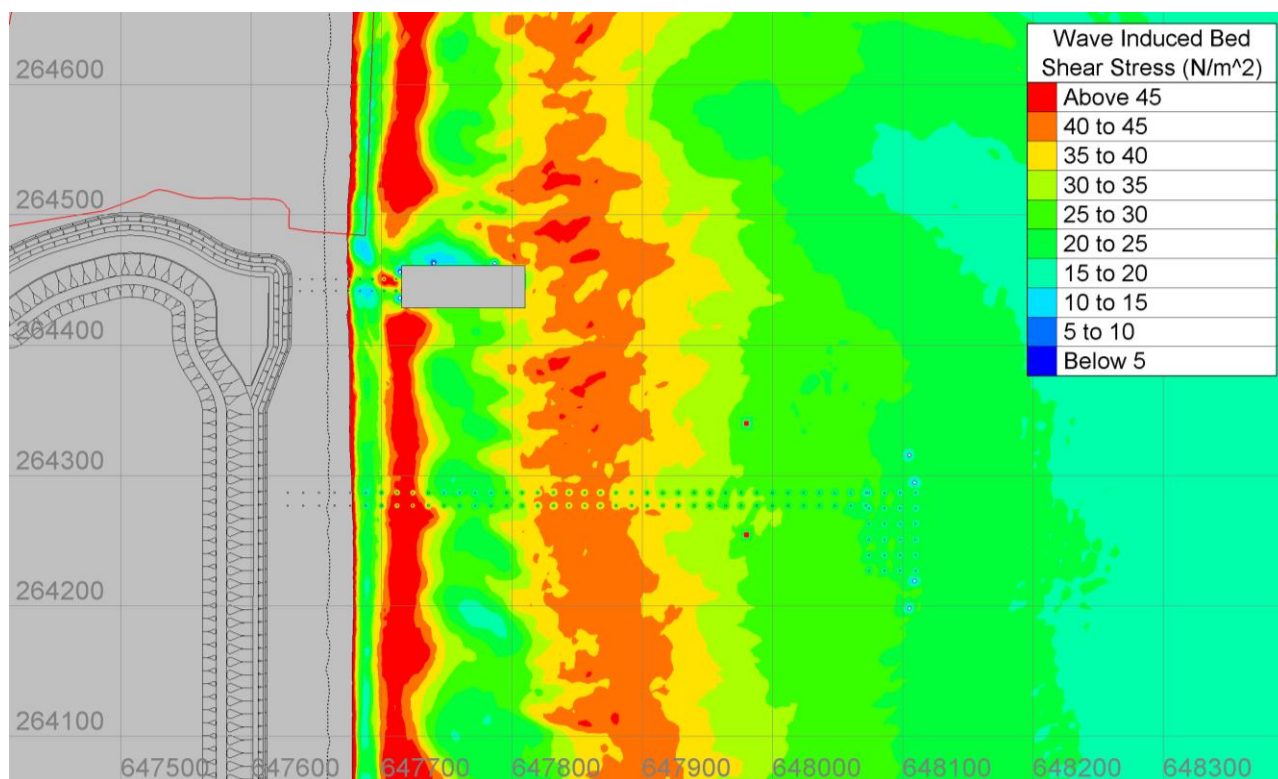
Figure 28: Wave-only (τ_w) bed shear stress for the temporary and permanent BLF structures plus grillage (1 in 20 year SE wave, peak ebb).

4.3.3 Combined wave and current bed shear stress

Figure 29 and Figure 30 show the mean (τ_m), and maximum (τ_{max}) combined bed shear stresses, respectively, for the temporary and permanent BLF structures plus grillage run.

As shown in Section 4.2.3, assessing change against a percentage difference can be misleading without consideration of the wider environmental context including the natural variability. As such, for the subsequent model scenarios, the analysis will focus on the magnitude of change in absolute bed shear stress. Figure 24 shows the effect of the BLF structures plus the grillage on the combined bed shear stress as represented by a difference in magnitude.

TR543 MODELLING OF THE TEMPORARY AND PERMANENT BLF AT SZC

NOT PROTECTIVELY MARKED
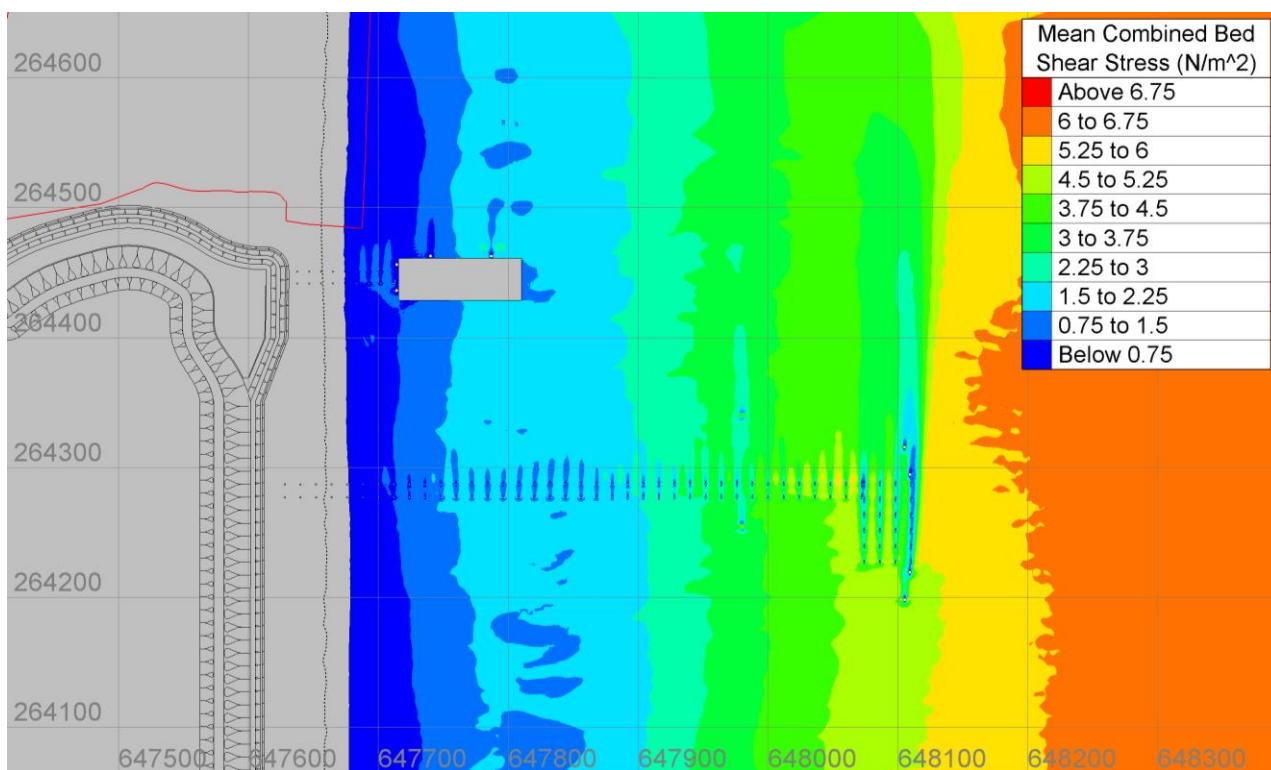
Figure 29: Mean combined bed shear stress (τ_m) for the temporary and permanent BLF structures plus grillage (1 in 20 year SE wave, peak ebb).

TR543 MODELLING OF THE TEMPORARY AND PERMANENT BLF AT SZC

NOT PROTECTIVELY MARKED
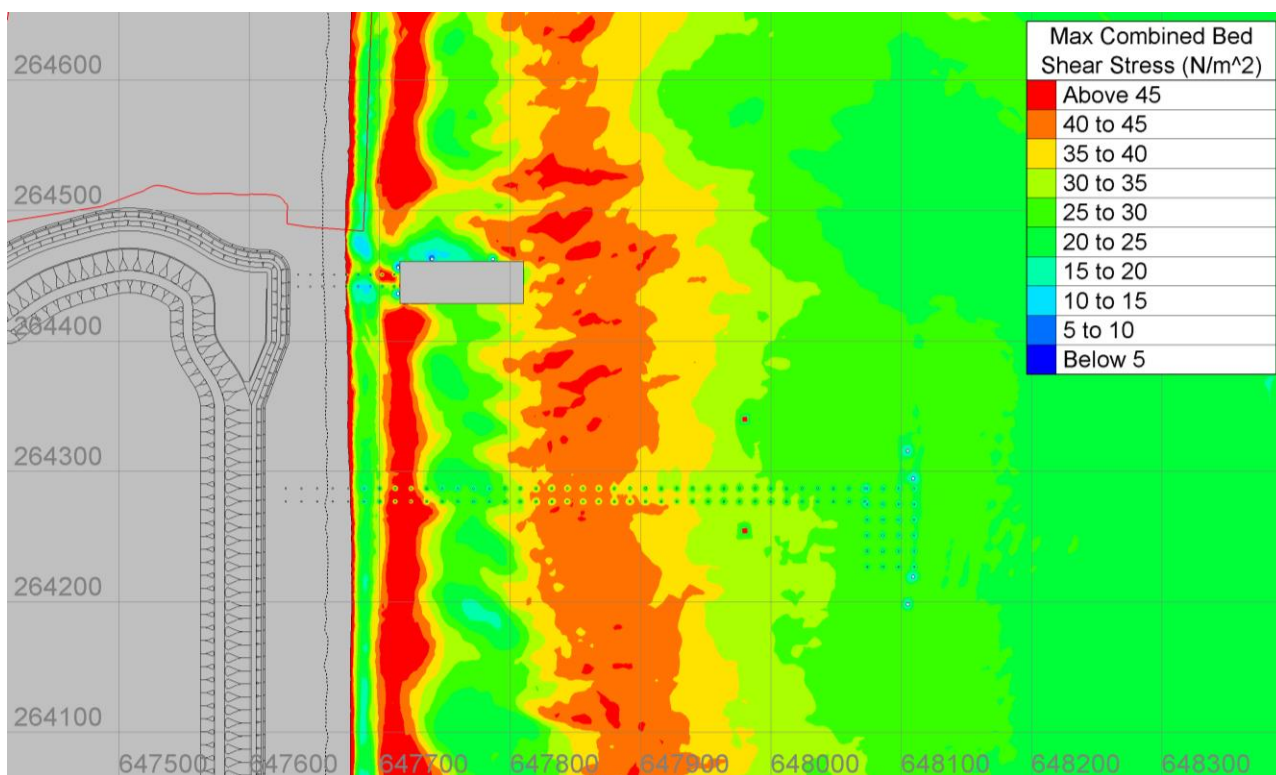
Figure 30: Maximum combined bed shear stress (τ_{max}) for the temporary and permanent BLF structures plus grillage (1 in 20 year SE wave, peak ebb).

TR543 MODELLING OF THE TEMPORARY AND PERMANENT BLF AT SZC

NOT PROTECTIVELY MARKED
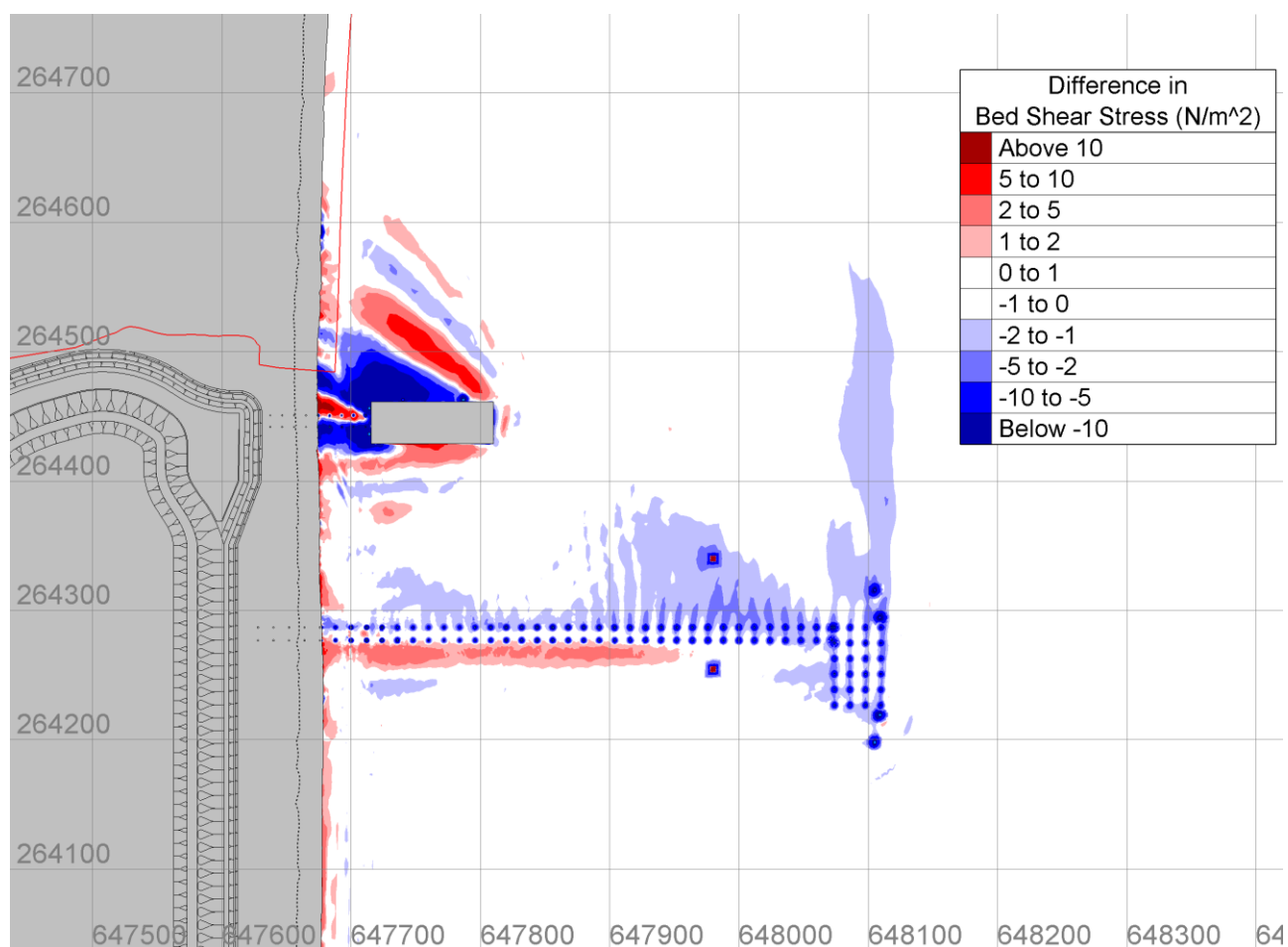
Figure 31: Magnitude of change in maximum bed shear stress for the temporary and permanent BLF structures with the grillage (1 in 20 year SE wave, peak ebb).

Results show that the baseline bed shear stresses over entire model domain are above the critical threshold of motion (0.216 N/m^2).

As expected, the grillage increases the area of change in bed shear stress compared to the BLF piles alone. Landward of the inner longshore bar, there is an area of increased bed shear stress of 3-6 N/m^2 extending 245 m into the Minsmere SPA/SAC. This is similar in magnitude to changes associated with the BLF structures only, albeit over a slightly longer frontage of the Minsmere SPA/SAC. The small increase in bed shear stress is still within natural variation along the Minsmere SPA/SAC frontage and is unlikely to be detectable beyond the environmental limits. The baseline bed shear stress conditions along the Minsmere frontage is 40-60 N/m^2. The baseline condition is 185 to 277 times larger than the critical threshold, meaning the subtidal sediment is already in motion. To the north of the grillage, bed shear stress is reduced by 15-22 N/m^2 but only over a short 45 m section of the inner longshore bar, and only for the SE wave condition. The baseline condition in this area is 40-50 N/m^2.

The BLF piles are transmissive so they would not block sediment transport. Whilst the shoreward end of the grillage sits above the bed, deflecting currents shoreward, the grillage does not act as a blockage as currents still pass over the top. Furthermore, the grillage sits on the outer flank of the inner longshore bar deeper than the intertidal zone, meaning longshore sediment transport still occurs shoreward of the grillage. The shoreward

deflection of tidal currents due to the grillage leads to an increase in bed shear stress amongst the final pairs of jetty piles of the permanent BLF. The peak increase in bed shear stress within this area the permanent BLF is 8-15 N/m^2 compared to a baseline of 30-45 N/m^2 in that particular location. However, that very localised increase is still within the wider baseline variation along the Sizewell C frontage of 30-65 N/m^2 (for a 1 in 20 yr wave height).

The patchwork of increased and decreased bed shear stress due to the piles and grillage is dependent on, and fluctuates with, the state of the tide and direction of waves. Continuous variation in the state of tide and waves means that the peak impact shown is not persistent and varies (lessens) over the tidal cycle. There are no areas of change within the model where a reduction in bed stress reduces below the critical threshold or an increase above the threshold where it was not previously. Patches of altered bed shear stress are sufficiently small in magnitude and scale that they are not expected to cause detectable change to the shoreline.

4.4 Temporary and Permanent BLFs plus ship

To investigate the effect of the presence of a 120 m ship at the temporary BLF in combination with the permanent and temporary BLF jetties into the domain, the peak ebb velocities, wave energy and bed shear stress results were compared to the baseline conditions with a 1.5 m wave (working limit of the ship). This scenario will occur when the temporary BLF is in use but the requirement for the permanent BLF during construction has finished.

4.4.1 Tidal current induced bed shear stress

To highlight the influence of the ship's presence at the temporary BLF on tidal currents, Figure 32 and Figure 33 show the flow velocities and the difference in velocities compared to the baseline. They show that the last row of temporary BLF piles, fenders and the ship slightly interrupt the shore parallel flow. Flow returns to within 0.1 m/s within 300m downstream of the ship. Due to the hydrodynamic profile of the ship, the lateral disturbance of velocities is much smaller. There is an increase of up to 0.2 m/s along the length of seaward side of the ship.
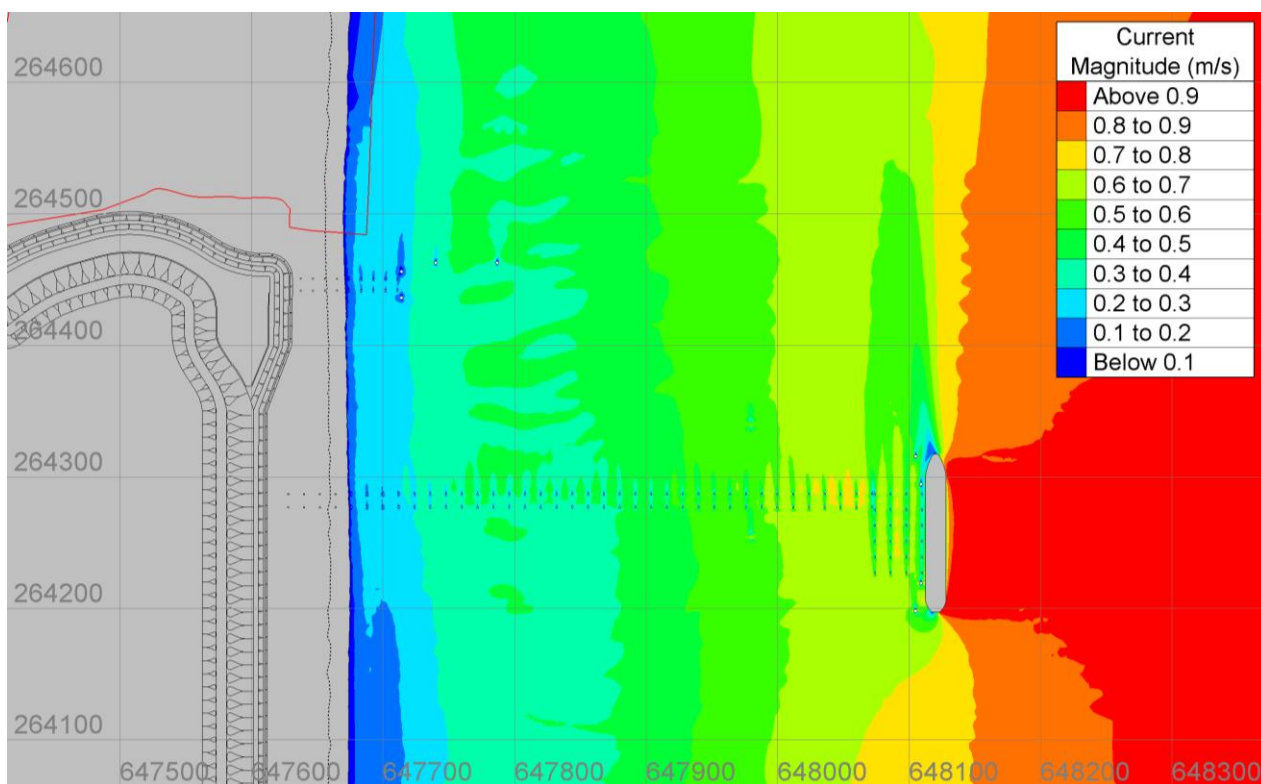
Figure 32: Peak ebb velocities around temporary and permanent BLF plus ship.

TR543 MODELLING OF THE TEMPORARY AND PERMANENT BLF AT SZC

NOT PROTECTIVELY MARKED
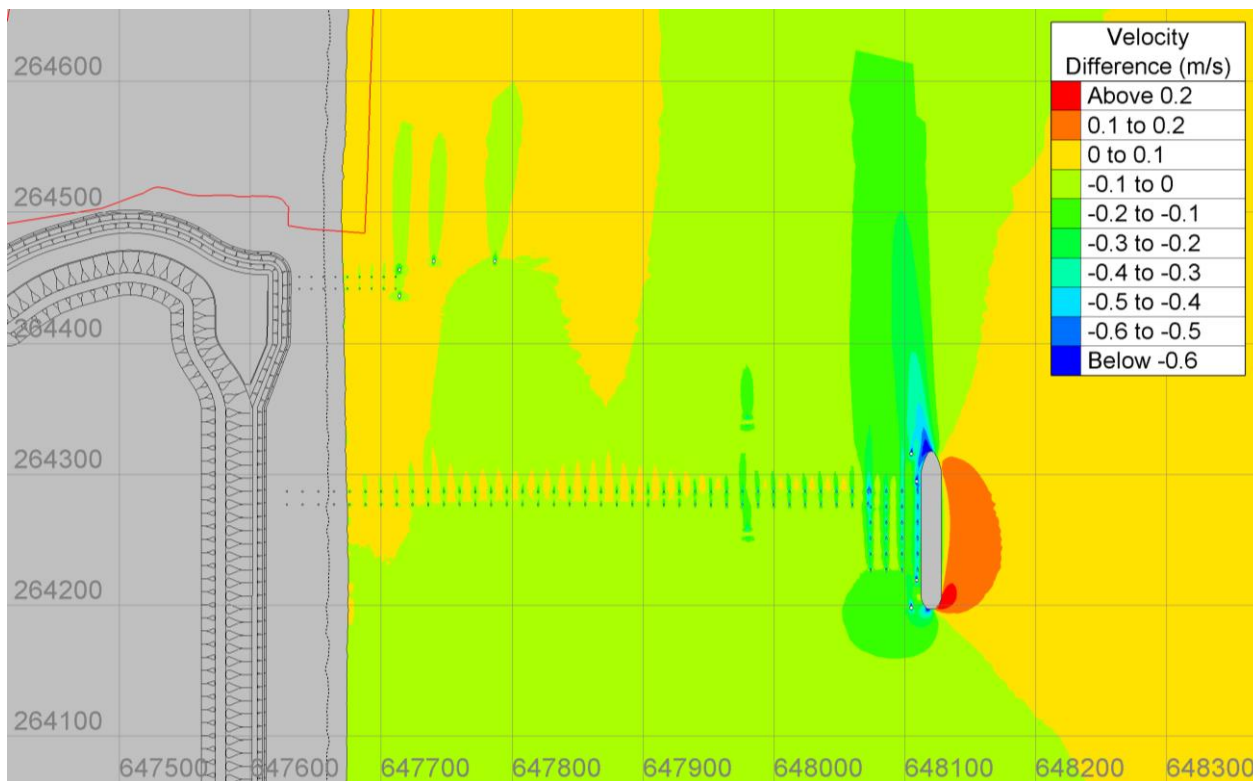
Figure 33: Difference in peak ebb velocity between the structures plus ship and baseline case.

TR543 MODELLING OF THE TEMPORARY AND PERMANENT BLF AT SZC

NOT PROTECTIVELY MARKED

Figure 34 shows the current-only (τ_c) bed shear stress for the temporary and permanent BLF structures with the ship present at the temporary BLF. Due to the shore parallel currents, the presence of the ship at the temporary BLF has no interaction with the permanent BLF, with regard to current induced bed shear stress. Whilst there is a small patch of very low bed shear stress at the leeward end of the ship which would imply a deposition, this will not be the case. The ship does not occupy the full water column, unlike how it is included in the model, meaning currents can still flow underneath the ship. Furthermore, as the tidal currents change direction, any sediment accumulation would be swept away on the reversing tide.
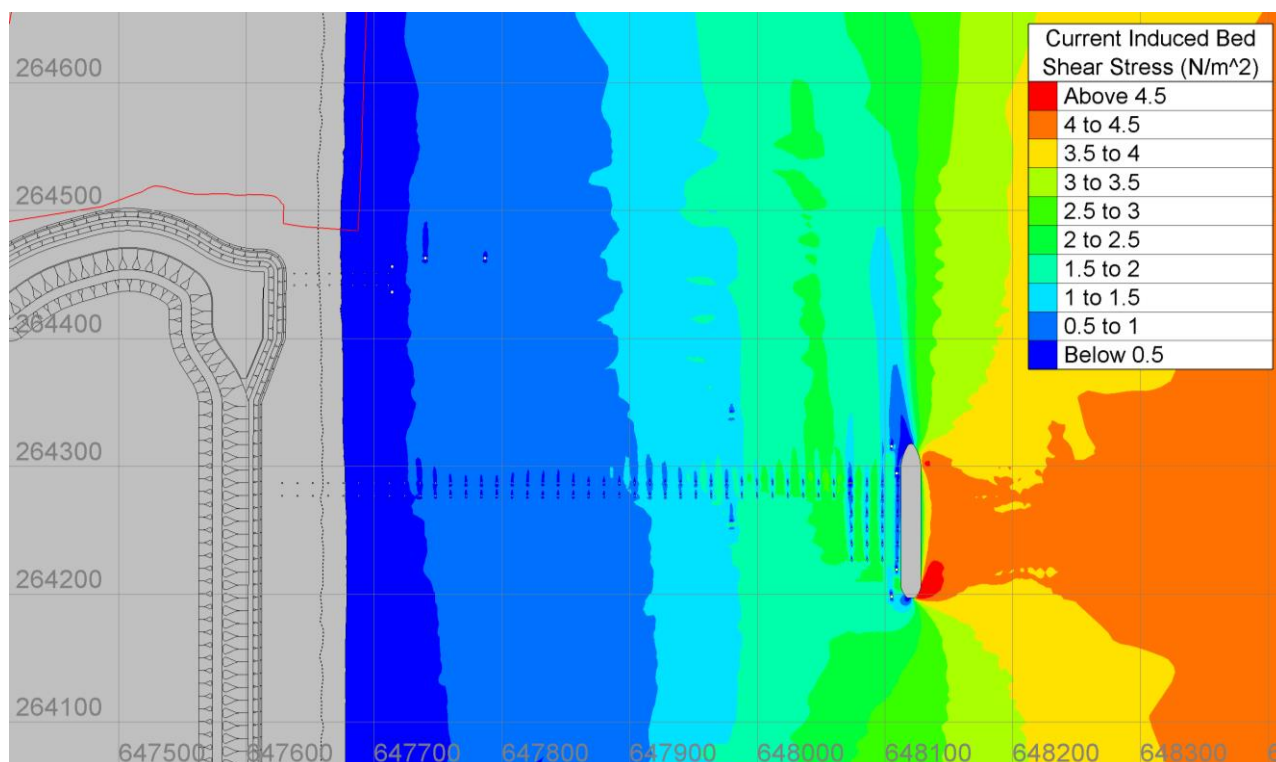
Figure 34: Current-only (τ_c) bed shear stress for the temporary and permanent BLF structures plus ship (peak ebb).

4.4.2   Wave induced bed shear stress

Figure 35 shows wave-only (τ_w) bed shear stress for the temporary and permanent BLF structures plus ship for a 1.5 m SE wave during peak ebb. The presence of the ship at the temporary BLF results in a bed shear stress reduction in the lee of the prevailing wave direction, extending from the ship across the inner and outer longshore bars. However, results show that the wave induced bed shear stress is still in excess of 10 times larger than the critical threshold at the temporary BLF head and 100 to 140 times larger along the inner longshore bar, meaning sediment is still in motion along these areas. The influence on sediment transport and shoreline change due to the reduction in the lee of the ship is discussed in more detail in Section 5.
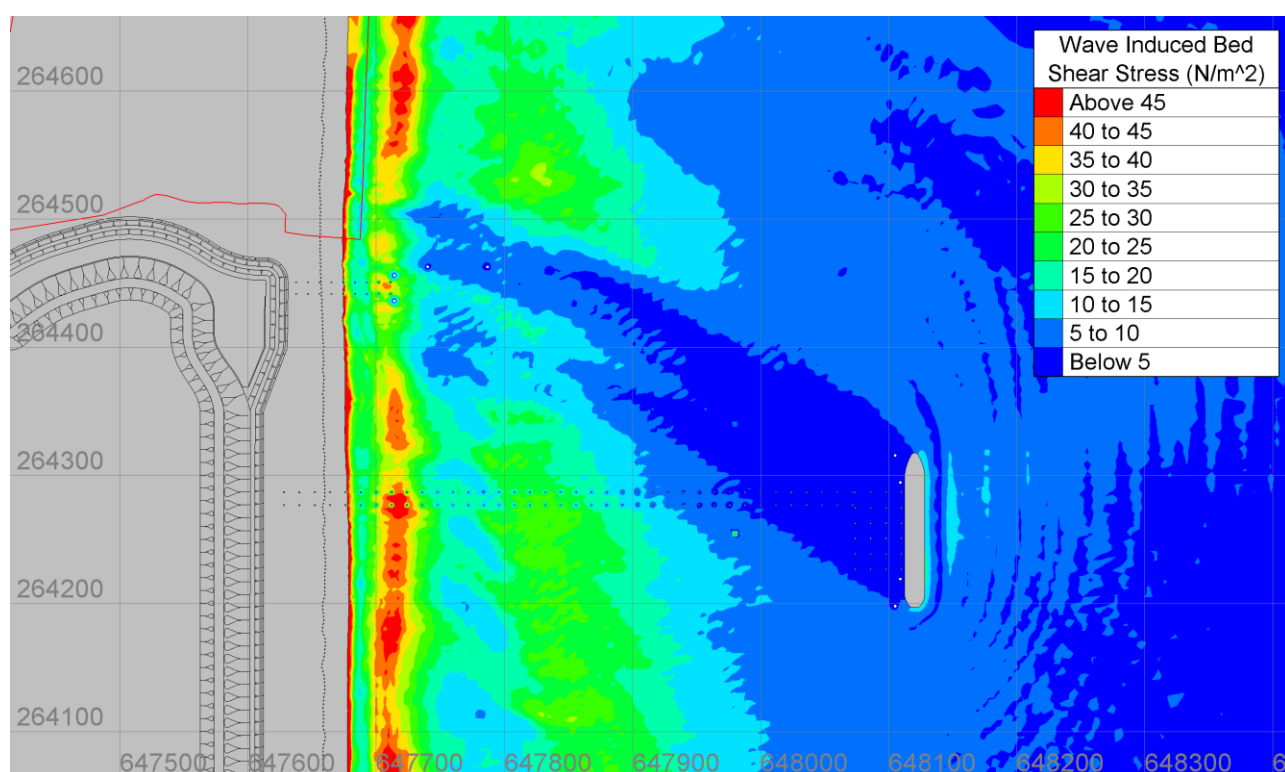
Figure 35: Wave-only (τ_w) bed shear stress for the temporary and permanent BLF structures plus ship (1.5 m SE wave, peak ebb).

4.4.3 Combined wave and current bed shear stress

Figure 36 and Figure 37 show the mean (τ_m), and maximum (τ_{max}) combined bed shear stresses, respectively, for the temporary and permanent BLF structures plus ship run. Figure 38 shows the effect of the BLF structures plus the ship on the combined bed shear stress as represented by a difference in magnitude. Results show that the baseline bed shear stresses over entire model domain are above the critical threshold of motion (0.216 N/m^2).
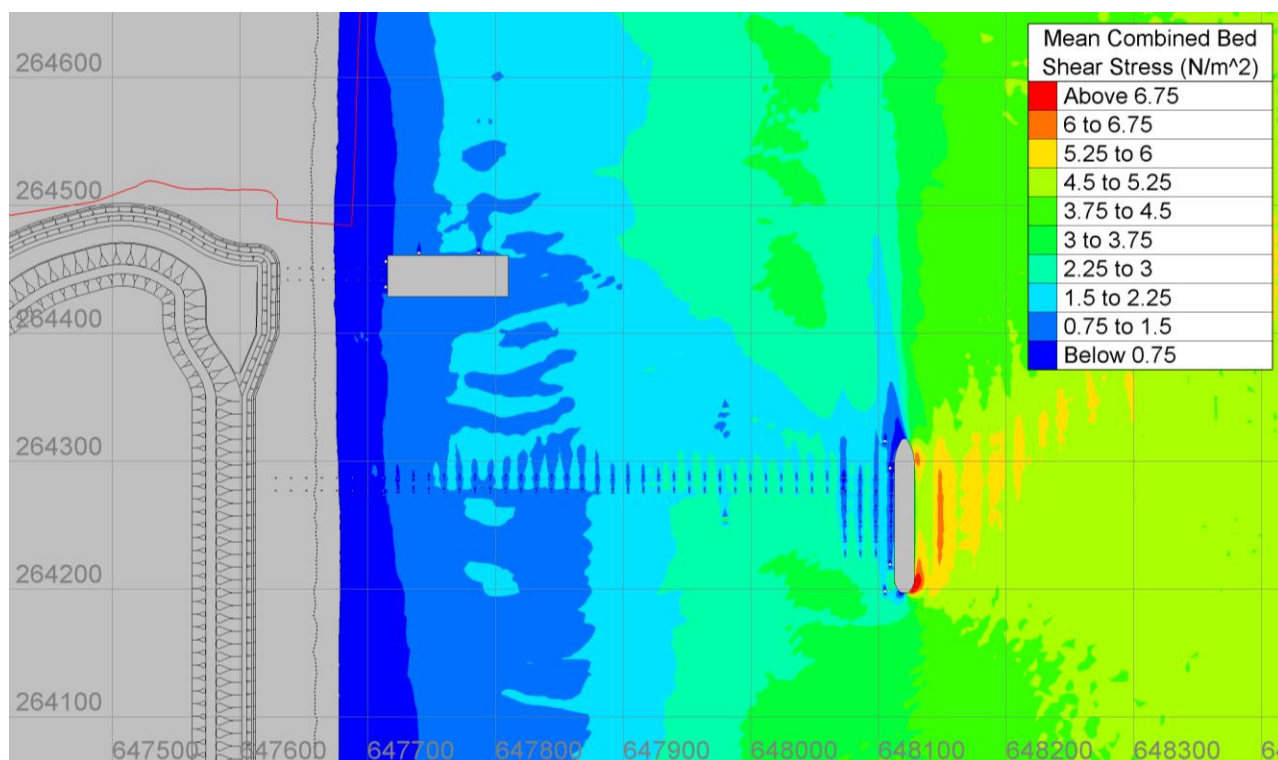
Figure 36: Mean combined bed shear stress (τ_m) for the temporary and permanent BLF structures plus ship (1.5 m SE wave, peak ebb).

TR543 MODELLING OF THE TEMPORARY AND PERMANENT BLF AT SZC

NOT PROTECTIVELY MARKED
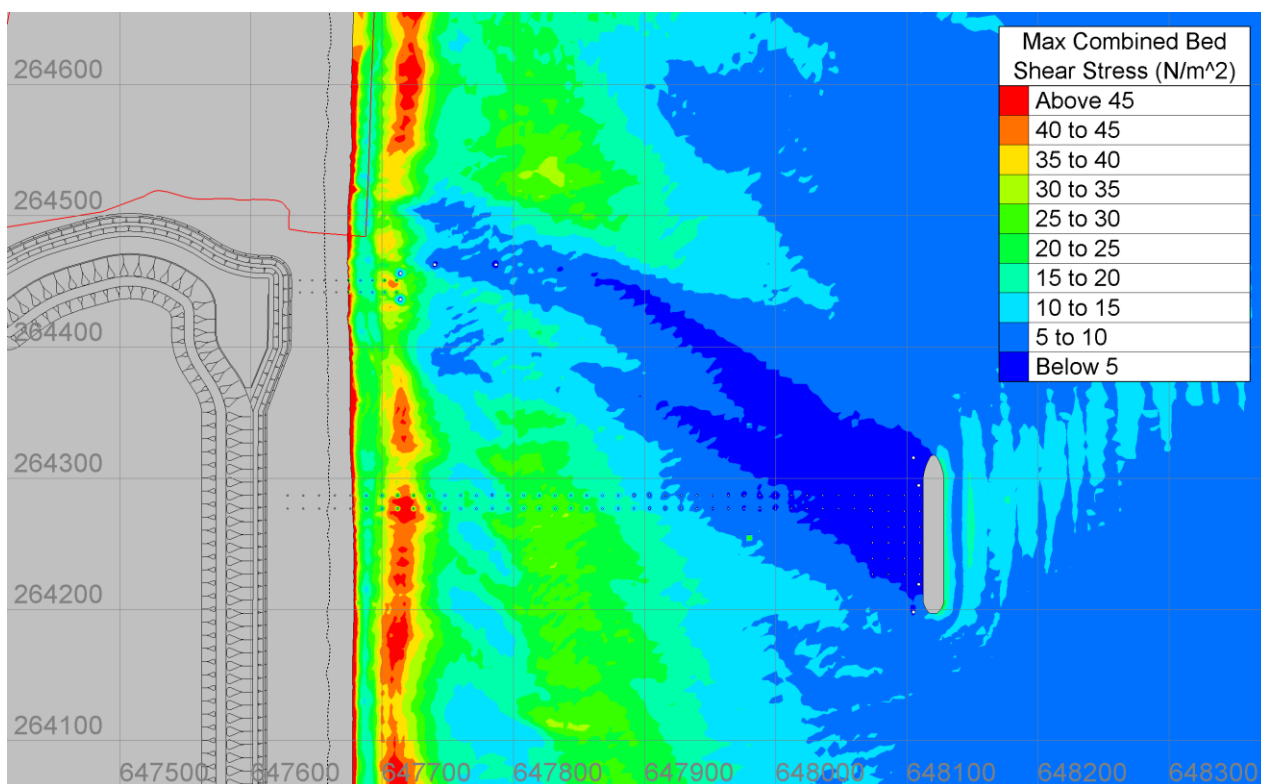
Figure 37: Maximum combined bed shear stress (τ_{max}) for the temporary and permanent BLF structures plus ship (1.5 m SE wave, peak ebb).

TR543 MODELLING OF THE TEMPORARY AND PERMANENT BLF AT SZC

NOT PROTECTIVELY MARKED
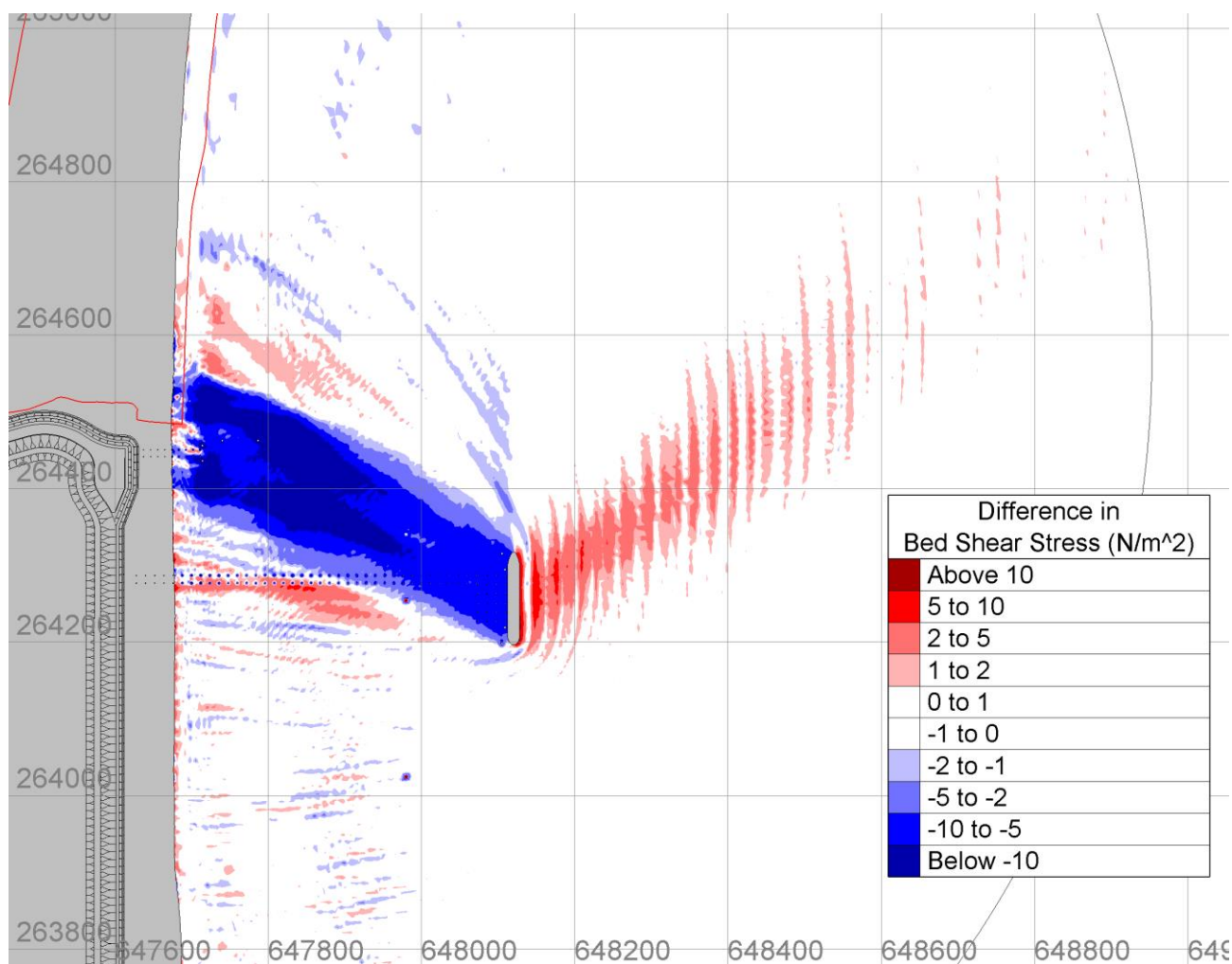
Figure 38: Magnitude of change in maximum bed shear stress for the temporary and permanent BLF structures with the ship (1.5 m SE wave, peak ebb).

The ship results in a reduction in bed shear stress in the lee of the prevailing wave direction. The ship is modelled as filling the entire water column, which is precautionary as in reality the ship would be floating and not resting on the seabed. The reduction in bed shear stress is between 15-20 N/m^2 along both the inner and outer longshore bar. The baseline bed shear stress along the outer bar is 20-30 N/m^2 and 40-50 N/m^2 along the inner longshore bar. No area is reduced below the critical threshold.

Shoreward of the inner bar, the reduction is smaller and predicted to be 5-10 N/m^2. This reduction extends approximately 60 m into the Minsmere SPA/SAC frontage. Despite this reduction, as evident in Figure 37, the bed shear stress shoreward of the inner bar is still in excess of 45 N/m^2. As well as the reduction along the Minsmere frontage, an area of increased bed shear stress, between 1-3 N/m^2, extends a further 400 m. Patches of altered bed shear stress are sufficiently small in magnitude and scale, and would migrate continuously, so that they are not expected to cause detectable change to the shoreline.

As noted previously, the patchwork of alternating bed shear stress due to the piles would change continuously with the state of the tide and direction of waves. These conditions are variable with the state of tide and waves, meaning the peak impact shown in the model results is not persistent over a tidal cycle. Furthermore, there

NOT PROTECTIVELY MARKED

are no areas of change within the model where a reduction in bed stress reduces below the critical threshold or an increase above the threshold where it was not previously.

4.5   Temporary and Permanent BLFs plus grillage and ship

To investigate the effect of the grillage at the permanent BLF and a 120-m-long ship at the temporary BLF, the peak ebb velocities, wave energy and bed shear stress results were compared to the baseline conditions with a 1.5 m wave (working limit of the ship). This scenario would occur when the temporary BLF is in use, but the permanent BLF is not.

4.5.1   Tidal current induced bed shear stress

To highlight the influence of the grillage with a ship's presence at the temporary BLF, Figure 39 shows the flow velocities around the temporary and permanent BLF and the ship present with Figure 40 showing the difference in velocities compared to the baseline.

Comparing the magnitude and velocity difference for the grillage and the ship, as shown in Figure 39 and Figure 40, with the grillage only (Figure 25 and Figure 26) and the ship only (Figure 32 and Figure 33), it can be seen that the grillage and ship do not interact, with respect to tidal currents. That is, the effect of the grillage and ship in isolation is the same when both are present.

At the temporary BLF the last row of deck piles, fenders and the ships presence slightly interrupt the shore parallel flow. Flow returns to within 0.1 m/s within 300m downstream of the ship. Due to the hydrodynamic profile of the ship, the lateral disturbance of velocities is much smaller. There is an increase of up to 0.2 m/s along the length of seaward side of the ship.

At the permanent BLF, the last pair of deck piles, fenders and the shoreward tip of the grillage slightly interrupt the shore parallel flow. This occurs where the shoreward tip of the grillage sits slightly above the bathymetry. The grillage does not act as a blockage as currents still pass over the top. This small decrease in the tidal currents in the lee of the piles and grillage returns to within 0.1 m/s within 45 m. There is also a minor increase of 0.1 m/s in flows created shoreward of the mooring fenders. Over the grillage there is a small increase of 0.075 m/s, although the grillage itself is a non-erodible structure so this would have no effect.

Figure 41 shows the current-only (τ_c) bed shear stress for the temporary and permanent BLF structures with the ship present at the temporary BLF.

TR543 MODELLING OF THE TEMPORARY AND PERMANENT BLF AT SZC

NOT PROTECTIVELY MARKED
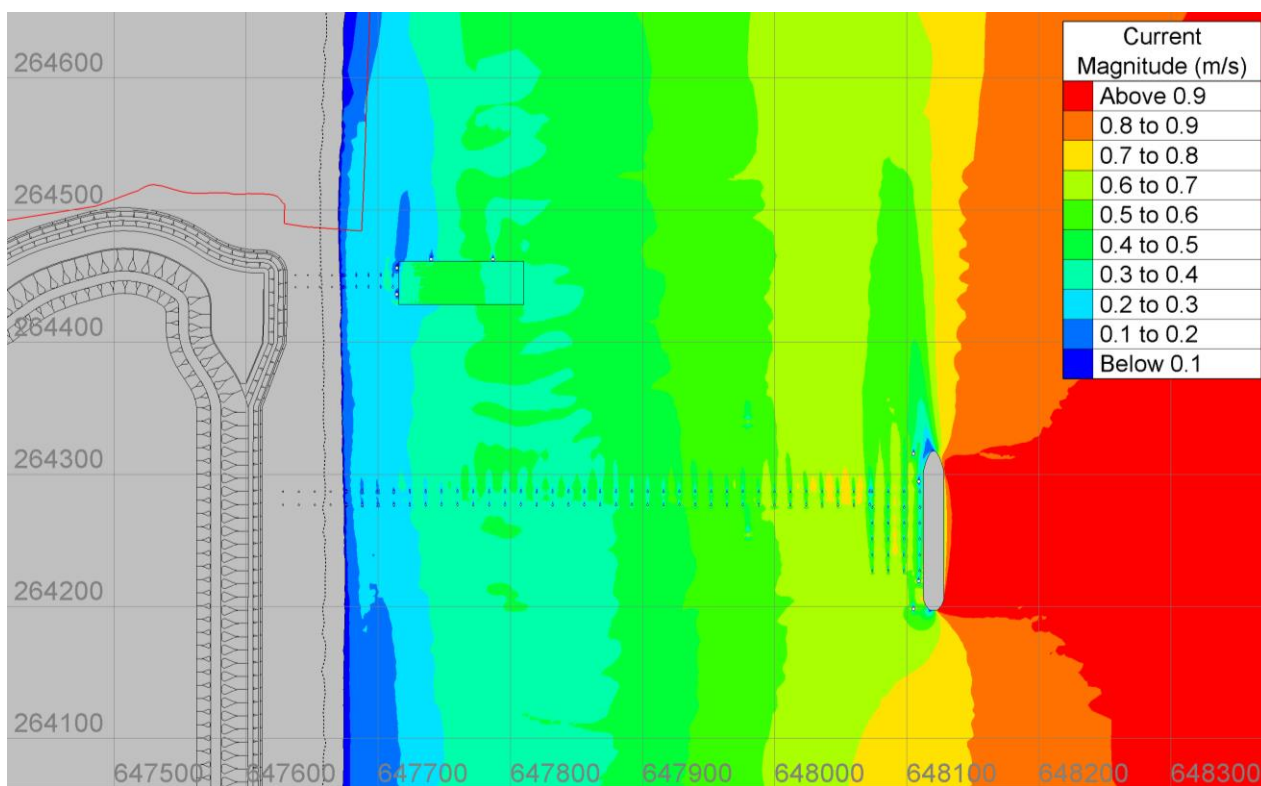
Figure 39: Peak ebb velocities around temporary and permanent BLF plus grillage and ship.

TR543 MODELLING OF THE TEMPORARY AND PERMANENT BLF AT SZC

NOT PROTECTIVELY MARKED
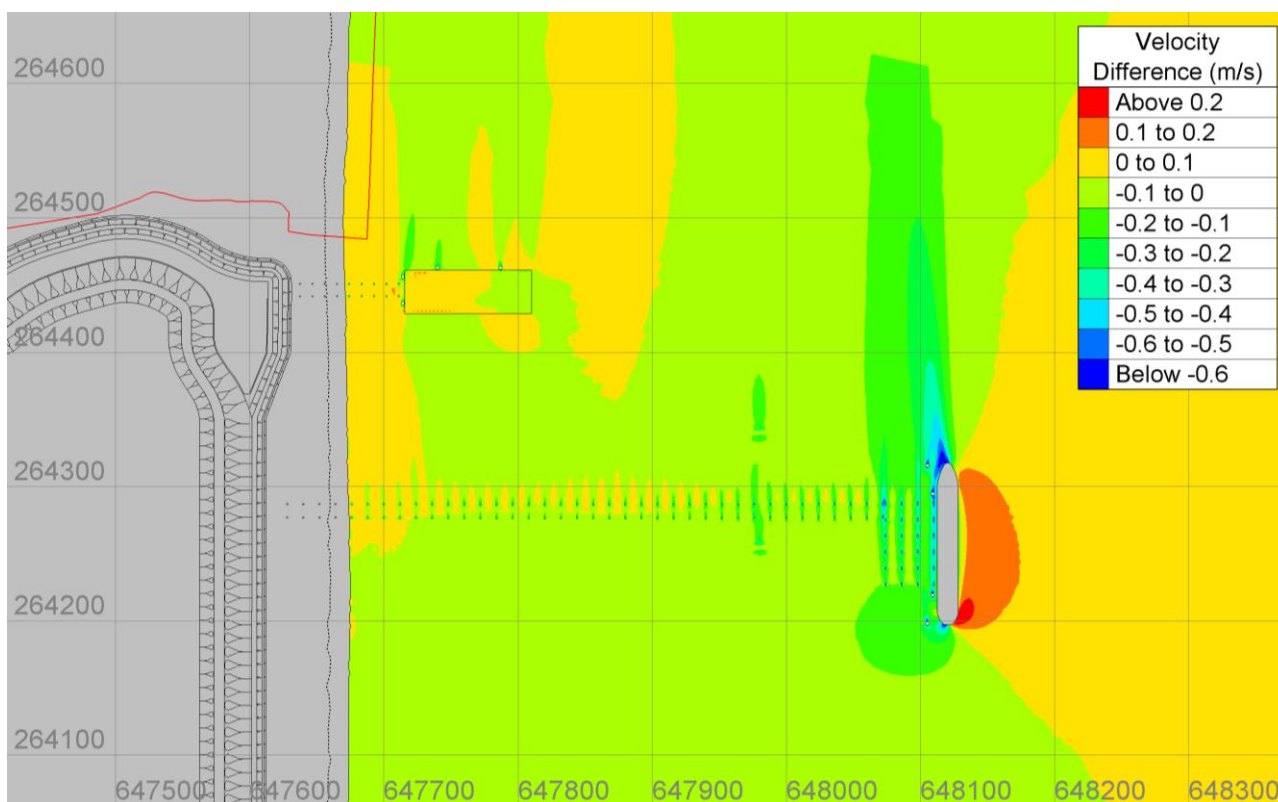
Figure 40: Difference in peak ebb velocity between the structures plus grillage and ship and baseline case.

TR543 MODELLING OF THE TEMPORARY AND PERMANENT BLF AT SZC

NOT PROTECTIVELY MARKED
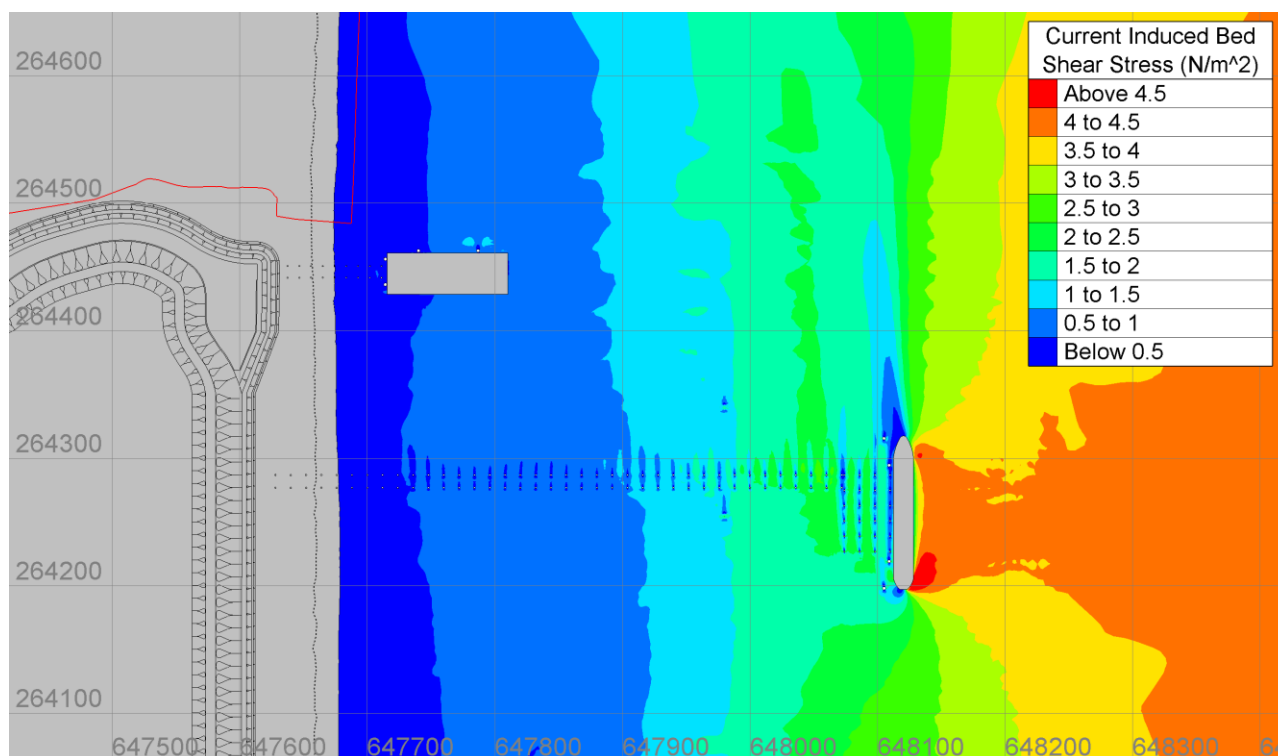
Figure 41: Current-only (τ_c) bed shear stress for the temporary and permanent BLF structures plus grillage and ship (peak ebb).

4.5.2 Wave induced bed shear stress

Figure 42 shows wave-only (τ_w) bed shear stress for the temporary and permanent BLF structures plus the grillage and ship for a 1.5 m SE wave during peak ebb.

The presence of the ship at the temporary BLF results in reduced bed shear stress in the lee of the prevailing wave direction, extending from the ship across the inner and outer longshore bars. However, results show that the wave induced bed shear stress is still in excess 10 times larger than the critical threshold at the temporary BLF head. For the SE wave direction, the wave shadow of the ship intersects with the grillage at the permanent BLF. The ships presence slightly enhances the reduction in bed shear stress at the shoreward edge of the grillage, with reductions in τ_w for approximately 80 m along the inner longshore bar. However, results show that the wave induced bed shear stress is still over 100 times larger than the critical threshold, meaning sediment is still in motion along the bar.
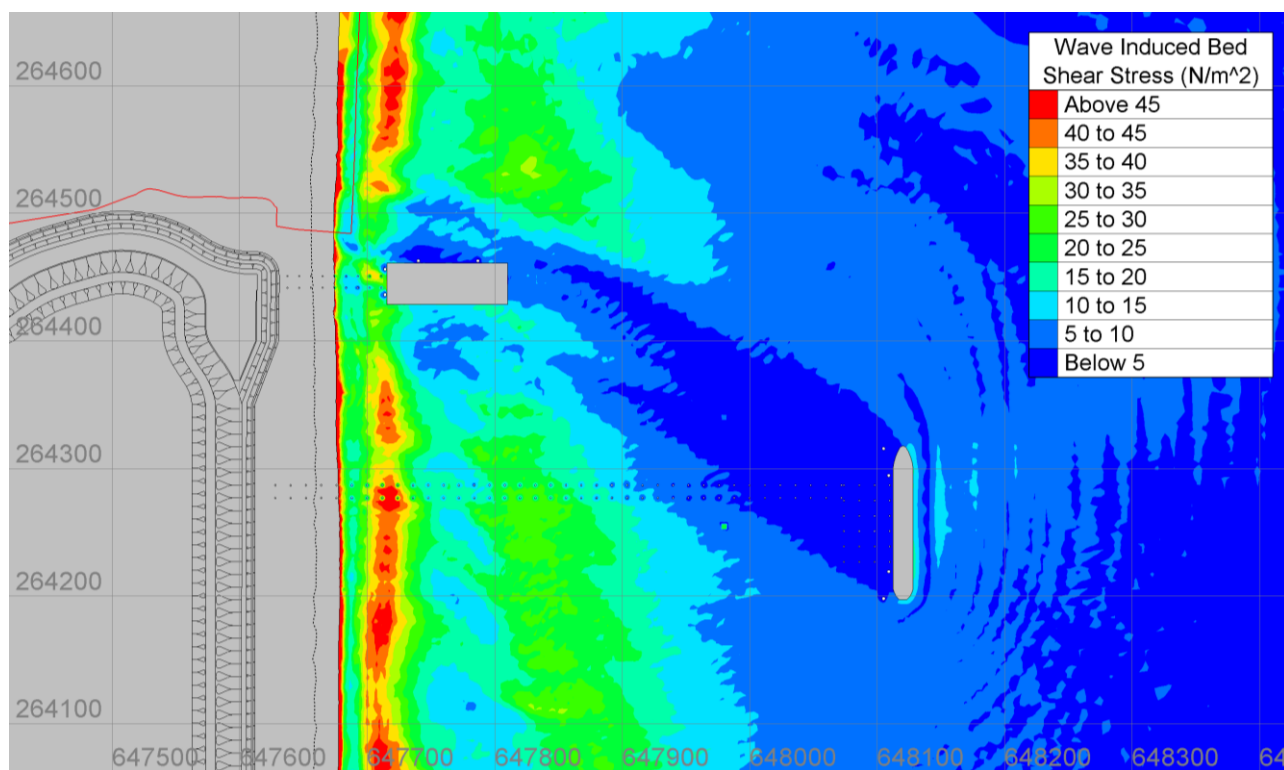
Figure 42: Wave-only (τ_w) bed shear stress for the temporary and permanent BLF structures plus grillage and ship (1.5 m SE wave, peak ebb).

TR543 MODELLING OF THE TEMPORARY AND PERMANENT BLF AT SZC

NOT PROTECTIVELY MARKED

4.5.3 Combined wave and current bed shear stress

Figure 43 and Figure 44 show the mean (τ_m), and maximum (τ_{max}) combined bed shear stresses, respectively, for the temporary and permanent BLF structures plus grillage and ship run. Figure 45 shows the effect of the BLF structures plus the grillage and ship on the combined bed shear stress as represented by a difference in magnitude. Results show that the baseline bed shear stresses over entire model domain are above the critical threshold of motion (0.216 N/m^2).
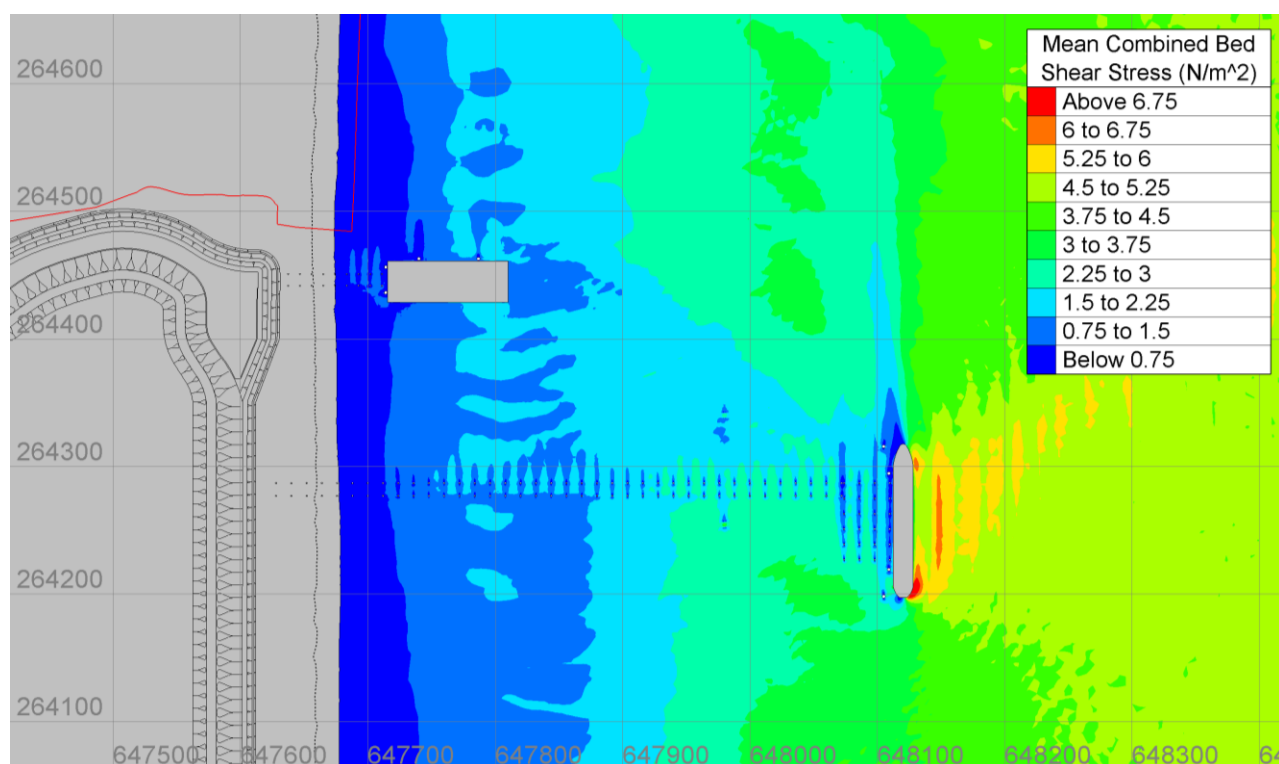
Figure 43: Mean combined bed shear stress (τ_m) for the temporary and permanent BLF structures plus grillage and ship (1.5 m SE wave, peak ebb).

TR543 MODELLING OF THE TEMPORARY AND PERMANENT BLF AT SZC

NOT PROTECTIVELY MARKED
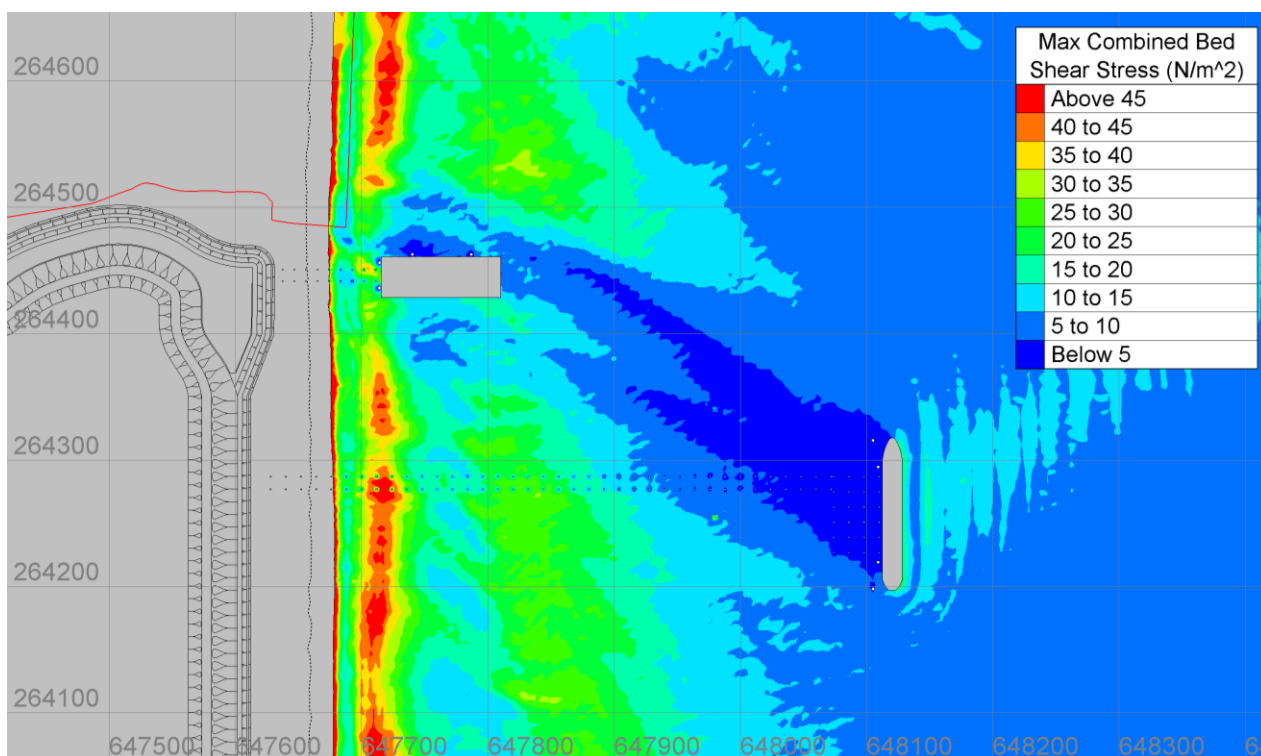
Figure 44: Maximum combined bed shear stress (τ_{max}) for the temporary and permanent BLF structures plus grillage and ship (1.5 m SE wave, peak ebb).

TR543 MODELLING OF THE TEMPORARY AND PERMANENT BLF AT SZC

NOT PROTECTIVELY MARKED
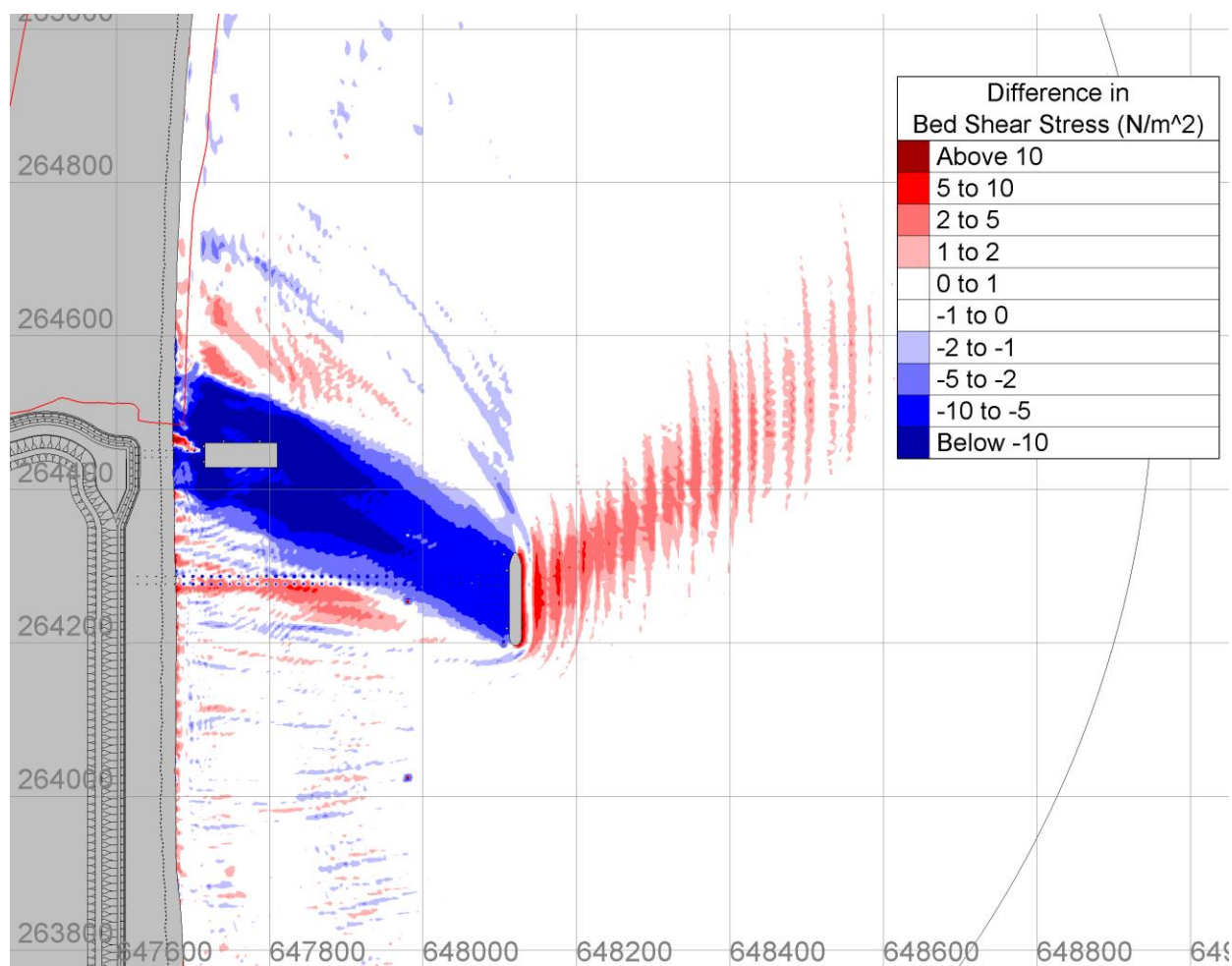
Figure 45: Magnitude of change in maximum bed shear stress for the temporary and permanent BLF structures with the grillage and ship (1.5 m SE wave, peak ebb).

Seaward of the grillage, the combined effects of the grillage and the ship are the same as the ship in isolation. The ship results in a reduction in bed shear stress in the lee of the prevailing wave direction. The ship is modelled as filling the entire water column, which is precautionary as in reality the ship would be floating and not resting on the seabed. The reduction in bed shear stress is between 15-20 N/m^2 along the outer longshore bar, whilst the baseline there is 20-30 N/m^2. No area is reduced below the critical threshold. The influence on sediment transport and shoreline change due to the reduction in the lee of the ship is discussed in more detail in Section 5. North of the grillage the magnitude of reduction along the inner longshore bar is similar 15-20 N/m^2, however, the extent is larger than the ship only case although still within the footprint of the ship's wave shadow.

Shoreward of the inner bar, the bed shear stress reduction is smaller at 5-10 N/m^2. This reduction extends approximately 60 m into the Minsmere SPA/SAC frontage but bed shear stress is still in excess of 45 N/m^2 (Figure 44) shoreward of the inner bar. An area of slightly increased bed shear stress (1-3 N/m^2) extends a further 400 m to the north. The small increase in bed shear stress is well within natural variation along the Minsmere SPA/SAC frontage.

NOT PROTECTIVELY MARKED

The BLF piles are transmissive and would not block sediment transport. However, the shoreward end of the grillage sits above the bed, deflecting currents shoreward, which leads to an increase amongst the final pairs of permanent BLF piles. The peak increase in bed shear stress within this area is 11 N/m^2 compared to a baseline of 40 N/m^2 in that location. However, that very localised increase is still within the wider baseline variation along the Sizewell C frontage of 30-65 N/m^2 (for a 1.5 m wave height).

The patchwork of alternating bed shear stress due to the piles would change continuously with the state of the tide and direction of waves. These conditions are variable with the state of tide and waves, meaning the peak impact shown in the model results is not persistent over a tidal cycle. Furthermore, there are no areas of change within the model where a reduction in bed stress reduces below the critical threshold or an increase above the threshold where it was not previously. Patches of altered bed shear stress along the shoreline are sufficiently small in magnitude and scale that they are not expected to cause detectable change to the shoreline.

4.6   Temporary and Permanent BLFs plus grillage, access dredge and barge

To investigate the effect of the presence of the grillage, access dredge (clipping the outer longshore bar to -3.5 m ODN) and barge at the permanent BLF in combination with the permanent and temporary BLF jetties into the domain, the peak ebb velocities, wave energy and bed shear stress results were compared to the baseline conditions with a 0.5 m wave (working limit of the barge). This scenario would occur during the construction phase when the permanent BLF is in use, but the temporary BLF is not.

4.6.1   Tidal current induced bed shear stress

To highlight the influence of the combination of the docked barge, grillage and access dredge at the permanent BLF, Figure 46 shows the flow velocities around the temporary and permanent BLF and the barge present with Figure 47 showing the difference in velocities compared to the baseline.

Figure 46 and Figure 47 show that the barge acts a barrier to the shore parallel tidal flows, as it occupies the entire water column once grounded. The flow is diverted around the shoreward and seaward ends of the barge, although it is important to note that barges would only be present for up to 22% of the April – October period (and infrequent during winter), and so the impacts described below are very transient. Flow is accelerated between the shore and the end of the barge and grillage, with a peak increase in tidal currents of 0.34 m/s between the last two pairs of piles of the permanent BLF. This increase in velocity returns to within 0.1 m/s within 140 m. The reduced flow to the north of the barge on the ebb tide returns to within 0.1 m/s within 835 m.

Figure 48 shows the current-only (τ_c) bed shear stress for the temporary and permanent BLF structures plus grillage, access dredge and barge during peak ebb. The effect of the grillage and barge on the bed shear stress can be seen to increase current induced bed shear stress shoreward of the grillage and barge, with a smaller increase in bed shear stress seaward of the grillage and barge. There is no indication of a change in bed shear stress associated with the access dredge at the seaward end of the barge.
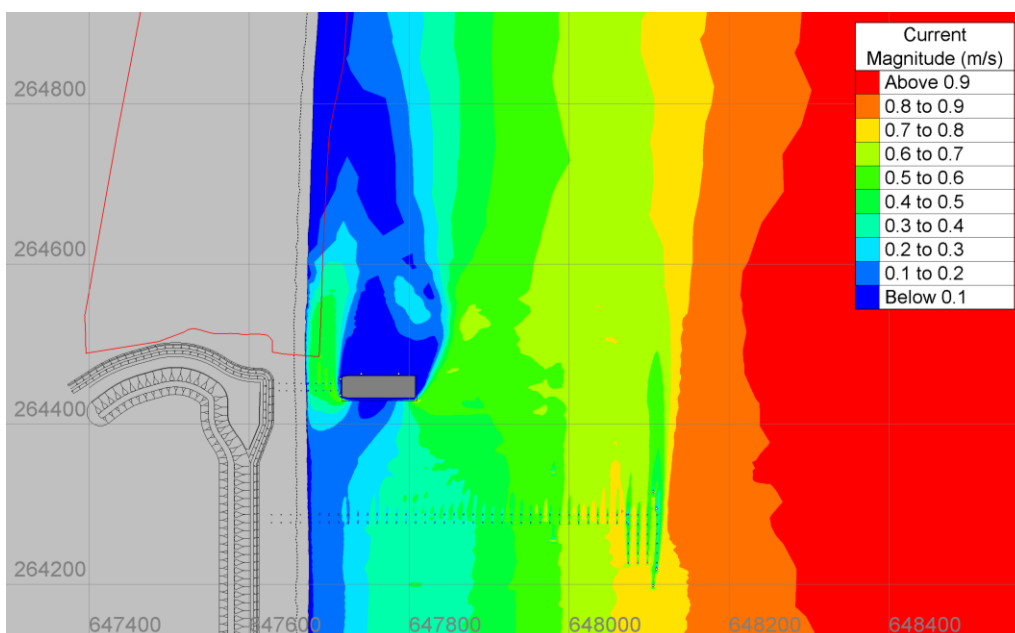
Figure 46: Peak ebb velocities around temporary and permanent BLF plus grillage, access dredge and barge.
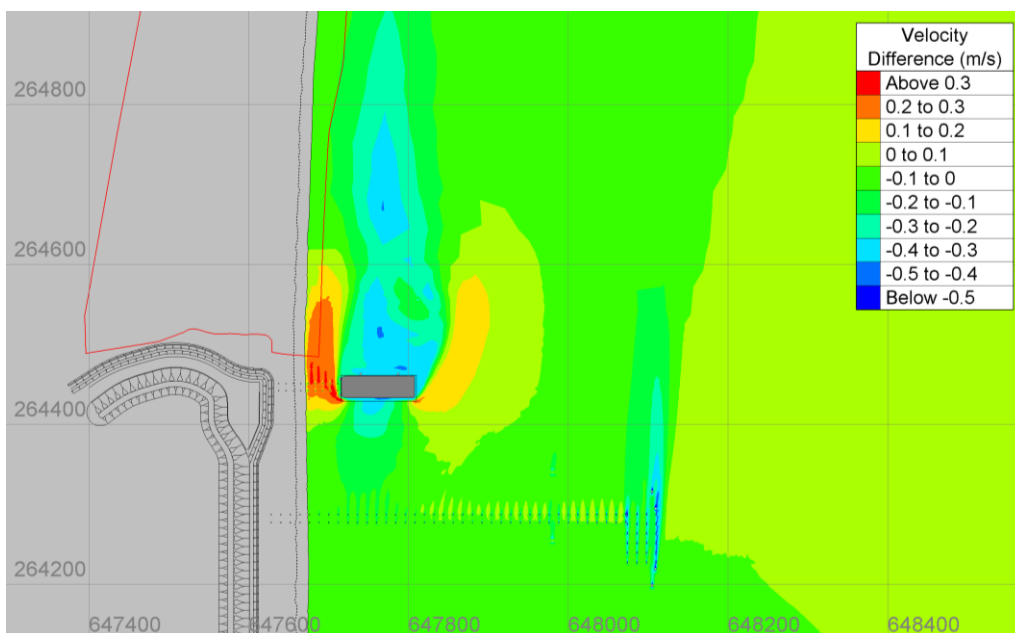
Figure 47: Difference in peak ebb velocity between the structures plus grillage, access dredge and barge and baseline case.

TR543 MODELLING OF THE TEMPORARY AND PERMANENT BLF AT SZC

NOT PROTECTIVELY MARKED
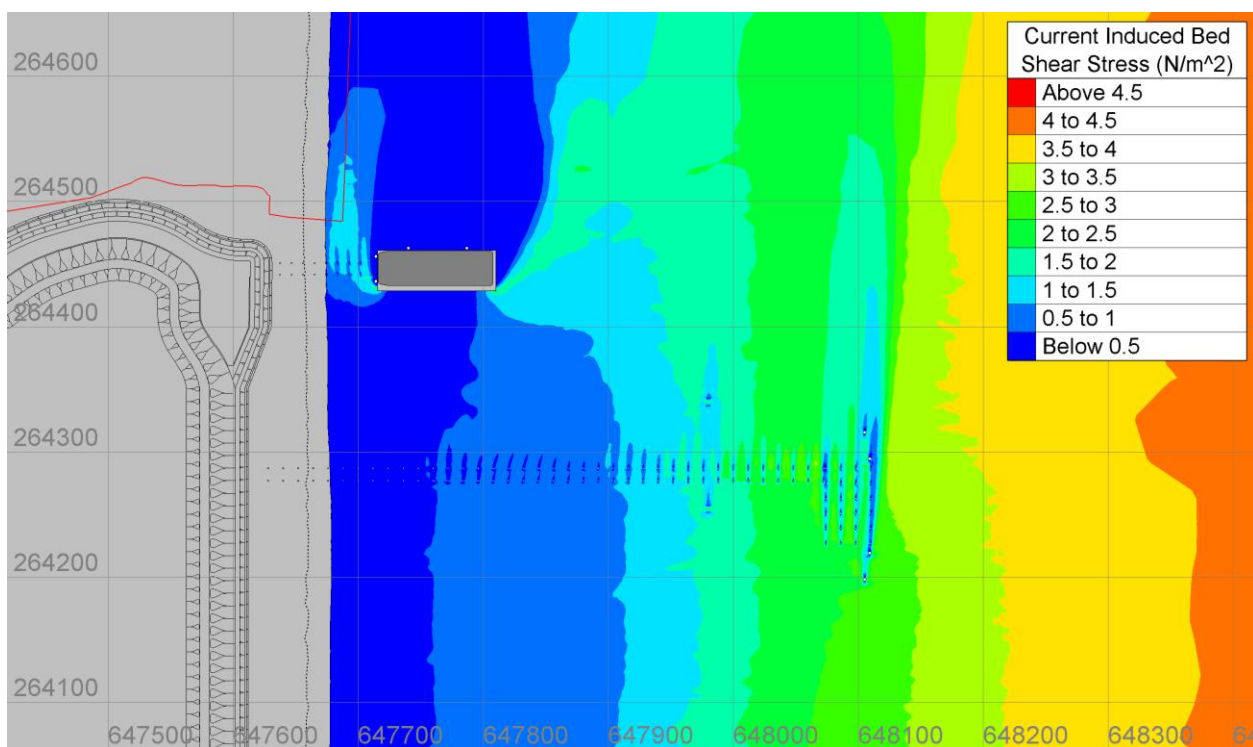
Figure 48: Current-only (τ_c) bed shear stress for the temporary and permanent BLF structures plus grillage, access dredge and barge (peak ebb).

4.6.2 Wave induced bed shear stress

Figure 49 shows the wave-only (τ_w) bed shear stress for the temporary and permanent BLFs plus grillage, access dredge and barge for a 0.5 m SE wave (barge limit) during peak ebb.

The effect of the grillage and barge on the wave induced bed shear stress is localised to the shoreward edge of the grillage, with reductions in τ_w for approximately 50 m along the inner longshore bar. However, results show that the wave induced bed shear stress is still over 13 times larger than the critical threshold, meaning sediment is still in motion along the bar. Due to the smaller working limit of the barge, the 0.5 m wave height shows a smaller interaction with the outer bar, with bed stresses approximately 4-5 times smaller along the outer longshore bar compared to the inner longshore bar.
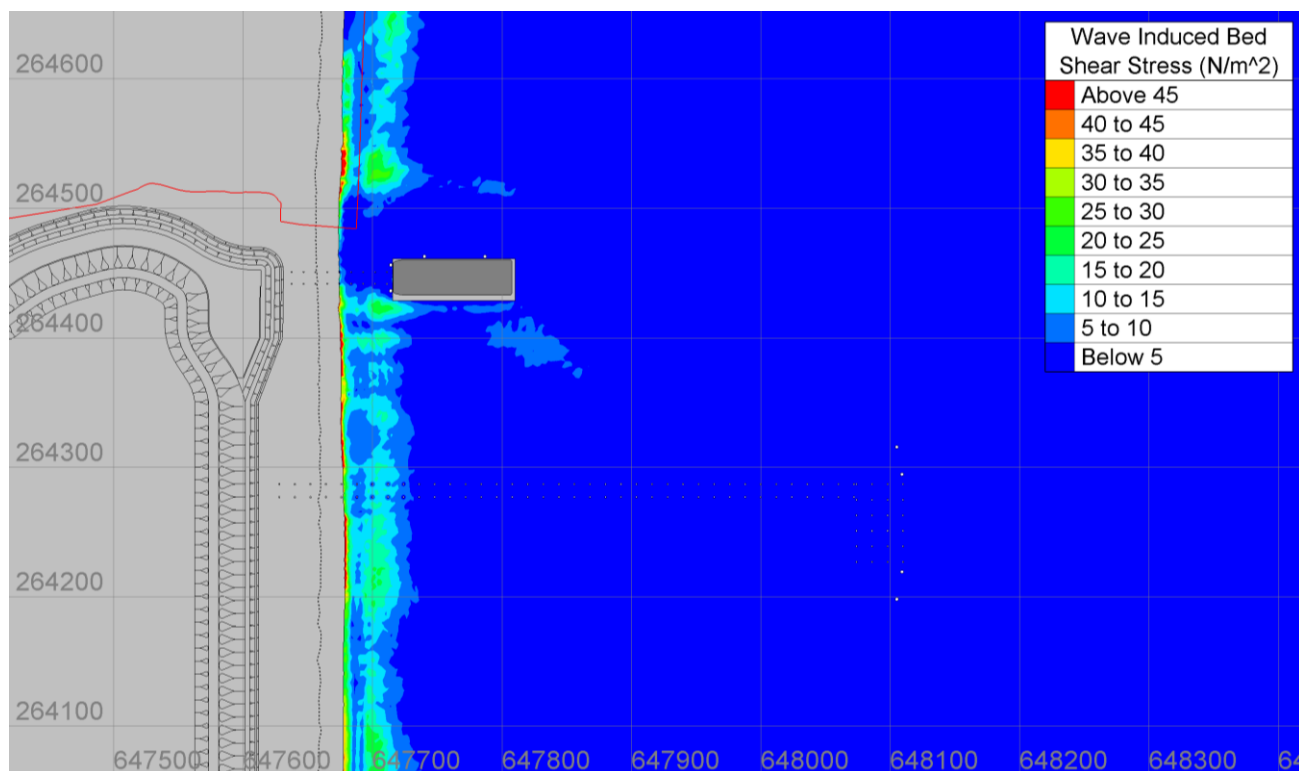
Figure 49: Wave-only (τ_w) bed shear stress for the temporary and permanent BLF structures plus grillage, access dredge and barge (0.5 m SE wave, peak ebb).

TR543 MODELLING OF THE TEMPORARY AND PERMANENT BLF AT SZC

NOT PROTECTIVELY MARKED

4.6.3   Combined wave and current bed shear stress

Figure 50 and Figure 51 show the mean (τ_m), and maximum (τ_{max}) combined bed shear stresses, respectively, for the temporary and permanent BLFs plus grillage, access dredge and barge model run. Figure 52 shows combined bed shear stress as represented by a difference in magnitude. Results show that the baseline bed shear stresses over entire model domain are above the critical threshold of motion (0.216 N/m^2).

Figure 50: Mean combined bed shear stress (τ_m) for the temporary and permanent BLF structures plus grillage, access dredge and barge (0.5 m SE wave, peak ebb).
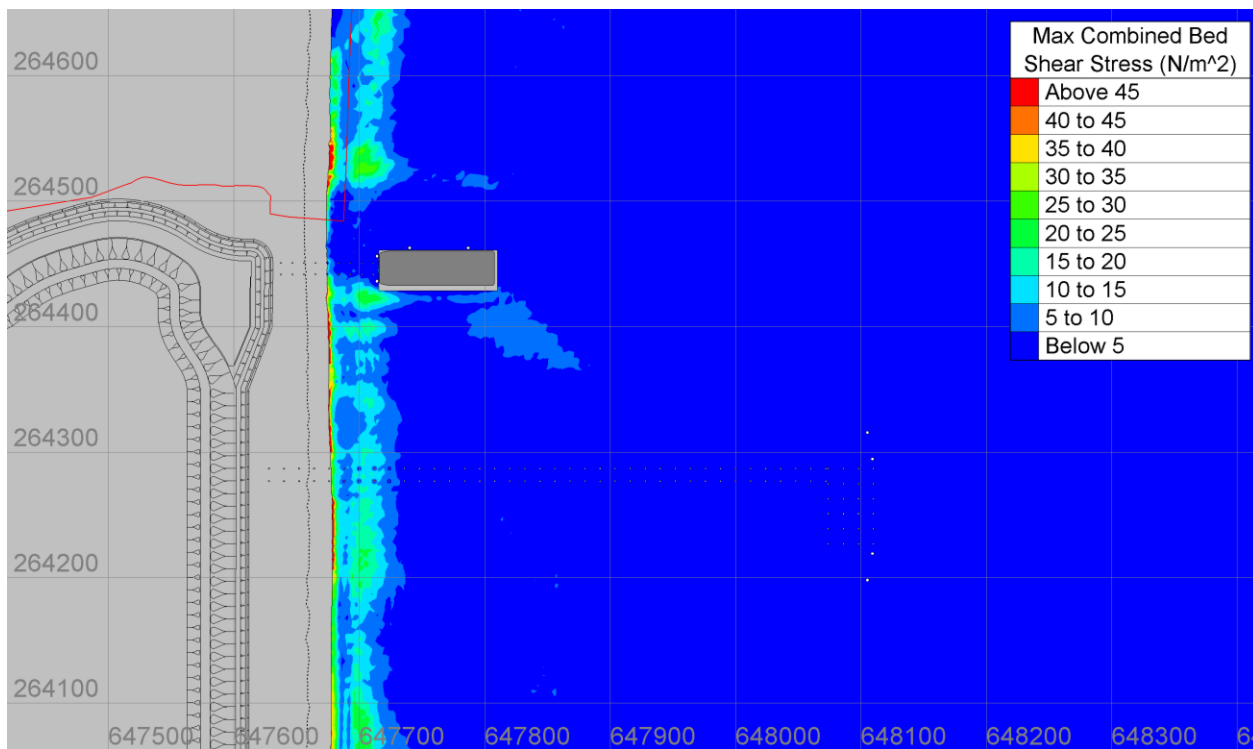
Figure 51: Maximum combined bed shear stress (τ_{max}) for the temporary and permanent BLF structures plus grillage, access dredge and barge (0.5 m SE wave, peak ebb).
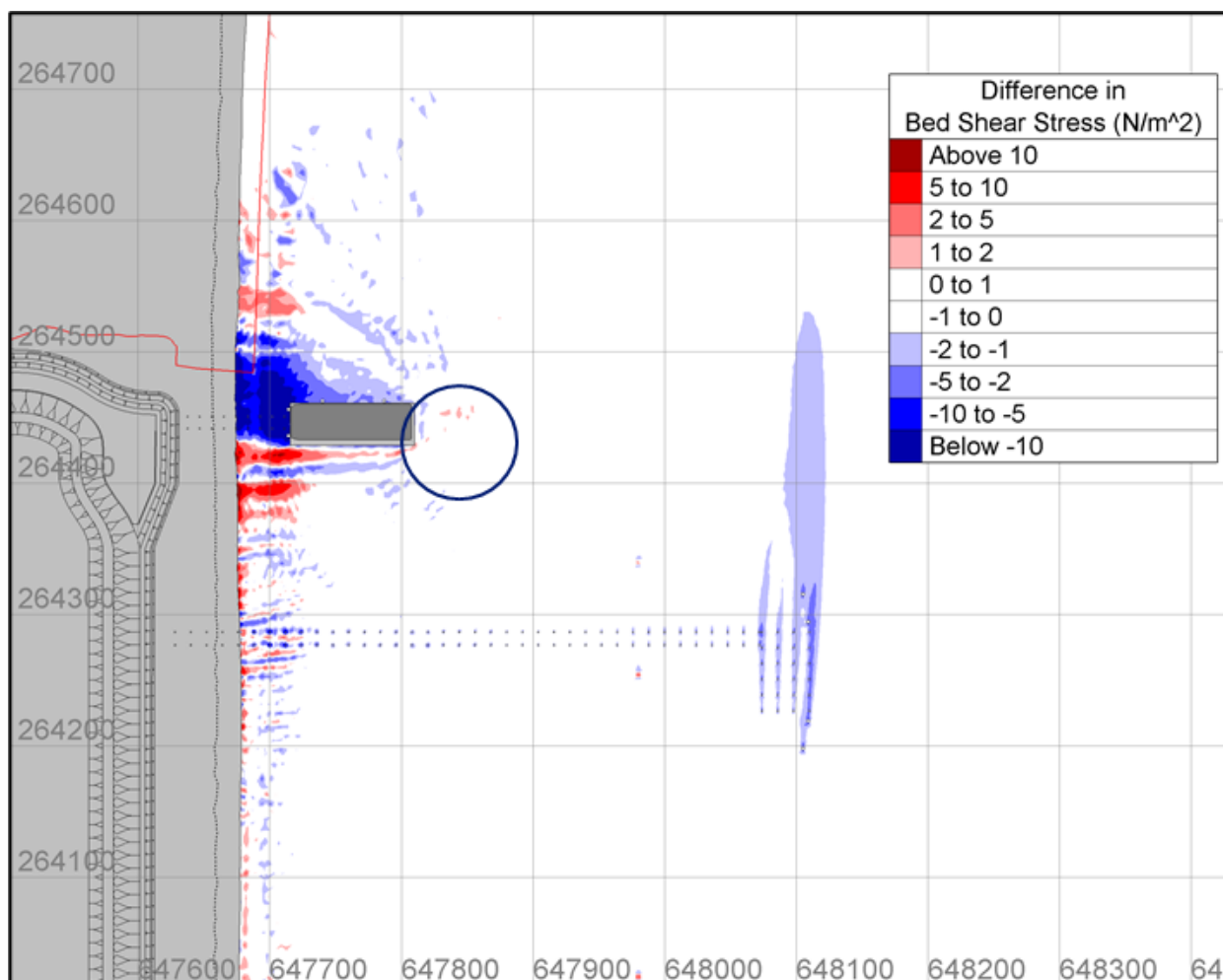
Figure 52: Magnitude of change in maximum bed shear stress for the temporary and permanent BLF structures with the grillage, access dredge and barge (0.5 m SE wave, peak ebb).

As evident by the lack of change in bed shear stress at the seaward end of the barge (marked with the circle in Figure 52), the access dredge shows no effect on the outer longshore bar.

Despite the increase in the current induced bed shear stress shoreward of the barge and grillage (Figure 48), results show, in Figure 52, that the blockage effect on waves leads to an overall reduction in bed shear stress between the shoreline and the barge. This is because the wave induced bed shear stress is significantly larger in the shallow waters than the current induced bed shear stress, even with a 0.5 m wave. That is, the increased stress due to tidal currents around the landward end of the barge is cancelled out by the reduction in stress due to wave sheltering.

The reduction in bed shear stress along the inner longshore bar between the barge and the shore is between 15-20 N/m². compared to a baseline of 20-25 N/m². Whilst the reduction peaks at 20 N/m² in places and the baseline is also 20 N/m² in places, these locations do not overlap. There is no area where a reduction in bed shear stress reduces below the critical threshold. The absolute bed shear stress is still 10-14 times larger than the critical threshold in this area. A 10-20 N/m² reduction in bed shear stress shoreward of the end of the barge

extends 30 m into the Minsmere SPA/SAC frontage, whilst a small 1-4 N/m² increase extends a further 145 m. The baseline bed shear stress along the Minsmere frontage is 20-40 N/m².

The patchwork of alternating bed shear stress would change continuously with the state of the tide and direction of waves. These conditions are variable with the state of tide and waves, meaning the peak impact shown in the model results is not persistent over a tidal cycle. Furthermore, there are no areas of change within the model where a reduction in bed stress reduces below the critical threshold or an increase above the threshold where it was not previously. Patches of altered bed shear stress along the shoreline are sufficiently small in magnitude and scale that they are not expected to cause detectable change to the shoreline.

4.7   Temporary and Permanent BLFs plus grillage, access dredge, barge and ship

To investigate the effect of the presence of the grillage, access dredge, the ship at the temporary BLF and the barge at the permanent BLF in combination with the permanent and temporary BLF jetties into the domain, the peak ebb velocities, wave energy and bed shear stress results were compared to the baseline conditions with a 0.5 m wave (working limit of the barge). This scenario would occur during the construction phase when both BLFs are in use.

4.7.1   Tidal current induced bed shear stress

To highlight the influence of the combination of the docked barge, grillage and access dredge at the permanent BLF and the ship at the temporary BLF, Figure 53 shows the flow fields and Figure 54 show the difference in velocities compared to the baseline.

Results show that the barge present at the permanent BLF in combination with the ship at the temporary BLF, produces a similar influence on the tidal currents as with the presence of the barge only. Figure 53 and Figure 54 show that the barge acts as a barrier to the shore parallel tidal flows because it occupies the entire water column once grounded. This blockage causes the flow to divert around the shoreward and seaward ends of the barge, although it is important to note that barges would only be present for up to 22% of the April – October period (and infrequent during winter), and so the impacts described below are very transient. However, there is a subtle interaction between the barge and the ship in that the presence of the ship reduces slightly the seaward acceleration of currents around the seaward end of the barge, reducing the total length of the velocity reduction in the lee of the barge. The reduced flow to the north of the barge on the ebb tide returns to within 0.1 m/s within 685 m, compared to 835 m when the ship is not present. Flow is accelerated between the shore and the end of the barge and grillage, with a peak increase in tidal currents of 0.33 m/s between the last two pairs of piles of the permanent BLF. This increase in velocity returns to within 0.1 m/s within 135 m. The effect of the ship on the tidal currents also reduces, with flows returning to within 0.1 m/s within 275 m downstream of the ship.

Figure 55 shows the current-only (τ_c) bed shear stress for the temporary and permanent BLFs plus grillage, access dredge, barge and ship during peak ebb. The effect of the grillage and barge on the bed shear stress can be seen to increase current induced bed shear stress shoreward of the grillage and barge, with a smaller increase in bed shear stress seaward of the grillage and barge. There is no indication of a change in bed shear stress associated with the access dredge at the seaward end of the barge.

TR543 MODELLING OF THE TEMPORARY AND PERMANENT BLF AT SZC

**NOT PROTECTIVELY MARKED**
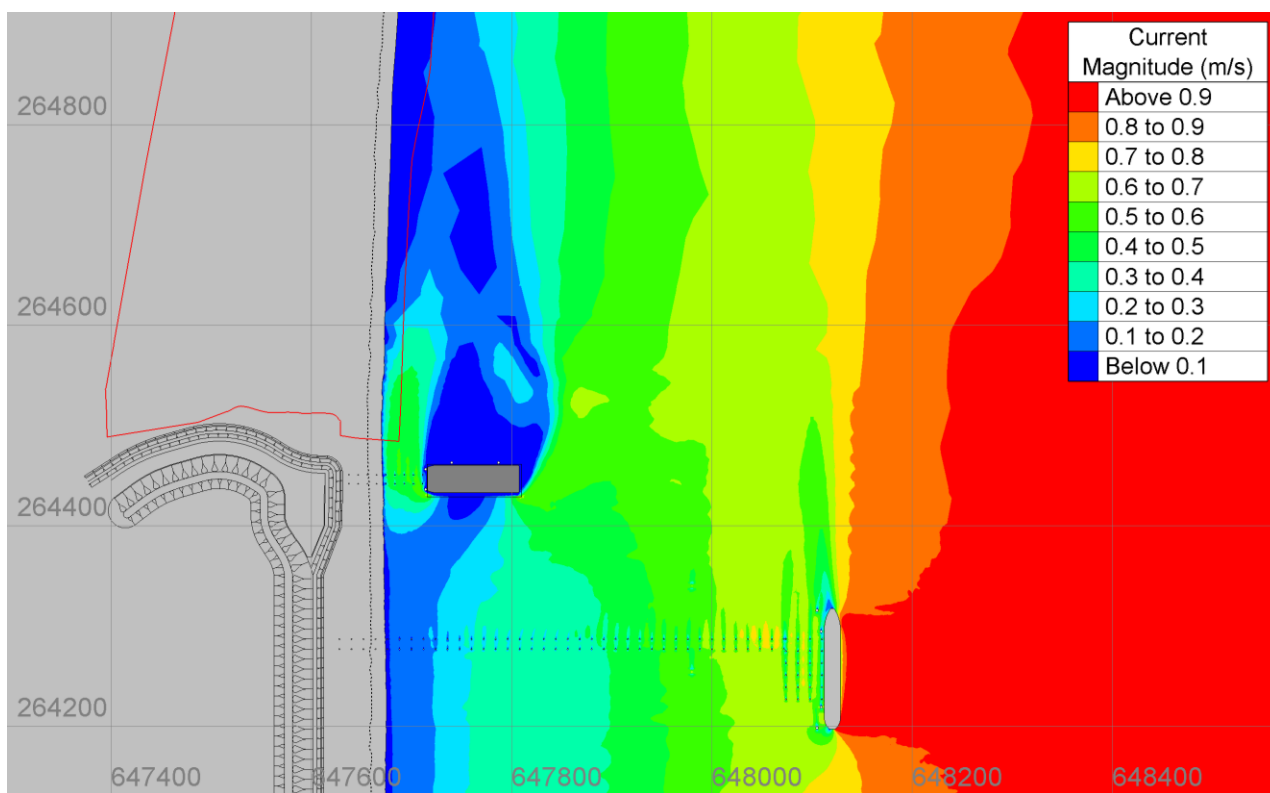
Figure 53: Peak ebb velocities around temporary and permanent BLF plus grillage, access dredge, barge and ship.

TR543 MODELLING OF THE TEMPORARY AND PERMANENT BLF AT SZC

NOT PROTECTIVELY MARKED
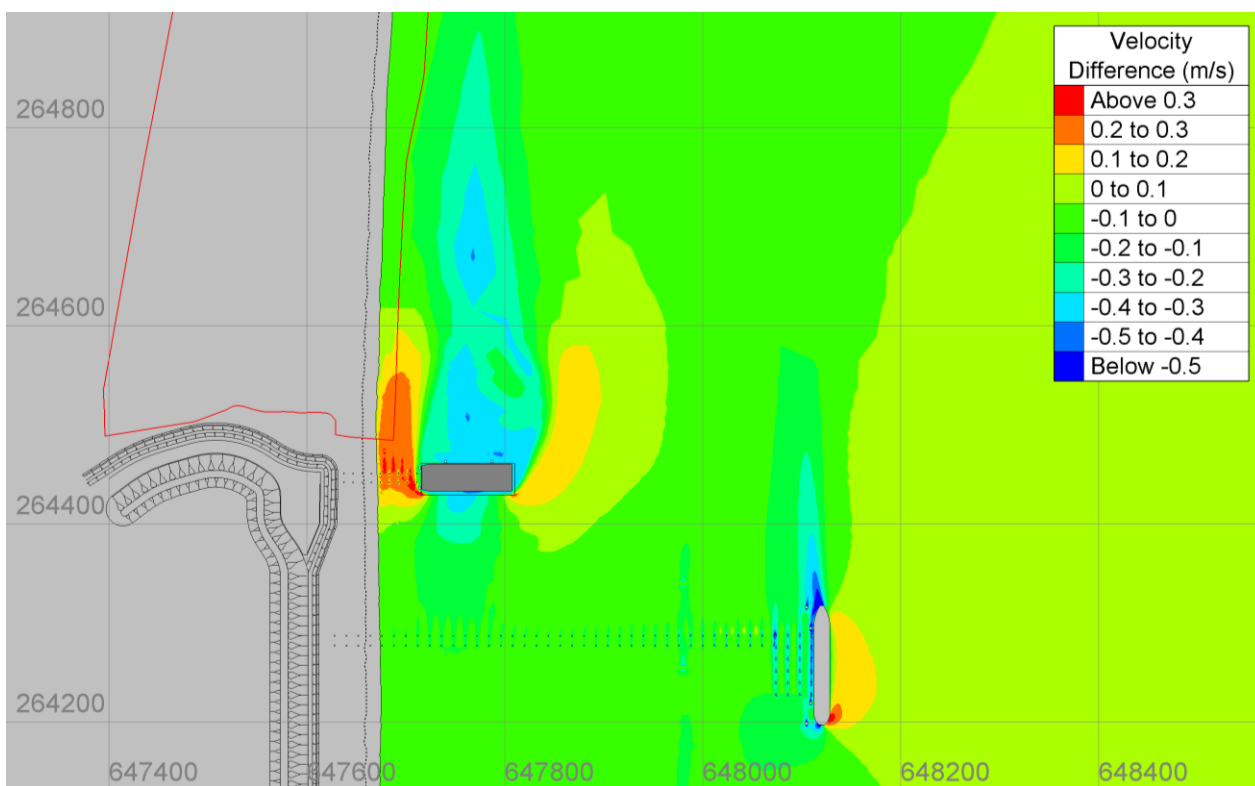
Figure 54: Difference in peak ebb velocity between the structures plus grillage, access dredge, barge and ship and baseline case.
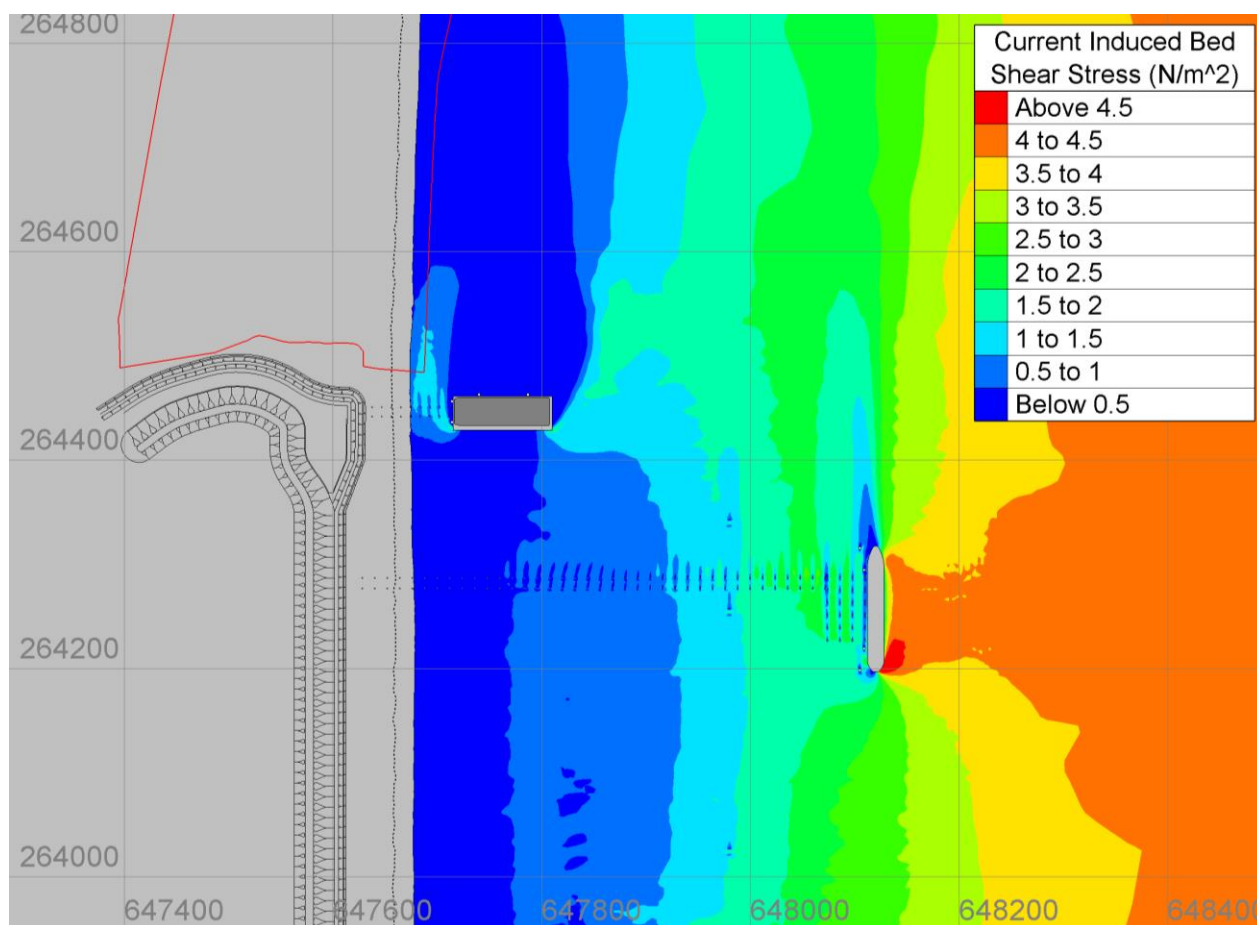
Figure 55: Current-only (τ_c) bed shear stress for the temporary and permanent BLF structures plus grillage, access dredge, barge and ship (peak ebb).

4.7.2 Wave induced bed shear stress

Figure 56 shows wave-only (τ_w) bed shear stress for the temporary and permanent BLFs plus grillage, access dredge and barge for a 0.5 m SE wave during peak ebb.

The effect of the grillage and barge on the wave induced bed shear stress is localised to the shoreward edge of the grillage, with reductions in τ_w for approximately 50 m along the inner longshore bar. However, results show that the wave induced bed shear stress is still more than 13 times larger than the critical threshold, meaning sediment is still in motion along the bar. Due to the smaller working limit of the barge, the 0.5 m wave height shows a smaller interaction with the outer bar, with bed stresses approximately 4-5 times smaller along the outer longshore bar compared to the inner longshore bar.

**TR543 MODELLING OF THE TEMPORARY AND PERMANENT BLF AT SZC**

NOT PROTECTIVELY MARKED

Figure 56: Wave-only (τ_w) bed shear stress for the temporary and permanent BLF structures plus grillage, access dredge, barge and ship (0.5 m SE wave, peak ebb).

4.7.3 Combined wave and current bed shear stress

Figure 57 and Figure 58 show the mean (τ_m), and maximum (τ_{max}) combined bed shear stresses, respectively, for the temporary and permanent BLFs plus grillage, access dredge, barge and ship run. Figure 59 shows the effect on the combined bed shear stress as represented by a difference in magnitude. Results show that the baseline bed shear stresses over entire model domain are above the critical threshold of motion (0.216 N/m^2).

Compared to the modelled higher waves associated with the working limit of the ship only, the wave shadow associated with the smaller wave height needed to allow barges to dock (0.5 m) is much smaller. The effect of the wave shadow only starts to appear in the shallow waters associated over the outer longshore bar. Beyond the reduction in bed shear over the outer longshore bar at the seaward end of the barge, the lack of change in bed shear stress at the seaward end of the barge, shows the access dredge has no effect on the outer longshore bar.
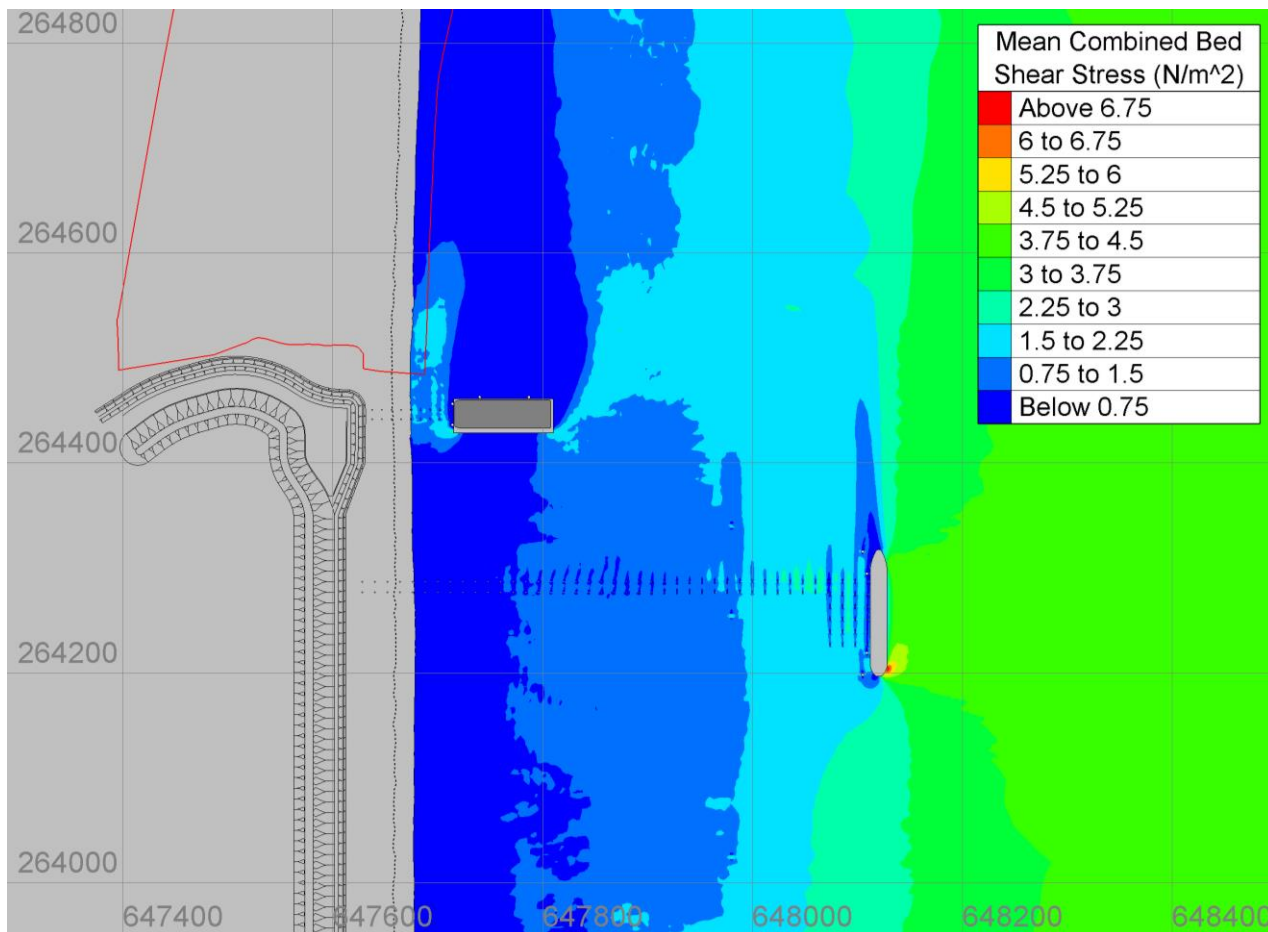
Figure 57: Mean combined bed shear stress (τ_m) for the temporary and permanent BLF structures plus grillage, access dredge, barge and ship (0.5 m SE wave, peak ebb).
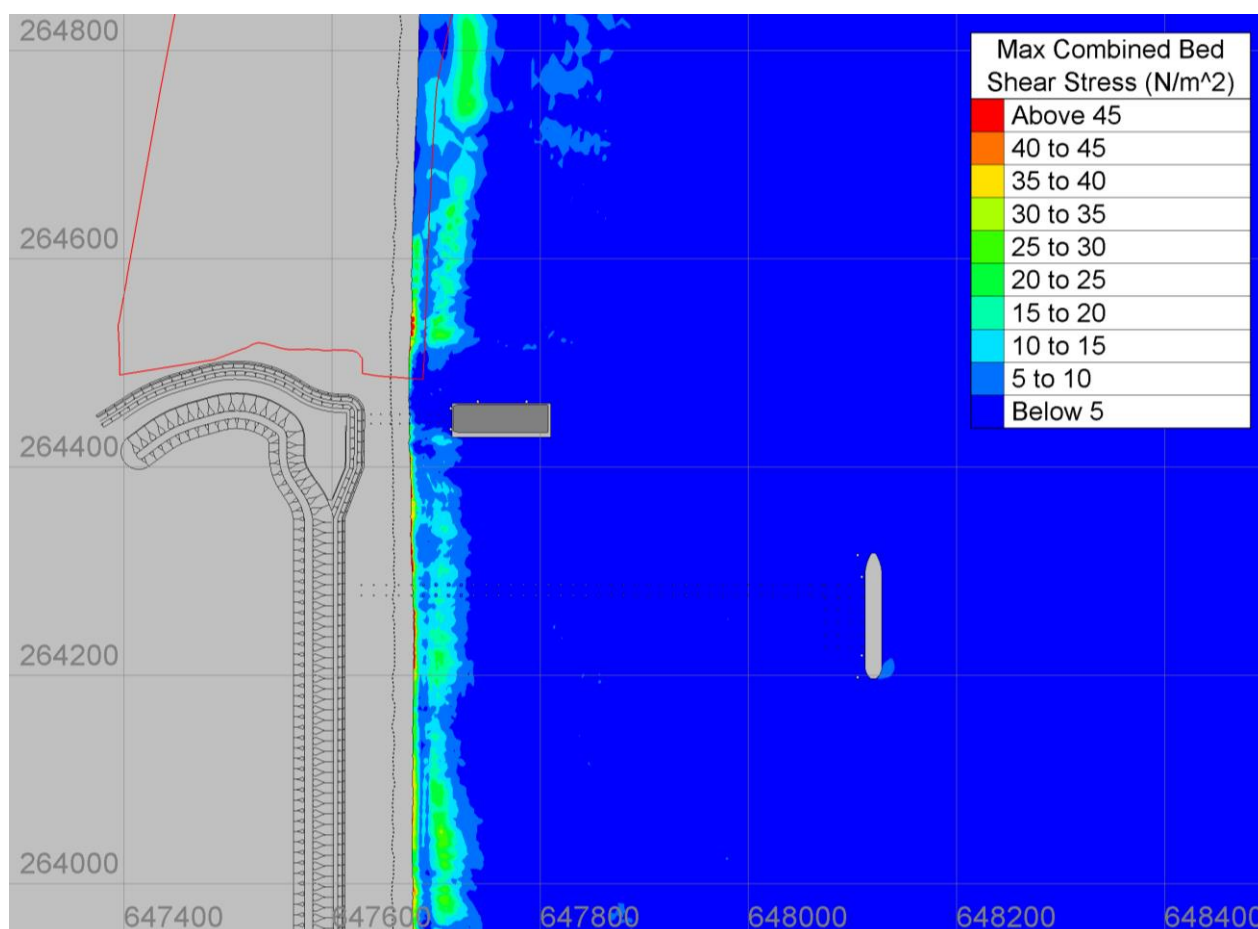
Figure 58: Maximum combined bed shear stress (τ_{max}) for the temporary and permanent BLF structures plus grillage, access dredge. Barge and ship (0.5 m SE wave, peak ebb).

Despite the increase in the current induced bed shear stress shoreward of the barge and grillage (Figure 55), results show, in Figure 58, that blockage effect to the waves leads to an overall reduction in bed shear stress between the shoreline and the barge. This is because the wave induced bed shear stress is significantly larger in the shallow waters than the current induced bed shear stress, even with a 0.5 m wave.

The reduction in bed shear stress along the inner longshore bar between the barge and the shore is up to 15-20 N/m² (Figure 59), compared to a baseline of 20-25 N/m². There is no area where a reduction in bed shear stress reduces below the critical threshold. The absolute bed shear stress is still 10-14 times larger than the critical threshold in this area. A 10-20 N/m² reduction in bed shear stress shoreward of the end of the barge extends 40 m into the Minsmere SPA/SAC frontage, whilst a small 1-4 N/m² increase extends a further 235 m. The baseline bed shear stress along the Minsmere SPA/SAC frontage is 20-40 N/m².

The patchwork of alternating bed shear stress due to the piles would change continuously with the state of the tide and direction of waves. These conditions are variable with the state of tide and waves, meaning the peak impact shown in the model results is not persistent over a tidal cycle. Furthermore, there are no areas of change within the model where a reduction in bed stress reduces below the critical threshold or an increase above the threshold where it was not previously. Patches of altered bed shear stress along the shoreline are

sufficiently small in magnitude and scale that they are not expected to cause detectable change to the shoreline.

Figure 59: Magnitude of change in maximum bed shear stress for the temporary and permanent BLF structures with the grillage, access dredge, barge and ship (0.5 m SE wave, peak ebb).

4.8   Permanent BLF structures only – SZC operational phase

To investigate the effect of the permanent BLF only (SZC operational phase), the peak ebb velocities, wave energy and bed shear stress results were compared to the baseline conditions with a 1 in 20 year return interval wave. This scenario will occur during the operational phase when the permanent BLF is not in use.

4.8.1   Tidal current induced bed shear stress

To highlight the influence of the BLF piles, Figure 60 shows the flow velocities around permanent BLF and Figure 61 shows the difference in velocities compared to the baseline. These figures show that the permanent BLF very slightly interrupts the shore parallel flow. There is a small decrease in the tidal currents in the lee of the piles, with flows returning to within 0.1 m/s within 4 m. There is also a minor increase in flows created shoreward of the mooring fenders. The reduction in tidal flows along the temporary BLF is very small.

Figure 62 shows the current-only (τ_c) bed shear stress during peak ebb currents. The effect of the BLF piles on the bed shear stress can be seen to be very localised around the jetty piles, due to the reduction caused by the scour pits around each pile.

TR543 MODELLING OF THE TEMPORARY AND PERMANENT BLF AT SZC

NOT PROTECTIVELY MARKED
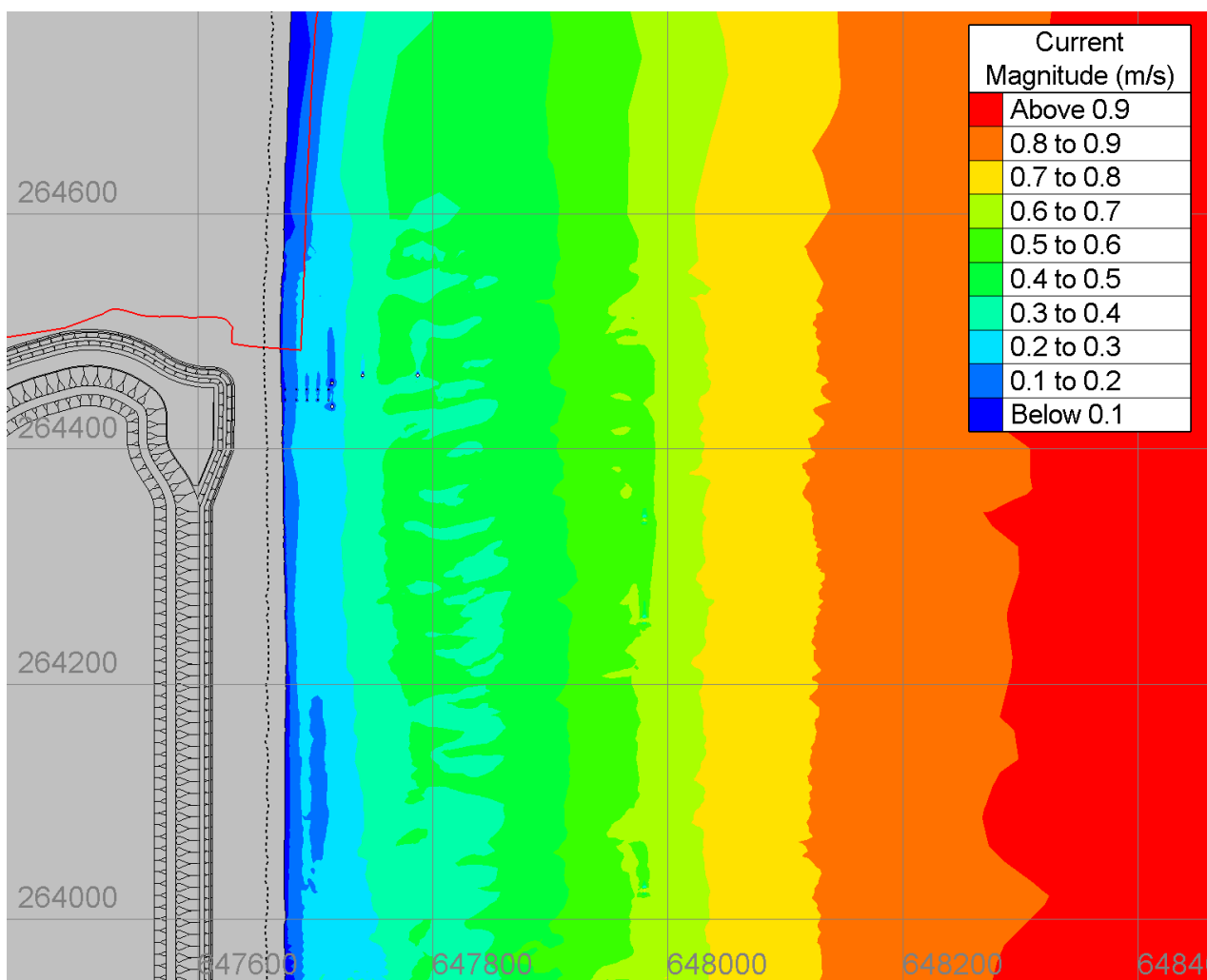
Figure 60: Peak ebb velocities around permanent BLF only.

TR543 MODELLING OF THE TEMPORARY AND PERMANENT BLF AT SZC

NOT PROTECTIVELY MARKED
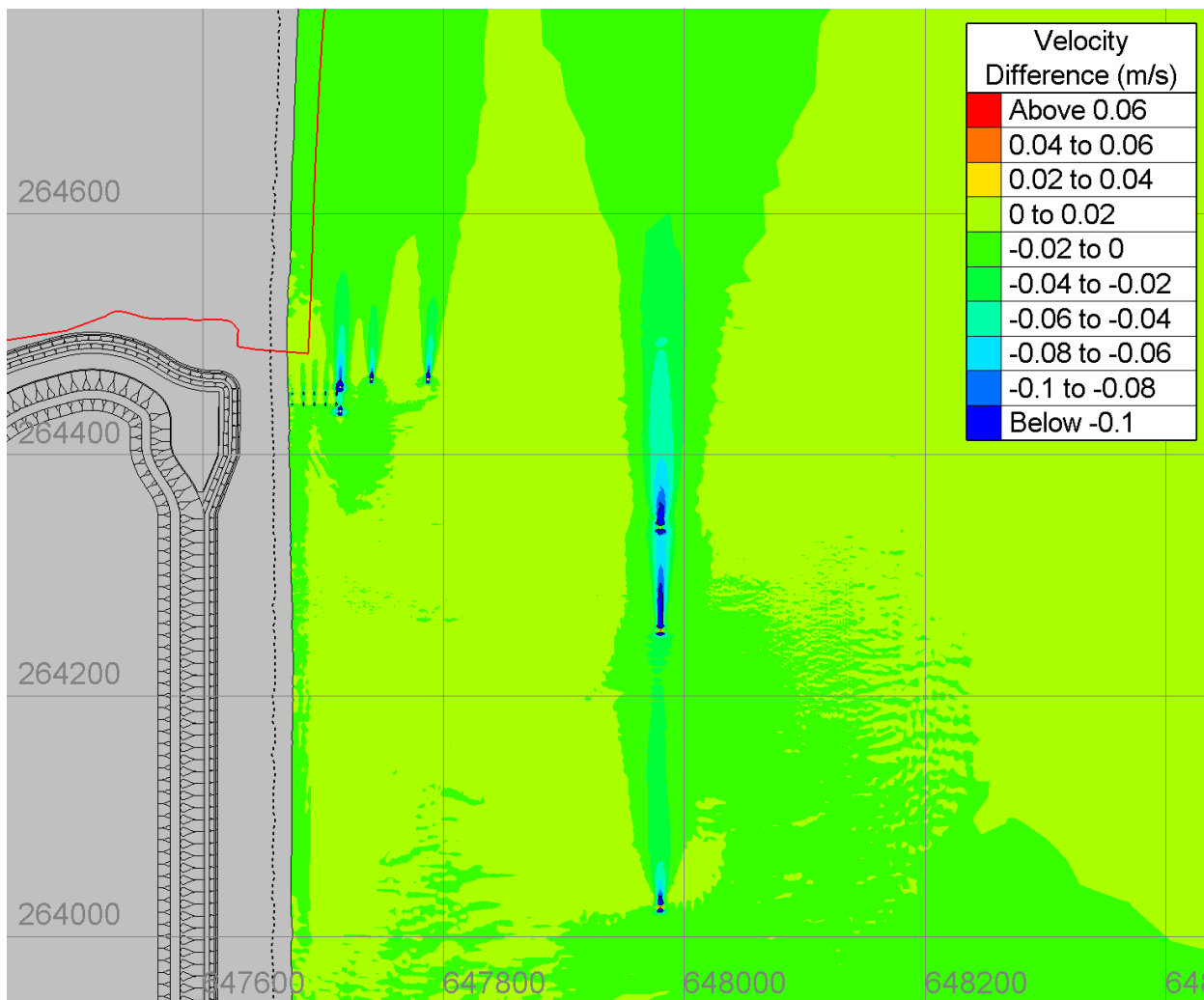
Figure 61: Difference in peak ebb velocity between the permanent BLF only and baseline case.

TR543 MODELLING OF THE TEMPORARY AND PERMANENT BLF AT SZC

NOT PROTECTIVELY MARKED
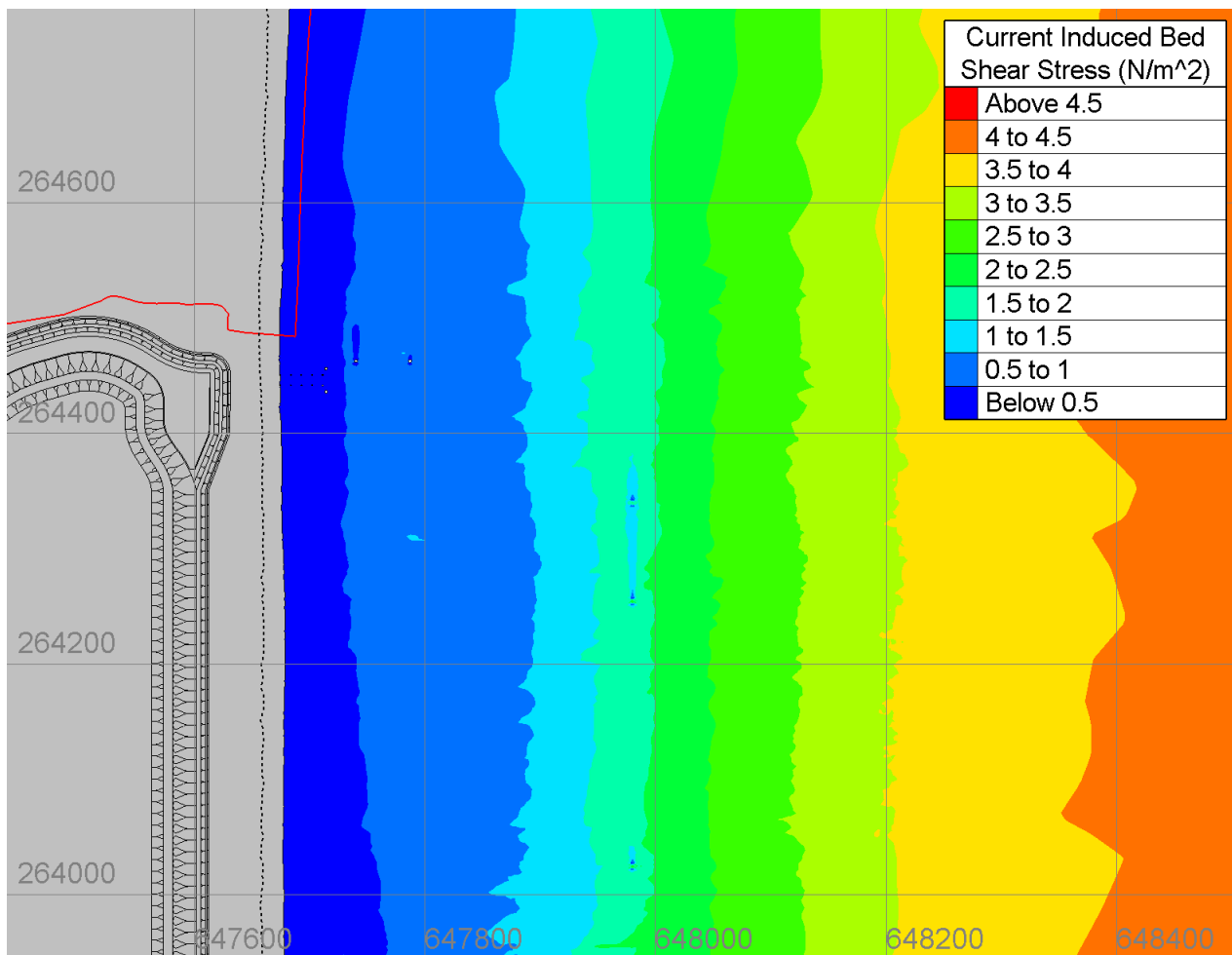
Figure 62: Current-only (τ_c) bed shear stress for the permanent BLF only (peak ebb).

TR543 MODELLING OF THE TEMPORARY AND PERMANENT BLF AT SZC

NOT PROTECTIVELY MARKED
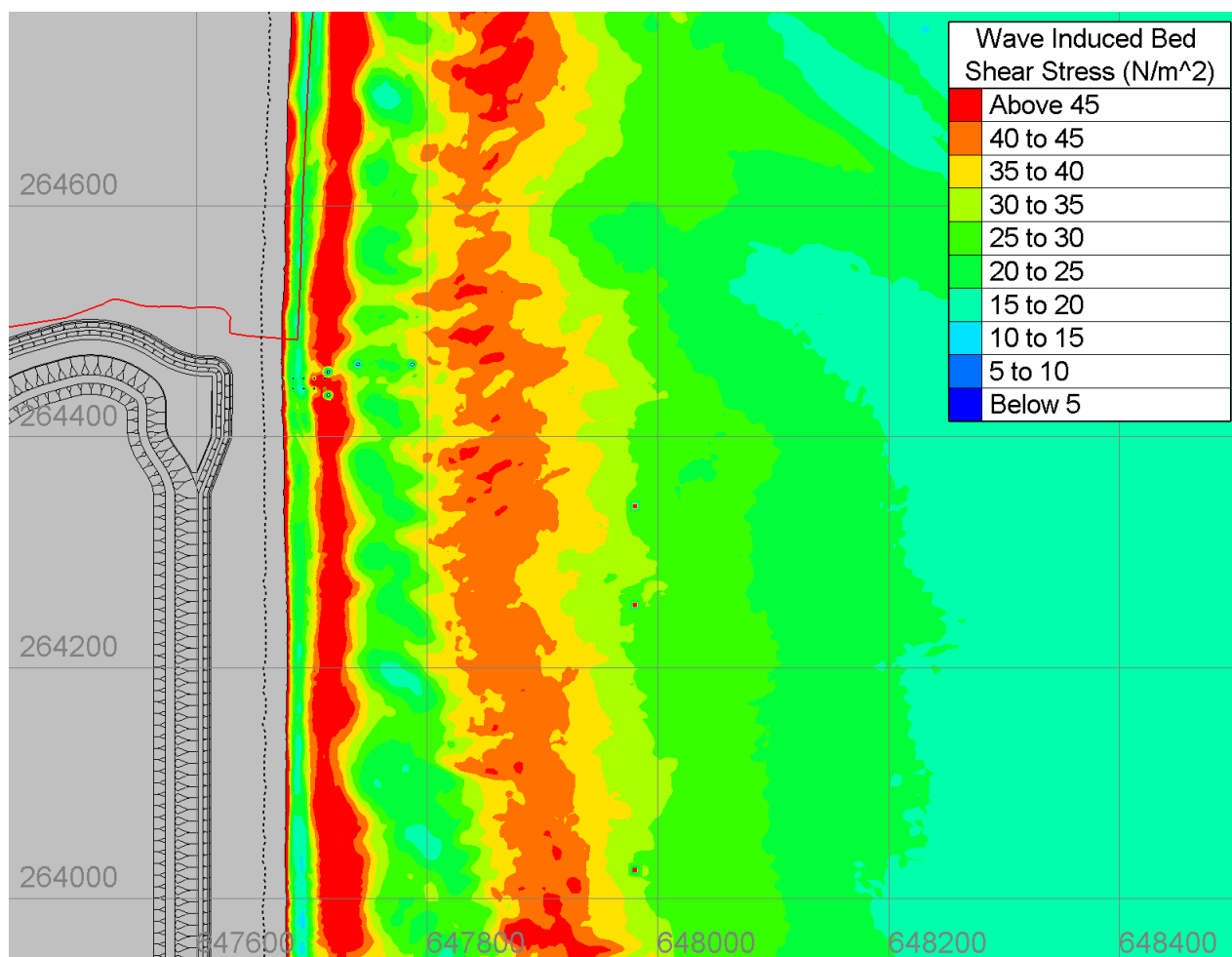
Figure 63: Wave-only (τ_w) bed shear stress for the permanent BLF only (1 in 20 year SE wave, peak ebb).

4.8.2   Wave induced bed shear stress

Figure 63 shows wave-only (τ_w) bed shear stress for the permanent BLF structures only for a 1 in 20 year SE wave during peak ebb. The effect of the jetty piles on the wave induced bed shear stress is very localised around the piles, with reductions in τ_w for approximately 3-5 m from the centre of the piles and fenders, respectively.

4.8.3   Combined wave and current bed shear stress

Figure 64 and Figure 65 show the mean (τ_m), and maximum (τ_{max}) combined bed shear stresses, respectively, for the permanent BLF only run. Figure 66 shows the effect on the combined bed shear stress as represented by a difference in magnitude. Results show that the baseline bed shear stresses over entire model domain are above the critical threshold of motion (0.216 N/m^2).

The spatial pattern of the magnitude of change of the permanent BLF only is almost the same as the combination of the permanent and temporary BLF. There is a small increase in bed shear stress of 2-5 N/m^2 extending 130 m into the Minsmere SPA/SAC, but this is very small compared to the baseline bed shear stresses of 40-60 N/m^2. That is, the baseline condition is 185 to 277 times larger than the critical threshold,

TR543 MODELLING OF THE TEMPORARY AND PERMANENT BLF AT SZC

NOT PROTECTIVELY MARKED

meaning the subtidal sediment is already in motion. The small increase in bed shear stress is well within natural variation along the frontage.

The BLF piles are transmissive and would not block sediment transport. The peak increase in bed shear stress within the permanent BLF is 11 N/m^2 compared to a baseline of 50 N/m^2 in that location. The patchwork of increased and decreased bed shear stress due to the piles are dependent on the state of the tide and direction of waves. These conditions vary with the state of tide and waves, meaning the peak impact is not persistent over a tidal cycle. There are no areas of change within the model where a reduction in bed stress reduces below the critical threshold or an increase above the threshold where it was not previously. Patches of altered bed shear stress are sufficiently small in magnitude and scale that they are not expected to cause detectable change to the shoreline.
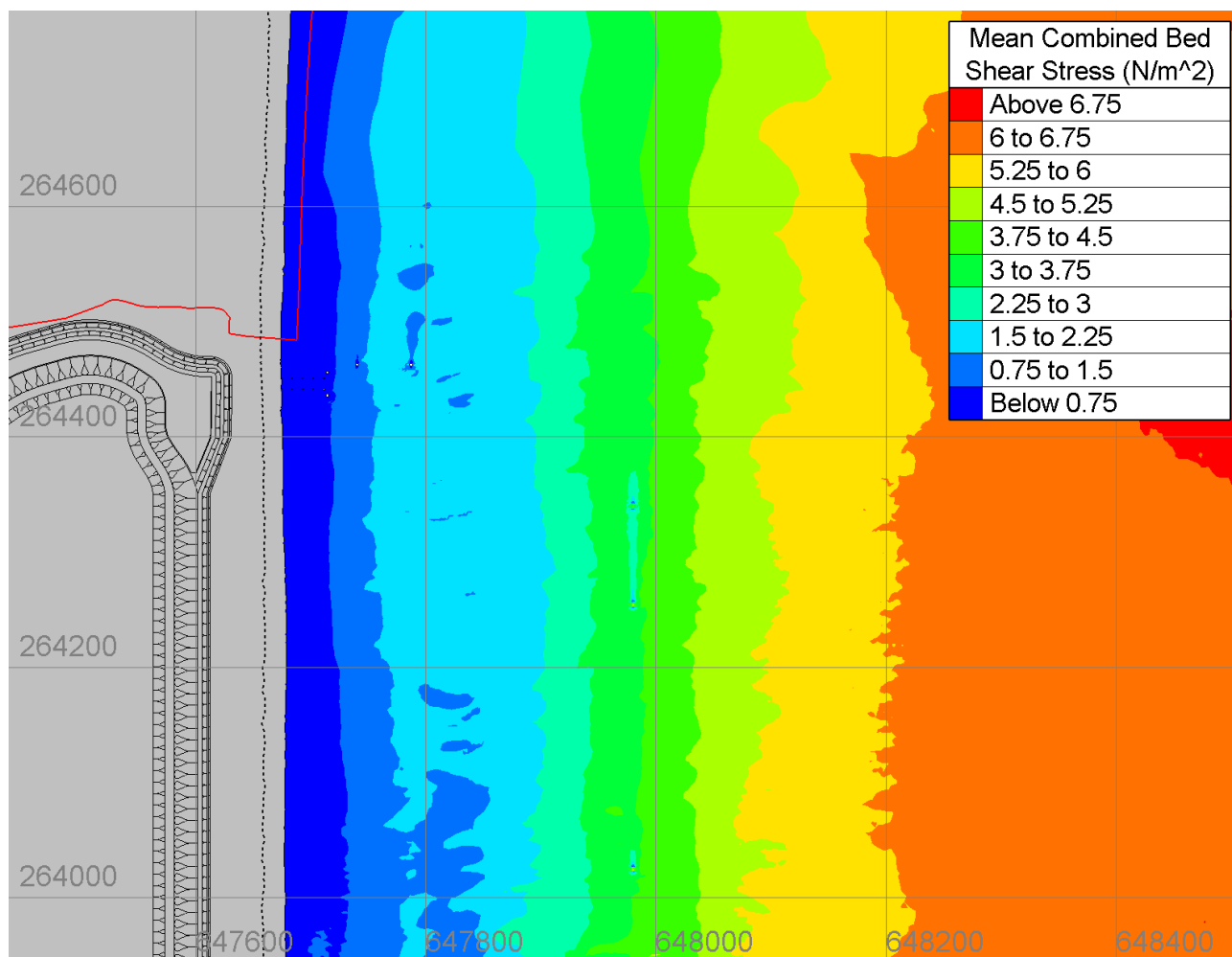
Figure 64: Mean combined bed shear stress (τ_m) for the permanent BLF only (1 in 20 year SE wave, peak ebb).

TR543 MODELLING OF THE TEMPORARY AND PERMANENT BLF AT SZC

NOT PROTECTIVELY MARKED
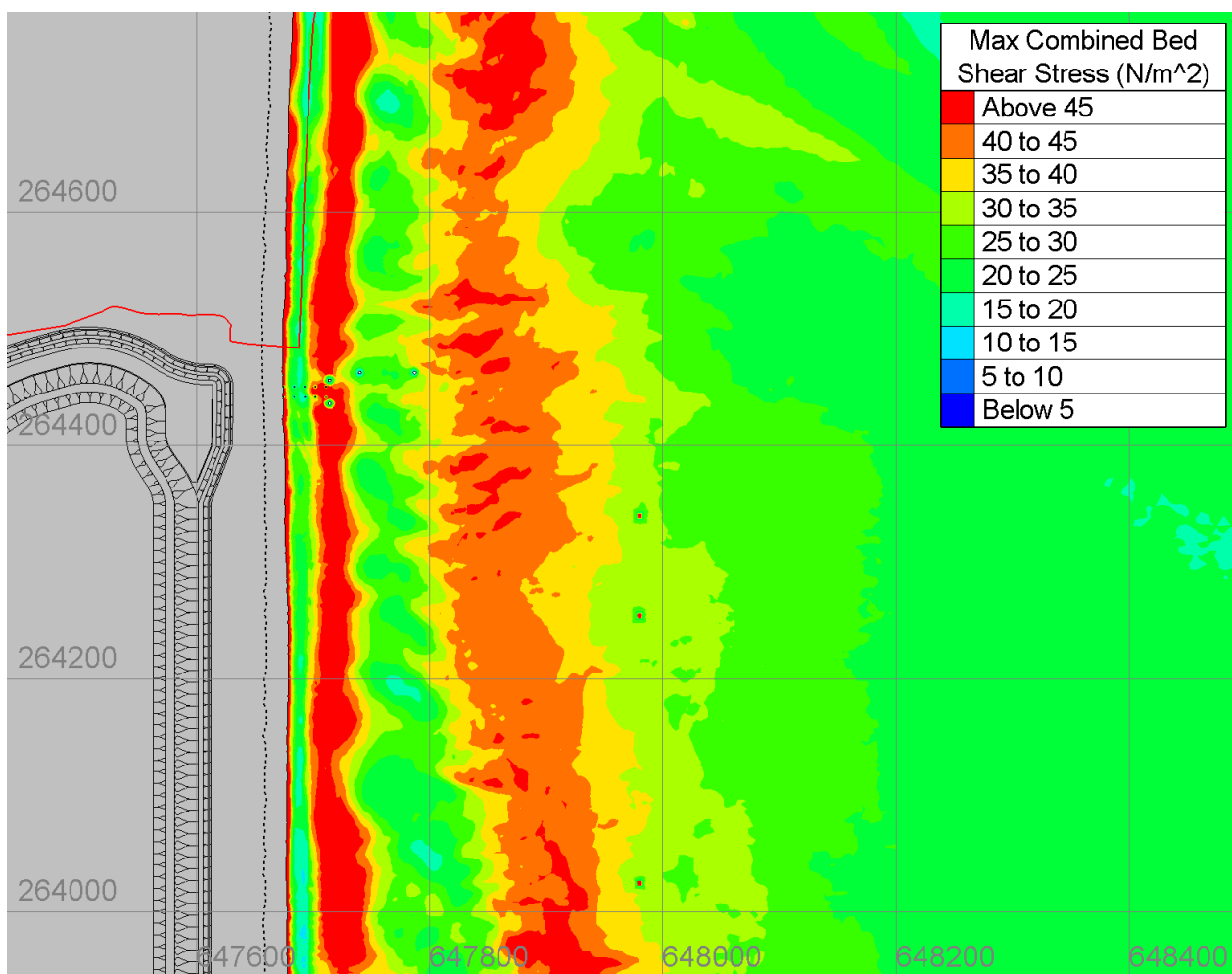
Figure 65: Maximum combined bed shear stress (τ_{max}) for the permanent BLF only (1 in 20 year SE wave, peak ebb).
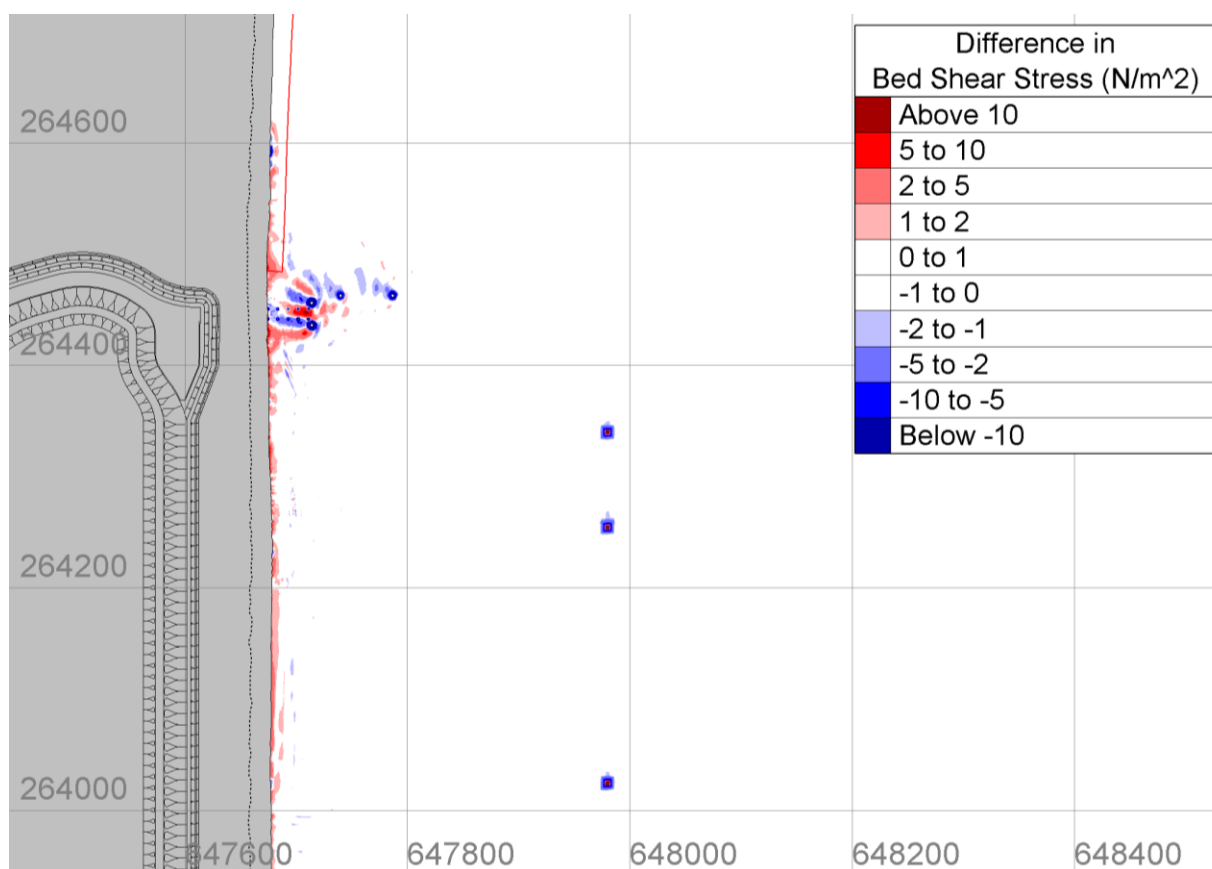
Figure 66: Magnitude of change in maximum bed shear stress for the permanent BLF only (1 in 20 year SE wave, peak ebb).

4.9   Permanent BLFs with grounding pocket and access dredge

To investigate the effect of the permanent BLF jetty and the reprofiled bed for the grounding pocket and navigational access, the peak ebb velocities, wave energy and bed shear stress results were compared to the baseline conditions with a 1 in 20 year return interval wave. This scenario is for the BLF use once every five to ten years during the operational phase.

4.9.1   Tidal current induced bed shear stress

To highlight the influence of the BLF piles, Figure 67 shows the flow velocities around the permanent BLF with Figure 68 showing the difference in velocities compared to the baseline.

Figure 67 and Figure 61 show that the grounding pocket only causes a minor change in the tidal currents, with a 0.1 m/s reduction within the deepest area of the grounding pocket and less than 0.1 m/s increase at the edges of the grounding pocket. The permanent BLF only slightly interrupts the shore parallel flow. With the addition of the grounding pocket, the small reduction in the less of the last row of piles and fenders returns to within 0.1 m/s within 10 m.

Figure 69 shows the current-only (τ_c) bed shear stress for the permanent BLF structures plus grounding pocket and access dredge during peak ebb. The effect of the grounding pocket on the bed shear stress can be seen to be very localised to the deeper parts of the grounding pocket, along with the northern and southern edge of the pocket. The access dredge shows very little effect of the current induced bed shear stress.

TR543 MODELLING OF THE TEMPORARY AND PERMANENT BLF AT SZC

NOT PROTECTIVELY MARKED
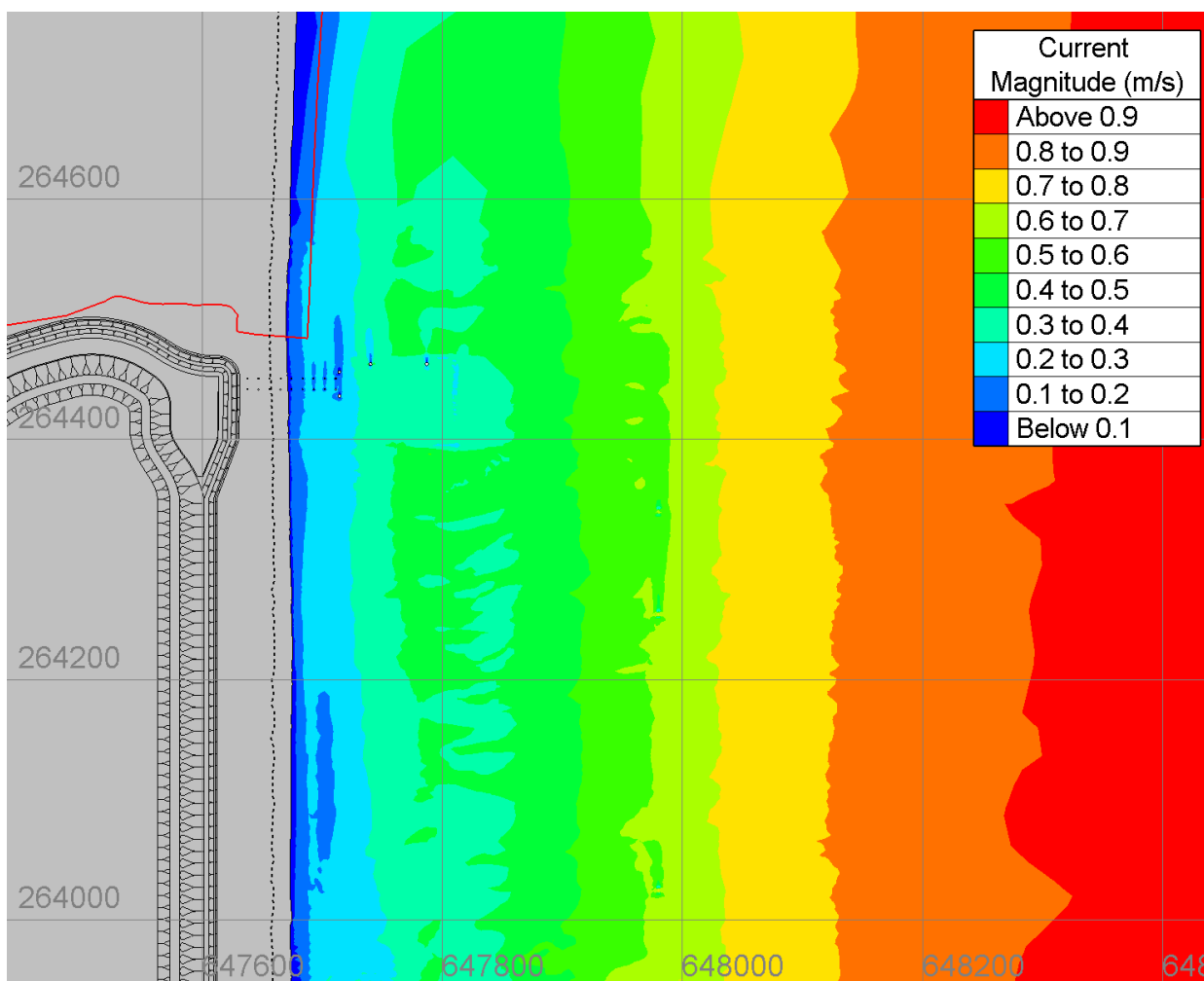
Figure 67: Peak ebb velocities around permanent BLF plus grounding pocket and access dredge.

TR543 MODELLING OF THE TEMPORARY AND PERMANENT BLF AT SZC

NOT PROTECTIVELY MARKED
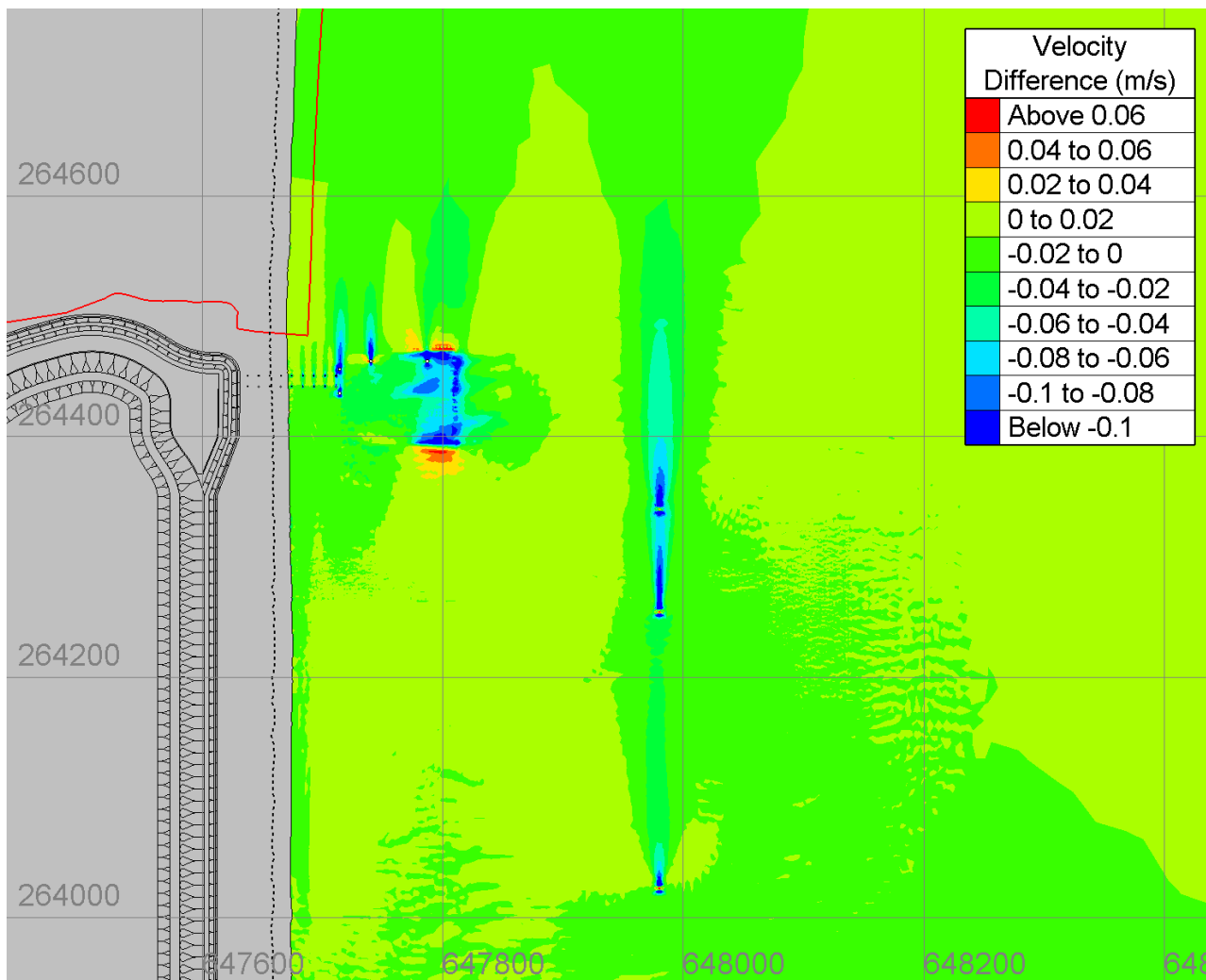
Figure 68: Difference in peak ebb velocity between the permanent BLF plus grounding pocket and access dredge and baseline case.
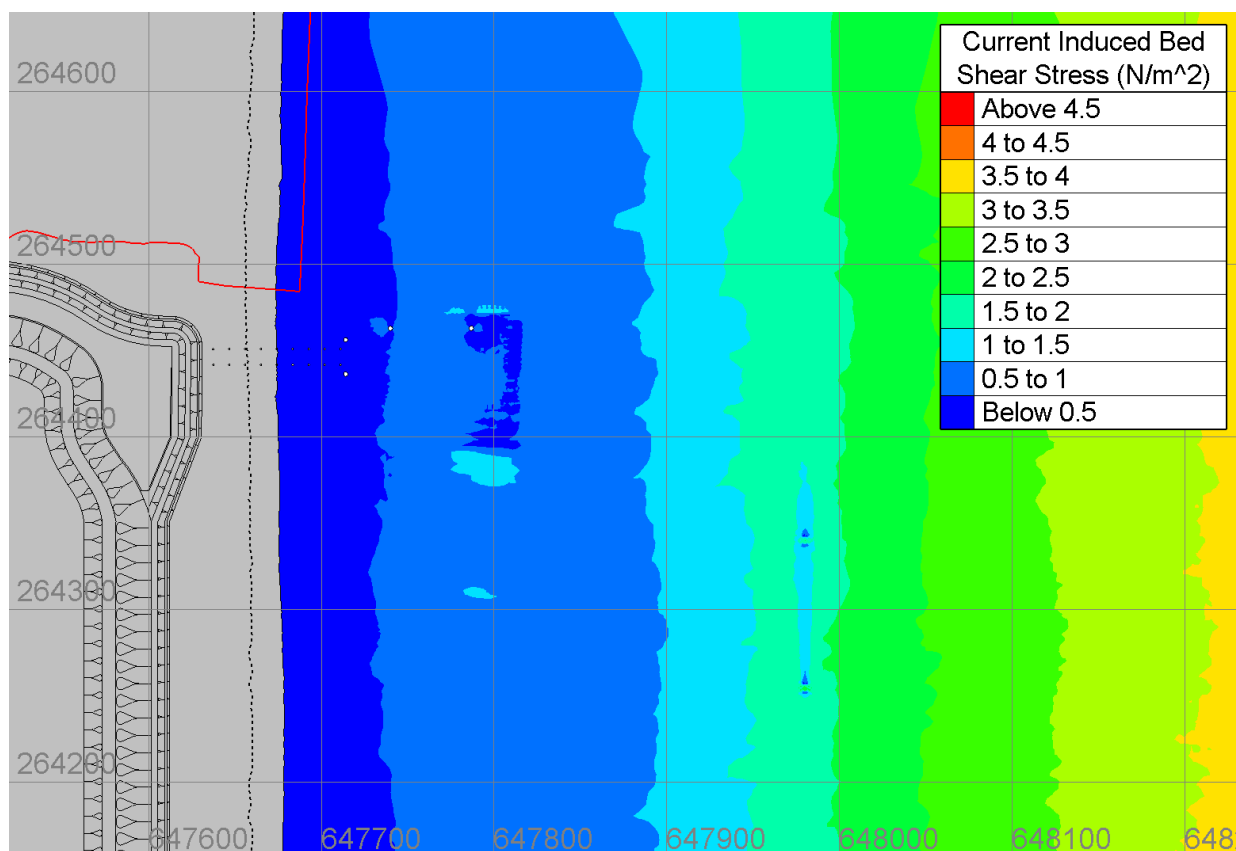
Figure 69: Current-only (τ_c) bed shear stress for the permanent BLF plus grounding pocket and access dredge (peak ebb).

4.9.2   Wave induced bed shear stress

Figure 70 shows wave-only (τ_w) bed shear stress for the permanent BLF plus the grounding pocket and access dredge for a 1 in 20 year SE wave during peak ebb.

The effect of the grounding pocket is a reduction in wave induced bed shear stress between the inner and outer longshore bars within the grounding pocket, along with a reduction in bed shear stress along 40 m of the inner bar north of the permanent BLF. For the larger wave heights associated with the 1 in 20 year return interval, the access dredge also shows a reduction in wave induced bed shear stress along the outer bar. This is in contrast to the smaller wave height of 0.5 m considered when the access dredge is required for the barge present scenarios, in Section 4.6 and 4.7, where the access dredge shows no discernible effect.
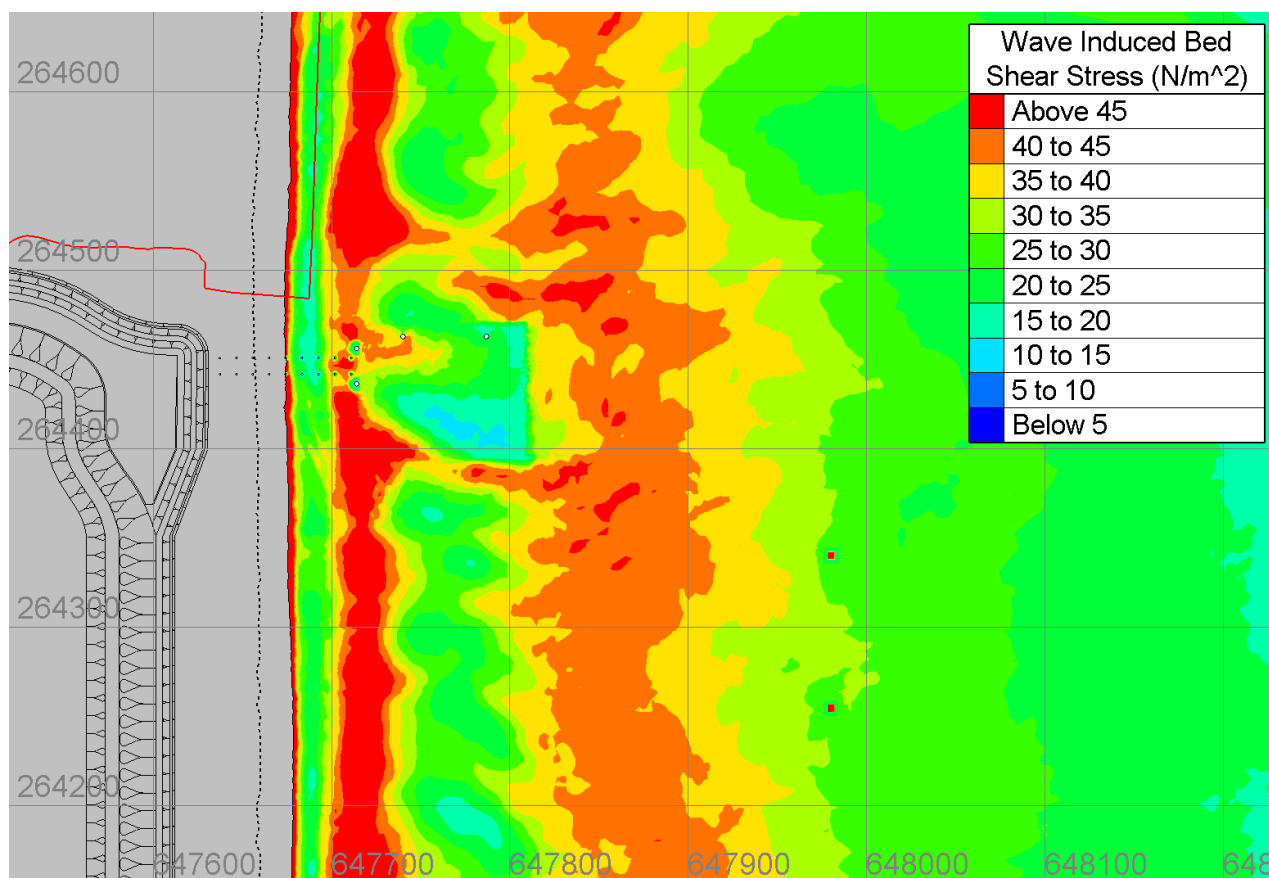
Figure 70: Wave-only (τ_w) bed shear stress for the permanent BLF plus grounding pocket and access dredge (1 in 20 year SE wave, peak ebb).

4.9.3   Combined wave and current bed shear stress

Figure 71 and Figure 72 show the mean (τ_m), and maximum (τ_{max}) combined bed shear stresses, respectively, for the permanent BLF plus the grounding pocket and access dredge run. Figure 73 shows the effect on the combined bed shear stress as represented by a difference in magnitude. Results show that the baseline bed shear stresses over entire model domain are above the critical threshold of motion (0.216 N/m²).

TR543 MODELLING OF THE TEMPORARY AND PERMANENT BLF AT SZC

NOT PROTECTIVELY MARKED
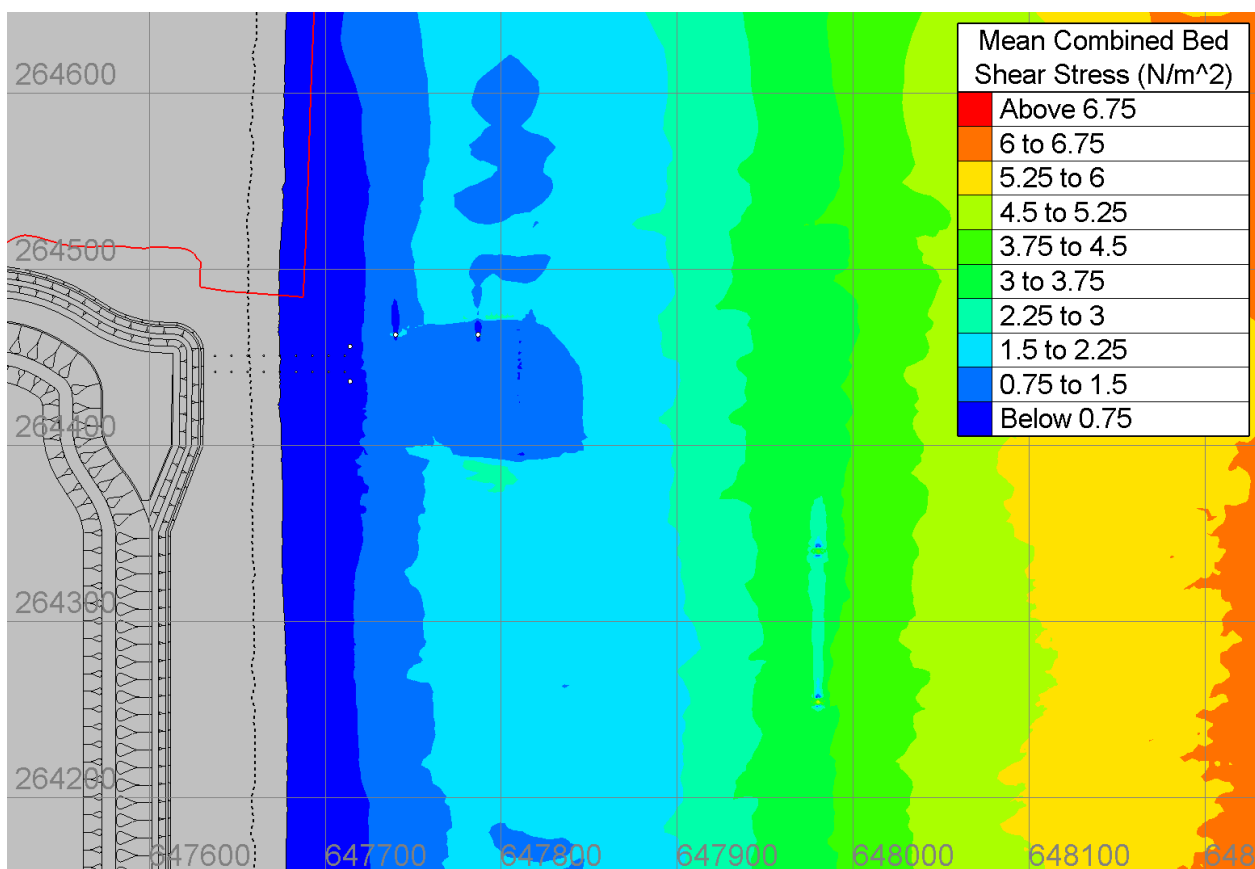
Figure 71: Mean combined bed shear stress (τ_m) for the permanent BLF plus grounding pocket and access dredge (1 in 20 year SE wave, peak ebb).

TR543 MODELLING OF THE TEMPORARY AND PERMANENT BLF AT SZC

NOT PROTECTIVELY MARKED
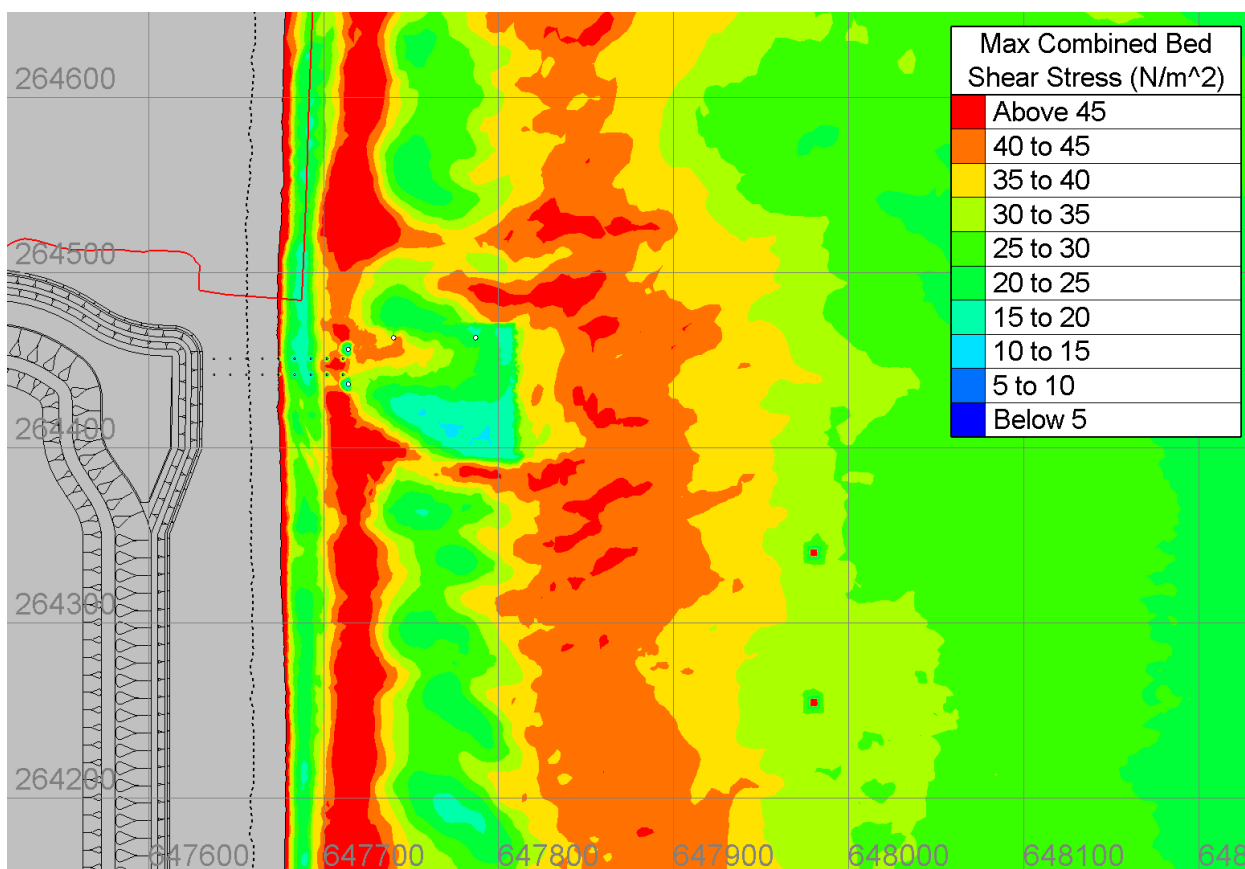
Figure 72: Maximum combined bed shear stress (τ_{max}) for the permanent BLF plus grounding pocket and access dredge (1 in 20 year SE wave, peak ebb).

NOT PROTECTIVELY MARKED
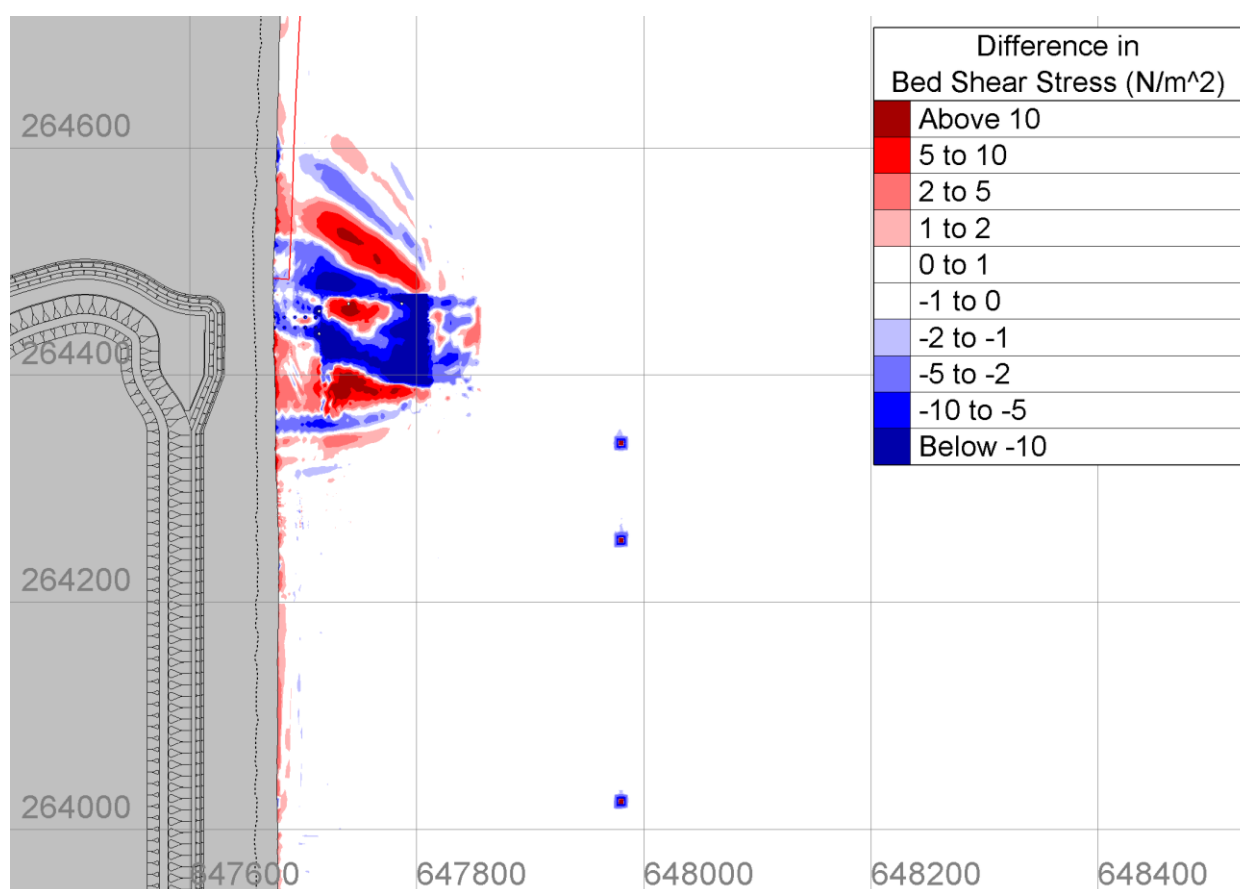
Figure 73: Magnitude of change in maximum bed shear stress for the permanent BLF plus grounding pocket and access dredge (1 in 20 year SE wave, peak ebb).

For the 1:20 year wave height, the access dredge does show an effect on the outer longshore bar. The patchiness of the change on the outer bar is due its spatial varying height being clipped to a constant depth of -3.5 m ODN.

Due to modification of bathymetry, the grounding pocket leads to an alternating pattern of increased/decreased in bed shear stress. The deepest parts of the grounding pocket show a reduction in bed shear stress of 10-15 N/m^2, whilst the shallowest areas have an increase of 8-10 N/m^2. The baseline within the grounding pocket is 25-30 N/m^2. There is no area where a reduction in bed shear stress reduces below the critical threshold.

A small 2-5 N/m^2 reduction in bed shear stress extends 35 m onto the Minsmere SPA frontage, followed by a small 3-6 N/m^2 increase for a further 195 m. The baseline bed shear stress along the Minsmere SPA/SAC frontage is 40-60 N/m^2. As the sediment is already substantially in motion, such small changes will not register detectable change at the bed.

The patchwork of alternating bed shear stress due to the grounding pocket would change continuously with the state of the tide and direction of waves. These conditions are variable with the state of tide and waves, meaning the peak impact shown in the model results is not persistent over a tidal cycle. Furthermore, reprofiling the grounding pocket would occur very infrequently during the operational phase, every 5-10 years. Therefore, it would have no effect on the shoreline.

5 Discussion

The effects of all the combinations of temporary and permanent BLFs have been assessed against the absolute change in combined wave and current bed shear stress, and comparison against entrainment thresholds and baseline conditions. An increase in bed shear stress does not necessarily mean an increase in erosion nor does a decrease necessarily mean an increase in deposition of sediment. From a coastal geomorphology perspective, any changes in absolute bed shear stress need to be considered with respect to the critical bed shear stress.

Along the Minsmere SPA/SAC frontage, the patchwork of increased and decreased bed shear stress due to the structures and vessels are dependent on the state of the tide and direction of waves. Furthermore, the peak impact shown by the models does not persist over a tidal cycle. There are no areas of change where a reduction in bed stress reduces below the critical threshold or an increase above the threshold where it was not previously prior to the modelled impacts. All changes along the Minsmere SPA/SAC frontage are within natural variation and unlikely to be distinguished from background conditions. The patches of altered bed shear stress are sufficiently small in magnitude and scale that they are not expected to cause detectable change to the shoreline.

The presence of the ship at the temporary BLF causes a reduction in bed shear stresses in the ship's lee which are up to an order of magnitude, are close to baseline values at its peak and extend across approximately 200 m of the beach frontage. The degree of reduction from the wave shadow lessens closer to the shore. However, the wave shadow never reduces below the critical threshold and sediment will remain entrained. For example, despite a 20 N/m^2 reduction, the absolute bed shear stress along the outer longshore bar is still 45 times larger than the critical threshold.

As bed shear stress drives the turbulence that maintains sediment in suspension, i.e. suspended sediment concentrations (SSC) rise with bed shear stress, a reduction in bed shear stress will mean less sediment in suspension. Therefore, a reduction in bed shear stress means less change or bed erosion than that which would naturally occur. In the case of the ship present at the temporary BLF, the relative higher areas of bed shear stress compared to baseline adjacent to the wave shadow could lead to a tendency for erosion with less erosion in the shadow (all areas in the shadow are still above critical threshold, so sediment mobilisation is still occurring). Whilst this tendency could form a salient, it is considered very unlikely that a salient would form.

The differences in bed shear stress along the shoreline are small compared to baseline, meaning that deposition and salient formation is very unlikely, as a long period of persistent wave conditions (non-varying, directionally) would be required. The following rationale further illustrates why salient formation is unlikely (or at best very small and short lived:

▶ The differences in bed shear stress are slight and shown for the maximum wave height condition. The differences lessen further with a reduction in wave height.

▶ Variation in wave directions would mean any tendency for deposition would be constantly moving, and so any small accumulation would be readily dispersed.

▶ Ships are not present all of the time, and least in winter when bed shear stress difference would be greatest. When ships are absent the reduction in stress would disappear.

TR543 MODELLING OF THE TEMPORARY AND PERMANENT BLF AT SZC

NOT PROTECTIVELY MARKED

▶ Treating the ship as a breakwater, which ignores the fact that it is buoyant, will heave with the waves, and is not grounded, provides a useful worst case. This approach shows that for a unidirectional wave climate (again conservative as Sizewell is bi-directional), the ratio of the ship's length (120 m) to its distance from shore (450 m) is 0.267, which is substantially less than the 0.5 value below which no deposition (i.e. a salient) is expected to occur (Nir, 1982). This aligns with, for example, local observations at Sea Palling, where multiple segmented breakwaters 150 m long and 230 m from shore (a ratio of 0.65, corresponding to predicted salient formation) only produce small salients at 230 m from shore compared to the ship at 450 m.

In summary, therefore, salient formation is very unlikely and, were it to occur, would amount to very small transient feature. As the differences in bed shear near the shore are very subtle and shown to be incapable of salient formation for several reasons, they would also not affect longshore transport in a detectable way.

As a salient formation is very unlikely and that longshore transport will not be affected, the BLFs and associated structures and vessels are not considered to act as a potential barrier to the restorative processes of the beach following natural erosion over the winter. The recovery phases of the beach and the landward movement of sand occur mainly during summer months when the waves are lower, meaning the reduction due to the presence of the ship is very small. Furthermore, the presence of the ship is lowest during the winter period when the effect shown would be most pronounced. Whilst it is possible the wave shadow could temporarily reduce SSC, there is a lag in between storms and SSC potentially by days. As such, there is still sediment available after a storm for inner and outer bars to recover as the wave heights fall and the effect of the shadow reduces.

For all of the scenarios considered in this report, the BLF structures and their associated activities are not considered to result in any detectable change to bed levels along the shoreline. Therefore, there would be no change beyond natural processes to the supratidal beach. As a result, there will be no additional change to the 'annual vegetation of drift lines' habitat (Minsmere to Walberswick Heaths and Marshes SAC) or the potential nesting sites for little tern (*Sterna albifrons*) (Minsmere to Walberswick SPA). The assessment of the impact on the annual vegetation drift lines or potential nesting sites is not conducted in this report but will be conducted in the shadow Habitats Regulation Assessment (HRA).

6 Summary

The effect of the temporary and permanent BLFs, grillage, dredging and presence of a ship and/or a barge on bed shear stress has been investigated using the ARTEMIS and TELEMAC2D models. The objective of this work was to investigate the impacts of the temporary and permanent BLFs, and associated activities (grillage, dredging, a ship at the temporary BLF and a barge at the permanent BLF), in all possible combinations, as the BLFs would be used in different ways at different times. The aim was to verify the conclusions of the updated EIA in the ES Addendum. Nine different combinations of the structures and vessels were investigated representing all possible combinations during the construction and operational phases. The magnitude of change in the absolute bed shear stress was calculated for each case and compared in consideration of the critical bed shear stress.

The shape and size of the BLF piles and fenders/dolphins, based on the design information supplied by SZC Co., were introduced into the ARTEMIS and TELEMAC2D models on a very fine scale mesh (20 cm). The numerical models were used to predict the effect of the jetty piles (including scour), vessels and reprofiled bed on the wave climate, current field and associated bed shear stresses.

For each of the nine combinations of structures and vessels, four scenarios were considered in ARTEMIS with different combinations of wave heights, wave direction and water levels (coincident with peak flood and ebb tidal conditions, extracted from TELEMAC2D results). In total, 58 wave and tide scenarios were modelled, including the baseline conditions with no structures or vessels.

In all the meshes, except for the baseline mesh, the presence of the Combined Drainage Outfall (CDO) and the two Fish Recovery and Return outfalls (FRR) has been included. Whilst the construction of the CDO and FRRs may not temporally overlap the use of the temporary BLF jetty, the structures have been included as a worst case.

The bed shear stress changes were estimated for all scenarios and a detailed analysis was presented for the scenario corresponding to the worst-case impact, defined as the greatest magnitude change, which was from south-easterly waves with peak ebb tidal currents (and its associated water level). Three wave heights were considered depending on whether the ship or barge was present: a 1 in 20 year return interval wave height (no vessels), 1.5 m (working limit of the ship) and 0.5 m (working limit of the barge).

For all scenarios considered, results show that the baseline bed shear stresses over entire model domain are above the critical threshold of motion ($0.216 \ N/m^2$). There are no areas of change within the model where a reduction in bed stress reduces below the critical threshold or an increase above the threshold where it was not previously.

For the temporary and permanent BLF piles only, there is an area of very small increase in bed shear stress ($2\text{-}5 \ N/m^2$) extending 140 m into the Minsmere SPA/SAC. This increase in bed shear stress is small compared to baseline conditions ($40\text{-}60 \ N/m^2$) and is well within natural variation along the Minsmere SPA/SAC frontage and unlikely to result in a detectable topographic change. The introduction of the permanent BLF leads to an alternating increase/decrease in bed shear stress along the shore, as the waves and flow interact with the permanent BLF structure. The BLF piles are transmissive and would not block sediment transport. There is an increase in bed shear stress within the permanent BLF with a peak of $11 \ N/m^2$ compared to a baseline of $50 \ N/m^2$ in that location. The temporary BLF causes a $2\text{-}3 \ N/m^2$ reduction in the leeward side of the structure from the prevailing wave direction with an $2\text{-}3 \ N/m^2$ increase in bed shear stress on the windward side of the structure. The baseline bed shear stress in this particular area is $30\text{-}40 \ N/m^2$.

NOT PROTECTIVELY MARKED

The patchwork of alternating bed shear stress due to the piles would change continuously with the state of the tide and direction of waves. These conditions are variable with the state of tide and waves, meaning the peak impact shown in the model results is not persistent over a tidal cycle. Patches of altered bed shear stress are sufficiently small in magnitude and scale that they are not expected to cause detectable change to the shoreline.

The presence of the CDO and FRR structures also show no detectable change in bed shear stress beyond their immediate scour pits and show no interaction with the temporary or permanent BLF.

The grillage, used for approximately four years at the permanent BLF, increases the area of changed bed shear stress compared to the BLF jetty piles alone. Inside of the inner longshore bar, there is an area of increased bed shear stress of 3-6 N/m^2 extending 245 m into the Minsmere SPA/SAC. This is similar in magnitude of change compared to the BLF structures only, albeit over a slightly longer frontage of the Minsmere SPA/SAC. In the lee of the grillage, there is an area of reduction of 15-22 N/m^2 extending approximately 45 m over the inner longshore bar. The baseline condition in this particular area is 40-50 N/m^2. The BLF piles are transmissive and would not block sediment transport. Whilst the shoreward end of the grillage sits above the bed, deflecting currents shoreward, the grillage does not act as a blockage as currents still pass over the top This leads to an increase amongst the final pairs of jetty piles of the permanent BLF. The peak increase in bed shear stress at the permanent BLF is 8-15 N/m^2 compared to a baseline of 30-45 N/m^2 in that location. However, that very localised increase is still within the wider baseline variation along the Sizewell C frontage of 30-65 N/m^2 (for a 1 in 20 yr wave height). Much like the BLF structures alone, the grillage and jetty piles create a patch work of increased and decreased bed shear stress which are dependent on non-persistent and variable state of the tide and direction of waves. Patches of altered bed shear stress are sufficiently small in magnitude and scale that they are not expected to cause detectable change to the shoreline.

The introduction of the ship at the temporary BLF combined with the permanent BLF (without grillage or dredging) results in reduction in bed shear stress in the lee of the prevailing wave direction. The ship is treated as a barrier to wave energy in the model, however in reality the ship does not occupy the full water column and would heave with the passage of waves, meaning that the model results show greater increases and decreases in bed shear stress than would be expected in reality. The reduction in bed shear stress is between 15-20 N/m^2 along both the inner and outer longshore bar. The baseline bed shear stress in the area of reduction is 20-30 N/m^2 along the outer bar and 40-50 N/m^2 along the inner longshore bar. No area is reduced below the critical threshold. The wave shadow caused by a ship in dock under large SE waves leads to a reduction in bed shear stress will mean less sediment in suspension and less change or bed erosion than that which would naturally occur. However, the differences in bed shear stress along the shoreline are small compared to baseline, meaning that deposition and salient formation is very unlikely, as a long period of persistent wave conditions (non-varying, directionally) would be required. Differences lessen with a reduction in wave height. Ships are not present all of the time, and least present in winter when bed shear stress difference would be greatest. When ships are absent the reduction in stress would disappear. Treating the ship as a breakwater (but noting the earlier comment that would not fully block wave energy) the ratio of the ship's length to its distance from shore is sufficiently small that no deposition (i.e. a salient) is expected to occur. In summary, therefore, salient formation is very unlikely but, were it to occur, it would amount to very small transient feature. As the differences in bed shear near the shore are very subtle and shown to be incapable of salient formation for several reasons, they would also not affect longshore transport in a detectable way.

As a salient formation is very unlikely and longshore transport will not be affected, the BLFs and associated structures and vessels are not considered to act as a potential barrier to the restorative processes of the beach following natural erosion over the winter. The recovery phases of the beach and the landward movement of

NOT PROTECTIVELY MARKED

sand occur mainly during summer months when the waves are lower, meaning the reduction due to the presence of the ship is very small.

Inclusion of the grillage for the combined BLFs and ship is the same as for the ship along, seaward of the grillage. Landward of the grillage, the bed shear stress reduction along the inner longshore bar is similar 15-20 N/m^2 but extends over a wider area (than the ship alone) but is still within the footprint of the wave shadow of the ship only case. Much like the grillage on its own, without the ship, the shoreward end of the grillage deflects currents shoreward. This leads to a peak increase of 11 N/m^2 amongst the final pairs of jetty piles of the permanent BLF compared to a baseline of 40 N/m^2 in that particular location. However, that very localised increase is still within the wider baseline variation along the Sizewell C frontage of 30-65 N/m^2 (for a 1.5 m wave height).

Unlike the grillage, which sits slightly proud of the seabed for part of its length, the grounded barge acts a barrier to the shore parallel tidal flows, as it occupies the entire water column once grounded. This blockage causes the flow to divert around the shoreward and seaward ends of the barge, although it is important to note that barges would only be present for up to 22% of the April – October period (and infrequent during winter), and so the impacts described below are very transient. Flow is accelerated between the shore and the end of the barge and grillage, with a peak increase in tidal currents of 0.34 m/s between the last two pairs of piles of the permanent BLF. This increase in velocity returns to within 0.1 m/s within 140 m. The reduced flow to the north of the barge on the ebb tide returns to within 0.1 m/s within 835 m.

Despite the resulting increase in the current induced bed shear stress shoreward of the barge and grillage, results show that blockage effect to the waves leads to an overall reduction in bed shear stress between the shoreline and the barge. This is because the wave induced bed shear stress is significantly larger in the shallow waters than the current induced bed shear stress, even with a 0.5 m wave. The reduction in bed shear stress along the inner longshore bar between the barge and the shore is between 15-20 N/m^2, compared to a baseline of 20-25 N/m^2. There is no area where a reduction in bed shear stress reduces below the critical threshold. The absolute bed shear stress is still 10-14 times larger than the critical threshold in this area.

Compared to the modelled higher waves associated with the working limit of the ship only (1.5 m), the wave shadow associated with the smaller working limit of the barge is substantially smaller and only starts to appear in the shallow waters associated over the outer longshore bar. As a result, the change in bed shear stress due to the presence of both the ship and the barge is similar to the barge only. The reduction in bed shear stress along the inner longshore bar between the barge and the shore is between 15-20 N/m^2, compared to a baseline of 20-25 N/m^2. There is no area where a reduction in bed shear stress reduces below the critical threshold. One difference between the presence of the ship and barge and the barge only, is the longer extent of change into the Minsmere SPA/SAC frontage (275 m vs 175 m). However, the magnitude of change is the same in both instances; a 10-20 N/m^2 reduction in bed shear stress shoreward of the end of the barge 30-40 m into the Minsmere SPA/SAC frontage with a small 1-4 N/m^2 increase further beyond. The baseline bed shear stress along the Minsmere frontage is 20-40 N/m^2.

For the operational phase, when only the permanent BLF is present, the spatial pattern of the bed shear stress change is almost identical to that of the permanent and temporary BLFs combined. The patchwork of increased and decreased bed shear stress due to the piles are dependent on the state of the tide and direction of waves. These conditions vary with the state of tide and waves, meaning the peak impact is not persistent over a tidal cycle. Patches of altered bed shear stress are sufficiently small in magnitude and scale that they are not expected to cause detectable change to the shoreline.

The bathymetric reprofiling required for the grounding pocket results in an alternating pattern of increased/decreased bed shear stress. The deepest parts of the grounding pocket have a reduction of 10-15 N/m^2, whilst the shallow areas have an increase of 8-10 N/m^2. The baseline within the grounding pocket is 25-

NOT PROTECTIVELY MARKED

30 N/m^2. A small change of 2-6 N/m^2 reduction in bed shear stress extends 230 m into the Minsmere SPA/SAC frontage compared to a baseline of 40-60 N/m^2.

The patchwork of increased and decreased bed shear stress due to the grounding pocket will vary with the state of tide and waves, meaning the peak impact shown by the models is not persistent over a tidal cycle. Furthermore, reprofiling the grounding pocket would occur very infrequently during the operational phase, every 5-10 years. Therefore, it would have no effect on the shoreline.

For all of the scenarios considered in this report, the BLF structures and their associated activities are not considered to result in any detectable change to bed levels along the shoreline. Therefore, there would be no change beyond natural processes to the supratidal beach. As a result, there will be no additional change to the 'annual vegetation of drift lines' habitat (Minsmere to Walberswick Heaths and Marshes SAC) or the potential nesting sites for little tern (*Sterna albifrons*) (Minsmere to Walberswick SPA). The assessment of the impact on the annual vegetation drift lines or potential nesting sites is not conducted in this report but will be conducted in the shadow HRA.

As per the original aim of this report, all the modelled predictions are consistent with the overall conclusions presented in the Environmental Statement Addendum and original Environmental Statement; namely that there was no significant effect on coastal geomorphology receptors due to the presence of the BLFs and/or associated operations.

7 References

Araujo, M. A., Fernand, L. and Bacon, J., 2018. Sensitivity analysis to reflection and diffraction in ARTEMIS. Proceedings of the XXVth TELEMAC-MASCARET User Conference, 9th - 11th October 2018, Norwich, UK. DOI: 10.14465/2018.tucxxv.nrw.

BEEMS Technical Report TR224. Overview of Telemac Hydrodynamic and Sediment Transport Modelling at Sizewell, Cefas, Lowestoft.

BEEMS Technical Report TR232 Edition 2. Sizewell Wave Model Setup and Validation. Cefas, Lowestoft.

BEEMS Technical Report TR233 Edition 2. Sizewell Tidal Modelling with Telemac2D – Validation. Cefas, Lowestoft.

BEEMS Technical Report TR310 Edition 2. Sizewell C Assessment of scour at the marine structures. Cefas, Lowestoft.

BEEMS Technical Report TR319. Derivation of extreme wave and surge events at Sizewell with initial results of the coastal wave modelling. Cefas, Lowestoft.

BEEMS Technical Report TR403. Expert Geomorphological Assessment of Sizewell's Future Shoreline Position. Cefas, Lowestoft.

BEEMS Technical Report TR480 Edition 2. Modelling of Sediment Dispersion of Dredge Material from SZC Construction and Operation. Cefas, Lowestoft.

BEEMS Technical Report TR487. Likely infill rates for the BLF access channel. Cefas, Lowestoft.

BEEMS Technical Report TR523. Sizewell coastal geomorphology monitoring plan. Cefas, Lowestoft.

Defra (2016) Joint Advice Note Principles for Flood and Coastal Risk Management Office for Nuclear Regulation and Environment Agency, 2016.

EDF, 2012. The TELEMAC Modelling System - Theoretical Note and User manual - Artemis software for Wave Agitation.

Grant, W. and Madsen, O., 1979. Combined wave and current interaction with a rough bottom. *Journal of Geophysical Research*, 84 (C4): 1797-1808.

Komar, P. D. and Miller, M. C.,1973. The threshold of sediment movement under oscillatory water waves. *Journal of Sedimentary Research*, Vol 43, No 4: 1101-1110.

Leeder, M.,1999. Sedimentology and Sedimentary Basins. Blackwell Science Ltd, London, UK.

Met Office 'ReMap' European wave model, http://wavenet.cefas.co.uk/hindcast

Nielsen, P.,1992. Coastal Bottom Boundary Layers and Sediment Transport. *Advanced Series on Ocean Engineering*, Vol 4. World Scientific Publishing, Singapore.

NOT PROTECTIVELY MARKED

Nir, Y., 1982. *Offshore Artificial Structures and Their Influence on the Israel and Sinai Mediterranean Beaches*, Proceedings, 18th International Coastal Engineering Conference, American Society of Civil Engineers, pp 1837-1856.

Osprey, 2017. Sizewell C BLF Operational Capability Statement. NNB GenCo Document Number: SZC-3RDSPY-XX-000-REP-100001.

Palmer M., Howard T., Tinker J., Lowe J., Bricheno, L., Calvert D., Edwards T., Gregory J., Harris G., Krijnen J., Pickering M., Roberts C. and Wolf J., 2018. UKCP18 Marine report. UK Met Office, 132pp.

Press, W., Teukolsky, S., Vetterling, W., and Flannery, B.,1986. Numerical Recipes in Fortran 77, vol 1. Cambridge University Press, Cambridge, UK., 2nd ed.

Putnam, J.A. and Johnson, J.W., 1949. The dissipation of wave energy by bottom friction. pp. 67-74.

Richardson, E. V. and Davis, S. R. (2001). *Evaluating Scour at Bridges.* Hydraulic. Engineering. Circular No. 18, US Department of Transport, Federal Highway Administration, Pub. No. FHWA NHI 01-001.

Shields, A.F., 1936. Application of similarity principles and turbulence research to bed-load movement. Berlin, Germany, Vol.26: 5-24.

Soulsby, R. L., 1993. Wave -current interaction within and outside the bottom boundary layer, Coastal Engineering 21, p41-69.

Soulsby, R. L., 1997. Dynamics of Marine Sands. London, Thomas Telford.

Soulsby, R L.,2006. Simplified calculation of wave orbital velocities. Report TR 155, Release 1.0, HR Wallingford.

Soulsby, R.L. and Whitehouse, R.J.,1997. Threshold of sediment motion in coastal environments. Proc Pacific Coasts and Ports 97 Conf., Christchurch 1, pp 149-154.

Truitt, C. and Herbich, J., 1986. Transmission of random waves through pile breakwaters. *Coastal Engineering*, Chapter 169: 2303-2313.

Van Rijn, L., 1993. Principles of Sediment Transport in Rivers, Estuaries and Coastal Seas. Aqua Publications, Amsterdam.

Van Weele, B., 1965. Wave reflection and transmission for cylindrical pile arrays. MS Thesis, May 1965, Reprint no 313. Fritz Laboratory Reports, Paper 183.

Whitehouse, R.J.S. (1998). *Scour at marine structures.* A manual for practical applications. Thomas Telford, London.

Zubier, K., Panchang, V., Demerbilek, Z., 2003. Simulation of waves at Duck (North Carolina) using two numerical models. *Coastal Engineering Journal*, Vol 45, No 3: 439-469.

NOT PROTECTIVELY MARKED

Appendix A Determining Bed Shear Stress

A.1   Combining waves and tides

The detailed procedure used by Soulsby (1997) to evaluate the components needed for the enhanced bed-shear stress is shown below and each component described:

1.   Calculate U_{rms} – root-mean-square wave orbital velocity

$$U_{rms} = \left(\frac{H_s}{4}\right)\left(\frac{g}{h}\right)^{\frac{1}{2}} \exp\left\{-\left[\frac{3.65}{T_z}\left(\frac{h}{g}\right)^{\frac{1}{2}}\right]^{2.1}\right\} \quad (2)$$

where H_s= significant wave height; h= still water depth; g= acceleration due to gravity and T_z= zero up-crossing wave period. The equation for U_{rms} used for this study is applied for a JONSWAP spectrum and uses an improved version derived in Soulsby (2006). It provides a simpler approach to the more complex and less accurate version in Soulsby (1997) and is appropriate for use in shallow water.

2.   Calculate U_w – near bed orbital velocity amplitude

$$U_w = \sqrt{2}\, U_{rms} \qquad (3)$$

This is applied to the equivalent monochromatic wave, having the same velocity variance as the full spectrum.

3.   Determine values for the physical characteristics: z_0, C_D, ρ_w and ν

For a rippled bed over the whole domain (typical of tidal currents over sand throughout fine-scale tide and wave domains), the roughness length (z_0) of 6 mm was assumed (Soulsby, 1997, Table 7). The drag coefficient (C_D) of steady current in absence of waves is obtained by interpolation of data in Soulsby's (1997, Table 10), which fits a series of models, giving the value C_D= 0.00458 for use here. The water density (ρ_w) is 1027 kg/m^3 and its kinematic viscosity ν = 1.36×10^{-6} m^2/s.

4.   Calculate f_w - wave friction factor

$$f_w = max(f_{wr}, f_{ws}) \qquad (4)$$

where the rough bed friction factor (f_{wr}) is calculated based on Soulsby formulation, using Eq. 5, and the smooth bed friction factor (f_{ws}) is obtained through Eq. 7.

$$f_{wr} = 1.39\left(\frac{A}{z_0}\right)^{-0.52} \qquad (5)$$

where A = the orbital amplitude of wave motion at the bed, which is given by:

$$A = \frac{U_w T_p}{2\pi} \qquad (6)$$

$$f_{ws} = B R_w^{-N} \qquad (7)$$

where,

$B = 2$,	$N = 0.5$	for	$R_w \leq 5 \times 10^5$
$B = 0.0521$,	$N = 0.187$	for	$R_w > 5 \times 10^5$

and R_w is the wave Reynolds number:

$$R_w = \frac{U_w A}{\nu} \qquad (8)$$

5. Calculate the wave-only bed shear stress (τ_w):

$$\tau_w = \frac{1}{2} \rho_w f_w U_w{}^2 \qquad (9)$$

6. Calculate the current-only bed shear stress (τ_c):

$$\tau_c = \rho_w C_D \bar{U}^2 \qquad (10)$$

where $\bar{U}$ = depth-averaged current speed.

Once the individual components of bed shear stress have been computed, the combined mean bed shear stress, τ_m, and maximum bed shear stress, τ_{max}, can be determined.

7. Calculate the combined mean bed shear stress:

$$\tau_m = \tau_c \left[1 + 1.2 \left(\frac{\tau_w}{\tau_c + \tau_w} \right)^{3.2} \right] \qquad (11)$$

8. Calculate the combined maximum bed shear stress:

$$\tau_{max} = [(\tau_m + \tau_w \cos \emptyset)^2 + (\tau_w \sin \emptyset)^2]^{\frac{1}{2}} \qquad (12)$$

where $\emptyset$ is the angle between current direction and direction of wave travel.

While τ_m is used for determining the sediment diffusion into the outer flow, τ_{max} is used to determine whether the threshold of sediment motion has been exceeded and for near bed diffusion.

A.2 Critical bed shear stress

The critical threshold conditions for sediment entrainment were determined following Soulsby (1997; chapter 6). Steady tidal currents and wave-orbital currents can be considered separately, as both have a threshold stress above which sand grains on the bed begin to mobilise. As the velocity of the fluid flow over a sand bed increases, there is a stage when the stress exerted by the fluid on the particles is enough to cause them to move into the flow. The threshold of sediment movement is fundamental when evaluating the sediment response to currents or waves. Under oscillatory waves, the complexity increases since the currents are continuously varying as the phase of the wave changes, and accelerations become important. In this case, the threshold of sediment motion cannot simply be related to the sediment grain size as is the case for unidirectional currents (Komar and Miller, 1973). In shallow water, near the bottom, the elliptical motion of water particles is reduced to a horizontal motion with a bottom orbital velocity amplitude which depends on

NOT PROTECTIVELY MARKED

wave height, period and water depth (see Eq. 2). Both modes of flow create a frictional force exerted on the bed, which is expressed as the bed shear stress.

The threshold value of the bed shear stress is, therefore, one of the most important factors when determining bed or suspended sediment response to hydrodynamic flow. The work of Shields (1936) developed the idea of a ratio of force exerted by the bed shear stress to the submerged weight of the grain countering it, producing a dimensionless value for bed shear stress known as the Shields Parameter (θ).

The entrainment threshold value of the Shields parameter (θ_{cr}) can be evaluated and is relevant for both steady currents and orbital wave currents. The size and density of both the sediment and fluid are the dominant factors determining the threshold of motion and are used to determine a threshold value.

Soulsby and Whitehouse (1997) gave an updated method to evaluate the threshold Shields parameter. Their method is much improved for fine (sand) grain sizes and is given by:

1.   Calculating the threshold Shields parameter:

$$\theta_{cr} = \frac{0.30}{1+1.2D_*} + 0.055[1 - \exp(-0.020D_*)] \qquad (13)$$

where D_* is the dimensionless grain size:

$$D_* = \left[\frac{g(s-1)}{v^2}\right]^{\frac{1}{3}} d_{50} \qquad (14)$$

where v is the kinematic viscosity of water, s the ratio of density of sand to water ($s = \rho_s/\rho_w$) and d_{50} the median diameter of sediment grains. The sand grain density is taken as a quartz grain, i.e. 2650 kg/m^3.

At the Sizewell site, sediment size is relatively coarse and the original work by Shields is fully applicable.

2.   Compute the critical threshold bed shear stress τ_{cr}

$$\tau_{cr} = \theta_{cr}g(\rho_s - \rho_w)d_{50} \qquad (15)$$

This method allows a direct comparison to be made of bed shear stress generated by hydrodynamic forcing, and a value at which sediment mobility is expected to occur.

TR543 MODELLING OF THE TEMPORARY AND PERMANENT BLF AT SZC

NOT PROTECTIVELY MARKED

Appendix B ARTEMIS and TELEMAC2D models

B.1   Mesh design

The major challenge in designing the mesh for the model was to provide node centres as small as 20 cm to create the shape of the tubular steel support piles whilst also replicating all bathymetric features over the wider region extending offshore (seaward of the BLFs) so that waves could propagate inshore from the boundary. The fine mesh density around the piles is crucial to allow reflection and diffraction of waves from these features of the structure. The node density is reduced away from the piles but is done gradually.

The high density of nodes in the mesh has implications for run-times of both the wave and tide models. For the wave model these are reasonable as it is a steady state model. The model simulation across the domain takes approximately two hours to complete using a High-Performance Computer in scalar (single processor) mode. For the tidal model runs, as the model is run over across several tides it takes much greater computational effort. The very small distance between the nodes requires an exceptionally short internal time-step in the tidal model (0.1 second) to ensure that the stability criteria of Courant-Friedrichs-Lewy is overcome. The criteria states that:

$$\frac{|v|\Delta t}{\Delta x} \leq 1 \qquad\qquad (16)$$

where v is the current velocity, Δt the internal timestep and Δx the distance between nodes (Press et al, 1986). The model simulation takes 5 hours using a High-Performance Computer in parallel (using 24 processors), to run a 48-hour tidal simulation.

To investigate the effect of the BLF structures and vessels, four base meshes were created (for ARTEMIS and TELEMAC2D). The first mesh excludes the presence of the BLF jetty piles and is referred to as the baseline conditions (i.e., the nearshore bathymetry based on data collected in 2017). The second mesh includes the piles from the temporary and permanent BLFs. These first two meshes are identical except for the piles, dolphins and fenders, whose circumferences were triangulated for the baseline simulations. As such, a comparison can then be made between the baseline conditions and the inclusion of the structures. The third mesh is identical in mesh structure to the second mesh (temporary and permanent BLFs) but includes of the ship docked at the temporary BLF. The fourth mesh includes only the piles of the permanent BLF. From these four base meshes, a further five meshes were created, which are structurally the same as the base meshes, but with modified bathymetry to represent the grillage, navigation access dredging, grounding pocket and barge. In all the meshes, except for the baseline mesh, the presence of the Combined Drainage Outfall (CDO) and the two Fish Recovery and Return outfalls (FRR) has been included. These structures have a dimension of 3 m by 3 m and sit 2.5 m above the seabed. Whilst the construction of the CDO and FRRs may not temporally overlap the use of the temporary BLF, the structures have been included as a worst case. Figure 5 shows the node density and mesh structure of the ARTEMIS and TELEMAC2D mesh structure, including the ship at the temporary BLF, the grillage and barge at the permanent BLF and the CDO and FRR outfalls.

B.2   ARTEMIS domain

The seaward boundary of the ARTEMIS wave model (at which waves are input from north-easterly and south-easterly directions) is semi-circular and covers the area 1.5 km north and 1.25 km south of the permanent BLF (Figure 74). The model boundary was designed as a semicircle to avoid corners or acute changes in boundary angle, which removes the need to determine how waves would reflect from boundaries internally as they leave the domain boundary. These effects are described fully in Section 3.5.2 of the ARTEMIS Technical Manual (EDF, 2012). The seaward (semi-circular) boundary is the only boundary that permits incident waves to

propagate over the domain. The shore boundary and the pile boundaries are both solid but treat incident waves differently with respect to reflection (see Section B.3).
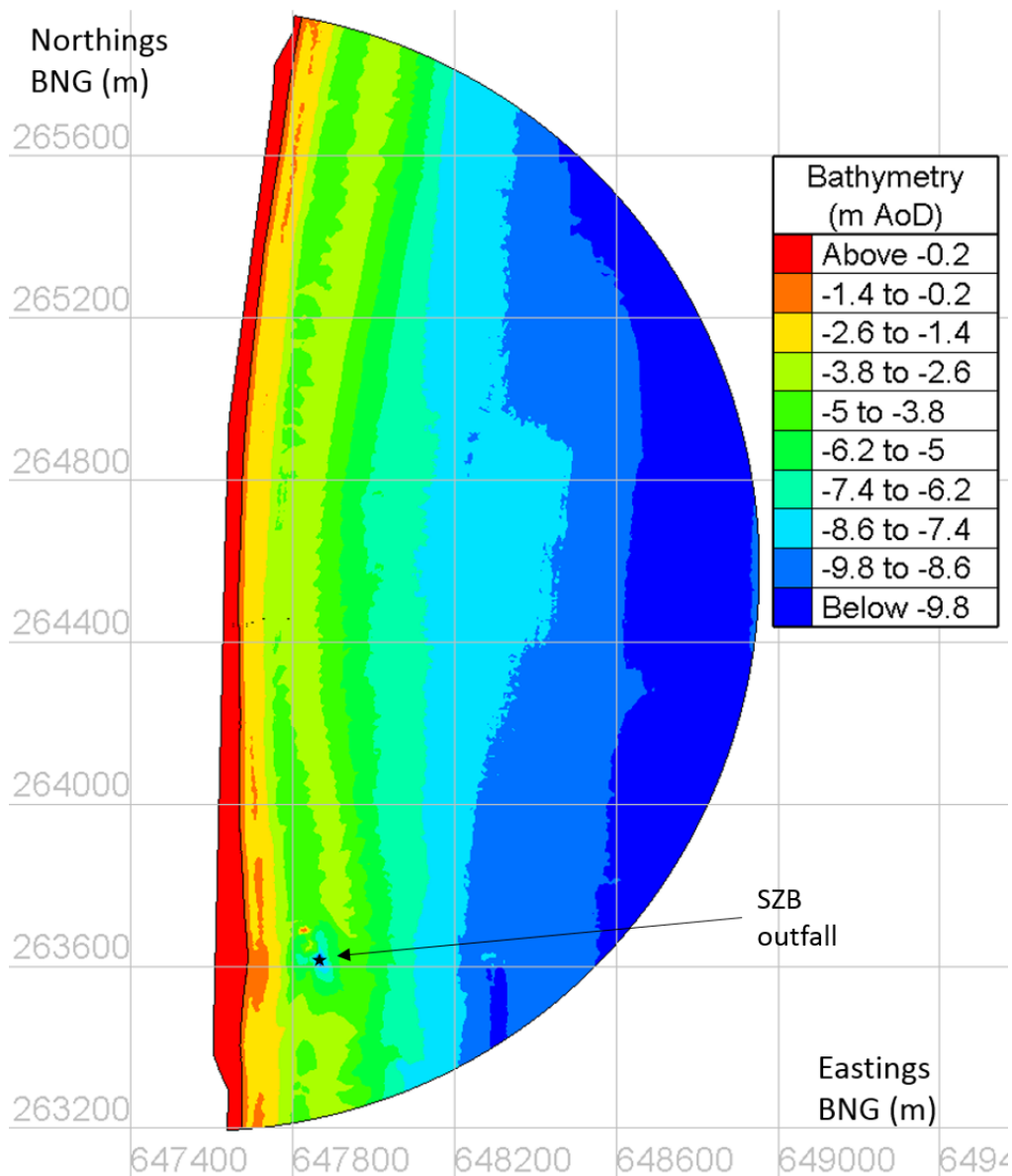

Figure 74: ARTEMIS model domain and bathymetry. The vertical black line represents the shoreline (0 m ODN).

The baseline mesh comprises 92,583 nodes. The mesh including the temporary and permanent BLF and the ship comprises of 89,995 nodes. The mesh density at the seaward boundary is 10 m, decreasing to 20 cm around piles.

An example of the fine detail of the mesh around the permanent BLF piles is shown in Figure 75. Figure 75 presents part of the ARTEMIS mesh that is used for the BLF piles and the baseline simulations, with the exception at the piles/dolphins/fenders location where the holes are triangulated for the baseline case (represented in black). The mesh including the structures appears in colour on top of the baseline mesh.
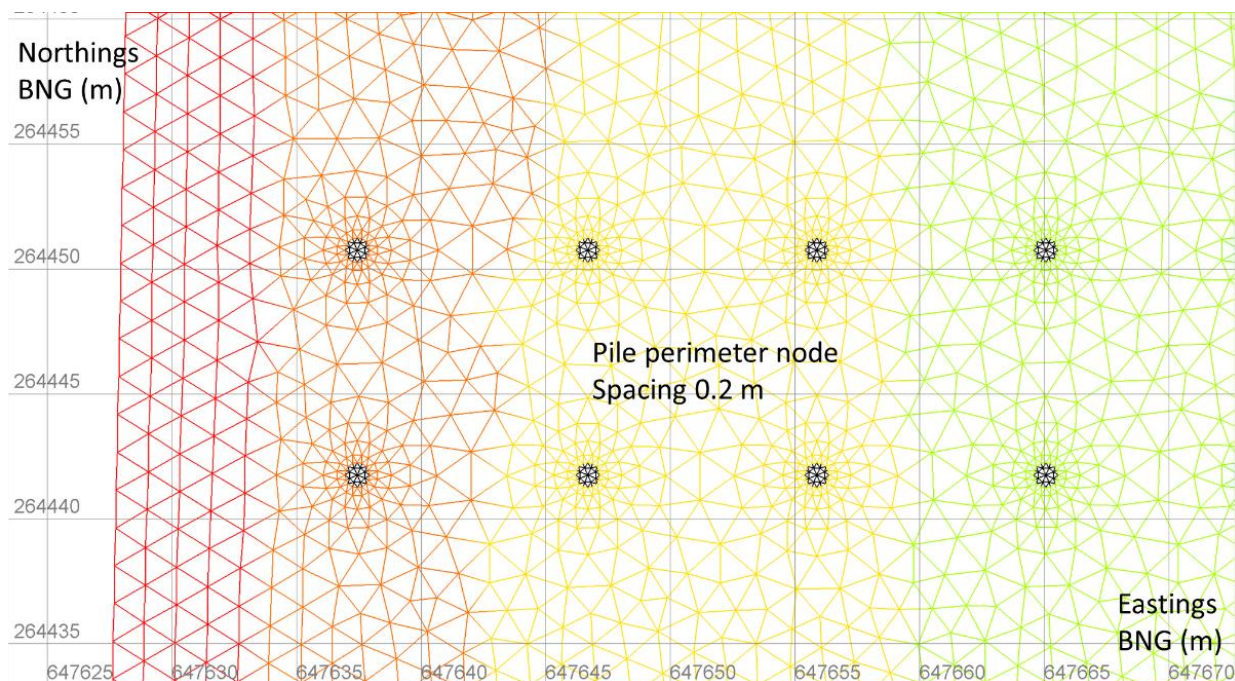
Figure 75: Part of ARTEMIS mesh around permanent BLF (in colour) and baseline (in black). High resolution of the mesh around the piles.

B.3   Determination of the ARTEMIS reflection coefficient

ARTEMIS is able to take into account the ability of a solid boundary (for example the support piles of the BLF jetties) to reflect wave energy. A coefficient of reflection is programmed for each boundary node, to evaluate at that location. That boundary node can be either at the shore or at the pile's boundary. The coefficient value can vary between one (perfect reflector – no absorption of wave energy) and zero (all energy is absorbed at the boundary). Along the shore boundary, a reflection coefficient of zero was considered. The effect of providing a reflection coefficient of one to the pile boundaries (no absorption of energy) means that no attenuation of waves occurs as they pass through the jetty. A reflection coefficient of zero has the opposite effect and each contact of wave with a pile boundary absorbs energy.

Research carried out at the Field Research Facility (FRF) at the US Army Corp of Engineers, Duck, North Carolina, during the last decade, shows some of the difficulties in determining the correct values for reflection, or absorption of wave energy by structures of this type. The facility at Duck includes a shore-normal jetty which extends from the shoreline, for 561 m into water with depth of ~6 m (see Figure 76). The jetty features two lines of support piles and the pile diameter is 0.85 m (i.e. similar to the proposed SZC BLF jetties). The FRF facility has hosted much coastal research during the last 20 years and provides comprehensive datasets of waves being attenuated by the jetty structure.
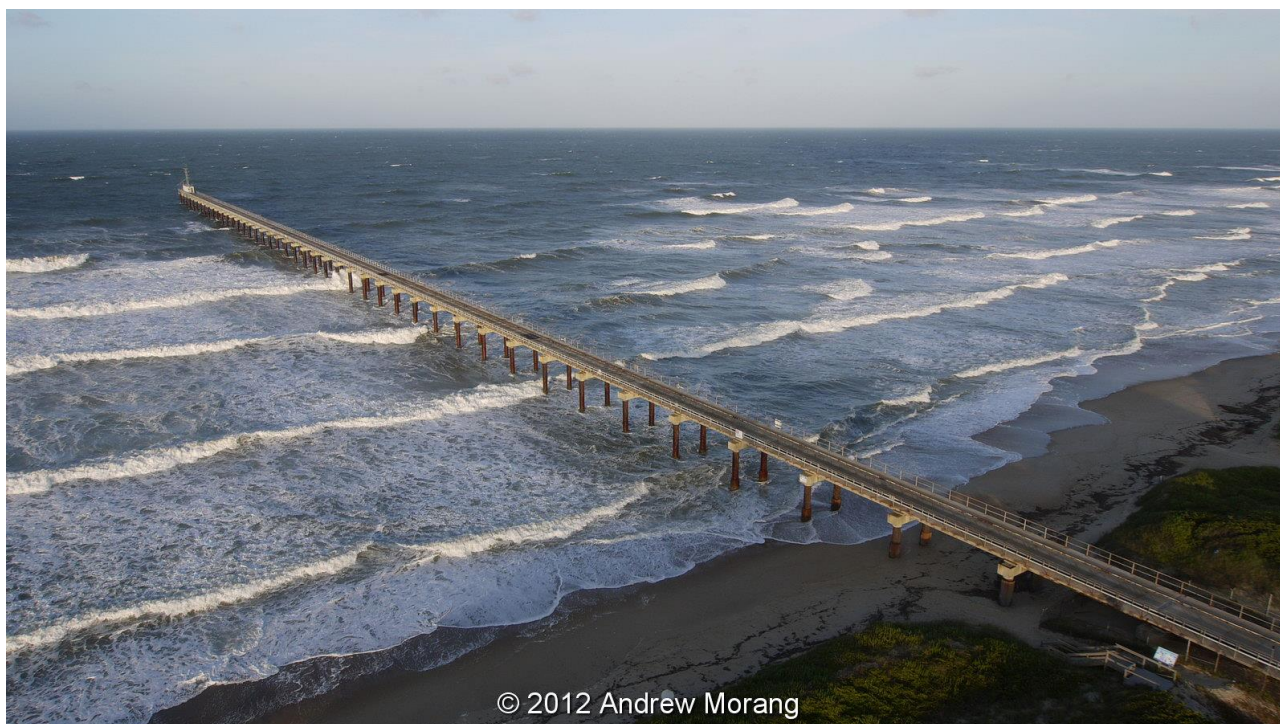
Figure 76: The jetty at the FRF facility at Duck, North Carolina. Two rows of 0.85 m diameter piles extend 560 m off-shore into water of ~6 m depth. The facility is one of the only centres in the world to have carried out research into wave attenuation by interaction of the support piles and wave orbital currents.

Zubier et al (2003) used FRF data to compare the performance of two wave models (CGWave and Swan) under storm conditions. The two models are less complex than ARTEMIS, although CGWave is closest to ARTEMIS as a phase resolving model and bases mesh density on wavelength (minimum 10 nodes per wavelength). Whereas Swan, a spectral energy model is closest in type to TOMAWAC and uses an orthogonal, 8 m grid based on bathymetry. A feature of the FRF jetty is a distinct bathymetric "low" under the structure and whilst design details are not known, would suggest local erosion (scour) has occurred due to turbulence generated by the piles emerging from the seabed. Due to the specific working of each model (CGWave includes a reflection/diffraction effect but Swan does not), direct comparison of the mechanisms causing wave attenuation was not possible. Zubier et al (2003) conclude that the pier piles had little effect to block propagating waves and that the effects seen were due to the bathymetric "trench" under the jetty.

Work carried out by Truitt and Herbich (1986) presents transmission coefficients for closely spaced lines of piles. Even when the gap is 0.2 times the pile diameter, their results show a transmission coefficient (ratio of transmitted to incident wave height) of 80% or more. For the SZC temporary and permanent BLF jetty, the pile spacing is about 9-10 times the diameter, respectively, so significantly higher transmission is expected than published studies including Truitt and Herbich (1986) and the piles will have little effect on the waves. Although there is a smaller distance between the two most offshore jetty piles and the fenders, their effect on the waves is also expected to be small. This view is confirmed by flume tests carried out by Van Weele (1965). Tests on a 4 x 4 array of piles with spacing 2 times the pile diameter gave transmission coefficients of 90-95%. Considering these previous studies, it is expected that the direct effect of the BLF piles on the waves will be less than of the bathymetric (scour) changes around the piles. Also, taking into account HR Wallingford's experience (who use typical reflection coefficients between 0.95 and 1.0) and considering that the piles in the real environment are unlikely to be perfect reflectors as incident waves induce vibration, the reflection

coefficient used in the simulations in this report was set to 0.95. The selected reflection coefficient is supported by a sensitivity analysis carried out, but not presented in this report (Araujo et al, 2018).

B.4   TELEMAC2D domain

The pre-existing validated and calibrated Sizewell regional hydrodynamic model is too coarse to provide the necessary information regarding the hydrodynamics surrounding the BLFs. To include the presence of the piles into the regional domain, at the required scale, would mean that the computational requirement of the model would be excessive. Instead, a smaller fine scale model domain that includes the jetty piles at the same scale as that of the ARTEMIS domain was created. To provide boundary conditions for this smaller domain, the fine mesh is nested within the regional domain, such that the node spacing on the seaward boundary match the node distribution of the regional domain. The relationship between the regional domain and the fine mesh is shown in Figure 77. As the Sizewell-Dunwich Bank plays an important role in the local wave environment and hydrodynamics, the fine mesh domain extends to encompass these bathymetric features, as shown in Figure 78.

In the same way as for the ARTEMIS simulations, a total of nine meshes were created for the different combinations of structures, which are the same except at the piles/dolphins/fenders location, where the holes were triangulated for the baseline case. The baseline mesh comprises 81,485 nodes. The mesh including the temporary and permanent BLF and the ship comprises of 78,897 nodes and is shown Figure 79.

B.5   Regional model validation

Figure 80 shows the regional mesh used to run the full tidal model, wave models and sediment transport computations used for geomorphology studies and flood risk analyses carried out in previous works. The design of the mesh structure for the computational domain is described fully in BEEMS Technical Report TR224. Report TR224 presents all the bathymetric sources used and a dataset forming a bathymetry gridded at 25 m resolution. That mesh was then adjusted in BEEMS Technical Report TR233 to provide the best balance of node density and is designated mesh_Z2. This is the mesh that was used in the present report for regional model simulations.

TR543 MODELLING OF THE TEMPORARY AND PERMANENT BLF AT SZC

NOT PROTECTIVELY MARKED
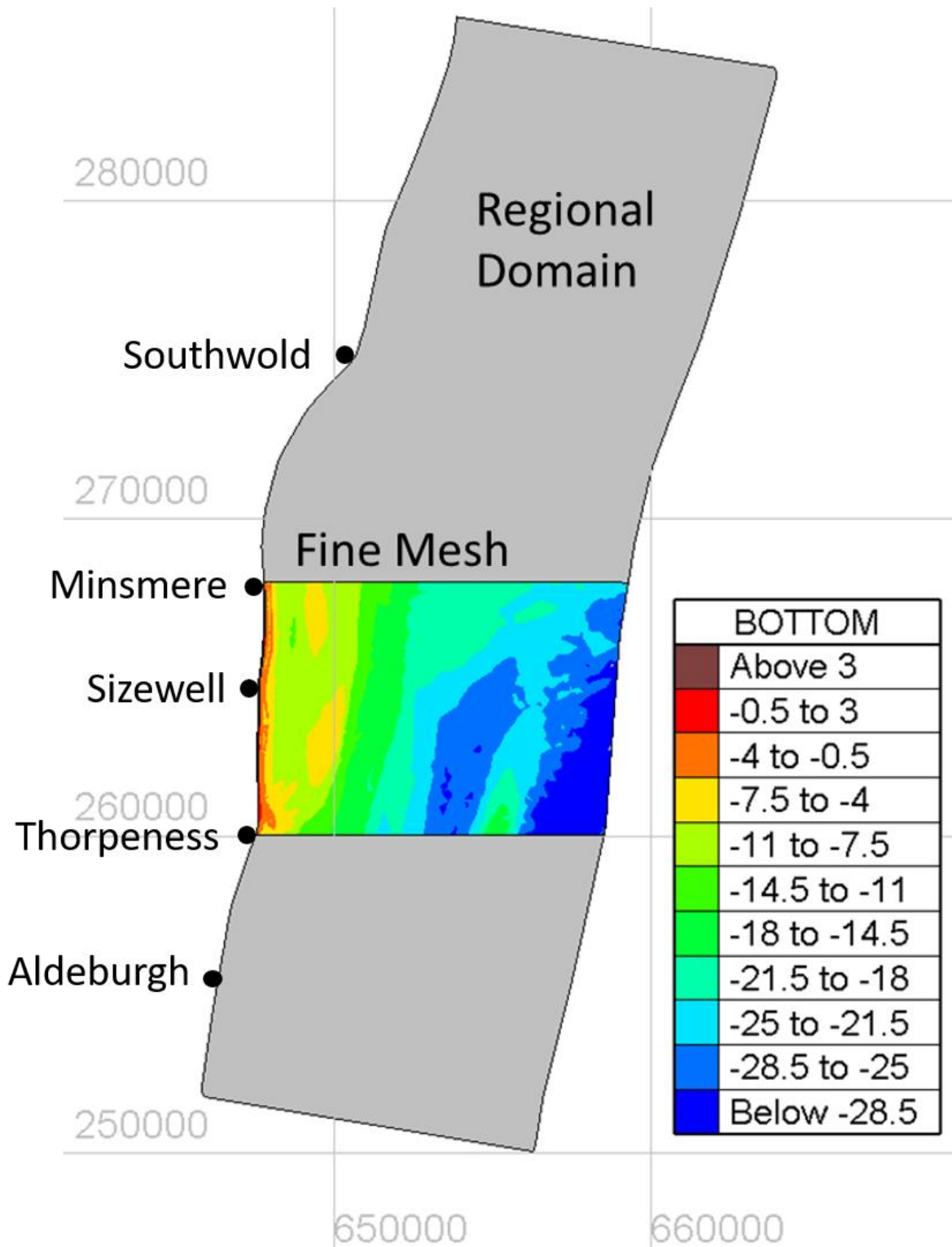
Figure 77: Fine mesh model domain nested within the Sizewell regional domain.

TR543 MODELLING OF THE TEMPORARY AND PERMANENT BLF AT SZC

NOT PROTECTIVELY MARKED
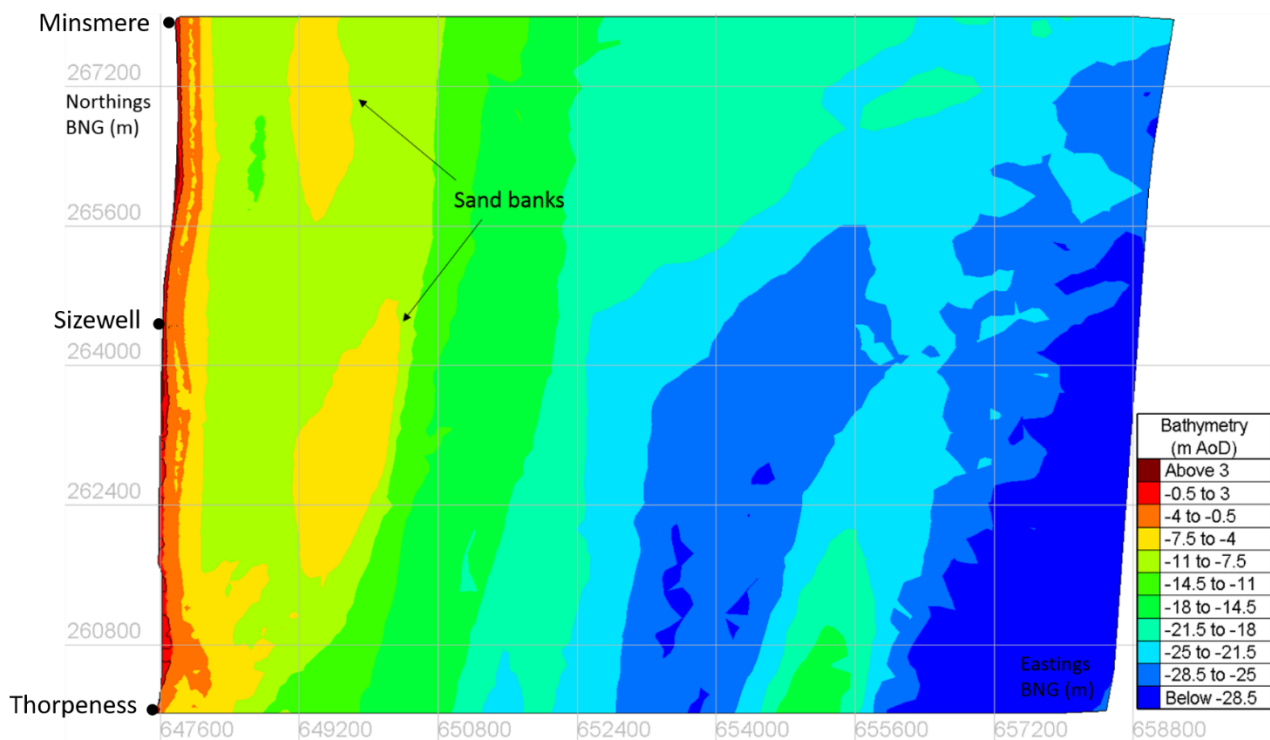
Figure 78: Detail of the bathymetry in TELEMAC2D domain. The sand banks, located at about 1,300 m offshore, are also represented. The vertical black line represents the shoreline (0 m ODN).

**TR543 MODELLING OF THE TEMPORARY AND PERMANENT BLF AT SZC**

NOT PROTECTIVELY MARKED
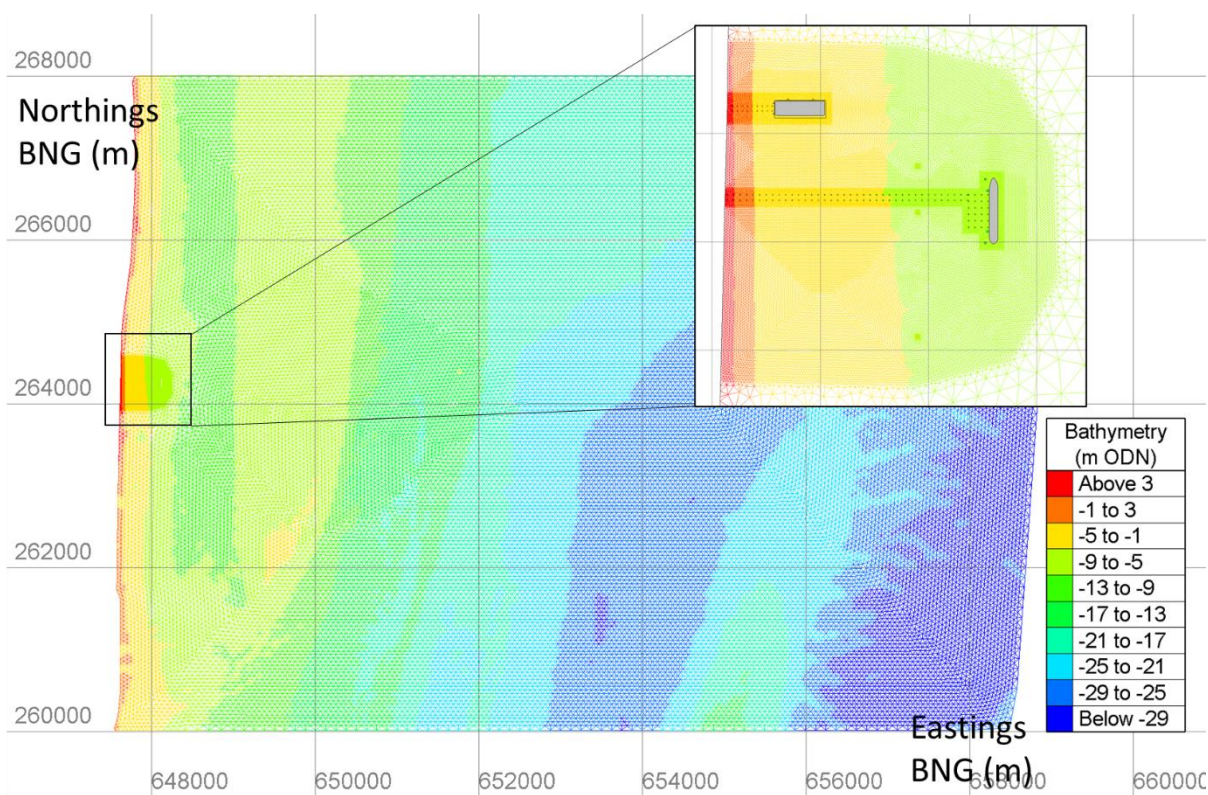
Figure 79: TELEMAC2D mesh used in BLF in use (in colour) and no BLF simulations (in black). As both meshes exactly overlap and the colour mesh in on top of the black mesh, it is possible to see the black mesh only at the pile locations, corresponding to when the piles are absent.

In 2017, multibeam bathymetry and aerial lidar data was acquired that covered the Sizewell part of the regional domain. This updated bathymetry (compared to that used in BEEMS Technical Report TR233) was used for the ARTEMIS and TELEMAC meshes. The updated bathymetry encompasses the entire ARTEMIS domain. Whereas, for the TELEMAC domain, a portion of the offshore section is missing. For this area, bathymetry from the original source for the regional domain is used. Figure 81 presents different sources of bathymetry with respect to the different model domains. The original bathymetry is presented in grey, and the regions where the bathymetry has been updated, corresponding to the multibeam and lidar data, are presented in colour.

The regional tidal model was used to generate the boundary conditions of the smaller tidal model run. Before rerunning the regional domain, its bathymetry was updated to include the 2017 bathymetric data. The validation of the regional domain was recompleted using the same observations, as described in BEEMS Technical Report TR233 Edition 2. The validation was conducted by comparing observed and modelled time series of velocity components U and V and free surface water elevation (E) at three lander positions, one offshore (OS1) and two inshore (IS1 and IS2) of Sizewell - Dunwich bank. The V component of velocity is aligned with the primary axis of the rectilinear tidal currents. The lander positions are represented in TR233 Edition 2. The validation was carried out for 29 days (from 7/11/2013 to 6/12/2013) and includes the December 2013 storm surge event.

Figure 82 to Figure 84 present the free surface elevation, and the V and U components of velocity for the offshore lander (OS1). The free surface elevation, and the V and U velocity for inshore IS1 lander are shown in Figure 85 to Figure 87. Results for the second inshore lander (IS2) are depicted in Figure 88 to Figure 90.

TR543 MODELLING OF THE TEMPORARY AND PERMANENT BLF AT SZC

NOT PROTECTIVELY MARKED

The results were very similar to those obtained in the previous calibration carried out in TR233 Edition 2. The free surface elevations replicated by the model with high accuracy but there are some differences presented, as before, namely for the U component (secondary velocities) Velocities along the Sizewell coast are highly rectilinear along the north-south axis meaning the U component is very small compared to the overall magnitude, i.e., 0.05 m/s vs >1 m/s. An error of approx. 0.05-0.1 m/s is well within EA guidelines for model calibration/validation (+/- 0.2 m/s error) and the model is considered acceptable for this study.
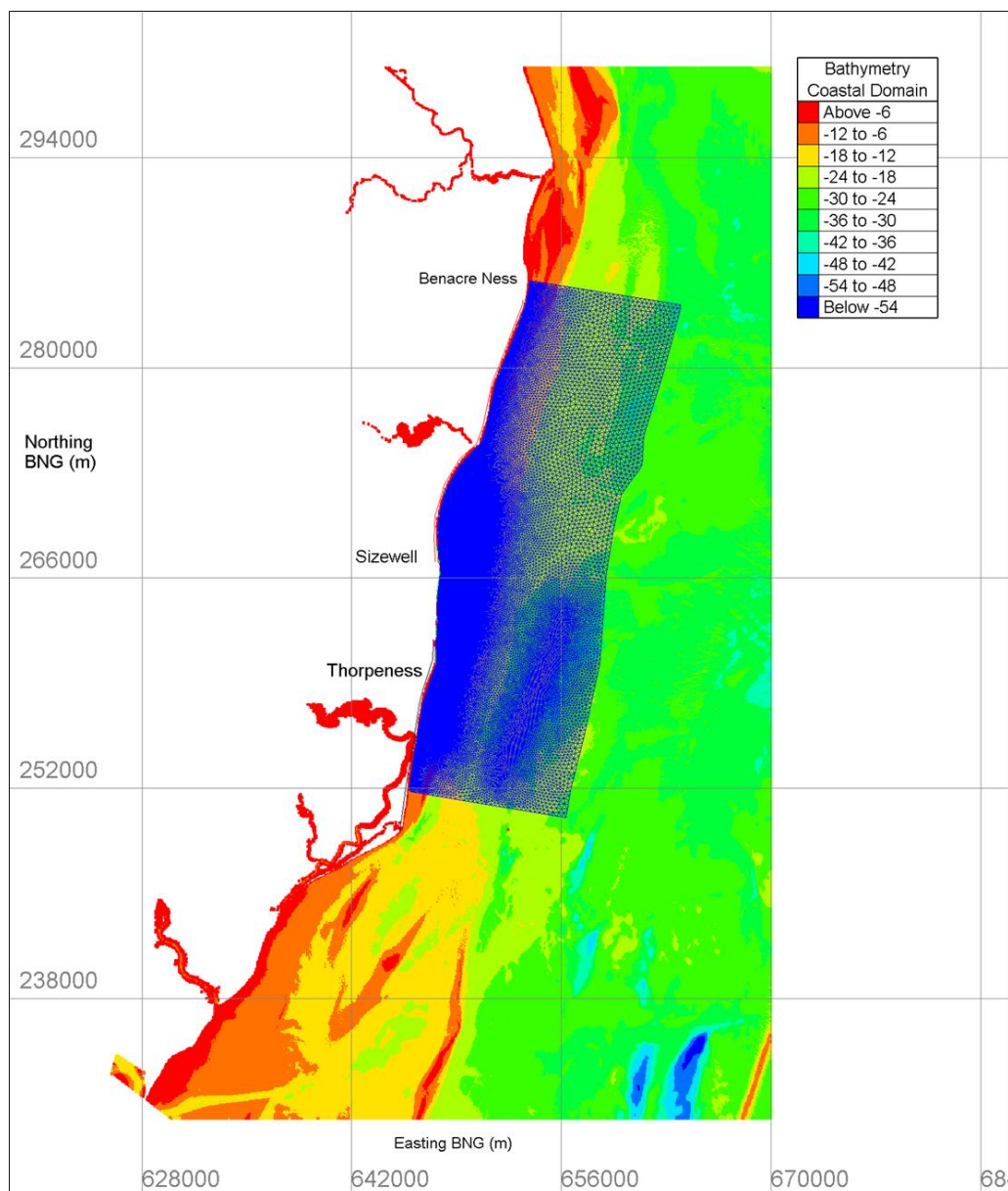
Figure 80: The regional TELEMAC model mesh used for tidal, wave and sediment transport calculations.

TR543 MODELLING OF THE TEMPORARY AND PERMANENT BLF AT SZC

NOT PROTECTIVELY MARKED
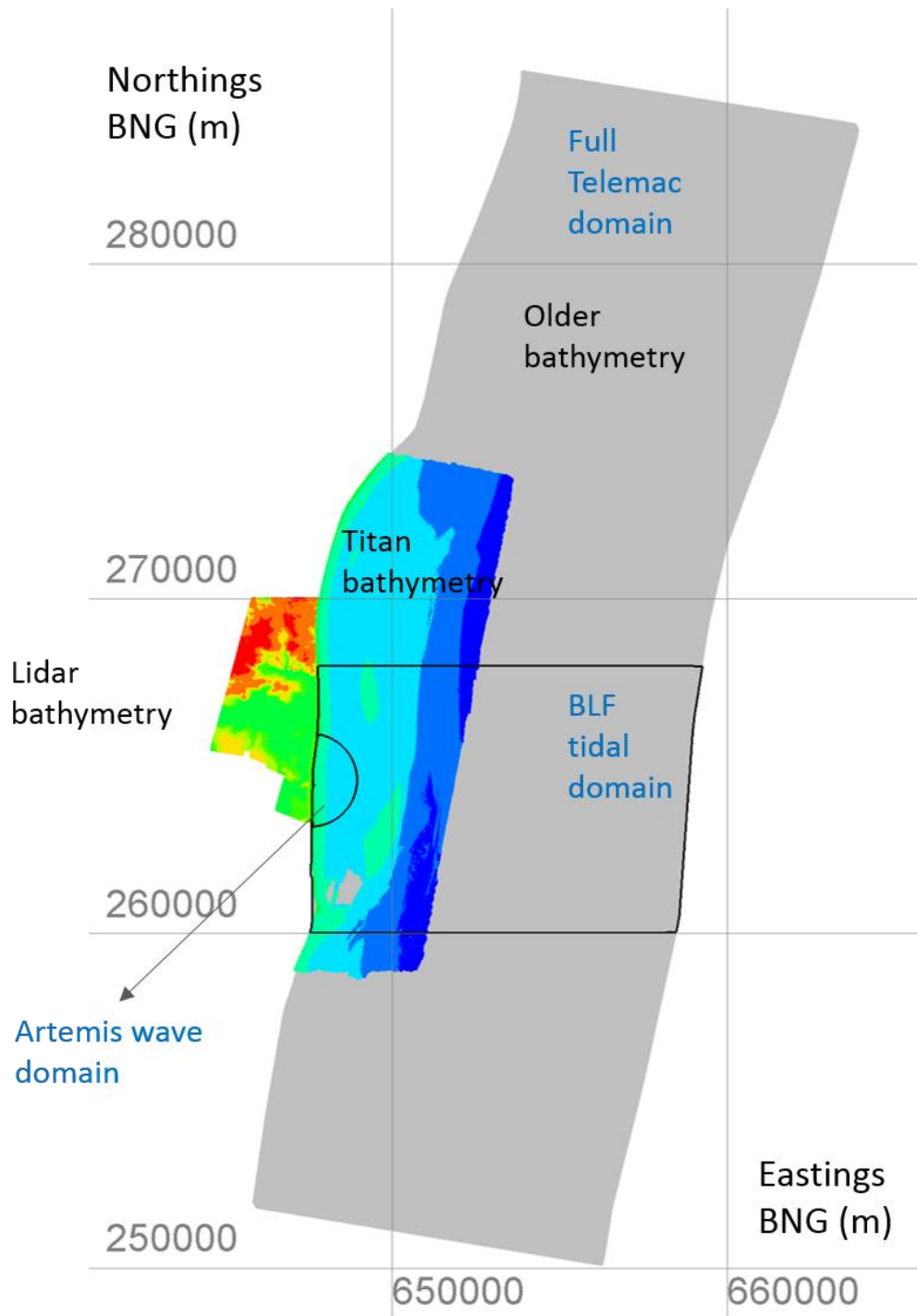
Figure 81: Map of the regional TELEMAC domain, BLF tidal and ARTEMIS wave domains. Representation of the old bathymetry (in grey) and the 2017 Titan and Lidar bathymetry (in colour).

TR543 MODELLING OF THE TEMPORARY AND PERMANENT BLF AT SZC

NOT PROTECTIVELY MARKED
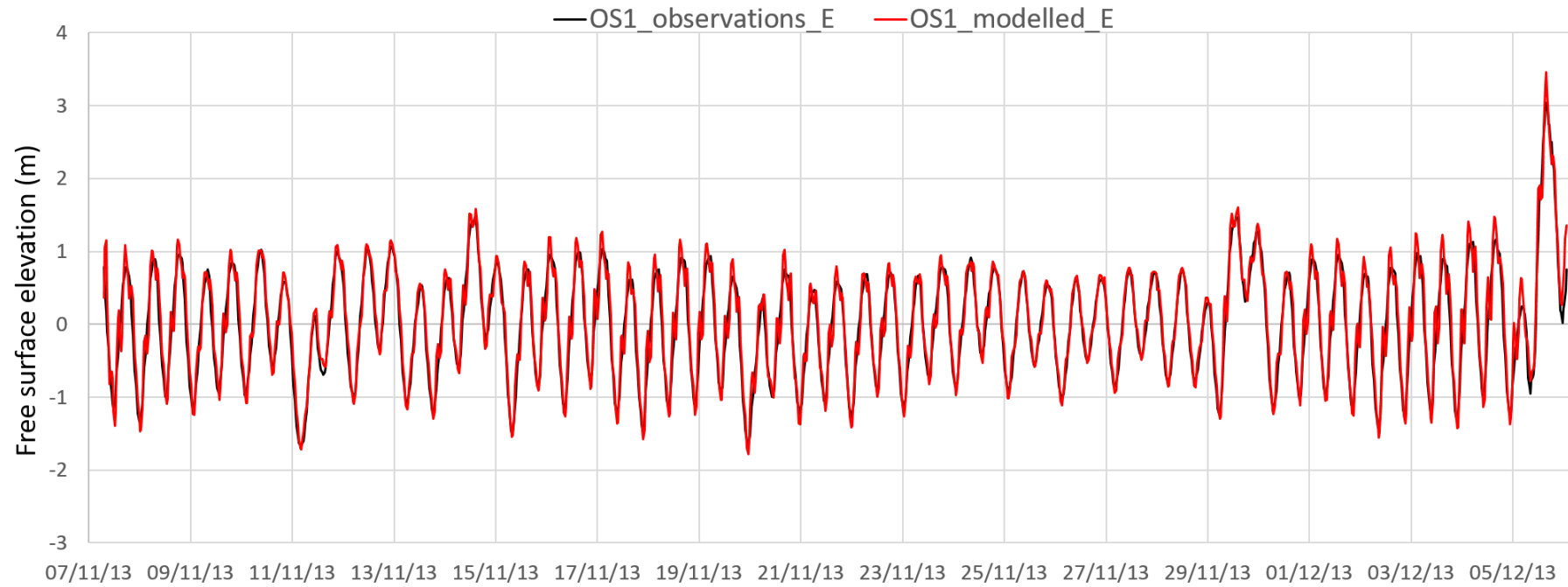
Figure 82: Comparison of vertical free surface elevation (m) at offshore lander (OS1): observations in black and modelled results in red.
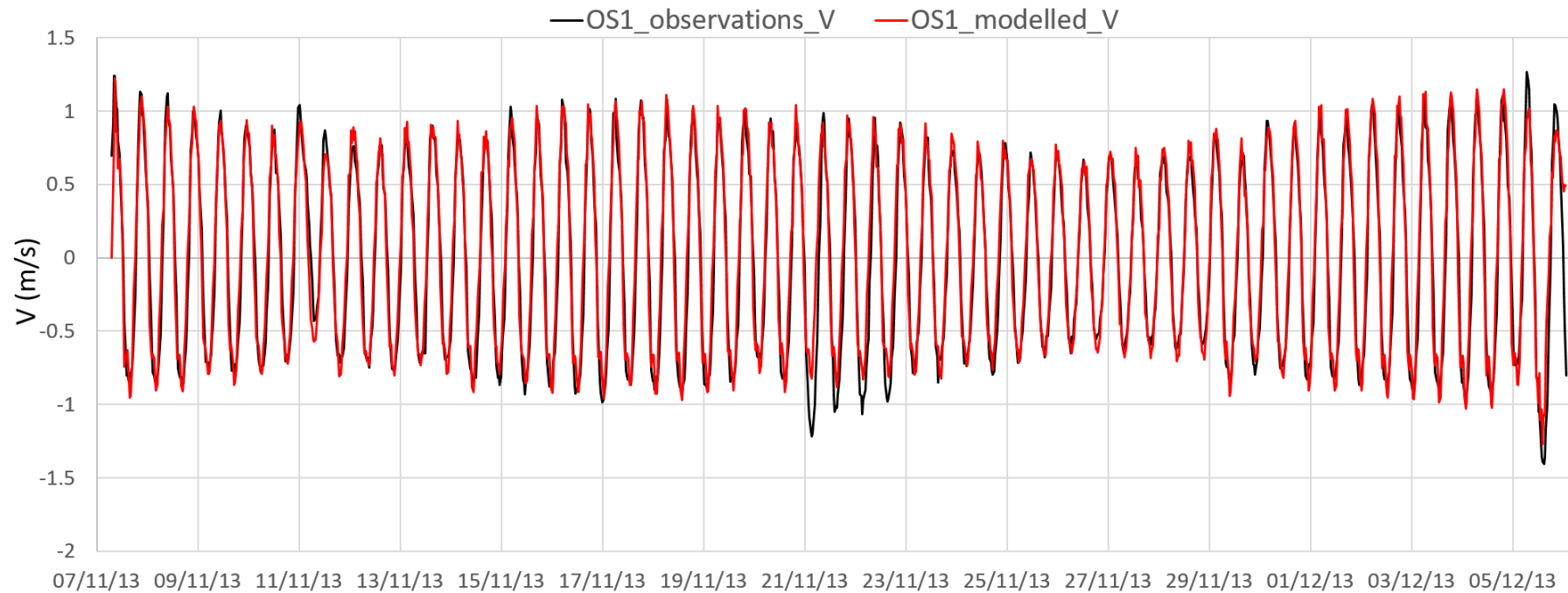
Figure 83: Comparison of velocity vector V (m/s) at offshore lander (OS1): observations in black and modelled results in red. Positive and negative velocities represent the movement northwards and southwards, respectively.

TR543 MODELLING OF THE TEMPORARY AND PERMANENT BLF AT SZC

NOT PROTECTIVELY MARKED
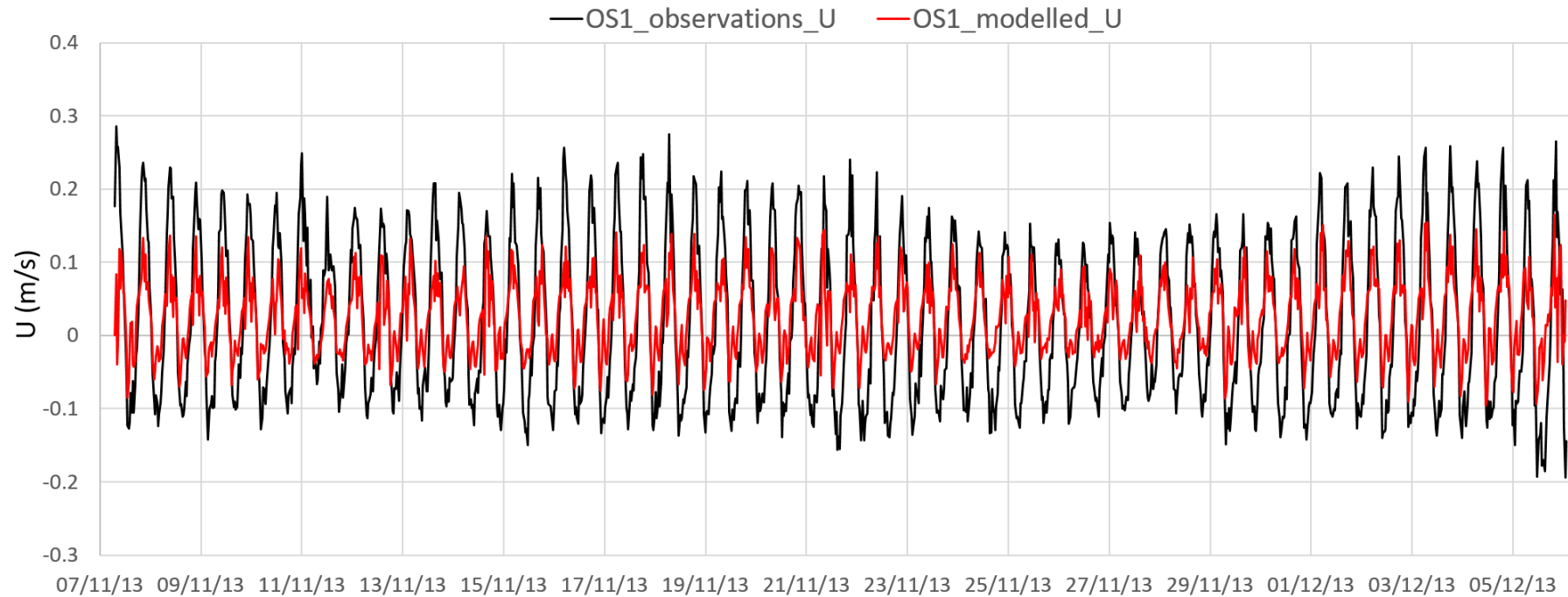
Figure 84: Comparison of velocity vector U (m/s) at offshore lander (OS1): observations in black and modelled results in red. Positive and negative velocities represent the movement eastwards and westwards, respectively.

TR543 MODELLING OF THE TEMPORARY AND PERMANENT BLF AT SZC

NOT PROTECTIVELY MARKED

Figure 85: Comparison of vertical free surface elevation (m) at inshore lander 1 (IS1): observations in black and modelled results in red.

Figure 86: Comparison of velocity vector V (m/s) at inshore lander 1 (IS1): observations in black and modelled results in red. Positive and negative velocities represent the movement northwards and southwards, respectively.
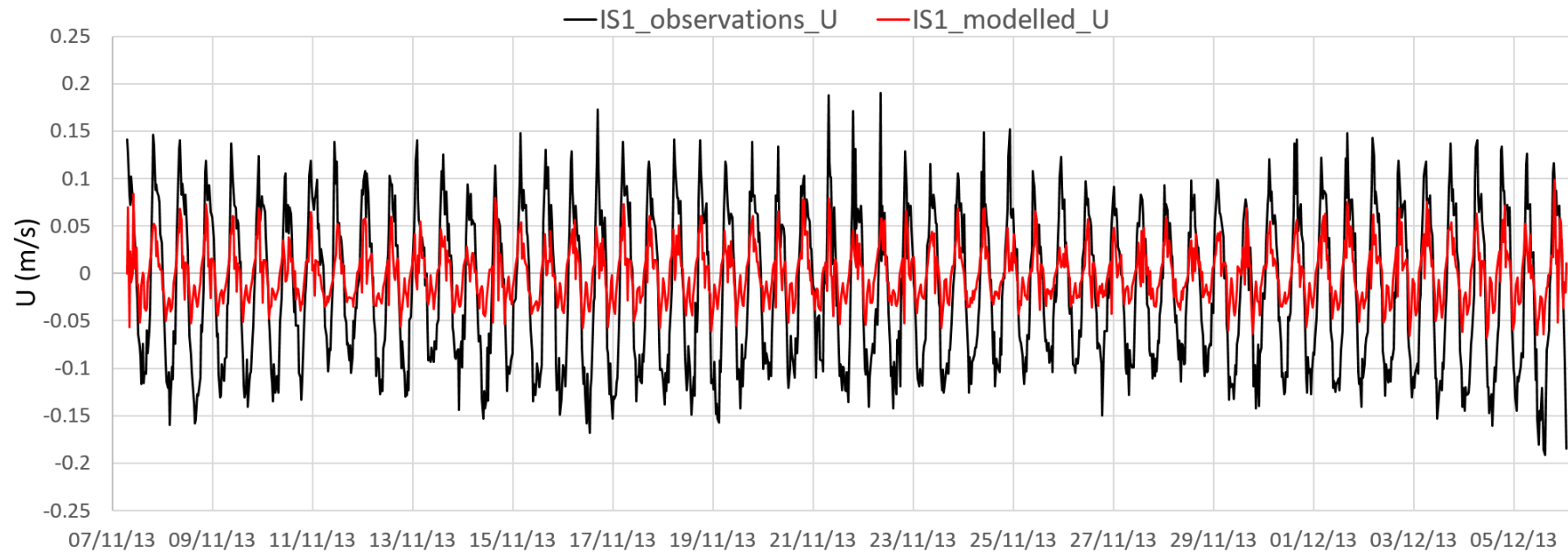
Figure 87: Comparison of velocity vector U (m/s) at inshore lander 1 (IS1): observations in black and modelled results in red. Positive and negative velocities represent the movement eastwards and westwards, respectively.

TR543 MODELLING OF THE TEMPORARY AND PERMANENT BLF AT SZC

NOT PROTECTIVELY MARKED

Figure 88: Comparison of vertical free surface elevation (m) at inshore lander 2 (IS2): observations in black and modelled results in red.

**TR543 MODELLING OF THE TEMPORARY AND PERMANENT BLF AT SZC**

NOT PROTECTIVELY MARKED

Figure 89: Comparison of velocity vector V (m/s) at inshore lander 2 (IS2): observations in black and modelled results in red. Positive and negative velocities represent the movement northwards and southwards, respectively.
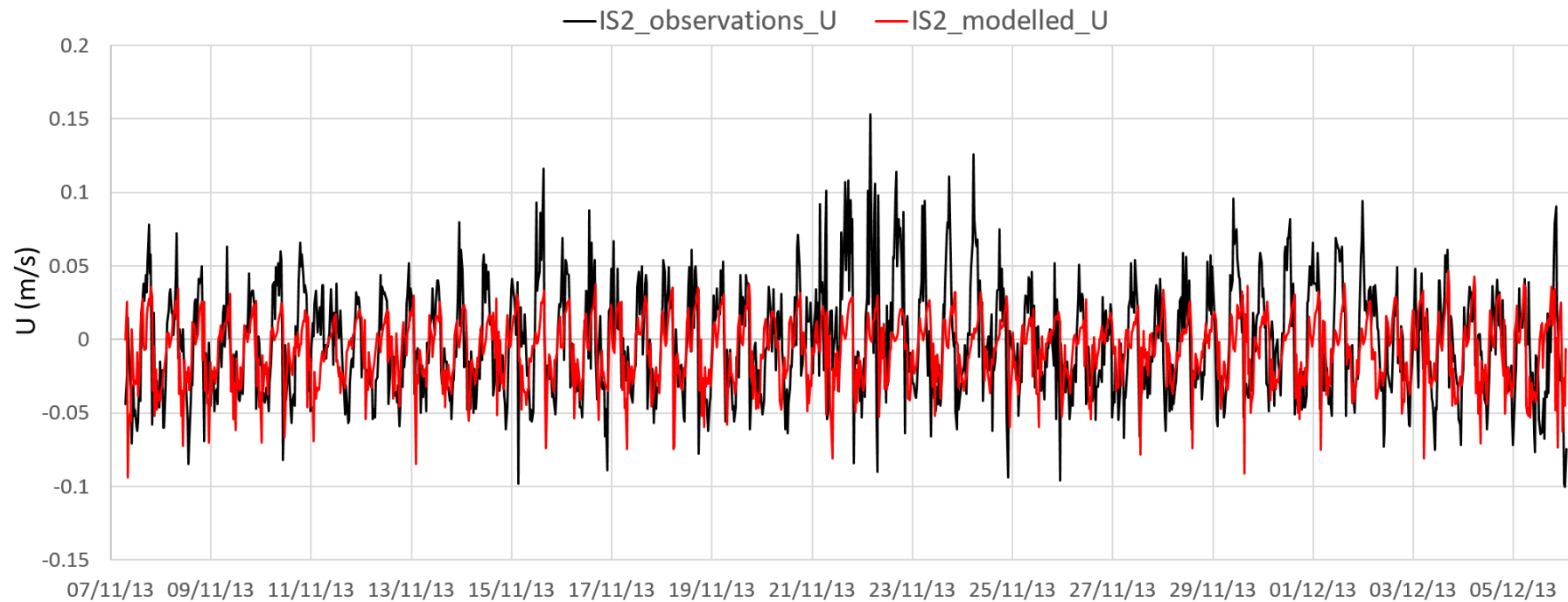
Figure 90: Comparison of velocity vector U (m/s) at inshore lander 2 (IS2): observations in black and modelled results in red. Positive and negative velocities represent the movement eastwards and westwards, respectively

B.6   Bed friction

Several options are permissible in ARTEMIS to apply friction at the bed. Values for sediment sizes d_{50} and d_{90} were used (d_{50}= 350 µm and d_{90}= 603 µm) to determine bed roughness value for skin and bedform friction following Putnam and Johnson (1949). The value for bed friction was uniformly applied to the whole model domain.

For the TELEMAC2D simulations, the Nikuradse law of bottom friction is used, which uses the roughness length, z_0, to compute friction. A constant value z_0 = 6 mm was applied uniformly to the whole model domain.

B.7   Pile scour

Once the BLFs are constructed, the seabed surrounding the piles will. It is expected that lowering of the bed will cease when continuity of volume of the tidal flow has been re-established. An empirical assessment of the localised scour around the piles was carried out in BEEMS Technical Report TR310 Edition 2, and the original bathymetry of the mesh was amended to include these scour dimensions. A detailed explanation of the scour calculations is presented in Appendix C, along with a layout of the piles and mooring dolphins of the temporary and permanent BLF as detailed in Figure 92 with the individual scour calculations for each pile summarised in Table 2.

For the permanent BLF, the scour depth for the piles is between 0.64 m and 0.84 m, with a scour extent between 1.21 m and 1.58 m. For the mooring dolphins, the scour depth is between 1.79 m and 2.07 m, with a scour extent between 3.37 m and 3.89 m. For the temporary BLF, the scour depth for the piles is between 0.26 m and 2.31 m, with a scour extent between 0.49 m and 4.35 m. The scour depth for the jetty piles of the head is between 1.63 m and 2.26 m, with a scour extent between 3.07m and 4.25 m. For the mooring dolphins the scour depth is between 2.67 m and 2.87 m, with a scour extent between 5.03 m and 5.39 m. Group scour was computed for the two piles of the permanent BLF and six piles of the temporary BLF, as detailed in Appendix C. The scour values are applied to both the ARTEMIS and TELEMAC2D model meshes.

The shape of the scour pit has been smoothed by using an angle of repose of 28° to produce suitable gradients away from the scoured depression (Soulsby, 1997). An example of the bathymetry and local lowering used in the ARTEMIS mesh around the permanent BLF is shown in Figure 91. Note there is a vertical exaggeration in the plot to aid visualisation.

TR543 MODELLING OF THE TEMPORARY AND PERMANENT BLF AT SZC

NOT PROTECTIVELY MARKED
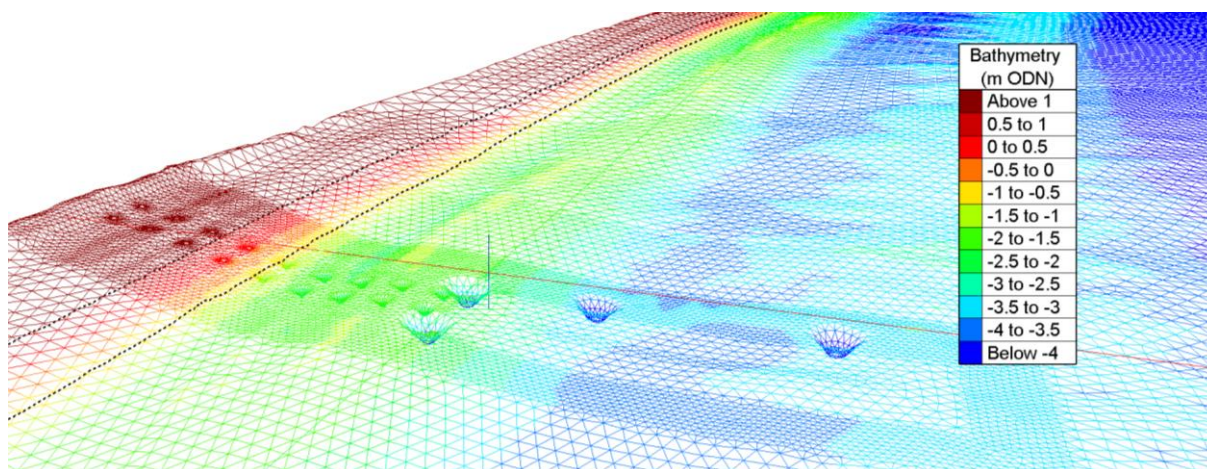
Figure 91: Example of the bathymetry around the permanent BLF jetty piles, including the addition of lowering the bathymetry around the piles due to scour. The vertical black lines represent the MHWS and MLWS contours.

Appendix C Scour Calculations

Scour calculations were undertaken for both BLFs according to the assessment methodology presented in BEEMS Technical Report TR310 Edition 2.

The Hydraulic Engineering Circular No. 18 (HEC18) methodology for either single slender piles or groups of piles was applied to determine scour depth, depending on the spacing between piles relative to their diameter (Richardson and Davis, 2001). Scour extent, defined as the distance from the structure to the edge of the scour pit, was calculated using scour depths based on an assumed sediment angle of repose of 28˚ (Soulsby, 1997). Scour depth and extent for each pile is presented in Figure 92 alongside water depth, current speed and pile group characteristics in and pile locations are shown in Table 2.

Scour depths ranged between 0.26 and 2.87 m and scour extent ranged between 0.49 and 5.39 m. Group scour effects were predicted at eight piles only.

The influence of waves was not incorporated into the scour assessment for input to the modelling since waves would act to reduce the scour depth and extent compared to a tidal current only scenario, and therefore predicted scour under waves or combined waves and currents does not represent the worst case.

The temporary BLF is 22 m from FRR2 and 52 m from the CDO at its closest point. The structures are sufficiently distant from each other for no interaction of scour pits to occur (group scour effects are expected where spacing is less than six times structure diameter (Whitehouse, 1998) and the larger diameter 3 m for the FRR and CDO does not exceed this threshold).

TR543 MODELLING OF THE TEMPORARY AND PERMANENT BLF AT SZC

NOT PROTECTIVELY MARKED
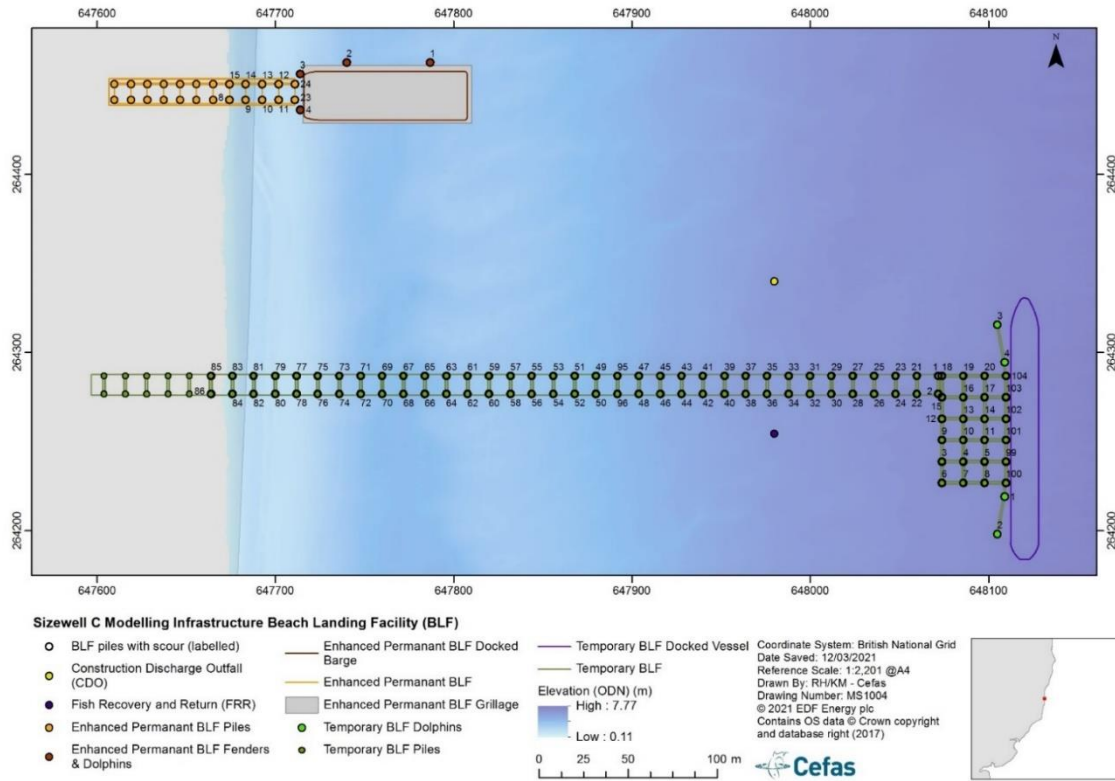
Figure 92: BLF piles with scour outlined bold, labelled according to pile references in Table 2.

Table 2: Calculation of the maximum scour depth and horizontal scour around the piles, as labelled in Figure 92.

Jetty and section	Pile Reference	Pile diameter (m)	Water depth (m)	Current velocity (m/s)	Pile group characteristics				Scour depth (m)	Scour extent (m)
					Distance to nearest pile (m)	Number of piles inline with flow	Number of piles perpendicular to flow	Group scour effects		
Permanent BLF – jetty piles	8	1	0.84	0.2	9	2	1		0.65	1.23
	9	1	1.65	0.23	9	2	1		0.77	1.45
	10	1	1.72	0.25	9	2	1		0.8	1.5
	11	1	1.38	0.27	9	2	1		0.8	1.5
	12	1	1.43	0.26	9	2	1		0.79	1.48
	13	1	1.73	0.24	9	2	1		0.79	1.49
	14	1	1.67	0.23	9	2	1		0.76	1.43
	15	1	0.86	0.19	9	2	1		0.64	1.21
	23	1	1.68	0.28	6.2	2	2		0.84	1.58
	24	1	1.68	0.28	6.2	2	2		0.83	1.57
	1	2.5	3.19	0.37	46	1	1		1.87	3.51

TR543 MODELLING OF THE TEMPORARY AND PERMANENT BLF AT SZC

NOT PROTECTIVELY MARKED

Permanent **BLF – dolphin piles**	2	2.5	3.17	0.34	26.8	1	1		1.79	3.37
	3	2.5	1.89	0.28	6.2	2	2	Yes	2.06	3.88
	4	2.5	1.79	0.29	6.2	2	2	Yes	2.07	3.89
Temporary BLF – jetty head piles	3	1.2	6.81	0.65	12	2	1		1.63	3.07
	4	1.2	6.9	0.66	12	2	1		1.64	3.09
	5	1.2	7	0.67	12	2	1		1.66	3.12
	6	1.2	6.78	0.65	12	2	1		1.63	3.07
	7	1.2	6.87	0.66	12	2	1		1.65	3.09
	8	1.2	6.96	0.67	12	2	1		1.66	3.12
	9	1.2	6.84	0.65	12	2	1		1.63	3.07
	10	1.2	6.92	0.66	12	2	1		1.64	3.09
	11	1.2	7.03	0.67	12	2	1		1.66	3.11
	12	1.2	6.84	0.65	12	2	1		1.63	3.07
	13	1.2	6.92	0.66	12	2	1		1.64	3.09
	14	1.2	7.05	0.66	12	2	1		1.65	3.11
	15	1.2	6.81	0.65	2.8	1	2	Yes	2.09	3.94

TR543 MODELLING OF THE TEMPORARY AND PERMANENT BLF AT SZC

NOT PROTECTIVELY MARKED

	16	1.2	6.9	0.66	12	2	1		1.64	3.09
	17	1.2	7.04	0.66	12	2	1		1.65	3.11
	18	1.2	6.78	**0.65**	2	1	2	Yes	2.26	4.25
	19	1.2	6.87	0.66	12	2	1		1.64	3.09
	20	1.2	7.02	0.66	12	2	1		1.65	3.11
	99	1.2	7.11	0.67	10	2	1		1.67	3.14
	100	1.2	7.08	0.68	7.74	2	1		1.67	3.14
	101	1.2	7.14	0.67	12	2	1		1.67	3.14
	102	1.2	7.15	0.67	12	2	1		1.66	3.13
	103	1.2	7.17	0.67	12	2	1		1.66	3.13
	104	1.2	7.17	0.67	7.74	2	1		1.66	3.12
Temporary BLF – jetty piles	1	1.2	6.77	0.65	2	2	2	Yes	2.31	4.35
	2	1.2	6.79	0.65	2.8	2	2	Yes	2.19	4.12
	21	1.2	6.68	0.64	10	2	1		1.62	3.04
	22	1.2	6.72	0.64	10	2	1		1.62	3.04
	23	1.2	6.56	0.64	10	2	1		1.61	3.03

TR543 MODELLING OF THE TEMPORARY AND PERMANENT BLF AT SZC

NOT PROTECTIVELY MARKED

24	1.2	6.6	0.63	10	2	1		1.61	3.02
25	1.2	6.43	0.63	10	2	1		1.6	3.01
26	1.2	6.44	0.63	10	2	1		1.6	3
27	1.2	6.35	0.62	10	2	1		1.59	2.99
28	1.2	6.34	0.62	10	2	1		1.59	2.98
29	1.2	6.24	0.61	10	2	1		1.57	2.96
30	1.2	6.19	0.62	10	2	1		1.57	2.96
31	1.2	6.08	0.61	10	2	1		1.56	2.94
32	1.2	6.02	0.61	10	2	1		1.56	2.94
33	1.2	5.92	0.6	10	2	1		1.54	2.9
34	1.2	5.87	0.6	10	2	1		1.54	2.9
35	1.2	5.77	0.58	10	2	1		1.52	2.87
36	1.2	5.72	0.59	10	2	1		1.53	2.87
37	1.2	5.56	0.57	10	2	1		1.5	2.82
38	1.2	5.49	0.58	10	2	1		1.5	2.83
39	1.2	5.39	0.56	10	2	1		1.48	2.78

TR543 MODELLING OF THE TEMPORARY AND PERMANENT BLF AT SZC

NOT PROTECTIVELY MARKED

40	1.2	5.35	0.56	10	2	1		1.48	2.79
41	1.2	5.2	0.54	10	2	1		1.45	2.73
42	1.2	5.16	0.55	10	2	1		1.46	2.75
43	1.2	4.97	0.52	10	2	1		1.43	2.68
44	1.2	4.81	0.54	10	2	1		1.43	2.7
45	1.2	4.76	0.51	10	2	1		1.4	2.64
46	1.2	4.62	0.52	10	2	1		1.41	2.65
47	1.2	4.48	0.5	10	2	1		1.38	2.59
48	1.2	4.42	0.51	10	2	1		1.38	2.6
49	1.2	3.89	0.48	10	2	1		1.33	2.5
50	1.2	3.94	0.47	10	2	1		1.32	2.49
51	1.2	3.6	0.47	10	2	1		1.3	2.44
52	1.2	3.74	0.46	10	2	1		1.29	2.44
53	1.2	3.4	0.45	10	2	1		1.27	2.39
54	1.2	3.47	0.44	10	2	1		1.26	2.38
55	1.2	3.24	0.44	10	2	1		1.24	2.34

56	1.2	3.26	0.43	10	2	1		1.24	2.34
57	1.2	3.08	0.42	10	2	1		1.22	2.29
58	1.2	3.03	0.43	10	2	1		1.22	2.29
59	1.2	3.01	0.41	10	2	1		1.19	2.25
60	1.2	2.99	0.41	10	2	1		1.2	2.25
61	1.2	3.11	0.39	10	2	1		1.18	2.22
62	1.2	3.12	0.4	10	2	1		1.19	2.24
63	1.2	3.46	0.38	10	2	1		1.18	2.22
64	1.2	3.4	0.39	10	2	1		1.19	2.24
65	1.2	3.77	0.38	10	2	1		1.19	2.24
66	1.2	3.71	0.39	10	2	1		1.2	2.26
67	1.2	3.85	0.39	10	2	1		1.21	2.27
68	1.2	3.89	0.39	10	2	1		1.21	2.28
69	1.2	3.67	0.39	10	2	1		1.21	2.27
70	1.2	3.72	0.39	10	2	1		1.2	2.27
71	1.2	3.51	0.38	10	2	1		1.19	2.23

72	1.2	3.35	0.38	10	2	1		1.18	2.22
73	1.2	2.92	0.35	10	2	1		1.12	2.1
74	1.2	2.78	0.36	10	2	1		1.13	2.12
75	1.2	2.04	0.34	10	2	1		1.05	1.97
76	1.2	2.1	0.35	10	2	1		1.06	1.99
77	1.2	1.54	0.31	10	2	1		0.97	1.82
78	1.2	1.53	0.31	10	2	1		0.97	1.83
79	1.2	1.48	0.31	10	2	1		0.97	1.83
80	1.2	1.5	0.3	10	2	1		0.96	1.8
81	1.2	1.63	0.23	10	2	1		0.87	1.63
82	1.2	1.64	0.25	10	2	1		0.89	1.68
83	1.2	0.65	0.18	10	2	1		0.68	1.28
84	1.2	0.61	0.15	10	2	1		0.62	1.17
85	1.2	0.13	0.07	10	2	1		0.37	0.69
86	1.2	0.08	0.04	10	2	1		0.26	0.49
95	1.2	4.22	0.48	10	2	1		1.35	2.54

TR543 MODELLING OF THE TEMPORARY AND PERMANENT BLF AT SZC

NOT PROTECTIVELY MARKED

	96	1.2	4.19	0.49	10	2	1		1.35	2.54
Temporary BLF – dolphin piles	1	2.5	7.08	0.68	7.73	2	1	Yes	2.87	5.39
	2	2.5	7.08	0.67	21.44	2	1		2.69	5.05
	3	2.5	7.07	0.67	21.44	2	1		2.67	5.03
	4	2.5	7.15	0.67	7.74	2	1	Yes	2.85	5.37

Appendix D Results of other modelled scenarios

D.1   Bed shear stress

Figure 93 to Figure 100 show the magnitude of change in maximum bed shear stress for each combination of wave direction and tidal current conditions for each combination of the temporary and permanent BLF plus the associated structures, dredging and vessels.
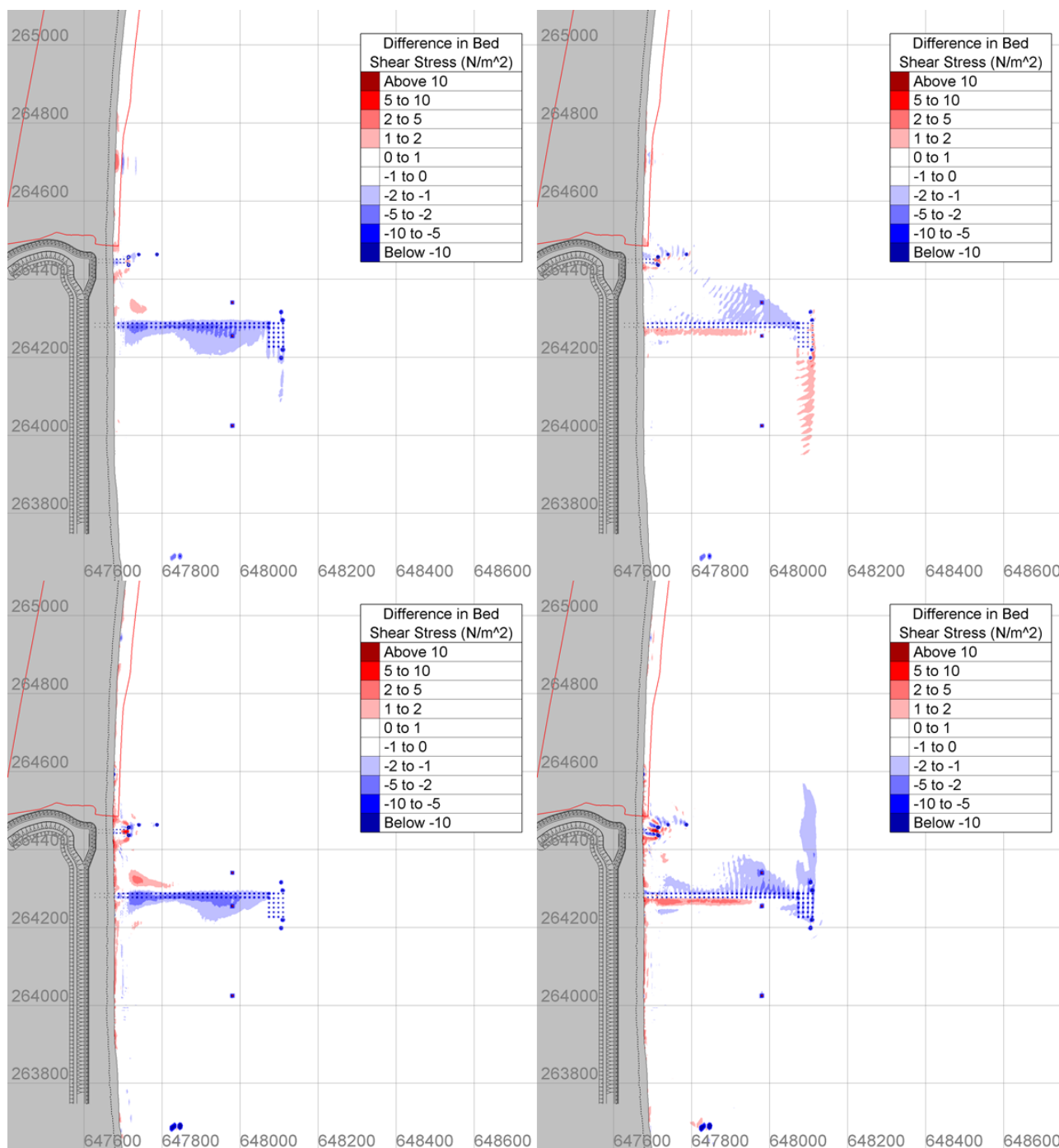
Figure 93: Magnitude of change in maximum bed shear stress for the temporary and permanent BLF structures only, for NE wave at peak flood, SE wave peak flood, SE wave peak ebb and SE peak ebb (clockwise from top left).

**TR543 MODELLING OF THE TEMPORARY AND PERMANENT BLF AT SZC**

NOT PROTECTIVELY MARKED
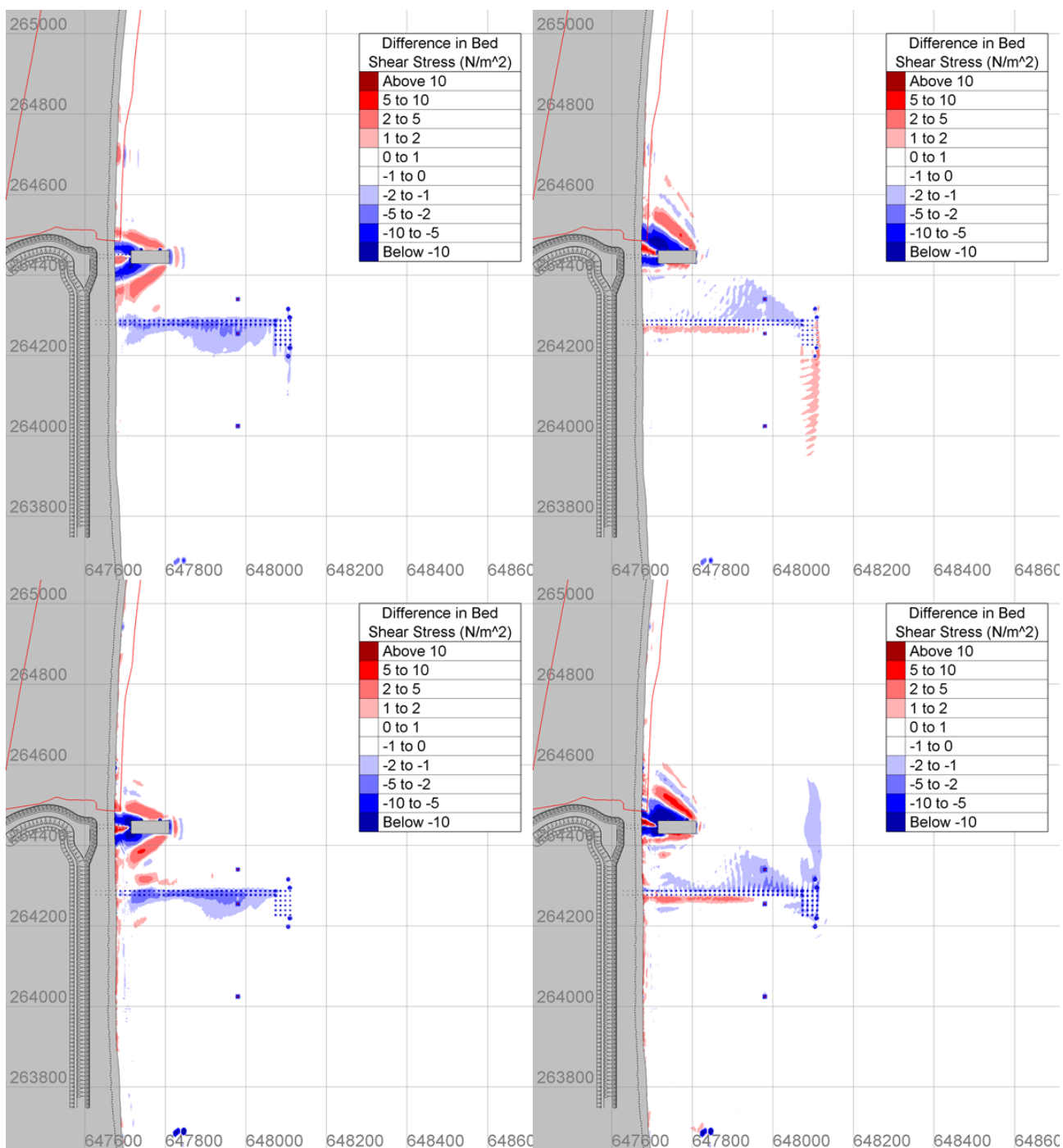
Figure 94: Magnitude of change in maximum bed shear stress for the temporary and permanent BLF structures with the grillage, for NE wave at peak flood, SE wave peak flood, SE wave peak ebb and SE peak ebb (clockwise from top left).

TR543 MODELLING OF THE TEMPORARY AND PERMANENT BLF AT SZC

NOT PROTECTIVELY MARKED
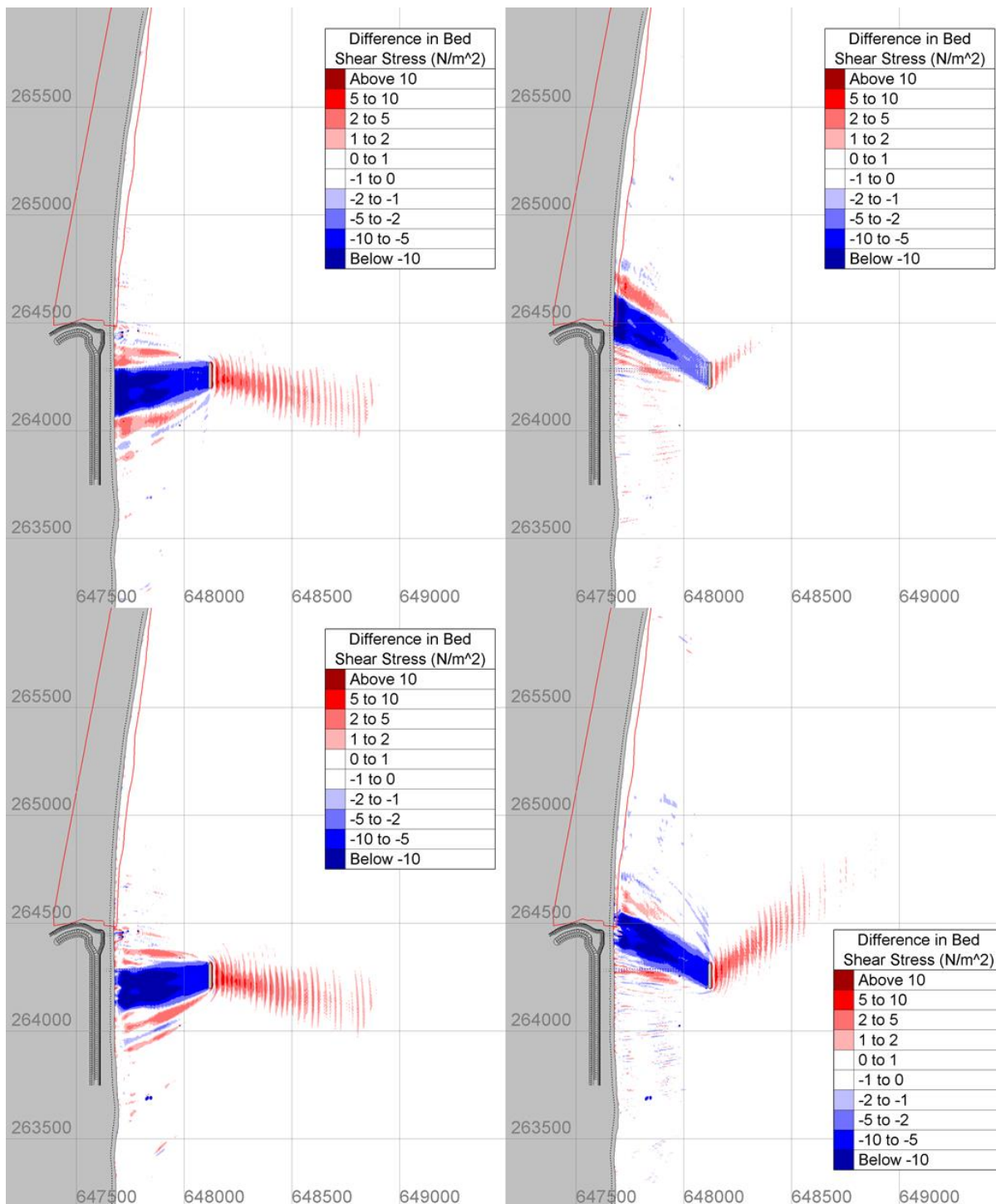
Figure 95: Magnitude of change in maximum bed shear stress for the temporary and permanent BLF structures with the ship, for NE wave at peak flood, SE wave peak flood, SE wave peak ebb and SE peak ebb (clockwise from top left).

**TR543 MODELLING OF THE TEMPORARY AND PERMANENT BLF AT SZC**

NOT PROTECTIVELY MARKED
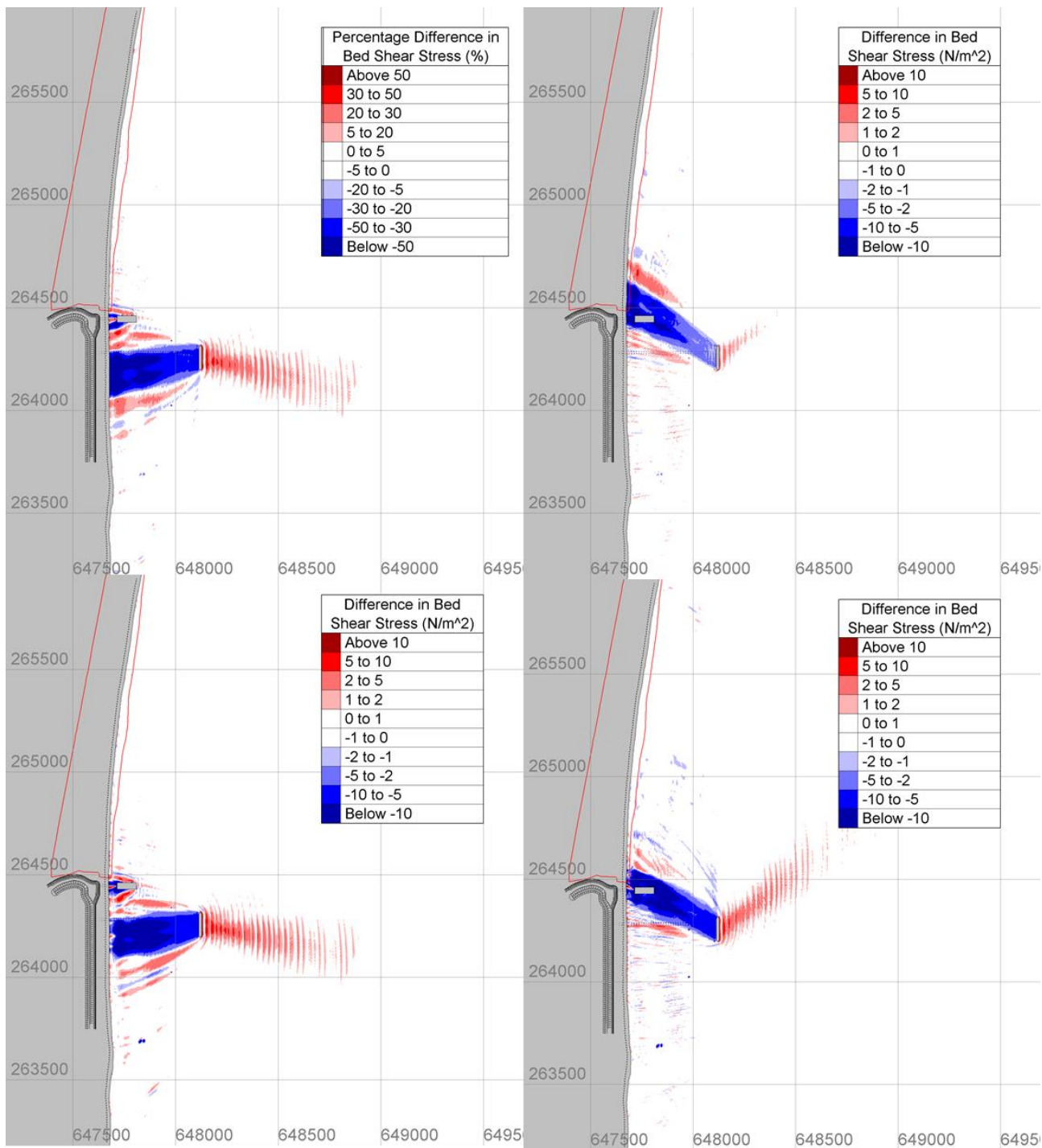
Figure 96: Magnitude of change in maximum bed shear stress for the temporary and permanent BLF structures with the grillage and ship, for NE wave at peak flood, SE wave peak flood, SE wave peak ebb and SE peak ebb (clockwise from top left).

**TR543 MODELLING OF THE TEMPORARY AND PERMANENT BLF AT SZC**

NOT PROTECTIVELY MARKED
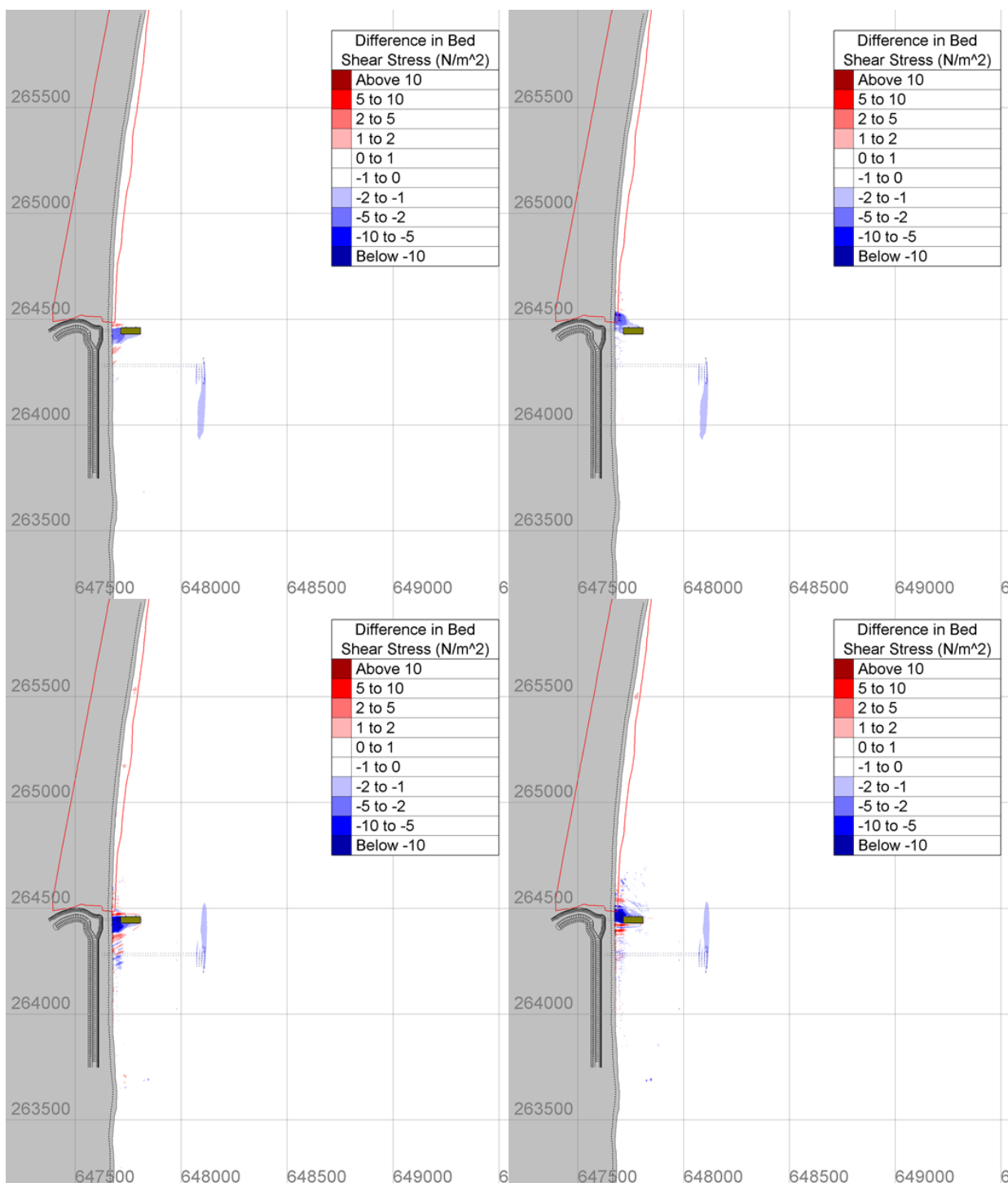
Figure 97: Magnitude of change in maximum bed shear stress for the temporary and permanent BLF structures with the grillage, access dredge and barge, for NE wave at peak flood, SE wave peak flood, SE wave peak ebb and SE peak ebb (clockwise from top left).

TR543 MODELLING OF THE TEMPORARY AND PERMANENT BLF AT SZC

NOT PROTECTIVELY MARKED
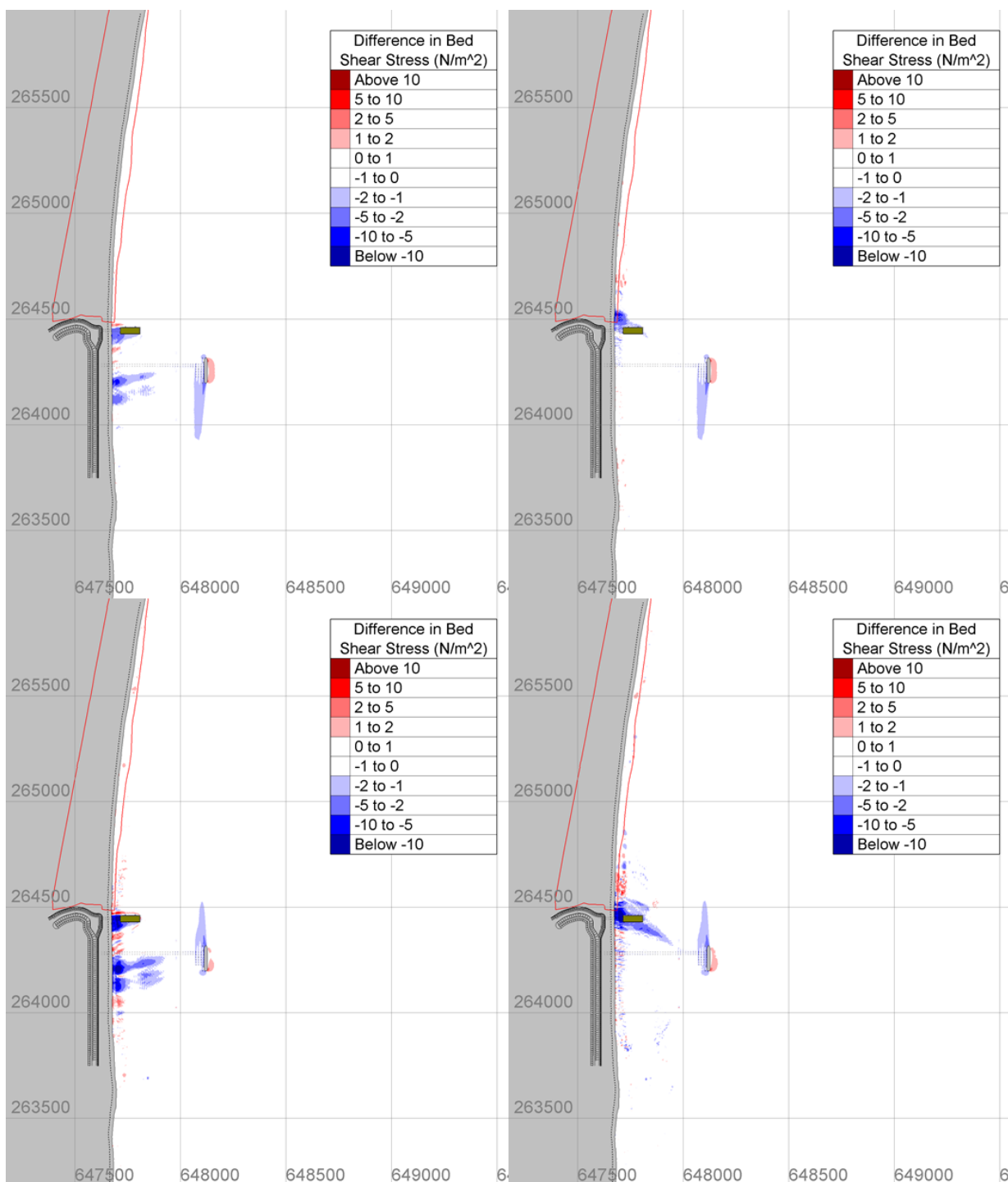
Figure 98: Magnitude of change in maximum bed shear stress for the temporary and permanent BLF structures with the grillage, access dredge, barge and ship, for NE wave at peak flood, SE wave peak flood, SE wave peak ebb and SE peak ebb (clockwise from top left).

**TR543 MODELLING OF THE TEMPORARY AND PERMANENT BLF AT SZC**

NOT PROTECTIVELY MARKED
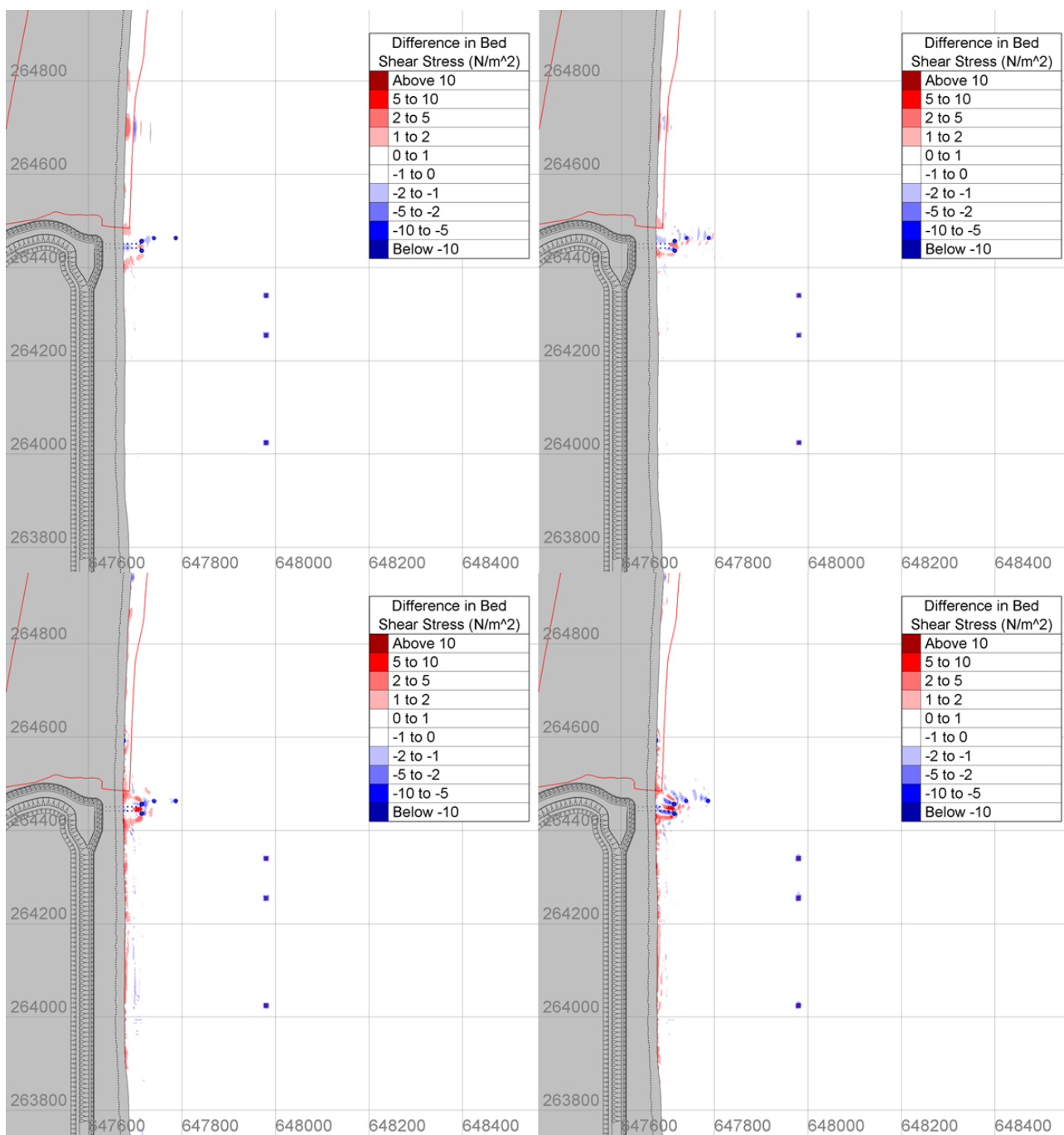
Figure 99: Magnitude of change in maximum bed shear stress for the permanent BLF only, for NE wave at peak flood, SE wave peak flood, SE wave peak ebb and SE peak ebb (clockwise from top left).

TR543 MODELLING OF THE TEMPORARY AND PERMANENT BLF AT SZC

NOT PROTECTIVELY MARKED
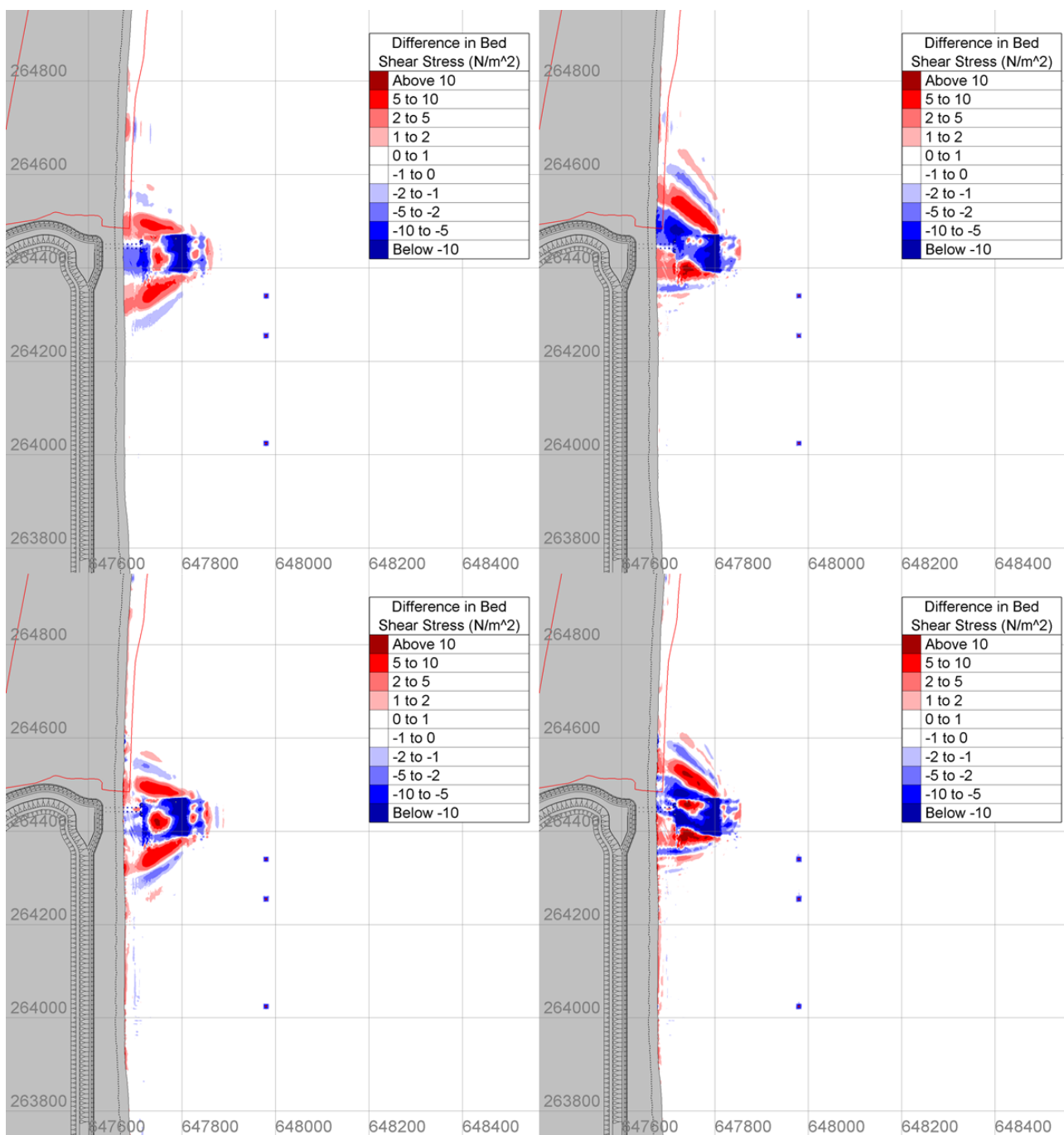
Figure 100: Magnitude of change in maximum bed shear stress for the permanent BLF plus grounding pocket and access dredge, for NE wave at peak flood, SE wave peak flood, SE wave peak ebb and SE peak ebb (clockwise from top left).